Holography beyond AdS/CFT

by

Nicholas S Salzetta

A dissertation submitted in partial satisfaction of the

requirements for the degree of

Doctor of Philosophy

in

Physics

in the

Graduate Division

of the

University of California, Berkeley

Committee in charge:

Professor Yasunori Nomura, Chair
Professor Ori Ganor
Assistant Professor Jessica Lu

Fall 2019

Holography beyond AdS/CFT

Abstract

Holography beyond AdS/CFT

by

Nicholas S Salzetta

Doctor of Philosophy in Physics

University of California, Berkeley

Professor Yasunori Nomura, Chair

Physicists have long sought to fully understand how gravity can be fully formulated within a quantum mechanical framework. A promising avenue of research in this direction was born from the idea of holography - that gravitational physics can be recast as a different theory living in fewer dimensions. Evidence of this phenomena was first observed in the arena of black hole physics, where the entropy of a black hole was calculated to scale with its area, not its volume. The advent of the Anti-de Sitter/Conformal Field Theory (AdS/CFT) correspondence provided an explicit realization of holography for gravitational theories in AdS space. This brought a flurry of activity dedicated to dissecting this correspondence. Ultimately, however, it will be necessary to move beyond the confines of AdS/CFT in order to understand our universe, as we live in a de Sitter type universe. The research presented in this dissertation attempts to broaden the scope of holgraphic theories to include more phenomenologically relevant universes. To do so, we utilize a top-down approach and take results from AdS/CFT that appear to be general holographic results and see how they can be applied in spacetimes other than AdS. In particular, we take the Ryu-Takayanagi (RT) formula, along with its related results, and investigate what we can learn by applying it to general spacetimes. Doing so naturally forces us to utilize holographic screens, as these are the largest such surfaces where the RT formula can be self-consistently applied. This approach allows us to examine properties of the purported boundary theory for general spacetimes, including the entanglement structure and propagation speeds of excitations dual to bulk excitations. This is done in chapters 2 and 3. In chapters 4 and 5, we use this lens of generalized holography to elucidate the nature of the relationship between entanglement and emergent geometry. Finally, in chapter 6, we revisit one the important underlying assumption that the RT formula is general and demonstrate the validity of this assumption.

To my parents, Meg and Paul

Contents

List of Figures

Acknowledgments

I owe my success to a number of individuals who have helped me throughout the course of my PhD career.

I am unbelievably grateful to my parents, Meg and Paul. Their undying support, love, and compassion, not only during my PhD, but throughout all throughout childhood and young adulthood have made me the person I am today. They fostered my curiosity, showed me the world, and entertained my maddening questions (at least until I was well enough equipped to browse Wikipedia). They have not only demonstrated the importance of hard work, but also the immense value of maintaining personal interests and relationships.

My advisor, Yasunori Nomura, has gone above and beyond in terms of mentorship and guidance. He has both shaped my understanding of the universe and developed my confidence as a researcher and communicator. I cannot thank him enough for his role in my PhD program.

I would like to thank all those that I collaborated with, in particular Sean Weinberg, Fabio Sanches, Pratik Rath, and Chitraang Murdia. You all taught me so much and I look forward to seeing your future successes.

Additionally, I would like to thank all of the members of the BCTP for providing a welcoming and engaging learning environment.

Chapter 1

Introduction

Both quantum mechanics and general relativity have enjoyed astounding empirical success since their theoretical foundations were laid in the early 1900s. Despite this, physicists have yet to fully understand how these two theories are reconciled with one another. A naive approach to address this problem is to directly quantize the Einstein-Hilbert action of general relativity, and treat it as a quantum field theory. However, this fails to give a complete picture of quantum gravity because the action is nonrenormalizable. This does not prohibit us from utilizing such an effective theory, however it indicates that there exists a high-energy scale at which the theory breaks down and one must find a creative way of describing phenomena at this scale [1, 2, 3].

The most promising theory to describe physics at this scale, which naturally includes gravitational interactions is string theory. String theory is wildly successful in that it has the capability to describe an extremely wide range of phenomena with minimal assumptions, while simultaneously including gravity [4, 5]. Despite this, string theory best describes perturbative interactions, for example the scattering between strings in various states. Unfortunately, classical spacetimes are described by an impossibly large number of interacting strings, and string theory in its current form is an unwieldy tool to address physics at this scale. Analogously, no one would try to calculate the pressure of air in a box by utilizing a fully quantum mechanical description of all $\sim 10^{23}$ particles interacting with one another.

To tackle questions in the regime of classical spacetime dynamics, one needs a different approach. Luckily, just as one can apply thermodynamic principles to address questions like calculating the pressure of gases, one can attempt to formulate thermodynamic principles of spacetime. This approach will aid in our understanding of the emergence of gravity from quantum mechanical systems. This direction of research began with the investigation of black hole evaporation and entropy by Bekenstein and Hawking [6, 7, 8, 9]. The revelation that black holes radiated and have temperature suggested that taking a thermodynamic approach to quantum gravity would be fruitful [10, 11]. Since then an understanding has developed that gravity and spacetime emerge from the complex interactions of massive numbers of quantum mechanical degrees of freedom [12]. Continuing the analogy, Einstein's equations of general relativity are like the ideal gas law - both formulas describe physics in a certain

regime, and both emerge from the interaction of many degrees of freedom.

One of the most astonishing results from this research direction is that the entropy of black holes is proportional to its area, rather than its volume [8]. This is in stark contrast to any theory with local degrees of freedom, which necessitates a volume law scaling of entropy. This suggests that a theory describing black hole dynamics requires one fewer dimension than that of the ambient spacetime. Additionally, this area law behavior provides an upper bound for the entropy of a region of spacetime - if one tried to violate this by adding more and more matter to a subregion of space then eventually the matter would collapse into a black hole, which has its entropy bounded by its area. This spurred the concept of holography - gravitational theories have an alternate formulation in one fewer dimension [13].

Hawking's calculation of black hole entropy merely alluded to the existence of an alternate theory in fewer dimensions, however, an explicit holographic correspondence was discovered in the late 90s. This correspondence is dubbed AdS/CFT, as it relates gravitational physics in an anti-de Sitter (AdS) spacetime of $d+1$ dimensions to a special conformal field theory (CFT) in d dimensions which "lives" at the conformal boundary of AdS [14, 15]. This correspondence has provided physicists with a playground to learn about quantum gravity. AdS/CFT tells us that any observable on the gravity side of the theory can be translated into observables in the CFT. Physicists have since been filling out entries in this "dictionary", relating CFT quantities to AdS ones. One of the most interesting dictionary entries is the Ryu-Takayanagi (RT) formula [16]. This relates entanglement entropy in the CFT to the area of geometric surfaces in AdS - a profound connection between quantum information and geometry. However, while AdS/CFT has immensely aided our understanding of quantum gravity, it is far from the whole story. The Hubble constant has been consistently measured to be positive [17, 18, 19, 20], which tells us that we do not live in an *anti*-de Sitter space, but rather a de Sitter (dS) space.

AdS has a number of properties that make it easier to deal with holographically compared to dS. For one, AdS has a natural timelike conformal boundary. This makes it easier to understand and visualize how time evolution in the bulk is related to time evolution in the boundary. Additionally, the volume of a region within AdS actually scales with the area of said region, due to the hyperbolic nature of the spacetime - this makes the existence of a holographic theory more palatable. Unfortunately, de Sitter and other spacetimes resembling the universe we live in do not have these nice properties. However, intuition from black hole entropy still suggests a holographic formulation should be possible.

Headway was made in addressing holographic principles in general spacetimes with the covariant entropy conjecture [21]. This introduced a holographic entropy bound that applies in all spacetimes. In particular, it provides a codimension-1 surface in all spacetimes that effectively bounds the entropy to the interior of the surface. Additionally, this surface, the holographic screen, has a unique foliation into "time-slices", dubbed leaves. Hence, we have a surface in all spacetimes that provides a holographic entropy bound and also has a preferred time direction. The holographic screen gives us a platform for investigating holography in general spacetimes [22].

This brings us to the focus of this thesis. To address holography in general spacetimes,

one could take a bottom up approach and attempt to find a new string-theoretic formulation of holography and go from there. Alternatively, one can work top-down, and attempt to extrapolate results and draw connections between established work in an effort to understand holography in general spacetimes. We will take the latter approach. In particular, we extract results from AdS/CFT that seem to be general holographic results as opposed to AdS/CFT specific, and understand how they should work in general spacetimes with holographic screens. One of these general results is the RT formula - indeed, one of the most intriguing aspects of the RT formula is that it seems to be unconcerned with the particularities of AdS/CFT. The proof of RT does not need the gravitational bulk to be AdS, nor does it need the boundary theory to be a CFT [23]. Additionally, a similar relationship between entanglement and geometry is observed in tensor networks [24, 25, 26], a completely different framework! Our work begins by assuming the RT formula (and related results [27, 28, 29]) should hold in general spacetimes, and we investigate the consequences. Interestingly, this naturally forces us to consider holographic screens. This is because the largest surface that one can anchor extremal surfaces to in a manner consistent with the RT formula is a leaf of a holographic screen [30, 31]. By then applying the RT formula to holographic screens, we can understand properties of the hypothetical boundary theory that lives on said screen. We can also "test" our assumptions by checking if our results pass a number of nontrivial self-consistency checks. By taking this top-down approach we can develop intuition as to how holography should work in all spacetimes, and from there try to find an underlying theory that matches our results.

This thesis presents a collection of papers that investigate holography in general spacetimes through this top-down perspective. The chapters are organized as follows,

- Chapter 2 introduces the general framework we adopt and shares key results and understandings. In particular, we explain how we apply the RT formula to holographic screens and calculate the entanglement entropy for theories dual to FRW and dS spacetimes. We also address the possible Hilbert space structure that houses the holographic states [32].

- Chapter 3 builds on the work in chapter 2 and investigates how boundary operators dual to bulk excitations evolve. This allows us to understand the dynamics of the boundary theory, as opposed to just the kinematics [33].

- Chapter 4 investigates how entanglement is related to emergent spacetime. We consider a number of spacetimes and examine their entanglement structure in relation to "how much" spacetime is present. We find the interesting result that spacetime emerges once a deviation from maximal entanglement occurs. This also helps to deepen our understanding of how holographic states may be organized within one Hilbert space. We further discuss possible candidates for boundary theories of FRW spacetimes [34].

- Chapter 5 uses our previously developed understanding of how regions of spacetime are holographically encoded in the boundary to explain how a coarse-graining procedure

of the boundary theory is related to a unique bulk surface. This helps us understand how and where different regions of the bulk are encoded in the boundary [31].

- Chapter 6 takes a step back and works to address one of the fundamental underlying assumptions used throughout. Namely, that the RT formula holds beyond AdS/CFT. We clarify some work and argue for the validity of the relationship in at least one theory beyond AdS/CFT. This bolsters all of our previous work [35].

This work, taken together, provides a new framework for thinking about quantum gravity in cosmological spacetimes. This is all begins by applying some of the most interesting results from AdS/CFT to settings outside of where they were discovered. Namely, by using the RT formula (and related discoveries) in general spacetimes we can investigate how quantum gravity manifests in general spacetimes. As argued in Chapter 6, the proof for the RT formula is independent of AdS/CFT's specifics, and as demonstrated in the preceding chapters (and proven in [30]) these results can be applied self-consistently in cosmological spacetimes. This lets us use general relativity calculations to peer behind the curtain of quantum gravity.

Most notably, we find that formulating a theory which lives on a holographic screen is most natural because this surface is the limiting point at where the RT formula can be applied consistently. Based on the entanglement structure for this supposed theory, we can deduce it must have long-range interactions. Further, based on how bulk excitations must be encoded, we find that the theory is not Lorentz invariant (i.e. excitations propagate faster than the speed of light). Our investigations extended beyond just characterizing this putative holographic theory to understanding more general aspects of holography. We use the same tools and intuition to show that spacetime emerges from a holographic theory only when considering states with sub-maximal entanglement. We also discover a new geometric object, the holographic slice, and explain how it naturally represents entanglement renormalization.

The natural continuation of this work is to try to develop the boundary holographic theory from a more fundamental direction. Recent investigations of $T\bar{T}$ deformed CFTs have yielded promising results from this direction [36]. Specifically, by performing this special deformation ($T\bar{T}$) to a holographic CFT, one can effectively pull the boundary in to the bulk of the emergent spacetime. By continuing this deformation, one can continue to pull the boundary deeper and deeper into the bulk, until the remaining spacetime is no longer AdS, but effectively flat. This remarkably provides us an explicit boundary theory that has a bulk dual that is not strictly AdS. By investigating $T\bar{T}$ deformed theories, one can hope to connect the results of this thesis with a more bottom-up approach.

There are two "big picture" implications of the work presented in this thesis. For one, we are inching towards a holographic theory that can describe cosmological spacetimes like the one in which we live. Discovering and understanding the quantum gravitational theory that governs our universe will help illuminate fundamental questions related to the birth and fate of our universe, dark energy, and perhaps even alternative explanations of dark matter. Simultaneously, at its core our work attempts to find mathematical dualities between different theories, a quantum mechanical theory and a gravitational one. Finding these connections

translates difficult, often intractable calculations in one theory into simple calculations in the other. Perhaps the most promising area in which this avenue of work can be applied is in understanding condensed matter systems. These systems comprise of complex interactions between many, many constituents. The ability to recast the physics of this system as a more simple, gravitational theory can help make some calculations feasible and ultimately illuminate characteristics of the system at hand. This could hopefully be used to better discover and understand new materials. By investigating holography in general spacetimes we will both further understand our place in the universe and help discover useful mathematical relationships between seemingly disparate theories.

Chapter 2

Toward holography for general spacetimes

This chapter is a replication of Nomura et al. "Toward a Holographic Theory for General Spacetimes", in *Phys. Rev.* D95.8 (2017), p. 086002, and is reproduced here in its original form.

2.1   Introduction

As with any other classical object, spacetime is expected to consist of a large number of quantum degrees of freedom. The first explicit hint of this came from the discovery that empty spacetime can carry entropy [9, 8, 10, 7, 6, 11]. What theory describes these degrees of freedom as well as the excitations on them, i.e. matter?

Part of the difficulty in finding such a theory is the large redundancies present in the description of gravitational spacetime. The holographic principle [37, 13, 22] suggests that the natural space in which the microscopic degrees of freedom for spacetime (and matter) live is a non-dynamical spacetime whose dimension is one less than that in the original description (as demonstrated in the special case of the AdS/CFT correspondence [14]). This represents a huge redundancy in the original gravitational description beyond that associated with general coordinate transformations. For general spacetimes, causality plays a central role in fixing this redundancy [38, 21]. A similar idea also plays an important role in addressing problems in the semiclassical descriptions of black holes [39] and cosmology [40, 41].

In this paper, we explore a holographic theory for general spacetimes. We follow a "bottom-up" approach given the lack of a useful description in known frameworks, such as AdS/CFT and string theory in asymptotically Minkowski space. We assume that our holographic theory is formulated on a holographic screen [42], a codimension-1 surface on which the information about the original spacetime can be encoded. This construction can be extended beyond the semiclassical regime by considering all possible states on all possible slices—called leaves—of holographic screens [40, 43], where the nonuniqueness of erecting a

holographic screen is interpreted as the freedom in fixing the redundancy associated with holography. The resulting picture is consistent with the recently discovered area theorem applicable to the holographic screens [44, 45, 46].

To study the structure of the theory, we use conjectured relationships between spacetime in the gravitational description and quantum entanglement in the holographic theory. Recently, it has become increasingly clear that quantum entanglement among holographic degrees of freedom plays an important role in the emergence of classical spacetime [16, 47, 48, 49, 50, 23, 51, 30, 52, 53, 54, 55]. In particular, Ref. [30] showed that the areas of the extremal surfaces anchored to the boundaries of regions on a leaf of a holographic screen satisfy relations obeyed by entanglement entropies, so that they can indeed be identified as the entanglement entropies associated with the corresponding regions in the holographic space. We analyze properties of these surfaces and discuss their implications for a holographic theory of general spacetimes.

We lay down our general framework in Section 2.2. We then study the behavior of extremal surfaces in cosmological Friedmann-Robertson-Walker (FRW) spacetimes in Section 3.3. Here we focus on initially expanding flat and open universes, in which the area of the leaves monotonically increases. We first consider universes dominated by a single component in the Friedmann equation, and we identify how screen entanglement entropies—the entanglement entropies among the degrees of freedom in the holographic space—encode information about the spacetimes. We discuss next how the screen entanglement entropies behave in a transition period in which the dominant component of the universe changes. We find an interesting theorem when the holographic screen is spacelike: the change of a screen entanglement entropy is always monotonic. The proof of this theorem is given in Appendix 2.6. If the holographic screen is timelike, no such theorem holds.

In Section 2.4, we study the structure of the holographic theory for general spacetimes, building on the results obtained earlier. In particular, we discuss how the holographic entanglement entropies for general spacetimes differ from those in AdS/CFT and how, nevertheless, the former reduce to the latter in an appropriate limit. We emphasize that the holographic entanglement entropies for cosmological spacetimes obey a volume law, rather than an area law, implying that the relevant holographic states are not ground states of local field theories. This is the case despite the fact that the dynamics of the holographic theory respects some sense of locality, indicated by the fact that the area of a leaf increases in a local manner on a holographic screen.

The Hilbert space of the theory is analyzed in Section 2.4 under two assumptions:

(i) The holographic theory has (effectively) a qubit degree of freedom per each volume of $4 \ln 2$ in Planck units. These degrees of freedom appear local at lengthscales larger than a microscopic cutoff l_c.

(ii) If a holographic state represents a semiclassical spacetime, the area of an extremal surface anchored to the boundary of a region Γ on a leaf σ and contained in the causal region associated with σ represents the entanglement entropy of Γ in the holographic theory.

We find that these two assumptions strongly constrain the structure of the Hilbert space, although they do not determine it uniquely. There are essentially two possibilities:

Direct sum structure — Holographic states representing different semiclassical space-times $\mathcal{M}$ live in different Hilbert spaces $\mathcal{H}_{\mathcal{M}}$ even if these spacetimes have the same boundary space (or leaf) B

$$\mathcal{H}_B = \bigoplus_{\mathcal{M}} \mathcal{H}_{\mathcal{M}}. \tag{2.1}$$

In each Hilbert space $\mathcal{H}_{\mathcal{M}}$, the states representing the semiclassical spacetime comprise only a tiny subset of all the states—the vast majority of the states in $\mathcal{H}_{\mathcal{M}}$ do not allow for a semiclassical interpretation, which we call "firewall" states borrowing the terminology in Refs. [56, 57, 58]. In fact, the states allowing for a semiclassical spacetime interpretation do not even form a vector space—their superposition may lead to a firewall state if it involves a large number of terms, of order a positive power of $\dim \mathcal{H}_{\mathcal{M}}$. This is because a superposition involving such a large number of terms significantly alters the entanglement entropy structure, so under assumption (ii) above we cannot interpret the resulting state as a semiclassical state representing $\mathcal{M}$. In this picture, small excitations over spacetime $\mathcal{M}$ can be represented by standard linear operators acting on the (suitably extended) Hilbert space $\mathcal{H}_{\mathcal{M}}$, which can be trivially promoted to linear operators in $\mathcal{H}_B$.

Spacetime equals entanglement — Holographic states that represent different semiclassical spacetimes but have same boundary space B are all elements of a single Hilbert space $\mathcal{H}_B$. And yet, the number of independent microstates representing *each* of these spacetimes, $\mathcal{M}, \mathcal{M}', \mathcal{M}'', \cdots$, is the dimension of $\mathcal{H}_B$:

$$|\Psi_i^{\mathcal{M}}\rangle, \ |\Psi_{i'}^{\mathcal{M}'}\rangle, \ |\Psi_{i''}^{\mathcal{M}''}\rangle, \ \cdots \in \mathcal{H}_B; \qquad i, i', i'', \cdots = 1, \cdots, \dim \mathcal{H}_B, \tag{2.2}$$

which implies that the microstates representing different spacetimes are not independent. This picture arises if we require the converse of assumption (ii) and is called "spacetime equals entanglement" [54]: if a holographic state has the form of entanglement entropies corresponding to a certain spacetime, then the state indeed represents that spacetime. The structure of Eq. (2.2) is then obtained because arbitrary unitary transformations acting in each cutoff size cell in B do not change the entanglement entropies, implying that the number of microstates for any geometry is $\dim \mathcal{H}_B$ (so they span a basis of $\mathcal{H}_B$). Despite the intricate structure of the states, this picture admits the standard many worlds interpretation for classical spacetimes, as shown in Ref. [54]. Small excitations over spacetime are represented by non-linear/state-dependent operators, along the lines of Ref. [59] (see also [60, 61, 62]), since a superposition of background spacetimes may lead to another spacetime, so that operators representing excitations must know the entire quantum state they act on.

We note that a dichotomy similar to the one described above was discussed earlier in Ref. [59], but the interpretation and the context in which it appears here are distinct. First,

the state-dependence of the operators representing excitations in the second scenario (as well as that of the time evolution operator) becomes relevant when the boundary space is involved in the dynamics as in the case of cosmological spacetimes. Hence, this particular state-dependence need not persist in the AdS/CFT limit. This does not imply anything about the description of the interior a black hole in the CFT. It is possible that the CFT does not provide a semiclassical description of the black hole interior, i.e. it gives only a distant description. Alternatively, there may be a way of obtaining a state-dependent semiclassical description of the black hole interior within a CFT, as envisioned in Ref. [59]. We are agnostic about this issue.

Second, Ref. [59] describes the dichotomy as state-dependence vs. firewalls. Our picture, on the other hand, does not have a relation with firewalls because the following two statements apply to *both* the direct sum and spacetime equals entanglement pictures:

- Most of the states in the Hilbert space, e.g. in the Haar measure, are firewalls in the sense that they do not represent smooth semiclassical spacetimes, which require special entanglement structures among the holographic degrees of freedom.

- The fact that most of the states are firewalls does not mean that these states are realized as a result of standard time evolution, in which the volume of the boundary space increases in time. In fact, the direct sum picture even has a built-in mechanism of eliminating firewalls through time evolution, as we will see in Section 2.4.[1]

Rather, the real tension is between the linearity/state-independence of operators representing observables (including the time evolution operator) and the spacetime equals entanglement hypothesis, i.e. the hypothesis that if a holographic state has entanglement entropies corresponding to a semiclassical spacetime, then the state indeed represents that spacetime. If we insist on the linearity of observables, we are forced to take the direct sum picture; if we adopt the spacetime equals entanglement hypothesis, then we must give up linearity.

Our analysis in Section 2.4 also includes the following. In Section 4.2, we discuss bulk reconstruction from a holographic state, which suggests that the framework provides a distant description for a dynamical black hole. In Section 2.4, we consider how the theory encodes information about spacetime outside the causal region of a leaf, which is needed for autonomous time evolution. Our analysis suggests a strengthened covariant entropy bound: the entropy on the *union* of two light sheets (future-directed ingoing and past-directed outgoing) of a leaf is bounded by the area of the leaf divided by 4. This bound is stronger than the original bound in Ref. [21], which says that the entropy on *each* of the two light sheets is bounded by the area divided by 4. In Section 2.4, we analyze properties of time evolution, in particular a built-in mechanics of eliminating firewalls in the direct sum picture and the required non-linearity of the time evolution operator in the spacetime equals entanglement

---

[1]This is natural because any dynamics leading to classicalization selects only a very special set of states as the result of time evolution: states interpreted as a superposition of a small number of classical worlds, where small means a number (exponentially) smaller than the dimension of the full microscopic Hilbert space.

picture. In Sections 2.4 and 2.4, we discuss how our framework may reduce to AdS/CFT and string theory in an asymptotically Minkowski background in the appropriate limits. We argue that the dynamics of these theories (in which the boundaries are sent to infinity) describe that of the general holographic theory modded out by "vacuum degeneracies" relevant for the dynamics of the boundaries and the exteriors.

In Section 3.4, we devote our final discussion to the issue of selecting a state. In general, specifying a system requires selection conditions on a state in addition to determining the theory. To address this issue in quantum gravity, we need to study the problem of time [63, 64]. We discuss possible signals from a past singularity or past null infinity, closed universes and "fine-tuning" of states, and selection conditions for the string theory landscape [65, 66, 67, 68], especially the scenario called the "static quantum multiverse" [69]. While our discussion in this section is schematic, it allows us to develop intuition about how quantum gravity might work at the fundamental level when applied to the real world.

Throughout the paper, we adopt the Schrödinger picture of quantum mechanics and take the Planck length to be unity, $l_{\rm P} = 1$. When the semiclassical picture is applicable, we assume the null and causal energy conditions to be satisfied. These impose the conditions $\rho \geq -p$ and $|\rho| \geq |p|$, respectively, on the energy density ρ and pressure p of an ideal fluid component. The equation of state parameter $w = p/\rho$, therefore, takes a value in the range $|w| \leq 1$.

2.2   Holography and Quantum Gravity

The holographic principle states that quantum mechanics of a system with gravity can be formulated as a non-gravitational theory in spacetime with dimension one less than that in the gravitational description. The covariant entropy bound, or Bousso bound, [21] suggests that this holographically reduced—or "boundary"—spacetime may be identified as a hypersurface in the original gravitational spacetime determined by a collection of light rays. Specifically, it implies that the entropy on a null hypersurface generated by a congruence of light rays terminating at a caustic or singularity is bounded by its largest cross sectional area $\mathcal{A}$; in particular, the entropy on each side of the largest cross sectional surface is bounded by $\mathcal{A}/4$ in Planck units.[2] It is therefore natural to consider that, for a fixed gravitational spacetime, the holographic theory lives on a hypersurface—called the holographic screen—on which null hypersurfaces foliating the spacetime have the largest cross sectional areas [42].

This procedure of erecting a holographic screen has a large ambiguity, presumably reflecting a large freedom in fixing the redundancy of the gravitational description associated with the holographic principle. A particularly useful choice advocated in Refs. [40, 43, 70] is to adopt an "observer centric reference frame." Let the origin of the reference frame follow a timelike curve $p(\tau)$ which passes through a fixed spacetime point p_0 at $\tau = 0$, and consider

---

[2]We will conjecture a stronger bound in Section 2.4.
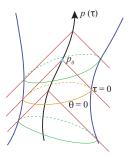
Figure 2.1: For a fixed semiclassical spacetime, the holographic screen is a hypersurface obtained as the collection of codimension-2 surfaces (labeled by τ) on which the expansion of the light rays emanating from a timelike curve $p(\tau)$ vanishes, $\theta = 0$. This way of erecting the holographic screen automatically deals with the redundancy associated with complementarity. The ambiguity of choosing $p(\tau)$ reflects a large freedom in fixing the redundancy associated with holography.

the congruence of past-directed light rays emanating from p_0.[3] The expansion of the light rays θ satisfies

$$\frac{\partial \theta}{\partial \lambda} + \frac{1}{2}\theta^2 \leq 0, \tag{2.3}$$

where λ is the affine parameter associated with the light rays. This implies that the light rays emitted from p_0 focus toward the past (starting from $\theta = +\infty$ at $\lambda = 0_+$), and we may identify the apparent horizon, i.e. the codimension-2 surface with

$$\theta = 0, \tag{2.4}$$

to be an equal-time hypersurface—called a leaf—of a holographic screen. Repeating the procedure for all τ, we obtain a specific holographic screen, with the leaves parameterized by τ, corresponding to foliating the spacetime region accessible to the observer at $p(\tau)$; see Fig. 2.1. Such a foliation is consonant with the complementarity hypothesis [39], which asserts that a complete description of a system is obtained by referring only to the spacetime region that can be accessed by a single observer.

With this construction, we can view a quantum state of the holographic theory as living on a leaf of the holographic screen obtained in the above observer centric manner. We can then consider the collection of all possible quantum states on all possible leaves, obtained by

---

[3]In Refs. [40, 43, 70], $p(\tau)$ was chosen to be a timelike geodesic with τ being the proper time measured at $p(\tau)$. We suspect that this simplifies the time evolution operator in the holographic theory.

considering all timelike curves in all spacetimes. We take the view that a state of quantum gravity lives in the Hilbert space spanned by all of these states (together with other states that do not admit a full spacetime interpretation) [40, 43]. It is often convenient to consider a Hilbert space $\mathcal{H}_B$ spanned by the holographic states that live on the "same" boundary space B.[4] The relevant Hilbert space can then be written as

$$\mathcal{H} = \sum_B \mathcal{H}_B, \tag{2.5}$$

where the sum of Hilbert spaces is defined by[5]

$$\mathcal{H}_1 + \mathcal{H}_2 = \{v_1 + v_2 \,|\, v_1 \in \mathcal{H}_1, v_2 \in \mathcal{H}_2\}. \tag{2.6}$$

This formulation is not restricted to descriptions based on fixed semiclassical spacetime backgrounds. For example, we may consider a state in which macroscopically different spacetimes are superposed; in particular, this picture describes the eternally inflating multiverse as a state in which macroscopically different universes are superposed [40, 69]. The space in Eq. (2.5) is called the covariant Hilbert space with observer centric gauge fixing.

Recently, Bousso and Engelhardt have identified two special classes of holographic screens [44, 45]: if a portion of a holographic screen is foliated by marginally anti-trapped (trapped) surfaces, then that portion is called a past (future) holographic screen. Specifically, denoting the two future-directed null vector fields orthogonal to a portion of a leaf by k^a and l^a, with k^a being tangent to light rays emanating from $p(\tau)$, the expansion of the null geodesic congruence generated by l^a satisfies $\theta_l > 0$ and < 0 for past and future holographic screens, respectively. They proved, building on earlier works [71, 72, 73, 74], that the area of leaves $\mathcal{A}(\tau)$ monotonically increases (decreases) for a past (future) holographic screen:

$$\begin{cases} \theta_k = 0 \\ \theta_l \gtrless 0 \end{cases} \quad \Leftrightarrow \quad \frac{d}{d\tau}\mathcal{A}(\tau) \gtrless 0; \tag{2.7}$$

see Fig. 2.2. In many regular circumstances, including expanding FRW universes, the holographic screen is a past holographic screen, so that the area of the leaves monotonically increases, $d\mathcal{A}(\tau)/d\tau > 0$. In this paper we mostly focus on this case, and we interpret the area theorem in terms of the second law of thermodynamics applied to the Hilbert space of

---

[4]The exact way in which the boundary spaces are grouped into different B's is unimportant. For example, one can regard the boundary spaces having the same area $\mathcal{A}$ within some precision $\delta\mathcal{A}$ to be in the same B, or one can discriminate them further by their induced metrics. This ambiguity does not affect any of the results, unless one takes $\delta\mathcal{A}$ to be exponentially small in $\mathcal{A}$ or discriminates induced metrics with the accuracy of order the Planck length (which corresponds to resolving microstates of the spacetime).

[5]Unlike Ref. [43], here we do not assume specific relations between $\mathcal{H}_B$'s; for example, $\mathcal{H}_{B_1}$ and $\mathcal{H}_{B_2}$ for different boundary spaces B_1 and B_2 may not be orthogonal. Also, we have included in the sum over B the cases in which B is outside the semiclassical regime, i.e. the cases in which the holographic space does not correspond to a leaf of a holographic screen in a semiclassical regime. These issues will be discussed in Section 2.4.
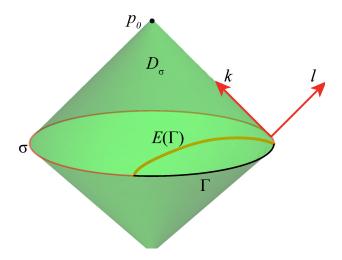
Figure 2.2: The congruence of past-directed light rays emanating from p_0 (the origin of the reference frame) has the largest cross sectional area on a leaf σ, where the holographic theory lives. At any point on σ, there are two future-directed null vectors orthogonal to the leaf: k^a and l^a. For a given region Γ of the leaf, we can find a codimension-2 extremal surface $E(\Gamma)$ anchored to the boundary $\partial\Gamma$ of Γ, which is fully contained in the causal region D_σ associated with σ.

Eq. (2.5). Moreover, in Ref. [46] it was proved that this area theorem holds locally on the holographic screen: the area of any fixed spatial portion of the holographic screen, determined by a vector field tangent to the holographic screen and normal to its leaves, increases monotonically in time. This implies that the dynamics of the holographic theory respects some notion of locality.

What is the structure of the holographic theory and how can we explore it? Recently, a conjecture has been made in Ref. [30] which relates geometries of general spacetimes in the gravitational description to the entanglement entropies of states in the holographic theory. This extends the analogous theorem/conjecture in the AdS/CFT context [16, 47, 48] to more general cases, allowing us to probe the holographic description of general spacetimes, including those that do not have an obvious spacetime boundary on which the holographic theory can live. In particular, Ref. [30] proved that for a given region Γ of a leaf σ, a codimension-2 extremal surface $E(\Gamma)$ anchored to the boundary $\partial\Gamma$ of Γ is fully contained in the causal region D_σ of σ:

D_σ : the domain of dependence of an interior achronal hypersurface whose only boundary is σ,

$$(2.8)$$

where the concept of the interior is defined so that a vector on σ pointing toward the interior takes the form $c_1 k^a - c_2 l^a$ with $c_1, c_2 > 0$ (see Fig. 2.2). This implies that the normalized

area of the extremal surface $E(\Gamma)$

$$S(\Gamma) = \frac{1}{4}\|E(\Gamma)\|, \tag{2.9}$$

satisfies expected properties of entanglement entropy, such as strong subadditivity, so that it can be identified with the entanglement entropy of the region Γ in the holographic theory. Here, $\|x\|$ represents the area of x. If there are multiple extremal surfaces in D_σ for a given Γ, then we must take the one with the minimal area.

In the rest of the paper, we study the holographic theory of quantum gravity for general spacetimes, adopting the framework described in this section. We first analyze FRW spacetimes and then discuss lessons learned from that analysis later.

2.3 Holographic Description of FRW Universes

In this section, we study the putative holographic description of $(3 + 1)$-dimensional FRW cosmological spacetimes:

$$ds^2 = -dt^2 + a^2(t)\left[\frac{dr^2}{1 - \kappa r^2} + r^2(d\psi^2 + \sin^2\psi\, d\phi^2)\right], \tag{2.10}$$

where $a(t)$ is the scale factor, and $\kappa < 0, = 0$ and > 0 for open, flat and closed universes, respectively. The Friedmann equation is given by

$$\left(\frac{\dot{a}}{a}\right)^2 + \frac{\kappa}{a^2} = \frac{8\pi}{3}\rho, \tag{2.11}$$

where the dot represents t derivative. Here, we include the energy density from the cosmological constant as a component in ρ having the equation of state parameter $w = -1$.

As discussed in the previous section, we describe the system as viewed from a reference frame whose origin follows a timelike curve $p(\tau)$, which we choose to be at $r = 0$. The holographic theory then lives on the holographic screen, an equal-time slice of which is an apparent horizon: a codimension-2 surface on which the expansion of the light rays emanating from $p(\tau)$ for a fixed τ vanishes. Under generic conditions, this horizon is always at a finite distance

$$r = \frac{1}{\sqrt{\dot{a}^2(t_*) + \kappa}} \equiv r_{\text{AH}}(t_*) < \infty, \tag{2.12}$$

where t_* is the FRW time on the horizon. Note that the symmetry of the setup makes the FRW time the same everywhere on the apparent horizon, and for an open universe, $\dot{a}(t_*) > \sqrt{-\kappa}$ is satisfied for values of τ before $p(\tau)$ hits the big crunch. For flat and open universes, we find that this surface is always marginally anti-trapped, i.e. a leaf of a past holographic screen, as long as the universe is initially expanding. On the other hand, for a closed universe the surface can change from marginally anti-trapped to marginally trapped

as τ increases, implying that the holographic screen may be a past holographic screen only until certain time τ. In this section, we focus our attention on initially expanding flat and open universes. Closed universes will be discussed in Section 3.4.

Below, we study entanglement entropies for subregions in the holographic theory—screen entanglement entropies—adopting the conjecture of Ref. [30]. Here we focus on studying the properties of these entropies, leaving their detailed interpretation for later. We first discuss "stationary" aspects of screen entanglement entropies, concentrating on states representing spacetime in which the expansion of the universe is dominated by a single component in the Friedmann equation. We study how screen entanglement entropies encode the information about the spacetime the state represents. We then analyze dynamics of screen entanglement entropies during a transition period in which the dominant component changes. Implications of these results in the broader context of the holographic description of quantum gravity will be discussed in the next section.

Holographic dictionary for FRW universes

Consider a Hilbert space $\mathcal{H}_B$ spanned by a set of quantum states living in the same codimension-2 boundary surface B. As mentioned in footnote 4, the definition of the boundary surface being the same has an ambiguity. For our analysis of states representing FRW spacetimes, we take the boundary B to be specified by its area $\mathcal{A}_B$ (within some precision $\delta\mathcal{A}_B$ that is not exponentially small in $\mathcal{A}_B$). In this subsection, we focus on a single Hilbert space $\mathcal{H}_* \in \{\mathcal{H}_B\}$ specified by a fixed (though arbitrary) boundary area $\mathcal{A}_*$.

Consider FRW universes with $\kappa \leq 0$ having vacuum energy ρ_Λ and filled with varying ideal fluid components.[6] For every universe with

$$\rho_\Lambda < \frac{3}{2\mathcal{A}_*}, \tag{2.13}$$

there is an FRW time t_* at which the area of the leaf of the past holographic screen is $\mathcal{A}_*$; see Fig. 2.3. This is because the area of the leaf of the past holographic screen is monotonically increasing [44], and the final (asymptotic) value of the area is given by

$$\mathcal{A}_\infty = \begin{cases} \frac{3}{2\rho_\Lambda}, & \text{for } \rho_\Lambda > 0, \\ +\infty, & \text{for } \rho_\Lambda \leq 0. \end{cases} \tag{2.14}$$

Any quantum state representing the system at any such moment is an element of $\mathcal{H}_*$. A question is what features of the holographic state encode information about the universe it represents.

To study this problem, we perform the following analysis. First, given an FRW universe specified by the history of the energy density of the universe, $\rho(t)$, we determine the FRW

---

[6]The ρ_Λ here represents the energy density of a (local) minimum of the potential near which fields in the FRW universe in question take values. In fact, string theory suggests that there is no absolutely stable de Sitter vacuum in full quantum gravity; it must decay, at least, before the Poincaré recurrence time [66].
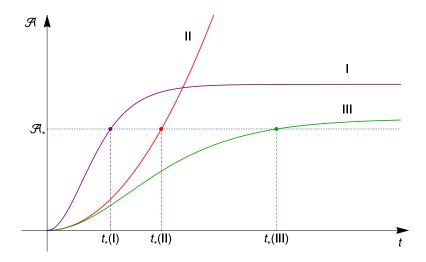
Figure 2.3: Various FRW universes, $\mathrm{I}, \mathrm{II}, \mathrm{III}, \cdots$, have the same boundary area $\mathcal{A}_*$ at different times, $t_*(\mathrm{I}), t_*(\mathrm{II}), t_*(\mathrm{III}), \cdots$. Quantum states representing universes at these moments belong to Hilbert space $\mathcal{H}_*$ specified by the value of the boundary area.

time t_* at which the apparent horizon σ_*, identified as a leaf of the past holographic screen, has the area $\mathcal{A}_*$:

$$\left\{ \begin{array}{l} \rho(t) \\ \mathcal{A}_* \end{array} \right. \;\rightarrow\; t_*, \tag{2.15}$$

where we assume Eq. (2.13). We then consider a spherical cap region of the leaf σ_* specified by an angle γ $(0 \leq \gamma \leq \pi)$:

$$L(\gamma): \quad t = t_*, \quad r = r_{\mathrm{AH}}(t_*), \quad 0 \leq \psi \leq \gamma, \tag{2.16}$$

where $r_{\mathrm{AH}}(t_*)$ is given by Eq. (2.12) (see Fig. 2.4), and determine the extremal surface $E(\gamma)$ which is codimension-2 in spacetime, anchored on the boundary of $L(\gamma)$, and fully contained inside the causal region D_{σ_*} associated with σ_*. According to Ref. [30], we interpret the quantity

$$S(\gamma) = \frac{1}{4}\|E(\gamma)\|, \tag{2.17}$$

to represent von Neumann entropy of the holographic state representing the region $L(\gamma)$, obtained after tracing out the complementary region on σ_*.

To determine the extremal surface $E(\gamma)$, it is useful to introduce cylindrical coordinates

$$\xi = r \sin \psi, \qquad z = r \cos \psi. \tag{2.18}$$

We find that the isometry of the FRW metric, Eq. (2.10), allows us to move the boundary on which the extremal surface is anchored, $\partial L(\gamma)$, on the $z = 0$ plane:

$$\partial L(\gamma): \quad t = t_*, \quad \xi = r_{\mathrm{AH}}(t_*) \sin \gamma \equiv \xi_{\mathrm{AH}}, \quad z = 0. \tag{2.19}$$
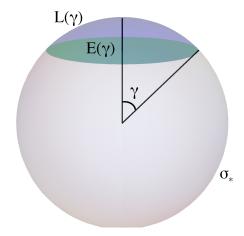
Figure 2.4: A region $L(\gamma)$ of the leaf σ_* is parameterized by an angle $\gamma : [0, \pi]$. The extremal surface $E(\gamma)$ anchored to its boundary, $\partial L(\gamma)$, is also depicted schematically. (In fact, $E(\gamma)$ bulges into the time direction.)

The surface to be extremized is then parameterized by functions $t(\xi)$ and $z(\xi)$ with the boundary conditions

$$t(\xi_{\mathrm{AH}}) = t_*, \qquad z(\xi_{\mathrm{AH}}) = 0, \tag{2.20}$$

and the area functional to be extremized is given by

$$2\pi \int_0^{\xi_{\mathrm{AH}}} a(t)\, \xi \sqrt{-\left(\frac{dt}{d\xi}\right)^2 + \frac{a^2(t)}{1 - \kappa(\xi^2 + z^2)}\left\{(1 - \kappa z^2) + (1 - \kappa \xi^2)\left(\frac{dz}{d\xi}\right)^2 + 2\kappa \xi z \frac{dz}{d\xi}\right\}}\, d\xi. \tag{2.21}$$

In all the examples we study (in this and next subsections), we find that the extremal surface does not bulge into the z direction. In this case, we can set $z = 0$ in Eq. (2.21) and find

$$\|E(\gamma)\| = \operatorname*{ext}_{t(\xi)} \left[2\pi \int_0^{r_{\mathrm{AH}}(t_*)\sin\gamma} a(t)\, \xi \sqrt{-\left(\frac{dt}{d\xi}\right)^2 + \frac{a^2(t)}{1 - \kappa \xi^2}}\, d\xi \right]. \tag{2.22}$$

The analysis described above is greatly simplified if the expansion of the universe is determined by a single component in the Friedmann equation, i.e. a single fluid component with the equation of state parameter w or negative spacetime curvature. We thus focus on the case in which the expansion is dominated by a single component in (most of) the region probed by the extremal surfaces. In realistic FRW universes this holds for almost all t, except for a few Hubble times around when the dominant component changes from one to another. Discussion about a transition period in which the dominant component changes will be given in the next subsection.

A flat FRW universe filled with a single fluid component

Suppose the expansion of the universe is determined dominantly by a single ideal fluid component with w. The scale factor is then given by

$$a(t) = c\,t^{\frac{2}{3(1+w)}}, \tag{2.23}$$

where c is a constant, and the metric in the region $r \leq r_{\mathrm{AH}}$ takes the form

$$ds^2 = -dt^2 + c^2\, t^{\frac{4}{3(1+w)}} \left[dr^2 + r^2(d\psi^2 + \sin^2\psi\, d\phi^2)\right], \tag{2.24}$$

where we have used the fact that $|\kappa\, r_{\mathrm{AH}}^2| \ll 1$. In this case, we find that the $\mathcal{A}_*$ dependence of screen entanglement entropy S_Γ for an arbitrarily shaped region Γ on σ_*—specified as a region on the ψ-ϕ plane—is given by

$$S_\Gamma = \tilde{S}_\Gamma \mathcal{A}_*, \tag{2.25}$$

where $\tilde{S}_\Gamma$ does not depend on $\mathcal{A}_*$. This can be seen in the following way.

Consider the causal region D_{σ_*} associated with σ_*. For certain values of w (i.e. $w \geq 1/3$), D_{σ_*} hits the big bang singularity. It is thus more convenient to discuss the "upper half" of the region:

$$D_{\sigma_*}^+ = \{p \in D_{\sigma_*} \mid t(p) \geq t_*\}. \tag{2.26}$$

In an expanding universe, the extremal surface anchored on the boundary of a region Γ on σ_* is fully contained in this region. Now, by performing t_*-dependent coordinate transformation

$$\rho = \frac{2}{3(1+w)} c\, t_*^{-\frac{1+3w}{3(1+w)}} r, \tag{2.27}$$

$$\eta = \frac{2}{3(1+w)} \left[\left(\frac{t}{t_*}\right)^{\frac{1+3w}{3(1+w)}} - 1\right], \tag{2.28}$$

the region $D_{\sigma_*}^+$ is mapped into

$$0 \leq \eta \leq 1, \qquad 0 \leq \rho \leq 1 - \eta, \tag{2.29}$$

and the metric in $D_{\sigma_*}^+$ is given by

$$ds^2\big|_{D_{\sigma_*}^+} = \frac{\mathcal{A}_*}{4\pi} \left(\frac{1+3w}{2}\eta + 1\right)^{\frac{4}{1+3w}} \left[-d\eta^2 + d\rho^2 + \rho^2(d\psi^2 + \sin^2\psi\, d\phi^2)\right], \tag{2.30}$$

where

$$\mathcal{A}_* = 9\pi(1+w)^2 t_*^2. \tag{2.31}$$

Since $\mathcal{A}_*$ appears only as an overall factor of the metric in Eqs. (2.29, 2.30), we conclude that the $\mathcal{A}_*$ dependence of $S_\Gamma \propto \|E_\Gamma\|$ is only through an overall proportionality factor, as in Eq. (2.25).

Due to the scaling in Eq. (2.25), it is useful to consider an object obtained by dividing S_Γ by a quantity that is also proportional to $\mathcal{A}_*$. We find it convenient to define the quantity

$$Q_\Gamma \equiv \frac{S_\Gamma}{V_\Gamma/4}, \tag{2.32}$$

where V_Γ is the (2-dimensional) "volume" of the region Γ or its complement $\bar{\Gamma}$ on the boundary surface σ_*, whichever is smaller. This quantity is independent of $\mathcal{A}_*$, and hence t_*. For the spherical region of Eq. (2.16), we find

$$Q(\gamma) = \frac{S(\gamma)}{V(\gamma)/4} = \frac{\|E(\gamma)\|}{V(\gamma)}, \tag{2.33}$$

where

$$V(\gamma) = \frac{1}{2}\left\{1 - \mathrm{sgn}\left(\frac{\pi}{2} - \gamma\right)\cos\gamma\right\}\mathcal{A}_*. \tag{2.34}$$

An explicit expression for $Q(\gamma)$ is given by

$$Q(\gamma) = \frac{1}{1 - \mathrm{sgn}(\frac{\pi}{2} - \gamma)\cos\gamma}\, \underset{f(x)}{\mathrm{ext}}\left[\int_0^{\sin\gamma} x\, f^{\frac{4}{1+3w}}\sqrt{1 - \left(\frac{2}{1+3w}\right)^2\left(\frac{df}{dx}\right)^2}\, dx\right], \tag{2.35}$$

where the extremization with respect to function $f(x)$ is performed with the boundary condition

$$f(\sin\gamma) = 1, \tag{2.36}$$

and we have used the fact that the extremal surface does not bulge into the z direction in the cylindrical coordinates of Eq. (4.87). From the point of view of the holographic theory, Q_Γ represents the amount of entanglement entropy per degree of freedom as viewed from the smaller of Γ and $\bar{\Gamma}$. As we will discuss in Section 2.4, the fact that this is a physically significant quantity has important implications for the structure of the holographic theory.

In Fig. 2.5, we plot $Q(\gamma)$ as a function of γ ($0 \le \gamma \le \pi/2$) for various values of w: -1 (vacuum energy), -0.98, -0.8, 0 (matter), $1/3$ (radiation), and 1. The value of $Q(\gamma)$ for $\pi/2 \le \gamma \le \pi$ is given by $Q(\gamma) = Q(\pi - \gamma)$. We find the following features:

- In the limit of a small boundary region, $\gamma \ll 1$, the value of $Q(\gamma)$ approaches unity regardless of the value of w:

$$Q_w(\gamma) \xrightarrow{\gamma \ll 1} 1. \tag{2.37}$$

  This implies that for a small boundary region, the entanglement entropy of the region is given by its volume in the holographic theory in Planck units:

$$S_w(\gamma) \xrightarrow{\gamma \ll 1} \frac{1}{4}V(\gamma). \tag{2.38}$$

  For larger γ ($\le \pi/2$), $Q(\gamma)$ becomes monotonically small as γ increases:

$$\frac{d}{d\gamma}Q_w(\gamma) < 0. \tag{2.39}$$
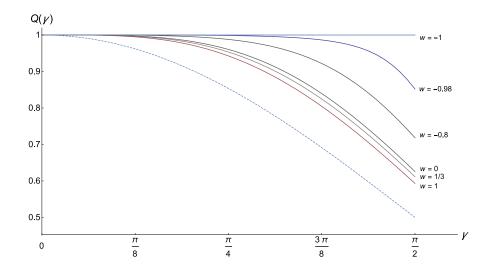
Figure 2.5: The value of $Q(\gamma)$ as a function of γ ($0 \leq \gamma \leq \pi/2$) for $w = -1$ (vacuum energy), -0.98, -0.8, 0 (matter), $1/3$ (radiation), and 1. The dotted line indicates the lower bound given by the flat space geometry, which can be realized in a curvature dominated open FRW universe.

The deviation of $Q(\gamma)$ from 1 near $\gamma = 0$ is given by

$$Q_w(\gamma) \overset{\gamma \ll 1}{=} 1 - c\,(1+w)\gamma^4 + \cdots, \tag{2.40}$$

where $c > 0$ is a constant that does not depend on w.

- For any fixed boundary region, γ, the value of $Q(\gamma)$ decreases monotonically in w:

$$\frac{d}{dw}Q_w(\gamma) < 0. \tag{2.41}$$

In particular, when w approaches -1 (from above), $Q(\gamma)$ becomes unity:

$$\lim_{w \to -1} Q_w(\gamma) = 1. \tag{2.42}$$

This implies that in the limit of de Sitter FRW ($w \to -1$), the state in the holographic theory becomes "randomly entangled" (i.e. saturates the Page curve [75]):[7]

$$\lim_{w \to -1} S_w(\gamma) = \frac{1}{4}V(\gamma). \tag{2.43}$$

---

[7]In the case of an exactly single component with $w = -1$, the expansion of light rays emanating from p_0, i.e. θ_k, becomes 0 only at infinite affine parameter λ. We view this as a result of mathematical idealization. A realistic de Sitter FRW universe is obtained by introducing an infinitesimally small amount of matter in addition to the $w = -1$ component, which avoids the above issue. The results obtained in this way agree with those by first taking $w > -1$ and then the limit $w \to -1$.
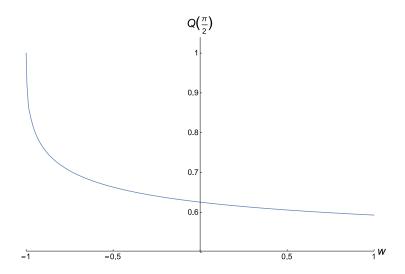
Figure 2.6: The value of $Q(\pi/2)$ as a function of w.

Note that $V(\gamma)$ is the smaller of the volume of $L(\gamma)$ and that of its complement on the leaf. The value of $Q(\pi/2)$ (the case in which $L(\gamma)$ is a half of the leaf) is plotted as a function of w in Fig. 2.6.

We will discuss further implications of these findings in Section 2.4.

We note that there are simple geometric bounds on the values of $Q_w(\gamma)$. This can be seen by adopting the maximin construction [30, 76]: the extremal surface is the one having the maximal area among all possible codimension-2 surfaces each of which is anchored on $\partial L(\gamma)$ and has minimal area on some interior achronal hypersurface bounded by σ. This implies that the area of the extremal surface, $\|E(\gamma)\|$, cannot be larger than the boundary volume $V(\gamma)$, giving $Q(\gamma) \leq 1$. Also, the extremal surface cannot have a smaller area than the codimension-2 surface that has the minimal area on a constant time hypersurface $t = t_*$: $\|E(\gamma)\| \geq \pi\{a(t_*)r_{\mathrm{AH}}(t_*)\sin\gamma\}^2$. Together, we obtain

$$\frac{\sin^2\gamma}{2\{1 - \mathrm{sgn}(\frac{\pi}{2} - \gamma)\cos\gamma\}} \leq Q_w(\gamma) \leq 1. \tag{2.44}$$

The lower edge of this range is depicted by the dashed line in Fig. 2.5. We find that the upper bound of Eq. (2.44) can be saturated with $w \to -1$, while the lower bound cannot with $|w| \leq 1$. If we formally take $w \to +\infty$, the lower bound can be reached. A fluid with $w > 1$, however, does not satisfy the causal energy condition (although it satisfies the null energy condition), so we do not consider such a component.

As a final remark, we show in Fig. 2.7 the shape of the extremal surface for $\gamma = \pi/2$ for the same values of w as in Fig. 2.5: -1, -0.98, -0.8, 0, 1/3, and 1. The horizontal axis is the cylindrical radial coordinate normalized by the apparent horizon radius, ξ/ξ_{AH}, and the
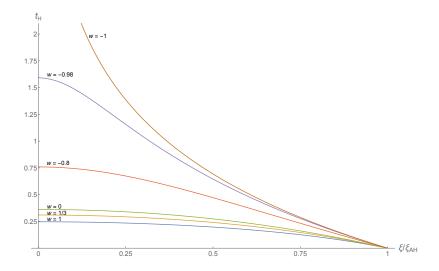
Figure 2.7: The shape of the extremal surfaces $E(\pi/2)$ for $w = -1, -0.98, -0.8, 0, 1/3$, and 1. The horizontal axis is the cylindrical radial coordinate normalized by the apparent horizon radius, ξ/ξ_{AH}, and the vertical axis is the Hubble time, t_{H}.

vertical axis is taken to be the Hubble time defined by

$$t_{\mathrm{H}} = \int_{t_*}^{t} \frac{\dot{a}(t)}{a(t)}\, dt = \frac{2}{3(1+w)} \ln \frac{t}{t_*}, \tag{2.45}$$

which reduces in the $w \to -1$ limit to the usual Hubble time $t_{\mathrm{H}} = H(t - t_*)$, where $H = \dot{a}/a$. We find that the extremal surface bulges into the future direction for any w. In fact, this occurs generally in an expanding universe and can be understood from the maximin construction: the scale factor increases toward the future, so that the area of the minimal area surface on an achronal hypersurface increases when the hypersurface bulges into the future direction in time. The amount of the bulge is $t_{\mathrm{H}} \approx O(1)$, except when $w \approx -1$. For $w \to -1$, the extremal surface probes $t_H \to +\infty$ as $\xi/\xi_{\mathrm{AH}} \to +0$, but its area is still finite, $\|E(\pi/2)\| \to \mathcal{A}_*/2$, as the surface becomes almost null in this limit.

An open FRW universe dominated by curvature

We now consider an open FRW universe dominated by curvature, i.e. the case in which the expansion of the universe is determined by the second term in the left-hand side of Eq. (2.11). This implies that the distance to the apparent horizon is much larger than the curvature length scale

$$\frac{-\kappa}{a^2(t)} \gg \frac{8\pi}{3} \rho(t) \quad \Longleftrightarrow \quad r_{\mathrm{AH}}(t) \gg \frac{1}{\sqrt{-\kappa}} \equiv r_{\mathrm{curv}}. \tag{2.46}$$

(Note that $\kappa < 0$ for an open universe.) As seen in Eqs. (2.11, 2.12), the value of $r_{\mathrm{AH}}(t)$ is determined by $\rho(t)$, which gives only a minor contribution to the expansion of the universe.

The scale factor is given by

$$a(t) = \sqrt{-\kappa}\, t. \tag{2.47}$$

The extremal surface can be found easily by noticing that the universe in this limit is a hyperbolic foliation of a portion of the Minkowski space: the coordinate transformation

$$\tilde{t} = t\sqrt{1 + \left(\sqrt{-\kappa}\, r\right)^2}, \tag{2.48}$$

$$\tilde{r} = \sqrt{-\kappa}\, t\, r, \tag{2.49}$$

leads to the Minkowski metric $ds^2 = -d\tilde{t}^2 + d\tilde{r}^2 + \tilde{r}^2(d\psi^2 + \sin^2\psi\, d\phi^2)$. The extremal surface is thus a plane on a constant $\tilde{t}$ hypersurface, which in the FRW (cylindrical) coordinates is given by

$$t_{\mathrm{H}} \approx \ln\frac{1}{\xi/\xi_{\mathrm{AH}}} \qquad (0 \le \xi/\xi_{\mathrm{AH}} \le 1), \tag{2.50}$$

where $\xi_{\mathrm{AH}} = r_{\mathrm{AH}}(t_*)\sin\gamma$, and t_{H} is the Hubble time

$$t_{\mathrm{H}} = \int_{t_*}^{t} \frac{\dot{a}(t)}{a(t)}\, dt = \ln\frac{t}{t_*}. \tag{2.51}$$

The resulting $Q(\gamma)$ is

$$Q(\gamma) \approx \frac{\sin^2\gamma}{2\{1 - \mathrm{sgn}(\frac{\pi}{2} - \gamma)\cos\gamma\}}. \tag{2.52}$$

This, in fact, saturates the lower bound in Eq. (2.44), plotted as the dashed line in Fig. 2.5.

Dynamics of screen entanglement entropies in a transition

Let us consider the evolution of an FRW universe. From the holographic theory point of view, it is described by a time-dependent state $|\Psi(\tau)\rangle$ living on $\sigma(\tau)$. Because of the area theorem of Refs. [44, 45], we can take τ to be a monotonic function of the leaf area, leading to

$$\frac{d}{d\tau}\mathcal{A}(\tau) > 0, \tag{2.53}$$

where $\mathcal{A}(\tau) \equiv \|\sigma(\tau)\|$. This evolution involves a change in the number of (effective) degrees of freedom, $\mathcal{A}(\tau)/4$, as well as that of the structure of entanglement on the boundary, $Q_\Gamma(\tau)$. For the latter, we mostly consider $Q(\gamma, \tau)$ associated with a spherical cap region $\Gamma = L(\gamma)$. A natural question is if a statement similar to Eq. (2.53) applies for screen entanglement entropies:

$$\frac{d}{d\tau}S(\gamma, \tau) \overset{?}{>} 0. \tag{2.54}$$

Here,

$$S(\gamma, \tau) = Q(\gamma, \tau)\frac{V(\gamma, \tau)}{4}, \tag{2.55}$$

with

$$V(\gamma, \tau) = \frac{1}{2}\left\{1 - \mathrm{sgn}\left(\frac{\pi}{2} - \gamma\right)\cos\gamma\right\}\mathcal{A}(\tau), \qquad (2.56)$$

being the smaller of the boundary volumes of $L(\gamma)$ and its complement.

There are some cases in which we can show that the relation in Eq. (2.54) is indeed satisfied. Consider, for example, a flat FRW universe filled with various fluid components having differing equations of states: w_i $(i = 1, 2, \cdots)$. As time passes, the dominant component of the universe changes from one having larger w to one having smaller w successively. This implies that $Q(\gamma, \tau)$ monotonically increases in time, so that Eq. (2.53) indeed implies Eq. (2.54) in this case. Another interesting case is when the holographic screen is spacelike. In this case, we can prove that the time dependence of $S(\gamma, \tau)$ is monotonic; see Appendix 2.6. In particular, if we have a spacelike past holographic screen (which occurs for $w > 1/3$ in a single-component dominated flat FRW universe), then the screen entanglement entropy for an arbitrary region increases in time: $dS_\Gamma(\tau)/d\tau > 0$.

What happens if the holographic screen is timelike? One might think that there is an obvious argument against the inequality in Eq. (2.54). Suppose the expansion of the early universe is dominated by a fluid component with w. Suppose at some FRW time t_0 this component is converted into another fluid component having a different equation of state parameter w', e.g. by reheating associated with the decay of a scalar condensate. If $w' > w$, then the Q value after the transition is smaller than that before

$$Q_{w'}(\gamma) - Q_w(\gamma) < 0. \qquad (2.57)$$

One may think that this can easily overpower the increase of $S(\gamma, \tau)$ from the increase of the area: $d\mathcal{A}(\gamma, \tau)/d\tau > 0$ [46]. In particular, if w is close to -1, then the increase of the area before the transition is very slow, so that the effect of Eq. (2.57) would win over that of the area increase. However, as depicted in Fig. 2.7, when $w \approx -1$ the extremal surface bulges into larger t by many Hubble times. Hence the time between the moments in which Eq. (2.55) can be used before and after the transition becomes long, opening the possibility that the relevant area increase is non-negligible.

To make the above discussion more explicit, let us compare the values of the screen entanglement entropy $S(\gamma)$ corresponding to two extremal surfaces depicted in Fig. 2.8: the "latest" extremal surface that is fully contained in the w region and the "earliest" extremal surface fully contained in the w' region, each anchored to the leaves at FRW times t_* and t_0. This provides the most stringent test of the inequality in Eq. (2.54) that can be performed using the expression of Eq. (2.55) for fixed w's. The ratio of the entanglement entropies is given by

$$R_{w'w}(\gamma) \equiv \frac{S_{\mathrm{after}}(\gamma)}{S_{\mathrm{before}}(\gamma)} = \frac{Q_{w'}(\gamma)}{Q_w(\gamma)}\frac{t_0^2}{t_*^2} = \frac{Q_{w'}(\gamma)}{Q_w(\gamma)}e^{3(1+w)t_{\mathrm{H},w}}, \qquad (2.58)$$

where $t_{\mathrm{H},w}$ is the Hubble time between t_* and t_0, given by Eq. (2.45) with $t \to t_0$. In Fig. 2.9, we plot $R_w \equiv R_{1w}(\pi/2)$; setting $w' = 1$ minimizes the ratio. We find that this ratio can
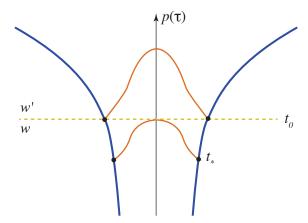
Figure 2.8: An FRW universe whose dominant component changes from w to w' at time t_0. Two surfaces depicted by orange lines are the latest extremal surface fully contained in the w region (bottom) and the earliest extremal surface fully contained in the w' region (top), each anchored to the leaves at t_* and t_0.

be smaller than 1 for $w \approx -1$. In fact, for $w \to -1$ we find the value obtained naively by assuming that the area does not change before the transition:

$$R_{-1} = \frac{Q_1\left(\frac{\pi}{2}\right)}{Q_{-1}\left(\frac{\pi}{2}\right)} = Q_1\left(\frac{\pi}{2}\right), \tag{2.59}$$

although for $w = -1$ there is no such thing as the latest extremal surface that is fully contained in the region before the transition (since $t_{\mathrm{H},-1} = +\infty$).

   This analysis suggests that screen entanglement entropies can in fact drop if the system experiences a rapid transition induced by some dynamics,[8] although the instantaneous transition approximation adopted above is not fully realistic. Of course, such a drop is expected to be only a temporary phenomenon—because of the area increase after the transition, the entropy generally returns back to the value before the transition in a characteristic dynamical timescale and then continues to increase afterward. We expect that the relation in Eq. (2.54) is valid in a coarse-grained sense

$$\frac{d}{d\tau}\bar{S}(\gamma,\tau) > 0; \qquad \bar{S}(\gamma,\tau) = \frac{1}{\tau_c}\int_{\tau}^{\tau+\tau_c} S(\gamma,\tau')\,d\tau', \tag{2.60}$$

but not "microscopically" in general. Here, τ_c must be taken sufficiently larger than the characteristic dynamical timescale, the Hubble time for an FRW universe.

---

[8]This does not mean that the second law of thermodynamics is violated. The entropy discussed here is the von Neumann entropy of a significant portion (half) of the whole system, which can deviate from the thermodynamic entropy of the region when the system experiences a rapid change.
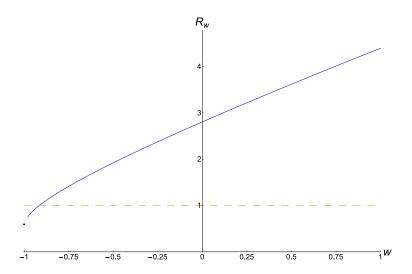
Figure 2.9: The ratio of the screen entanglement entropies, $R_w = R_{1w}(\pi/2)$, before and after the transition from a universe with the equation of state parameter w to that with $w' = 1$, obtained from Figs. 2.6 and 2.7 using Eq. (2.58). The dot at $w = -1$ represents $R_{-1} = R_{1-1}(\pi/2)$ obtained in Eq. (2.59).

For further illustration, we perform numerical calculations for how the area of a leaf hemisphere, $\|L(\pi/2, t)\|$, and the associated screen entanglement entropy, calculated using $S(\pi/2, t) = \|E(\pi/2, t)\|/4$, evolve in time during transitions from a $w = -1$ to a $w' = 0$ flat FRW universe. Here, we take the FRW time t as the time parameter. For this purpose, we consider a scalar field ϕ having a potential $V(\phi)$ that has a flat portion and a well, with the initial value of ϕ being in the flat portion. We first note that a transformation of the potential of the form

$$V(\phi) \to V'(\phi) = \epsilon^2 V(\phi), \tag{2.61}$$

leads to rescalings of the scalar field, $\phi(t)$, and the scale factor, $a(t)$, obtained as the solutions to the equations of motion:

$$\phi'(t) = \phi(\epsilon t), \qquad a'(t) = a(\epsilon t). \tag{2.62}$$

Plugging these in Eq. (2.22), we find that the area functionals before and after the transformation Eq. (2.61) are related by simple rescaling $t \to t/\epsilon$ and $\xi \to \xi/\epsilon$, so that

$$\left\| E'\left(\frac{\pi}{2}, t\right) \right\| = \frac{1}{\epsilon^2} \left\| E\left(\frac{\pi}{2}, \frac{t}{\epsilon}\right) \right\|. \tag{2.63}$$

These scaling properties imply that the leaf hemisphere area and the screen entanglement entropy for the transformed potential are read off from those for the untransformed one by

$$\left\| L'\left(\frac{\pi}{2}, t\right) \right\| = \frac{1}{\epsilon^2} \left\| L\left(\frac{\pi}{2}, \frac{t}{\epsilon}\right) \right\|, \qquad \left\| S'\left(\frac{\pi}{2}, t\right) \right\| = \frac{1}{\epsilon^2} \left\| S\left(\frac{\pi}{2}, \frac{t}{\epsilon}\right) \right\|. \tag{2.64}$$

We therefore need to be concerned only with the shape of the potential, not its overall scale. In particular, we can always be in the semiclassical regime by performing a transformation with $\epsilon \ll 1$.

In Fig. 2.10, we show the results of our calculations for "steep" and "broad" potentials. The explicit forms of the potentials are given by

$$V(\phi) = 1 - e^{-k(\phi-\phi_0)^2} + s(\phi - \phi_0)\tanh(p(\phi-\phi_0)), \tag{2.65}$$

with

$$\text{Steep}: \quad k = 5000, \quad s = 0.01, \quad p = 20, \quad \phi_0 = 0.045, \tag{2.66}$$
$$\text{Broad}: \quad k = 25, \quad s = 0.01, \quad p = 2, \quad \phi_0 = 0.5, \tag{2.67}$$

although their detailed forms are unimportant. For the steep potential, plotted in Fig. 2.10(a), we show the time evolutions of $\phi(t)$, $\|L(\pi/2, t)\|$, and $S(\pi/2, t)$ in Figs. 2.10(b)–(d) for the initial conditions of $\phi(0) = \dot{\phi}(0) = 0$ and $a(0) = 0.01$. The same are shown for the broad potential, Fig. 2.10(e), in Figs. 2.10(f)–(h) for the initial conditions of $\phi(0) = \dot{\phi}(0) = 0$ and $a(0) = 10^{-11}$. In either cases, the leaf hemisphere area increases monotonically while the screen entanglement entropy experiences drops as the field oscillates around the minimum. The fractional drops from the first, second, and third peaks are $\simeq 1.3\%$, 0.9%, and 0.6%, respectively, for the steep potential and $\simeq 2.5\%$, 1.6%, and 1.2%, respectively, for the broad potential.

We thus find that screen entanglement entropies may decrease in a transition period. The interpretation of this result, however, needs care. Since the system is far from being in a "vacuum" during a transition, true entanglement entropies for subregions in the holographic theory may have contributions beyond that captured by the simple formula of Eq. (2.17). This would require corrections of the formula, possibly along the lines of Refs. [28, 29, 77], and with such corrections the drop of the entanglement entropy we have found here might disappear. We leave a detailed study of this issue to future work.

2.4   Interpretation: Beyond AdS/CFT

The entanglement entropies in the holographic theory of FRW universes seen so far show features different from those in CFTs of the AdS/CFT correspondence. Here we highlight these differences and see how properties characteristic to local CFTs are reproduced when bulk spacetime becomes asymptotically AdS. We also discuss implications of our findings for the structure of the holographic theory. In particular, we discuss the structure of the Hilbert space for quantum gravity applicable to general spacetimes. While we cannot determine the structure uniquely, we can classify possibilities under certain general assumptions. The issues discussed include bulk reconstruction, the interior and exterior regions of the leaf, and time evolution in the holographic theory.

(a) Steep potential.

(e) Broad potential.

(b) $\phi(t)$ for the steep potential.

(f) $\phi(t)$ for the broad potential.

(c) $\|L(\pi/2, t)\|$ for the steep potential.

(g) $\|L(\pi/2, t)\|$ for the broad potential.

(d) $S(\pi/2, t)$ for the steep potential.

(h) $S(\pi/2, t)$ for the broad potential.
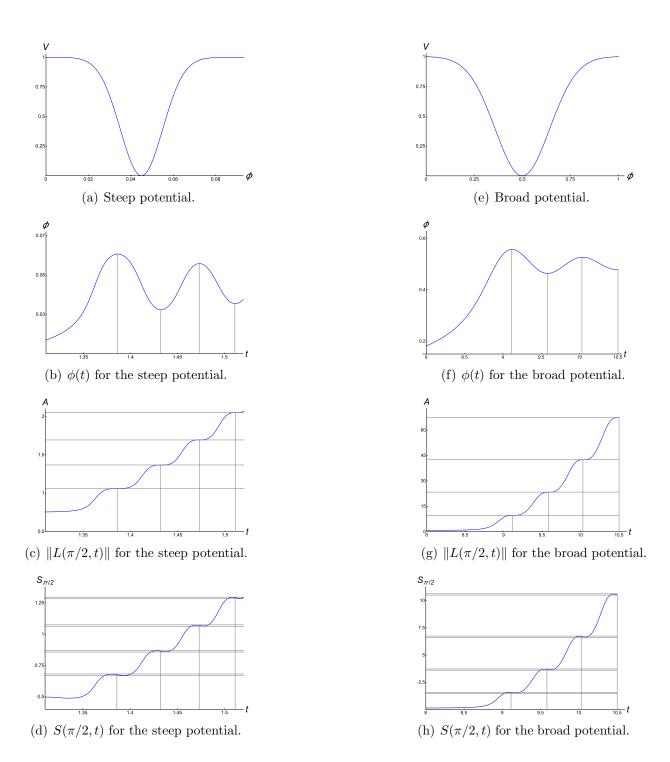
Figure 2.10: A steep potential (a) leading to the time evolution of the scalar field (b), the area of a leaf hemisphere (c), and the screen entanglement entropy (d). The same for a broad potential (e)–(h).

Volume/area law for screen entanglement entropies

One can immediately see that holographic entanglement entropies for FRW universes have two features that are distinct from those in AdS/CFT. First, unlike entanglement entropies in CFTs, the holographic entanglement entropies for FRW universes are finite for a finite value of $\mathcal{A}_*$. Second, as seen in Section 2.3, e.g. Eq. (2.25), these entropies obey a volume law, rather than an area law.[9] (Note that $\mathcal{A}_*$ is a volume from the viewpoint of the holographic theory.) In particular, in the limit that the region Γ in the holographic theory becomes small, the entanglement entropy S_Γ becomes proportional to the volume V_Γ *with a universal coefficient*, which we identified as $1/4$ to match the conventional results in Refs. [9, 8, 10, 7, 6, 11]. (For a small enough subsystem, we expect that the entanglement entropy agrees with the thermal entropy.) From the bulk point of view, this is because the extremal surface E_Γ approaches Γ itself, so that $\|E_\Gamma\| \to V_\Gamma$.

What do these features mean for the holographic theory? The finiteness of the entanglement entropies implies that the cutoff length of the holographic theory is finite, i.e. the number of degrees of freedom in the holographic theory is finite, at least effectively. In particular, our identification implies that the holographic theory effectively has a qubit degree of freedom per volume of $4\ln 2$ (in Planck units), although it does not mean that the cutoff length of the theory is necessarily $\simeq \sqrt{4\ln 2}$. It is possible that the cutoff length is $l_c > \sqrt{4\ln 2}$ and that each cutoff size cell has $N = l_c^2/4\ln 2$ (> 1) degrees of freedom. In fact, since the string length l_s and the Planck length are related as $l_s^2 \sim n$, where n is the number of species in the low energy theory (including the moduli fields parameterizing the extra dimensions) [79], it seems natural to identify l_c and N as l_s and n, respectively.

The volume law of the entangled entropies implies that a holographic state corresponding to an FRW universe is not a ground state of local field theory, which is known to satisfy an area law [80, 81]. This does not necessarily mean that the holographic theory for FRW universes must be nonlocal at lengthscales larger than the cutoff l_c; it might simply be that the relevant states are highly excited ones. In fact, the dynamics of the holographic theory is expected to respect some aspects of locality as suggested by the fact that the area theorem applies locally on a holographic screen [46]. Of course, it is also possible that the holographic states for FRW universes are states of some special class of nonlocal theories.

The features of screen entangled entropies described here are not specific to FRW universes but appear in more general "cosmological" spacetimes, spacetimes in which the holographic screen is at finite distances and the gravitational dynamics is not frozen there. If the interior region of the holographic screen is (asymptotically) AdS, these features change. In this case, the same procedure as in Section 2.2 puts the holographic screen at spatial infinity (the AdS boundary), and the AdS geometry makes the area of the extremal surface anchored to the boundary $\partial\Gamma$ of a small region Γ on a leaf proportional to the area of $\partial\Gamma$ with a diverging coefficient: $\|E_\Gamma\| \sim \|\partial\Gamma\|/\epsilon$ ($\epsilon \to 0$). This makes the screen entanglement entropies obey an area law, so that the holographic theory can now be a ground state of a

---

[9] A similar property was argued for holographic entropies for Euclidean flat spacetime in Ref. [78].

local field theory. In fact, the theory is a CFT [14, 82, 15], consistent with the fact that we could take the cutoff length to zero, $l_c \sim \epsilon \to 0$.

The structure of holographic Hilbert space

We now discuss implications of our analysis for the structure of the Hilbert space of quantum gravity for general spacetimes. We work in the framework of Section 2.2; in particular, we assume that when a holographic state represents a semiclassical spacetime, the area of the extremal surface contained in D_σ and anchored to the boundary of a region Γ on a leaf represents the entanglement entropy of the region Γ in the holographic theory, Eq. (2.9). Note that this does not necessarily mean that the converse is true; there may be a holographic state in which entanglement entropies for subregions do not correspond to the areas of extremal surfaces in a semiclassical spacetime.

Consider a holographic state representing an FRW spacetime. The fact that for a small enough region Γ the area of the extremal surface anchored to its boundary approaches the volume of the region on the leaf, $\|E_\Gamma\| \to V_\Gamma$, implies that the degrees of freedom in the holographic theory are localized and that their density is, at least effectively, one qubit per $4 \ln 2$ (although the cutoff length of the theory may be larger than $\sqrt{4 \ln 2}$). We take these for granted as anticipated in the original holographic picture [37, 13]. This suggests that the number of holographic degrees of freedom which comprise FRW states on the leaf σ_* with area $\mathcal{A}_*$ is $\mathcal{A}_*/4$ *for any value of w.*

Given these assumptions, there are still a few possibilities for the structure of the Hilbert space of the holographic theory. Below we enumerate these possibilities and discuss their salient features.

Direct sum structure

Let us first assume that state vectors representing FRW universes with different w's are independent of each other, as indicated in the left portion of Fig. 2.11. This implies that the Hilbert space $\mathcal{H}_* \in \{\mathcal{H}_B\}$, which contains holographic states for FRW universes at times when the leaf area is $\mathcal{A}_*$, has a direct sum structure

$$\mathcal{H}_* = \bigoplus_w \mathcal{H}_{*,w}. \tag{2.68}$$

Here, we regard universes with the equation of state parameters falling in a range $\delta w \ll 1$ to be macroscopically identical, where δw is a small number that does not scale with $\mathcal{A}_*$.[10] This is the structure envisioned originally in Ref. [43].

What is the structure of $\mathcal{H}_{*,w}$? A natural possibility is that each of these subspaces has dimension

$$\ln \dim \mathcal{H}_{*,w} = \frac{\mathcal{A}_*}{4}. \tag{2.69}$$

---

[10]If we consider FRW universes with multiple fluid components, the corresponding spaces must be added in the right-hand side of Eq. (2.68).

$$\mathcal{H}_* \subset \sum_B \mathcal{H}_B$$

Direct Sum

$$\mathcal{H}_* = \bigoplus_w \mathcal{H}_{*,w}$$

Russian Doll
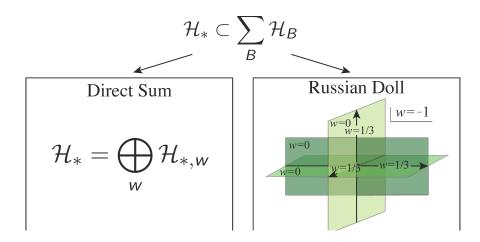
Figure 2.11: Possible structures of the Hilbert space $\mathcal{H}_*$ for a fixed boundary space B. In the direct sum structure (left), each semiclassical spacetime in D_{σ_*} has its own Hilbert space $\mathcal{H}_{*,w}$. The Russian doll structure (right) corresponds to the scenario of "spacetime equals entanglement," i.e. the entanglement entropies of the holographic degrees of freedom determine spacetime in D_{σ_*}. This implies that a superposition of exponentially many semiclassical spacetimes can lead to a different semiclassical spacetime.

This is motivated by the fact that arbitrary unitary transformations acting in each cutoff size cell do not change the structure of screen entanglement entropies, and they can lead to $e^{\mathcal{A}_*/4}$ independent holographic states that have the screen entanglement entropies corresponding to the FRW universe with the equation of state parameter w. If we regard all of these states as microstates for the FRW universe with w, then we obtain Eq. (2.69). This, however, does not mean that the holographic states representing the FRW universe with w comprise the Hilbert space $\mathcal{H}_{*,w}$. Since these states form a basis of $\mathcal{H}_{*,w}$, their superposition can lead to a state which has entanglement entropies far from those corresponding to the FRW universe with w. In fact, we can even form a state in which degrees of freedom in different cells are not entangled at all. This is a manifestation of the fact that entanglement cannot be represented by a linear operator.

This implies that states representing the semiclassical FRW universe are "preferred basis states" in $\mathcal{H}_{*,w}$, and their arbitrary linear combinations may lead to states that do not admit a semiclassical interpretation. We expect that these preferred axes are "fat": we have to superpose a large number of basis states, in fact exponentially many in $\mathcal{A}_*$, to obtain a state that is not semiclassical (because we need that many states to appreciably change the entanglement structure, as illustrated in a toy qubit model in Appendix 2.6). It is, however, true that most of the states in $\mathcal{H}_{*,w}$, including those having the entanglement entropy structure corresponding to a universe with another w, are states that do not admit a semiclassical spacetime interpretation. Drawing an analogy with the work in Refs. [56,

[57, 58], we may call them "firewall" states. In Section 2.4, we argue that these states are unlikely to be produced by standard semiclassical time evolution.

The dimension of $\mathcal{H}_*$ is given by

$$\ln \dim \mathcal{H}_* = \ln \sum_w e^{\frac{\mathcal{A}_*}{4}} \approx \frac{\mathcal{A}_*}{4} - \ln \delta w \simeq \frac{\mathcal{A}_*}{4}, \tag{2.70}$$

as expected from the covariant entropy bound (unless δw is exponentially small in $\mathcal{A}_*$, which we assume not to be the case). Small excitations over the FRW universes may be represented in suitably extended spaces $\mathcal{H}_{*,w}$. Since entropies associated with the excitations are typically subdominant in $\mathcal{A}_*$ [37, 83], they have only minor effects on the overall picture, e.g. Eq. (2.70). (Note that the excitations here do not contain the degrees of freedom attributed to gravitational, e.g. Gibbons-Hawking, radiation. These degrees of freedom are identified as the microscopic degrees of freedom of spacetimes, i.e. the vacuum degrees of freedom [84, 85, 86], which are already included in Eq. (2.69).) The operators representing the excitations can be standard linear operators acting on the Hilbert space $\mathcal{H}_*$, at least in principle.

We also mention the possibility that the logarithm of the number of independent states N_w representing the FRW universe with w is smaller than $\mathcal{A}_*/4$. For example, it might be given approximately by twice the entanglement entropy for a leaf hemisphere $S_w(\pi/2) = Q_w(\pi/2)\mathcal{A}_*/8$:

$$\ln N_w \approx Q_w\left(\frac{\pi}{2}\right)\frac{\mathcal{A}_*}{4}. \tag{2.71}$$

The basic picture in this case is not much different from that discussed above; for example, the difference of the values of $\ln \dim \mathcal{H}_*$ is higher order in $1/\mathcal{A}_*$ (although this possibility makes the issue of the equivalence condition for the boundary space label B nontrivial). We will not consider this case separately below.

Russian doll structure: spacetime equals entanglement

In the picture described above, the structures of $\mathcal{H}_{*,w}$'s are all very similar. Each of these spaces has the dimension of $\mathcal{A}_*/4$ and has $e^{\mathcal{A}_*/4}$ independent states that represent the FRW universe with a fixed value of w. An arbitrary linear combination of these states, however, is not necessarily a state representing the FRW universe with w. In the previous picture, we identified all such states as the firewall (or unphysical) states, but is it possible that some of these states, in fact, represent other FRW universes? In particular, is it possible that all the $\mathcal{H}_{*,w}$ spaces are actually the *same* space, i.e. $\mathcal{H}_{*,w_1} = \mathcal{H}_{*,w_2}$ for all $w_1 \neq w_2$?

A motivation to consider this possibility comes from the fact that if w does not by itself provide an independent label for states, then the $e^{\mathcal{A}_*/4}$ independent microstates for the FRW universe with a fixed w can form a basis for the configuration space of the $\mathcal{A}_*/4$ holographic degrees of freedom. This implies that we can superpose these states to obtain many—in fact $e^{\mathcal{A}_*/4}$—independent states that have the entanglement entropies corresponding

to the FRW universe with any $w' \neq w$, which we can identify as the states representing the FRW universe with w'.[11] In essence, this amounts to saying that the converse of the statement made at the beginning of this subsection is true: when a holographic state has the form of entanglement entropies corresponding to a certain spacetime, then the state indeed represents that spacetime. This scenario was proposed in Ref. [54] and called "spacetime equals entanglement." It is depicted in the right portion of Fig. 2.11.

One might think that the scenario does not make sense, since it implies that a superposition of classical universes can lead to a different classical universe. Wouldn't it make any reasonable many worlds interpretation of spacetime impossible? In Ref. [54], it was argued that this is not the case. First, for a given FRW universe, we expect that the space of its microstates is "fat"; namely, a superposition of less than $e^{O(\delta w \mathcal{A}_*)}$ microstates representing a classical universe leads only to another microstate representing the same universe. This implies that the $e^{\mathcal{A}_*/4}$ microstates of a classical universe generate an "effective vector space," unless we consider a superposition of an exponentially large, $\gtrsim e^{O(\delta w \mathcal{A}_*)}$, number of states.

What about a superposition of different classical universes? In particular, if states representing universes with w_1 and w_2 ($\neq w_1$) are superposed, then how does the theory know that the resulting state represents a superposition of two classical universes, and not another—perhaps even non-classical—universe? A key point is that the Hilbert space we consider has a special basis, determined by the $\mathcal{A}_*/4$ local degrees of freedom in the holographic space:[12]

$$\mathcal{H}_* = (\mathbf{C}^2)^{\otimes \frac{\mathcal{A}_*}{4}}. \tag{2.72}$$

From the result in Section 2.3, we know that a state representing the FRW universe with w_1 is more entangled than that representing the FRW universe with w_2 ($> w_1$). This implies that when expanded in the natural basis $\{|\Psi_i\rangle\}$ for the structure of Eq. (2.72), i.e. the product state basis for the $\mathcal{A}_*/4$ local holographic degrees of freedom, then a state $|\Psi_{w_1}\rangle$ representing the universe with w_1 effectively has exponentially more terms than a state $|\Psi_{w_2}\rangle$ representing the universe with w_2. Namely, we expect that

$$|\Psi_w\rangle \approx \sum_{i=1}^{e^{f(w)\frac{\mathcal{A}_*}{4}}} a_i |\Psi_i\rangle, \tag{2.73}$$

where $f(w)$ is a monotonically decreasing function of w taking values of $O(1)$, and a_i are coefficients taking generic random values. The normalization condition for $|\Psi_w\rangle$ then implies

$$|a_i| \approx O\big(e^{-f(w)\frac{\mathcal{A}_*}{8}}\big), \tag{2.74}$$

---

[11]The same argument applies to the FRW universes with multiple fluid components, so that the states representing these universes also live in the same Hilbert space as the single component universes.

[12]For simplicity, here we have assumed that the degrees of freedom are qubits, but the subsequent argument persists as long as the number of independent states for each degree of freedom does not scale with $\mathcal{A}_*$. In particular, it persists if the correct structure of $\mathcal{H}_*$ appears as $(\mathbf{C}^N)^{\otimes \mathcal{A}_*/l_c^2}$ as discussed in Section 2.4.

i.e. the size of the coefficients in product basis expansion is exponentially different for states with different w's. This, in particular, leads to

$$\langle \Psi_{w_1} | \Psi_{w_2} \rangle \lesssim O\big(e^{-\{f(w_1)-f(w_2)\}\frac{\mathcal{A}_*}{8}}\big), \tag{2.75}$$

i.e. microstates for different universes are orthogonal up to exponentially suppressed corrections.

Now consider a superposition state

$$|\Psi\rangle = c_1 |\Psi_{w_1}\rangle + c_2 |\Psi_{w_2}\rangle, \tag{2.76}$$

where $|c_1|^2 + |c_2|^2 = 1$ up to the correction from exponentially small overlap $\langle \Psi_{w_1} | \Psi_{w_2} \rangle$. We are interested in the reduced density matrix for a subregion Γ in the holographic theory

$$\rho_\Gamma = \mathrm{Tr}_{\bar{\Gamma}} |\Psi\rangle\langle\Psi|, \tag{2.77}$$

where Γ occupies less than a half of the leaf volume. The property of Eq. (2.75) then ensures that

$$\rho_\Gamma = |c_1|^2 \rho_\Gamma^{(1)} + |c_2|^2 \rho_\Gamma^{(2)}, \tag{2.78}$$

up to corrections exponentially suppressed in $\mathcal{A}_*$. Here, $\rho_\Gamma^{(1)}$ ($\rho_\Gamma^{(2)}$) are the reduced density matrices we would obtain if the state were genuinely $|\Psi_{w_1}\rangle$ ($|\Psi_{w_2}\rangle$). The matrix ρ_Γ thus takes the form of an incoherent classical mixture for the two universes. Similarly, the entanglement entropy for the region Γ is also incoherently added

$$S_\Gamma = |c_1|^2 S_\Gamma^{(1)} + |c_2|^2 S_\Gamma^{(2)} + S_{\Gamma,\mathrm{mix}}, \tag{2.79}$$

where $S_\Gamma^{(1,2)}$ are the entanglement entropies obtained if the state were $|\Psi_{w_{1,2}}\rangle$, and

$$S_{\Gamma,\mathrm{mix}} = -|c_1|^2 \ln |c_1|^2 - |c_2|^2 \ln |c_2|^2, \tag{2.80}$$

is the entropy of mixing (classical Shannon entropy), suppressed by factors of $O(\mathcal{A}_*)$ compared with $S_\Gamma^{(1,2)}$. The features in Eqs. (2.78, 2.79) indicate that unless $|c_1|$ or $|c_2|$ is suppressed exponentially in $\mathcal{A}_*$, the state $|\Psi\rangle$ admits the usual interpretation of a superposition of macroscopically different universes with $w_{1,2}$.

In fact, unless a superposition involves exponentially many microstates, we find

$$|\Psi\rangle = \sum_i c_i |\Psi_{w_i}\rangle \quad \Rightarrow \quad \begin{array}{l} \rho_\Gamma = \sum_i |c_i|^2 \rho_\Gamma^{(i)}, \\ S_\Gamma = \sum_i |c_i|^2 S_\Gamma^{(i)} + S_{\Gamma,\mathrm{mix}}, \end{array} \tag{2.81}$$

with exponential accuracy. Here, $S_{\Gamma,\mathrm{mix}} = -\sum_i |c_i|^2 \ln |c_i|^2$ and is suppressed by a factor of $O(\mathcal{A}_*)$ compared with the first term in S_Γ. This indicates that the standard many worlds interpretation applies to classical spacetimes under any reasonable measurements (only) in the limit that $e^{-\mathcal{A}_*}$ is regarded as zero, i.e. unless a superposition involves exponentially

many terms or an exponentially small coefficient. This is consonant with the observation that classical spacetime has an intrinsically thermodynamic nature [12], supporting the idea that it consists of a large number of degrees of freedom. In Ref. [54], the features described above were discussed using a qubit model in which the states representing the FRW universes exhibit a "Russian doll" structure as illustrated in Fig 2.11. We summarize this model in Appendix 2.6 for completeness.

We conclude that the states representing FRW universes with a leaf area $\mathcal{A}_*$ can all be elements of a single Hilbert space $\mathcal{H}_*$ with dimension

$$\ln \dim \mathcal{H}_* = \frac{\mathcal{A}_*}{4}. \tag{2.82}$$

Any such universe has $e^{\mathcal{A}_*/4}$ independent microstates, which form a basis of $\mathcal{H}_*$. This implies that matter and spacetime must have a sort of unified origin in this picture, since a superposition that changes the spacetime geometry must also change the matter content filling the universe. How could this be the case?

Consider, as discussed in Section 2.4, that the cutoff length of the holographic theory is of order $l_s \sim \sqrt{n}$, where n (> 1) is the number of species at energies below $1/l_s$. This implies that the $\mathcal{A}_*/4$ degrees of freedom can be decomposed as

$$\frac{\mathcal{A}_*}{4} \sim n \frac{\mathcal{A}_*}{l_s^2}, \tag{2.83}$$

representing n fields living in the holographic space of cutoff length l_s. Now, to obtain the $e^{\mathcal{A}_*/4}$ microstates for an FRW universe we need to consider rotations for all the n degrees of freedom in each cutoff size cell. This may suggest that the identity of a matter species at the fundamental level may not be as adamant as in low energy semiclassical field theories. The reason why all the n degrees of freedom can be involved could be because the "local effective temperature," defined analogously to de Sitter space, diverges at the holographic screen.

Finally, we expect that small excitations over FRW universes in this picture are represented by non-linear/state-dependent operators in the (suitably extended) $\mathcal{H}_*$ space, along the lines of Ref. [59] (see Refs. [60, 61, 62] for earlier work). This is because a superposition of background spacetimes may lead to another background spacetime, so that operators representing excitations should know the entire quantum state they are acting on.

Bulk reconstruction from holographic states

We have seen that the entanglement entropies of the $\mathcal{A}_*/4$ local holographic degrees of freedom in the holographic space σ_* encode information about spacetime in the causal region D_{σ_*}. Here we discuss in more detail how this encoding may work in general.

While we have focused on the case in which the future-directed ingoing light rays emanating orthogonally from σ_* (i.e. in the k^a directions in Fig. 2.2) meet at a point p_0, our discussion can be naturally extended to the case in which the light rays encounter a spacetime singularity before reaching a caustic. This may occur, for example, if a black hole
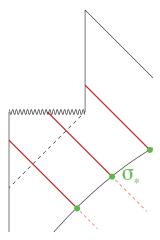
Figure 2.12: If a black hole forms inside the holographic screen, future-directed ingoing light rays emanating orthogonally from the leaf σ_* at an intermediate time may hit the singularity before reaching a caustic. While the diagram here assumes spherical symmetry for simplicity, the phenomenon can occur more generally.

forms in a universe as depicted in Fig. 5.4, where we have assumed spherical symmetry for collapsing matter and taken $p(\tau)$ to follow its center. We see that at intermediate times, the future-directed ingoing light rays emanating from leaves encounter the black hole singularity before reaching a caustic.[13] Our interpretation in this case is similar to the case without a singularity. The entanglement entropies of the holographic degrees of freedom encode information about D_{σ_*}.

In what sense does a holographic state on σ_* contain information about D_{σ_*}? We assume that the theory allows for the reconstruction of D_{σ_*} from the data in the state on σ_*. On the other hand, it is not the case that the collection of extremal surfaces for all possible subregions on σ_* probes the entire D_{σ_*}. This suggests that the full reconstruction of D_{σ_*} may need bulk time evolution.

There is, however, no a priori guarantee that the operation corresponding to bulk time evolution is complete within $\mathcal{H}_*$. This means that there may be no arrangement of operators defined in $\mathcal{H}_*$ that represents certain operators in D_{σ_*}. For these subsets of D_{σ_*}, bulk reconstruction would involve operators defined on other boundary spaces. In other words, the operators supported purely in $\mathcal{H}_*$ may allow for a direct spacetime interpretation only for a portion of D_{σ_*}, e.g. the outside of the black hole horizon in the example of Fig. 5.4 (in which case some of the operators would represent the stretched horizon degrees of freedom). Our

---

[13]At these times, the specific construction of the holographic screen in Section 2.2 cannot be applied exactly. This is not a problem as the fundamental object is the state in the holographic space, and not $p(\tau)$. The purpose of the discussion in Section 2.2 is to illustrate our observer centric choice of fixing the holographic redundancy in formulating the holographic theory.
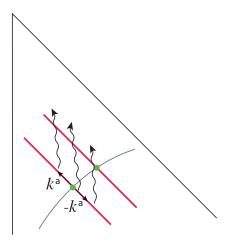
Figure 2.13: To determine a state in the future, we need information on the "exterior" light sheet, the light sheet generated by light rays emanating from σ_* in the $-k^a$ directions, in addition to that on the "interior" light sheet, i.e. the one generated by light rays emanating in the $+k^a$ directions.

assumption merely says that the operators in $\mathcal{H}_*$ acting on the state contain data equivalent to specifying the system on a Cauchy surface for D_{σ_*}.

The consideration above implies that the information in a holographic state on σ_*, when interpreted through operators in $\mathcal{H}_*$, may only be partly semiclassical. We expect that this becomes important when the spacetime has a horizon. In particular, for the $w = -1$ FRW universe, the leaf σ_* is formally beyond the stretched de Sitter horizon as viewed from $p(\tau)$. This may mean that some of the degrees of freedom represented by operators defined in $\mathcal{H}_*$ can only be viewed as non-semiclassical stretched horizon degrees of freedom.

Information about the "exterior" region

The information about D_{σ_*}, contained in the screen entanglement entropies, is not sufficient to determine future states obtained by time evolution. This information corresponds to that on the "interior" light sheet, i.e. the light sheet generated by light rays emanating in the $+k^a$ directions from σ_*.[14] However, even barring the possibility of information sent into the system from a past singularity or past null infinity (which we will discuss in Section 3.4), determining a future state requires information about the "exterior" light sheet, i.e. the one generated by light rays emanating in the $-k^a$ directions; see Fig. 2.13.[15] How is this

---

[14]If the light sheet encounters a singularity before reaching a caustic, then the information about the singularity may also be contained.

[15]This light sheet is terminated at a singularity or a caustic. Note that the information beyond a caustic is not needed to specify the state [70], since it is timelike related with the information on the interior light sheet [87] so that the two do not provide independent information.

information encoded in the holographic state? Does it require additional holographic degrees of freedom beyond the $\mathcal{A}_*/4$ degrees of freedom considered so far?

The simplest possibility is that the $e^{\mathcal{A}_*/4}$ microstates for each interior geometry (i.e. a fixed screen entanglement entropy structure) contain all the information associated with both the interior and exterior light sheets. If this is indeed the case, then we do not need any other degrees of freedom in the holographic space σ_* beyond the $\mathcal{A}_*/4$ ones discussed earlier. It also implies the following properties for the holographic theory:

- **Autonomous time evolution** — Assuming the absence of a signal sent in from a past singularity or past null infinity (see Section 3.4), the evolution of the state is autonomous. In particular, an initial pure state evolves into a pure state.

- **S-matrix description for a dynamical black hole** — As a special case, a pure state representing initial collapsing matter to form a black hole will evolve into a pure state representing final Hawking radiation, even if $p(\tau)$ hits the singularity at an intermediate stage (at least if the leaf stays outside the black hole); see Fig. 5.4.

- **Strengthened covariant entropy bound** — According to the original proposal of the covariant entropy bound [21, 22], the entropy on *each* of the interior and exterior light sheets is bounded by $\mathcal{A}_*/4$, implying that

$$\ln \dim \mathcal{H}_* = 2 \times \frac{\mathcal{A}_*}{4} = \frac{\mathcal{A}_*}{2}, \tag{2.84}$$

  where $\mathcal{H}_*$ is the Hilbert space associated with σ_*. The present picture instead says

$$\ln \dim \mathcal{H}_* = \frac{\mathcal{A}_*}{4}, \tag{2.85}$$

  implying that the entropy on the *union* of the interior and exterior light sheets is bounded by $\mathcal{A}_*/4$.[16] Note that the bound does not say that the entropy on each of the interior and exterior light sheets is separately bounded by $\mathcal{A}_*/8$, and so is profoundly holographic. This bound is consistent with the fact that in any known realistic examples the covariant entropy bound is saturated only in one side of a leaf [88].

The picture described here is, of course, a conjecture, which needs to be tested. For example, if a realistic case is found in which the $\mathcal{A}_*/4$ bound is violated by the contributions from both the interior and exterior light sheets, then we would have to modify the framework, e.g., by adding an extra $\mathcal{A}_*/4$ degrees of freedom on the holographic space. It is interesting that there is no known system that requires such a modification.

We finally discuss the connection with AdS/CFT. In the limit that the spacetime becomes asymptotically AdS, the location of the holographic screen is sent to spatial infinity, so that $\mathcal{A}_* \to \infty$. This implies that there are $N_* = e^{\mathcal{A}_*/4} \to \infty$ microstates for any spacetime

---

[16]This bound was anticipated earlier [83] based on more phenomenological considerations.

configuration in D_{σ_*} for a leaf σ_*, including the case that it is a portion of the empty AdS space. Wouldn't this contradict the statement that the vacuum of a CFT is unique?

As we will discuss in Section 3.4, the degrees of freedom associated with N_* correspond to a freedom of sending information into the system at a later stage of time evolution, i.e. that of inserting operators at locations other than the point $x_{-\infty}$ corresponding to $\tau = -\infty$ on the conformally compactified AdS boundary. It is with this freedom that the CFT corresponds to the AdS limit of our theory including the N_* degrees of freedom:

$$\text{CFT} \iff \lim_{\mathcal{M} \to \text{asymptotic AdS}} \mathcal{T}, \tag{2.86}$$

where $\mathcal{M}$ is the spacetime inside the holographic screen, and $\mathcal{T}$ represents the theory under consideration. Here, we have taken the holographic screen to stay outside the cutoff surface (corresponding to the ultraviolet cutoff of the CFT) which is also sent to infinity.

This implies that if we want to consider a setup in which the evolution of the state is "autonomous" within the bulk, then we need to fix a configuration of operators at $x \neq x_{-\infty}$, i.e. we need to fully fix a boundary condition at the AdS boundary. The correspondence to our theory in this case is written as

$$\text{autonomous} \quad \text{CFT} \iff \lim_{\mathcal{M} \to \text{asymptotic AdS}} \mathcal{T} \big/ N_*. \tag{2.87}$$

The conventional vacuum state of the CFT corresponds to a special configuration of the N_* degrees of freedom that does not send in any signal to the system at later times (the simple reflective boundary conditions at the AdS boundary). Given the correspondence between the N_* degrees of freedom and boundary operators, we expect that this configuration is unique. The state corresponding to the CFT vacuum in our theory is then unique: the vacuum state of the theory $\mathcal{T}/N_*$ with the configuration of the N_* degrees of freedom chosen uniquely as discussed above.

Time evolution

Another feature of the holographic theory of general spacetimes beyond AdS/CFT is that the boundary space changes in time. This implies that we need to consider the theory in a large Hilbert space containing states living in different boundary spaces, Eq. (2.5). For states representing FRW universes, the relevant space can be written as

$$\mathcal{H} = \sum_{\mathcal{A}} \mathcal{H}_{\mathcal{A}}, \tag{2.88}$$

where $\mathcal{A}$ is the area of the leaf, and the sum of the Hilbert spaces is defined by Eq. (2.6).[17] While the microscopic theory involving time evolution is not yet available, we can derive its

---

[17]More precisely, $\mathcal{H}_{\mathcal{A}}$ contains states whose leaf areas fall in the range between $\mathcal{A}$ and $\mathcal{A} + \delta\mathcal{A}$. The precise choice of $\delta\mathcal{A}$ is unimportant unless it is exponentially small in $\mathcal{A}$. For example, the dimension of $\mathcal{H}_{\mathcal{A}}$ is $e^{\mathcal{A}/4}\delta\mathcal{A}$, so that the entropy associated with it is $\mathcal{A}/4 + \ln\delta\mathcal{A}$, which is $\mathcal{A}/4$ at the leading order in $1/\mathcal{A}$ expansion.

salient features by assuming that it reproduces the semiclassical time evolution in appropriate regimes. Here we discuss this issue for both direct sum and Russian doll structures. In particular, we consider a semiclassical time evolution in which a state having the leaf area $\mathcal{A}_1$ evolves into that having the leaf area $\mathcal{A}_2$ ($> \mathcal{A}_1$).

Direct sum structure

In this case there is a priori no need to introduce non-linearity in the algebra of observables, so we may assume that time evolution is described by a standard unitary operator acting on $\mathcal{H}$. In particular, time evolution of a state in $\mathcal{H}_{\mathcal{A}_1}$ into that in $\mathcal{H}_{\mathcal{A}_2}$ is given by a linear map from elements of $\mathcal{H}_{\mathcal{A}_1}$ to those in $\mathcal{H}_{\mathcal{A}_2}$.

Consider microstates $|\Psi_i^w\rangle$ ($i = 1, \cdots, e^{\mathcal{A}_1/4}$) representing the FRW universe with w when the leaf area is $\mathcal{A}_1$, $|\Psi_i^w\rangle \in \mathcal{H}_{\mathcal{A}_1, w} \subset \mathcal{H}_{\mathcal{A}_1}$; see Eq. (2.68). Assuming that all these states follow the standard semiclassical time evolution,[18] their evolution is given by

$$|\Psi_i^w\rangle \to |\Phi_i^w\rangle, \tag{2.89}$$

where $\{|\Phi_i^w\rangle\}$ is a subset of the microstates $|\Phi_j^w\rangle$ ($j = 1, \cdots, e^{\mathcal{A}_2/4}$) representing the FRW universe with w when the leaf area is $\mathcal{A}_2$, $|\Phi_j^w\rangle \in \mathcal{H}_{\mathcal{A}_2, w} \subset \mathcal{H}_{\mathcal{A}_2}$. This has an important implication. Suppose that the initial state of the universe is given by

$$|\Psi\rangle = \sum_i a_i |\Psi_i^w\rangle. \tag{2.90}$$

As we discussed before, if the effective number of terms in the sum is of order $e^{\mathcal{A}_1/4}$, namely if there are $e^{\mathcal{A}_1/4}$ nonzero a_i's with size $|a_i| \sim e^{-\mathcal{A}_1/8}$, then the state $|\Psi\rangle$ is not semiclassical, i.e. a firewall state (because a superposition of that many microstates changes the structure of the entanglement entropies). After the time evolution, however, this state becomes

$$|\Psi\rangle \to |\Phi\rangle = \sum_i a_i |\Phi_i^w\rangle, \tag{2.91}$$

where the number of terms in the sum is $e^{\mathcal{A}_1/4}$ because of the linearity of the map. This implies that the state $|\Phi\rangle$ is *not* a firewall state, since the number of terms is much (exponentially) smaller than the dimensionality of $\mathcal{H}_{\mathcal{A}_2, w}$: $e^{\mathcal{A}_1/4} \ll e^{\mathcal{A}_2/4}$. In particular, the state $|\Phi\rangle$ represents the standard semiclassical FRW universe with the equation of state parameter w.

This shows that this picture has a "built-in" mechanism of eliminating firewalls through time evolution, at least when the leaf area increases in time as we focus on here. This process happens very quickly—any macroscopic increase of the leaf area makes the state semiclassical regardless of the initial state.

---

[18]Here we ignore the possibility that the equation of state changes between the two times, e.g., by a conversion of the matter content or vacuum decay. This does not affect our discussion below.

Spacetime equals entanglement

In this case, time evolution from states in $\mathcal{H}_{\mathcal{A}_1}$ to those in $\mathcal{H}_{\mathcal{A}_2}$ is expected to be non-linear. Consider microstates $|\Psi_i^w\rangle$ ($i = 1, \cdots, e^{\mathcal{A}_1/4}$) representing the FRW universe with w when the leaf area is $\mathcal{A}_1$, $|\Psi_i^w\rangle \in \mathcal{H}_{\mathcal{A}_1}$. As before, requiring the standard semiclassical evolution for all the microstates, we obtain

$$|\Psi_i^w\rangle \rightarrow |\Phi_i^w\rangle, \tag{2.92}$$

where $\{|\Phi_i^w\rangle\}$ is a subset of the microstates $|\Phi_j^w\rangle$ ($j = 1, \cdots, e^{\mathcal{A}_2/4}$) representing the FRW universe with w when the leaf area is $\mathcal{A}_2$, $|\Phi_j^w\rangle \in \mathcal{H}_{\mathcal{A}_2}$. Suppose the initial state

$$|\Psi\rangle = \sum_i a_i |\Psi_i^w\rangle \equiv |\Psi^{w'}\rangle, \tag{2.93}$$

represents the FRW universe with $w' < w$. This is possible if the effective number of terms in the sum is of order $e^{\mathcal{A}_1/4}$, i.e. if there are $e^{\mathcal{A}_1/4}$ nonzero a_i's with size $|a_i| \sim e^{-\mathcal{A}_1/8}$. Now, if the time evolution map were linear, then this state would evolve into

$$|\Psi^{w'}\rangle \rightarrow |\Phi\rangle = \sum_i a_i |\Phi_i^w\rangle. \tag{2.94}$$

This state, however, is not a state representing the FRW universe with w', since the effective number of terms in the sum, $e^{\mathcal{A}_1/4}$, is exponentially smaller than $e^{\mathcal{A}_2/4}$, the required number to obtain a state with w' from the microstates $|\Phi_i^w\rangle$. To avoid this problem, the map from $\mathcal{H}_{\mathcal{A}_1}$ into $\mathcal{H}_{\mathcal{A}_2}$ must be non-linear so that $|\Psi^{w'}\rangle$ evolves into $|\Phi^{w'}\rangle$ containing $e^{\mathcal{A}_2/4}$ terms when expanded in terms of $|\Phi_i^w\rangle$.

Here we make two comments. First, the non-linearity of the map described above does not necessarily mean that the time evolution of semiclassical degrees of freedom (given as excitations on the background states considered here) is non-linear, since the definition of these degrees of freedom would also be non-linear at the fundamental level. In fact, from observation this evolution must be linear, at least with high accuracy. This requirement gives a strong constraint on the structure of the theory. Second, the non-linearity seen above arises when the area of the boundary space changes, $\mathcal{A}_1 \rightarrow \mathcal{A}_2 \neq \mathcal{A}_1$. Since the area of the boundary is fixed in the AdS/CFT limit (with the standard regularization and renormalization procedure), this non-linearity does not show up in the CFT time evolution, generated by the dilatation operator with respect to the $t = -\infty$ point in the compactified Euclidean space.[19]

We finally discuss relations between different $\mathcal{H}_B$'s. While we do not know how they are related, for example they could simply exist as a direct sum in the full Hilbert space $\mathcal{H} = \bigoplus_B \mathcal{H}_B$, an interesting possibility is that their structure is analogous to the Russian

---

[19]This does not mean that the interior of a black hole is described by state-independent operators in the CFT. It is possible that the CFT does not provide a description of the black hole interior; see discussion in Section 4.2.

doll structure within a single $\mathcal{H}_B$. Specifically, let us introduce the notation to represent the Russian doll structure as

$$\{|\Psi^w\rangle\} \prec \{|\Psi^{w'}\rangle\} \quad \text{for} \quad w' < w, \tag{2.95}$$

meaning that the left-hand side is a measure zero subset of the closure of the right-hand side. We may imagine that states $|\Psi_B\rangle$ representing spacetimes with boundary B and states $|\Psi_{B'}\rangle$ representing those with boundary B' are related similarly as

$$\{|\Psi_B\rangle\} \prec \{|\Psi_{B'}\rangle\} \quad \text{for} \quad \|B\| < \|B'\|. \tag{2.96}$$

(The relation may be more complicated; for example, some of the $|\Psi_B\rangle$'s are related with $|\Psi_{B'}\rangle$'s and some with $|\Psi_{B''}\rangle$'s with $B'' \neq B'$.) Ultimately, all states in realistic (cosmological) spacetimes may be related with those in asymptotically Minkowski space as

$$\{|\Psi_B\rangle\} \prec \{|\Psi_{B'}\rangle\} \cdots \prec \{|\Psi_{\text{Minkowski}}\rangle\}, \tag{2.97}$$

since the boundary area for asymptotically Minkowski space is infinity, $\mathcal{A}_{\text{Minkowski}} = \infty$. Does string theory formulated in an asymptotically Minkowski background (using S-matrix elements) correspond to the present theory as

$$\text{String theory} \iff \lim_{\mathcal{M} \to \text{asymptotic Minkowski}} \mathcal{T}? \tag{2.98}$$

Here, the $\mathcal{T}/N_{\text{Minkowski}}$ portion is described by the scattering dynamics, and the $N_{\text{Minkowski}}$ degrees of freedom are responsible for the initial conditions, where $N_{\text{Minkowski}} = e^{\mathcal{A}_{\text{Minkowski}}/4}$; see the next section. If this is indeed the case, then it would be difficult to obtain a useful description of cosmological spacetimes directly in that formulation, since they would correspond to a special measure zero subset of the possible asymptotic states.

2.5   Discussion

In this final section, we discuss some of the issues that have not been addressed in the construction so far. This includes the possibility of sending signals from a past singularity or past null infinity (in the course of time evolution) and the interpretation of a closed universe in which the area of the leaf changes from increasing to decreasing once the scale factor at the leaf starts decreasing. We argue that these issues are related to that of "selecting a state"—even if the theory is specified we still need to provide selection conditions on a state, usually given in the form of boundary conditions (e.g. initial conditions). Our discussion here is schematic, but it allows us to develop intuition about how quantum gravity in general spacetimes might work at the fundamental level.
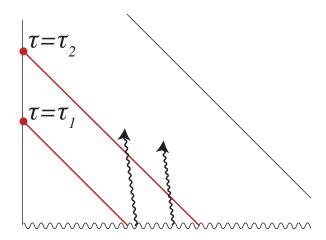
Figure 2.14: In a universe beginning with a big bang, obtaining a future state requires a specification of signals from the big bang singularity, in addition to the information contained in the original state. In an FRW universe this is done by imposing spatial homogeneity and isotropy, which corresponds to selecting a fine-tuned state from the viewpoint of the big bang universe.

Signals from a past singularity or past null infinity

As mentioned in Section 2.4, the evolution of a state in the present framework is not fully autonomous. Consistent with the covariant entropy bound, we may view a holographic state to carry the information on the two (future-directed ingoing and past-directed outgoing) light sheets associated with the leaf it represents. However, this is not enough to determine a future state because there may be signals sent into the system from a past singularity or past null infinity (signals originating from the lower right direction between the two 45° lines in Fig. 2.13).

To be specific, let us consider a (not necessarily FRW) universe beginning with a big bang. As shown in Fig. 2.14, obtaining a future state (represented by the upper 45° line) in general requires a specification of signals from the big bang singularity, in addition to the information contained in the original state (the lower 45° line). We usually avoid this issue by requiring the "cosmological principle," i.e. spatial homogeneity and isotropy, which determines what conditions one must put at the singularity—with this requirement, the state of the universe is determined by the energy density content in the universe at a time. Imposing this principle, however, corresponds to choosing a very special state. This is because there is no reason to expect that signals sent from the singularity at different times τ (defined holographically) are correlated in such a way that the system appears as homogeneous and isotropic in some time slicing. In fact, this was one of the original motivations for inflationary cosmology [89, 90, 91].

In some cases, appropriate conditions can be obtained by assuming that the spacetime

under consideration is a portion of larger spacetime. For example, if the universe is dominated by negative curvature at an early stage, it may arise from bubble nucleation [92], in which case the homogeneity and isotropy would result from the dynamics of the bubble nucleation [93]. Even in this case, however, we would still need to specify similar conditions in the ambient space in which our bubble forms, and so on. More generally, the analysis here says that to obtain a future state, we need to specify the information coming from the directions tangent to the past-directed light rays. This, however, is morally the same as the usual situation in physics in which we need to specify boundary (e.g. initial) conditions beyond the dynamical laws the system obeys.

The situation is essentially the same in the limit of AdS/CFT; we only need to consider the AdS boundary instead of the big bang singularity. To obtain future states, it is not enough to specify the initial state, given by a local operator inserted at the point $x_{-\infty}$ corresponding to $\tau = -\infty$ on the conformally compactified AdS boundary. We also have to specify other (possible) boundary operators inserted at points other than $x_{-\infty}$.

String theory formulated in terms of the S-matrix deals with this issue by adopting an asymptotically Minkowski time slice in which all the necessary information is viewed as being in the initial state. This, however, does not change the amount of information needed to specify the state, which is infinite in asymptotically Minkowski space (because one can in principle send an infinite amount of information into the system from past null infinity).

Closed universes—time in quantum gravity

Consider a closed universe in which the vacuum energy is negligible throughout its history. In such a universe, the area of the leaf changes from increasing to decreasing in the middle of its evolution. On the other hand, we expect that the area of the leaf for a "generic" state increases monotonically, since the number of independent states representing spacetime with the leaf area $\mathcal{A}$ goes as $e^{\mathcal{A}/4}$. What does this imply?

We interpret that states representing universes like these are "fine-tuned," so that they do not obey the usual second law of thermodynamics as applied to the Hilbert space of quantum gravity. This does not mean that they are meaningless states to consider. Rather, it means that we need to scrutinize carefully the concept of time in quantum gravity.

There are at least three different views of time in quantum gravity; see, e.g., Ref. [94]. First, since time parameterization in quantum gravity is nothing other than a gauge choice, the state $|\tilde{\Psi}\rangle$ of the *full* system—whatever its interpretation—satisfies the constraint [63, 64]

$$H|\tilde{\Psi}\rangle = 0, \tag{2.99}$$

where H is the time evolution operator, in our context the generator of a shift in τ. In this sense, the concept of time evolution does not apply to the full state $|\tilde{\Psi}\rangle$.[20] However, this of

---

[20]Reference [63] states that Eq. (2.99) need not apply in an infinite world; for example, the state of the system $|\Psi_\infty\rangle$ may depend on time in asymptotically Minkowski space. We view that Eq. (2.99) still applies in this case by interpreting $|\tilde{\Psi}\rangle$ to represent the full system, including the "exterior" degrees of freedom

course does not mean that *physical time* we perceive is nonexistent. Time we observe can be defined as correlations between subsystems (e.g. between an object playing the role of a clock and the rest) [63, 95], at least in some branch of $|\tilde{\Psi}\rangle$. Another way to define time is through probability flow in $|\tilde{\Psi}\rangle$. Suppose $|\tilde{\Psi}\rangle$ is expanded in a set of states $|\Psi_i\rangle$ each of which represents a well-defined semiclassical spacetime when such an interpretation is applicable:

$$|\tilde{\Psi}\rangle = \sum_i c_i |\Psi_i\rangle. \tag{2.100}$$

According to the discussion in Section 2.4, $|\Psi_i\rangle$'s are approximately orthogonal in the appropriate limit, and the constraint in Eq. (2.99) implies

$$\sum_j c_j U_{ij} = c_i, \qquad U_{ij} \equiv \langle\Psi_i|e^{-iH\delta\tau}|\Psi_j\rangle, \tag{2.101}$$

where U_{ij} is (effectively) unitary

$$\sum_j U_{ij}U_{kj}^* = \sum_j U_{ji}U_{jk}^* = \delta_{ik}. \tag{2.102}$$

Multiplying Eq. (2.101) with its conjugate and using Eq. (2.102), we obtain

$$0 = -|c_i|^2 \sum_{j\neq i} |U_{ji}|^2 + \sum_{j\neq i} |c_j|^2 |U_{ij}|^2$$
$$+ \sum_{j\neq i} c_i c_j^* U_{ii} U_{ij}^* + \sum_{j\neq i} c_j c_i^* U_{ij} U_{ii}^* + \sum_{\substack{j,k\neq i \\ j\neq k}} c_j c_k^* U_{ij} U_{ik}^*. \tag{2.103}$$

In the regime where the WKB approximation is applicable, the terms in the second line are negligible compared with those in the first line because of a rapid oscillation of the phases of $c_{j,k}$'s, so that

$$|c_i|^2 \sum_{j\neq i} |U_{ji}|^2 = \sum_{j\neq i} |c_j|^2 |U_{ij}|^2, \tag{2.104}$$

implying that the "current of probability" is conserved. We may regard this current as time flow. The time defined in this way—which we call *current time*—need not be the same as the physical time defined through correlations, although in many cases the former agrees approximately with the latter or the negative of it (up to a trivial shift and rescaling).

In a closed universe (with a negligible vacuum energy), it is customary to impose the boundary condition

$$c_i = 0 \quad \text{for} \quad \{|\Psi_i\rangle \,|\, a = 0\}, \tag{2.105}$$

discussed in Section 2.4 (the degrees of freedom corresponding to $N_{\text{Minkowski}}$ below Eq. (2.98)) as well as the "interior" degrees of freedom represented by $|\Psi_\infty\rangle$. The time evolution of $|\Psi_\infty\rangle$ is then understood as correlations between the interior and exterior degrees of freedom, as described below.

i.e. the wavefunction vanishes when the scale factor goes to zero [63]. With this boundary condition, current time τ flows in a closed circuit. The direction of the flow agrees with that of physical time in the branches where $da/d\tau > 0$, while the two are exactly the opposite in the branches where $da/d\tau < 0$. (The latter statement follows, e.g., from the analysis in Ref. [96], which shows that given a lower entropy final condition the most likely history of a system is the CPT conjugate of the standard time evolution.) Our time evolution in earlier sections concerns the flow of current time. The (apparent) violation of the second law of thermodynamics then arises because the condition of Eq. (2.105) selects a special, "standing wave" solution from the viewpoint of the current time flow. This is, however, not a fine-tuning from the point of view of the quantum theory in a similar way as the electron energy levels of the hydrogen atom are not regarded as fine-tuned states.

The fact that current time flows toward lower entropy states does not mean that a physical observer living in the $da/d\tau < 0$ phase sees a violation of the second law of thermodynamics. Since the whole system evolves as time reversal of a standard entropy increasing process, *including memory states of the observer*, a physical observer always finds the evolution of the system to be the standard one [43, 96]; in particular, he/she always finds that the universe is expanding.

Static quantum multiverse—selecting the state in the landscape

The analysis of string theory suggests that the theory has a multitude of metastable vacua each of which leads to a distinct low energy effective theory [65, 66, 67, 68]. Combining this with the fact that many of these vacua lead to inflation (which is future eternal at the semiclassical level) leads to the picture of the inflationary multiverse [97, 98, 99, 100]. The picture suggests that our universe is one of many bubble universes, and it cannot be a closed universe that will eventually collapse as the one discussed above. How is the state of the multiverse selected then?

A naive semiclassical picture implies that the state of the multiverse evolves asymptotically into a superposition of supersymmetric Minkowski worlds and (possibly) "singularity worlds" resulting from the big crunches of AdS bubble universes [43]. This is because any other universe is expected to decay eventually. There are basically two possibilities for the situation in a full quantum theory.

The first possibility is that the multiverse is in a "scattering state." This essentially preserves the semiclassical intuition. From the viewpoint of the current time flow, the multiverse begins as an asymptotic state, experiences nontrivial cosmology at an intermediate stage, and then dissipates again into the asymptotic Minkowski and singularity worlds. In the earlier stage of the evolution in which the coarse-grained entropy decreases in τ, the directions of current and physical time flows are opposite, while in the later stage of increasing entropy, the flows of the two times are in the same direction. The resulting picture is similar to that of Ref. [101]: the multiverse evolves asymptotically into both forward and backward in (current) time. This, however, does not mean that a physical observer, who is a part of

the system, sees an entropy decreasing universe; the observer always finds that his/her world obeys the second law of thermodynamics.

A problem with this possibility is that specifying the theory of quantum gravity, e.g. the structure of the Hilbert space and Hamiltonian, is not enough to obtain the state of the multiverse and hence make predictions. We would need a separate theory to specify initial conditions. Furthermore, having a lower course-grained entropy at the turn-around point (the point at which the coarse-grained entropy changes from decreasing to increasing in the current time evolution) requires a more carefully chosen initial condition. This leads to the issue of understanding why we are "ordinary observers," carrying course-grained entropies (much) smaller than that needed to have any consciousness—a variant of the well-known Boltzmann brain problem [102, 103, 104] (the argument applied to space of initial conditions, rather than to a thermal system).

The alternative, and perhaps more attractive, possibility is that the multiverse is in a "bound state" [69]. Specifically, the multiverse is in a *normalizable* state satisfying the constraint of Eq. (2.99) (as well as any other constraints):

$$|\tilde{\Psi}\rangle = \sum_i c_i |\Psi_i\rangle; \qquad \sum_i |c_i|^2 < \infty. \tag{2.106}$$

This is a normalization condition in spacetime, rather than in space as in usual quantum mechanics, and it allows us to determine, in principle, the state of the multiverse once the theory is given.[21] As in the case of a collapsing closed universe, current time flows in a closed circuit(s) to the extent that this concept is applicable. This suggests that the multiverse does not probe an asymptotic supersymmetric Minkowski region or the big crunch singularity of an AdS bubble. The origin of this phenomenon must be intrinsically quantum mechanical as it contradicts the naive semiclassical picture. In fact, such a situation is not new in physics. As is well known, the hydrogen atom cannot be correctly described using classical mechanics: any orbit of the electron is unstable with respect to the emission of synchrotron radiation. The situation in the quantum multiverse may be similar—quantum mechanics is responsible for the very existence of the system.

Once the state of the multiverse is determined, we should be able to use it to give predictions or explanations. This requires us to develop a prescription for extracting answers to physical questions about the state. The prescription would certainly involve coarse-graining (as one cannot even store the information of all possible microstates of the multiverse within the multiverse), and it should reproduce the standard Born rule giving probabilistic predictions in the appropriate regime. Perhaps, the normalization condition of Eq. (2.106) is required in order for this prescription to be well-defined.

---

[21]If there are multiple solutions $|\tilde{\Psi}_I\rangle$, it is natural to assume that the multiverse is in the maximally mixed state $\rho = \frac{1}{N} \sum_{I=1}^{N} |\tilde{\Psi}_I\rangle\langle\tilde{\Psi}_I|$ (in the absence of more information). Here, we have taken $|\tilde{\Psi}_I\rangle$'s to be orthonormal.

2.6   Appendix

Spacelike Monotonicity Theorem

Let H be a past holographic screen, foliated by compact marginally anti-trapped surfaces i.e. leaves, $\{\sigma_r\}$. Here, r is a (non-unique) real parameter taken to be a monotonically increasing function of the leaf area. For each leaf we can construct the two future-directed null vector fields (up to overall normalization) and denote them k^a and l^a, which satisfy

$$\theta_k = 0, \qquad \theta_l > 0. \tag{2.107}$$

Now let h^a a leaf-orthogonal vector field tangent to H and normalized by the condition $h^a \partial_a r = 1$. Note that h^a must point in the direction of increasing area. We can always put $h^a = \alpha l^a + \beta k^a$ for some smooth real-valued functions α and β on H. The Bousso-Engelhardt area theorem implies that $\alpha > 0$ everywhere. There is no restriction on the sign of β: it can even have indefinite sign on a single leaf.

Let A_r be a $d - 2$ dimensional region in a leaf σ_r and let ∂A_r denote its boundary, where d is the spacetime dimension. This region can be transported to a region $A_{r'}$ in a nearby leaf $\sigma_{r'}$ by following the integral curves of the leaf-orthogonal vector field h^a. While Ref. [46] pointed out that $\|A_r\|$ is an increasing function of r, this by itself does not guarantee that $S(A_r)$ monotonically increases. Nonetheless, we now show that $S(A_r)$ indeed monotonically increases if h^a is spacelike.

Theorem 1. *Suppose that H is a past holographic screen foliated by leaves $\{\sigma_r\}$ and assume that the parameter r is oriented to increase as leaf area increases. Assume that H is spacelike on some particular leaf which we take to be σ_0 by shifting r if necessary. Let A_0 be a subregion of σ_0 and define $A_r \subset \sigma_r$ by transporting points in A_0 along the integral curves of the leaf-orthogonal vector field in H. Then, $S(A_r)$ is a monotonically increasing function of r.*

Proof. Let h^a be the leaf-orthogonal vector field tangent to H with $h^a \partial_a r = 1$ and note that $h^a\big|_{\sigma_0}$ is spacelike. The compactness of σ_0 now allows us to find $r_0 > 0$ such that $h^a\big|_{H[-r_0,r_0]}$ is spacelike. Here we have introduced the convenient notation

$$H[r_1, r_2] = \bigcup_{r_1 \leq r \leq r_2} \sigma_r. \tag{2.108}$$

In what follows, we will assume that the extremal surface $E(A_r)$ anchored to ∂A_r deforms smoothly as a function of r at $r = 0$. If this is not the case, a phase transition occurs at $r = 0$ which will give rise to a discontinuity in the derivative of $S(A_r)$. However, we can then note that our theorem applies at r slightly greater than zero (where H is still spacelike and where no phase transition occurs) and also at r slightly smaller than zero. This implies that $S(A_r)$ is monotonically increasing at $r = 0$ even if $E(A_r)$ "jumps" at $r = 0$ so that the derivative of $\|E(A_r)\|$ has a discontinuity.

The maximin construction of $E(A_0)$ ensures that there exists $\Sigma_0 \in \mathcal{C}_{\sigma_0}$ such that $E(A_0) = \min(A_0, \Sigma_0)$. Here, $\mathcal{C}_\sigma$ denotes the collection of all complete codimension-1 achronal surfaces lying in D_σ that are anchored to σ, and $\min(A, \Sigma)$ denote the $d-2$ dimensional surface of minimal area lying in Σ that is homologous to A. If $0 < \epsilon < r_0$, let

$$\Sigma_\epsilon = \Sigma_0 \cup H[0, \epsilon]. \tag{2.109}$$

We claim that $\Sigma_\epsilon \in \mathcal{C}_{\sigma_\epsilon}$ for small ϵ. First we check that Σ_ϵ is achronal. Since Σ_0 and $H[0, \epsilon]$ are achronal independently, we focus on their intersection at σ_0. The definition of $\mathcal{C}_{\sigma_0}$ requires that Σ_0 lies in D_{σ_0} so that a vector pointing from σ_0 to Σ_0 has the form $c_1 k^a - c_2 l^a$ with $c_1, c_2 > 0$. Meanwhile, a vector pointing from σ_0 to $H[0, \epsilon]$ is proportional to $h^a\big|_{\sigma_0} = |\alpha|l^a - |\beta|k^a$. Here we have made use of the fact that $\alpha > 0$ and $\beta < 0$ for a spacelike past holographic screen. We see now that Σ_0 lies "inside" σ_0 while h^a points toward the "outside." This ensures that Σ_ϵ is achronal for sufficiently small ϵ. All that is left to check is that Σ_ϵ lies inside of D_{σ_ϵ}. But this is clear because a vector pointing from σ_ϵ toward Σ_ϵ is proportional to $-h^a\big|_{\sigma_\epsilon} = -|\alpha|l^a + |\beta|k^a$ which is indeed directed into D_{σ_ϵ}. That $\Sigma_\epsilon \in \mathcal{C}_{\sigma_\epsilon}$ is now clear for small ϵ.

We now construct an ϵ-dependent family of $d-2$ dimensional surfaces lying on Σ_0 that are anchored to ∂A_0, which we will denote by Ξ_ϵ. Begin by fixing a small ϵ with $0 < \epsilon < r_0$ and defining a projection function $\pi_\epsilon : H[0, \epsilon] \to \sigma_0$ in the natural way: if $p \in H[0, \epsilon]$, follow the integral curves of h^a, starting from p, until a point in σ_0 is reached. The result is $\pi_\epsilon(p)$. We can now define Ξ_ϵ:

$$\Xi_\epsilon = \Big(\min(A_\epsilon, \Sigma_\epsilon) \cap \Sigma_0 \Big) \bigcup \pi_\epsilon \Big(\min(A_\epsilon, \Sigma_\epsilon) \cap H[0, \epsilon] \Big). \tag{2.110}$$

If ϵ is sufficiently small, the fact that $H[0, \epsilon]$ has a positive definite metric, along with the fact that $E(A_0)$ is not tangent to σ_0 anywhere, ensures that $\|\pi_\epsilon\big(\min(A_\epsilon, \Sigma_\epsilon) \cap H[0, \epsilon]\big)\| < \|\min(A_\epsilon, \Sigma_\epsilon) \cap H[0, \epsilon]\|$. From this it follows that

$$\|\Xi_\epsilon\| < \|\min(A_\epsilon, \Sigma_\epsilon)\|. \tag{2.111}$$

On the other hand, because $\pi_\epsilon(\partial A_\epsilon) = \partial A_0$, we know that Ξ_ϵ is a codimension-2 surface anchored to ∂A_0 that lies only on Σ_0. Thus,

$$4S(A_0) = \|\min(A_0, \Sigma_0)\| \leq \|\Xi_\epsilon\|. \tag{2.112}$$

Noting that the maximin construction of $E(A_\epsilon)$ requires

$$\|\min(A_\epsilon, \Sigma_\epsilon)\| \leq 4S(A_\epsilon), \tag{2.113}$$

we find $S(A_0) < S(A_\epsilon)$. $\qquad\qquad\qquad\qquad\qquad\qquad\qquad\qquad\qquad\qquad\quad\square$

Qubit Model

Model and applications to quantum gravity

Here we describe a toy model for holographic states representing FRW universes, presented originally in Ref. [54]. We consider a Hilbert space for N ($\gg 1$) qubits $\mathcal{H} = (\mathbf{C}^2)^{\otimes N}$. Let Δ ($\leq N$) be a nonnegative integer and consider a typical superposition of 2^Δ product states

$$|\Psi\rangle = \sum_{i=1}^{2^\Delta} a_i \,|x_1^i x_2^i \cdots x_N^i\rangle, \tag{2.114}$$

where $\{a_i\}$ is a normalized complex vector, and $x_{1,\cdots,N}^i \in \{0,1\}$. Given an integer n with $1 \leq n < N$, we can break the Hilbert space into a subsystem Γ for the first n qubits and its complement $\bar{\Gamma}$. We are interested in computing the entanglement entropy S_Γ of Γ.

Suppose $n \leq N/2$. If $\Delta \geq n$, then i in Eq. (4.86) runs over an index that takes many more values than the dimension of the Hilbert space for Γ, so that Page's argument [75] tells us that Γ has maximal entanglement entropy: $S_\Gamma = n \ln 2$. On the other hand, if $\Delta < n$ then the number of terms in Eq. (4.86) is much less than both the dimension of the Hilbert space of Γ and that of $\bar{\Gamma}$, which limits the entanglement entropy: $S_\Gamma = \Delta \ln 2$. We therefore obtain

$$S_\Gamma = \begin{cases} n & n \leq \Delta, \\ \Delta & n > \Delta, \end{cases} \tag{2.115}$$

for $\Delta < N/2$, while

$$S_\Gamma = n, \tag{2.116}$$

for $\Delta \geq N/2$. Here and below, we drop the irrelevant factor of $\ln 2$. The value of S_Γ for $n > N/2$ is obtained from $S_\Gamma = S_{\bar{\Gamma}}$ since $|\Psi\rangle$ is pure.

The behavior of S_Γ in Eqs. (2.115, 2.116) models that of $S(\gamma)$ in Section 2.3. The correspondence is given by

$$\frac{n}{N} \leftrightarrow \frac{\|\Gamma\|}{\mathcal{A}_*}, \tag{2.117}$$

$$\frac{\Delta}{N} \leftrightarrow \frac{1}{2} Q_w \left(\frac{\pi}{2}\right), \tag{2.118}$$

for $\Delta \leq N/2$.[22] The identification of Eq. (2.117) is natural if we regard the $N = \mathcal{A}_*/4$ qubits as distributing over a leaf σ_* with each qubit occupying a volume of 4 in Planck units. The quantity Δ controls what universe a state represents. For fixed Δ, different choices of the product states $|x_1^i x_2^i \cdots x_N^i\rangle$ and the coefficients a_i give e^N independent microstates for the FRW universe with $w = f(\Delta/N)$. The function f is determined by Eq. (2.118); in particular, $f = -1$ (> -1) for $\Delta/N = 1/2$ ($< 1/2$).

---

[22]States with $\Delta > N/2$ cannot be discriminated from those with $\Delta = N/2$ using S_Γ alone. Below, we only consider the states with $N/4 \leq \Delta \leq N/2$.

This model can be used to argue for features of the holographic theories discussed in Section 2.4. We consider two cases:

Direct sum structure — In this case, each of the subspaces $\mathcal{H}_{*,w}$ is modeled by the N qubit system described here. Consider $\mathcal{H}_{*,w}$ with a fixed w. States representing the FRW universe with w then encompass e^N independent microstates in this space. These microstates form "effective vector space" in that a superposition involving less than $e^{O(\delta w N)}$ of them leads only to another microstate representing the same FRW universe with w. (We say that these states comprise "fat" preferred axes.) Most of the states in $\mathcal{H}_{*,w}$, containing more than $e^{O(\delta w N)}$ of the w microstates, are regarded as non-semiclassical, i.e. firewall or unphysical, states.

Russian doll structure — In this case, the entire $\mathcal{H}_*$ space is modeled by the N qubits, and the states representing various FRW universes are all elements of this single Hilbert space of dimension e^N. An important point is that the set of states with *any* fixed Δ_w provide a complete basis for the whole Hilbert space, where $\Delta_w \equiv N f^{-1}(w)$. This implies that we can obtain a state with any $w' < w$ by superposing $e^{\Delta_{w'} - \Delta_w}$ states with Δ_w, and we can also obtain a state with $w' > w$ as a superposition of carefully chosen e^{Δ_w} states with Δ_w. We call this the "Russian doll" structure, which is depicted schematically in Fig. 2.11.

Effective incoherence of superpositions

We now focus on the latter case and consider a normalized superposition

$$|\Psi\rangle = c_1|\Psi_1\rangle + c_2|\Psi_2\rangle, \tag{2.119}$$

of two states

$$|\Psi_1\rangle = \sum_{i=1}^{2^{\Delta_1}} a_i \, |x_1^i x_2^i \cdots x_N^i\rangle \qquad \left(\sum_{i=1}^{2^{\Delta_1}} |a_i|^2 = 1 \right), \tag{2.120}$$

$$|\Psi_2\rangle = \sum_{i=1}^{2^{\Delta_2}} b_i \, |y_1^i y_2^i \cdots y_N^i\rangle \qquad \left(\sum_{i=1}^{2^{\Delta_2}} |b_i|^2 = 1 \right), \tag{2.121}$$

with $\Delta_1 \neq \Delta_2$ and

$$\Delta_1, \Delta_2 \leq \frac{N}{2}. \tag{2.122}$$

Here, the coefficients a_i and b_i are random, as are the binary values $x_{1,\cdots,N}^i$ and $y_{1,\cdots,N}^i$, and $|c_1|^2 + |c_2|^2 = 1$ up to an exponentially suppressed correction arising from $\langle\Psi_1|\Psi_2\rangle \neq 0 \lesssim O(2^{-|\Delta_1 - \Delta_2|/2})$. We are interested in the reduced density matrix

$$\rho_{1\cdots n} = \text{Tr}_{n+1\cdots N}\, \rho, \tag{2.123}$$

obtained by performing a partial trace on

$$\rho = |\Psi\rangle\langle\Psi| = |c_1|^2|\Psi_1\rangle\langle\Psi_1| + |c_2|^2|\Psi_2\rangle\langle\Psi_2| + c_1c_2^*|\Psi_1\rangle\langle\Psi_2| + c_2c_1^*|\Psi_2\rangle\langle\Psi_1|, \qquad (2.124)$$

over the subsystem consisting of the first n qubits. We will only consider the case where $n < N/2$.

We begin our analysis by considering $\mathrm{Tr}_{n+1\cdots N}|\Psi_1\rangle\langle\Psi_1|$. It is convenient to write

$$|\Psi_1\rangle\langle\Psi_1| = \sum_{i=1}^{2^{\Delta_1}} |a_i|^2 \, |x_1^i \cdots x_N^i\rangle\langle x_1^i \cdots x_N^i| + \sum_{\substack{i,j=1 \\ i\neq j}}^{2^{\Delta_1}} a_i a_j^* \, |x_1^i \cdots x_N^i\rangle\langle x_1^j \cdots x_N^j|. \qquad (2.125)$$

Upon performing the partial trace over $|\Psi_1\rangle\langle\Psi_1|$, the first sum gives a diagonal contribution to the reduced density matrix

$$D_{11} = \sum_{i=1}^{2^{\Delta_1}} |a_i|^2 \, |x_1^i \cdots x_n^i\rangle\langle x_1^i \cdots x_n^i|. \qquad (2.126)$$

The second sum gives a correction

$$\tilde{D}_{11} = \sum_{\substack{i,j=1 \\ i\neq j}}^{2^{\Delta_1}} a_i a_j^* \, |x_1^i \cdots x_n^i\rangle\langle x_1^j \cdots x_n^j| \, \delta_{x_{n+1}^i, x_{n+1}^j} \cdots \delta_{x_N^i, x_N^j}. \qquad (2.127)$$

We now consider two cases:

(i) $\Delta_1 > n$.
    Because $2^{\Delta_1} \gg 2^n$, it is clear that D_{11} is a $2^n \times 2^n$ diagonal matrix with every diagonal entry approximately given by

$$\frac{2^{\Delta_1}}{2^n} \left\langle |a_i|^2 \right\rangle = 2^{-n}. \qquad (2.128)$$

   (Note that $\langle |a_i|^2 \rangle = 2^{-\Delta_1}$ because $|\Psi_1\rangle$ is normalized and random.) Thus, D_{11} is a fully mixed state. Now observe that $\tilde{D}_{11}$ consists of almost all zeros. In fact, looking at Eq. (2.127) we see that there are $2^{2\Delta_1 - N + n}$ nonzero entries of average absolute value $2^{-\Delta_1}$. Given that $\Delta_1 \leq N/2$, we conclude that $\tilde{D}_{11}$ has exponentially fewer nonzero entries than D_{11}, and that each nonzero entry has exponentially smaller size than the entries of D_{11}.

(ii) $\Delta_1 \leq n$.
    In this case, D_{11} is a diagonal matrix having 2^{Δ_1} nonzero entries of order $2^{-\Delta_1}$. The number of nonzero entries in $\tilde{D}_{11}$ is, again, $2^{2\Delta_1 - N + n}$, each having the average absolute value $2^{-\Delta_1}$. The effect of $\tilde{D}_{11}$ is highly suppressed because its number of nonzero entries

is exponentially smaller than that of D_{11}. In fact, for the number of nonzero entries in $\tilde{D}_{11}$ to compete with that in D_{11}, we would need $2\Delta_1 - N + n \geq \Delta_1$, which, however, mean

$$\Delta_1 \geq N - n > \frac{N}{2}, \tag{2.129}$$

a contradiction.

Summarizing, $\mathrm{Tr}_{n+1\cdots N}|\Psi_1\rangle\langle\Psi_1| = D_{11} + \tilde{D}_{11}$ is a diagonal matrix having $2^{\min\{\Delta_1,n\}}$ nonzero entries of order $2^{-\min\{\Delta_1,n\}}$, up to exponentially suppressed effects. The same analysis obviously applies to $\mathrm{Tr}_{n+1\cdots N}|\Psi_2\rangle\langle\Psi_2| = D_{22} + \tilde{D}_{22}$ with $\Delta_1 \to \Delta_2$.

We now turn our attention to the matrix $\mathrm{Tr}_{n+1\cdots N}|\Psi_1\rangle\langle\Psi_2|$, which we denote as $\tilde{D}_{12}$:

$$\tilde{D}_{12} = \sum_{i=1}^{2^{\Delta_1}}\sum_{j=1}^{2^{\Delta_2}} a_i b_j^* \, |x_1^i \cdots x_n^i\rangle\langle y_1^j \cdots y_n^j| \delta_{x_{n+1}^i, y_{n+1}^j} \cdots \delta_{x_N^i, y_N^j}. \tag{2.130}$$

We argue, along similar lines to the above, that $\tilde{D}_{12}$ is exponentially smaller than $|c_1|^2 D_{11} + |c_2|^2 D_{22}$, unless $|c_1|$ or $|c_2|$ is exponentially suppressed. Once again, we have several cases:

(i) $\Delta_1, \Delta_2 \leq n$.
In this case, $|c_1|^2 D_{11} + |c_2|^2 D_{22}$ is a diagonal matrix having 2^{Δ_1} nonzero entries of order $2^{-\Delta_1}$ and 2^{Δ_2} nonzero entries of order $2^{-\Delta_2}$. Considering Eq. (2.130), $\tilde{D}_{12}$ consists of zeros except for $2^{\Delta_1+\Delta_2-N+n}$ nonzero entries with the average absolute value $\langle|a_i b_j^*|\rangle = 2^{-(\Delta_1+\Delta_2)/2}$. The number of these entries, however, is exponentially smaller than 2^{Δ_1}, since having $\Delta_1 + \Delta_2 - N + n \geq \Delta_1$ would require $\Delta_2 \geq N - n > N/2$; similarly, it is also exponentially smaller than 2^{Δ_2}. Moreover the changes of the exponentially rare eigenvalues affected are at most of $O(1)$. We conclude that the effect of $\tilde{D}_{12}$ is exponentially suppressed.

(ii) $\Delta_1, \Delta_2 > n$.
In this case, the condition that $|c_1|^2 + |c_2|^2 = 1$ ensures that $|c_1|^2 D_{11} + |c_2|^2 D_{22}$ is a $2^n \times 2^n$ unit matrix multiplied by 2^{-n}. Meanwhile, $\tilde{D}_{12}$ consists of zeros except for $2^{\Delta_1+\Delta_2-N+n} \ll 2^n$ nonzero entries of size $2^{-(\Delta_1+\Delta_2)/2} \ll 2^{-n}$.

(iii) $\Delta_1 \leq n < \Delta_2$.
In this case, D_{22} is a $2^n \times 2^n$ unit matrix multiplied by 2^{-n} while D_{11} is a diagonal matrix having 2^{Δ_1} nonzero entries of order $2^{-\Delta_1}$. Once again, the number of nonzero entries in $\tilde{D}_{12}$ is exponentially smaller than 2^{Δ_1}, since $\Delta_1 + \Delta_2 - N + n \geq \Delta_1$ would require $\Delta_2 \geq N - n > N/2$, and the fractional corrections to eigenvalues from these entries are of order $2^{-(\Delta_2-n)}$. This implies that the effect of $\tilde{D}_{12}$ is negligible. The same argument also applies to the case that $\Delta_2 \leq n < \Delta_1$.

We conclude that for $n < N/2$, we find

$$\rho_{1\cdots n} = |c_1|^2 D_{11} + |c_2|^2 D_{22} = \sum_{i=1}^{2^{\Delta_1}} |a_i|^2 |x_1^i \cdots x_n^i\rangle\langle x_1^i \cdots x_n^i| + \sum_{i=1}^{2^{\Delta_2}} |b_i|^2 |y_1^i \cdots y_n^i\rangle\langle y_1^i \cdots y_n^i|,$$
(2.131)

up to effects exponentially suppressed in $N \approx O(\mathcal{A}_*)$. This implies that the reduced density matrix for the state $|\Psi\rangle$ takes the form of an incoherent classical mixture

$$\rho_{1\cdots n} = |c_1|^2 \rho_{1\cdots n}^{(1)} + |c_2|^2 \rho_{1\cdots n}^{(2)},$$
(2.132)

where $\rho_{1\cdots n}^{(k)} = \mathrm{Tr}_{n+1\cdots N} |\Psi_k\rangle\langle\Psi_k|$ $(k = 1, 2)$ are the reduced density matrices we would obtain if the state were $|\Psi_k\rangle$.

The form of Eq. (2.131) also implies that the entanglement entropy

$$S_{1\cdots n} = -\mathrm{Tr}_{1\cdots n}(\rho_{1\cdots n} \ln \rho_{1\cdots n}),$$
(2.133)

obeys a similar linear relation

$$S_{1\cdots n} = |c_1|^2 S_{1\cdots n}^{(1)} + |c_2|^2 S_{1\cdots n}^{(2)} + O(1),$$
(2.134)

unless $|c_1|$ or $|c_2|$ is exponentially small. Here, $S_{1\cdots n}^{(k)} = -\mathrm{Tr}_{1\cdots n}(\rho_{1\cdots n}^{(k)} \ln \rho_{1\cdots n}^{(k)})$. This can be seen by considering the same three cases as above. If $\Delta_1, \Delta_2 \leq n$, $\rho_{1\cdots n}$ is a diagonal matrix having 2^{Δ_1} nonzero entries with average value $|c_1|^2 2^{-\Delta_1}$ and 2^{Δ_2} nonzero entries with average value $|c_2|^2 2^{-\Delta_2}$. In this case,

$$S_{1\cdots n} = -|c_1|^2 \ln \frac{|c_1|^2}{2^{\Delta_1}} - |c_2|^2 \ln \frac{|c_2|^2}{2^{\Delta_2}} = |c_1|^2 \Delta_1 \ln 2 + |c_2|^2 \Delta_2 \ln 2 + O(1),$$
(2.135)

while we have $S_{1\cdots n}^{(k)} = \Delta_k \ln 2$. The $O(1)$ correction from linearity is the entropy of mixing, given by

$$S_{1\cdots n,\mathrm{mix}} = -|c_1|^2 \ln |c_1|^2 - |c_2|^2 \ln |c_2|^2.$$
(2.136)

If $\Delta_1, \Delta_2 > n$, then $\rho_{1\cdots n}$ is a unit matrix multiplied by 2^{-n}. From this it follows that $S_{1\cdots n} = n \ln 2 = |c_1|^2 n \ln 2 + |c_2|^2 n \ln 2$, which is desirable given that $S_{1\cdots n}^{(k)} = n \ln 2$ for $\Delta_k > n$.[23] Finally, if $\Delta_1 < n < \Delta_2$, $\rho_{1\cdots n}^{(1)}$ has 2^{Δ_1} nonzero entries of mean value $2^{-\Delta_1}$ while $\rho_{1\cdots n}^{(2)}$ is a unit matrix multiplied by 2^{-n}. Because $2^{-\Delta_1} \gg 2^{-n}$ the total density matrix $\rho_{1\cdots n}$ given by Eq. (2.131) is diagonal and has 2^{Δ_1} entries of size $|c_1|^2 2^{-\Delta_1}$ and 2^n entries of size $|c_2|^2 2^{-n}$. We thus find that $S_{1\cdots n} = |c_1|^2 \Delta_1 \ln 2 + |c_2|^2 n \ln 2 + S_{1\cdots n,\mathrm{mix}} = |c_1|^2 S_{1\cdots n}^{(1)} + |c_2|^2 S_{1\cdots n}^{(2)} + O(1)$. (This expression is valid for $\Delta_1 = n < \Delta_2$ as well.)

---

[23]The absence of the mixing contribution in this case is an artifact of the specific qubit model considered here, arising from the fact that two universes cannot be discriminated unless n is larger than one of $\Delta_{1,2}$; see Eq. (2.115). In realistic cases, the mixing contribution should always exist for any macroscopic region in the holographic space as two different universes can be discriminated in that region; see, e.g., Fig. 2.5.

Chapter 3

Butterfly Velocities for Holographic Theories of General Spacetimes

This chapter is a replication of Nomura and Salzetta, "Butterfly Velocities for Holographic Theories of General Spacetimes", in *JHEP* 10 (2017), p. 187, and is reproduced here in its original form.

3.1 Introduction

The quantum theory of gravity is expected to be formulated in a non-gravitational spacetime whose dimension is less than that of the bulk gravitational spacetime [37, 13, 22]. The holographic theories for general spacetimes are not explicitly known, but we expect that they are strongly coupled based on the known holographic correspondence between conformal field theories (CFT) and quantum gravity in asymptotically anti-de Sitter (AdS) spacetimes [14]. If cosmological spacetimes do indeed admit holographic descriptions, it is critical to find the appropriate dual theories in order to understand the quantum nature of gravity in our universe. In an effort to find such theories, we take a bottom-up approach and calculate quantities that can help identify them.

A particular quantity that characterizes a strongly coupled system is the butterfly velocity [105, 106, 107], which can be viewed as the effective speed of the spread of information relevant for an ensemble of states. Recently, Qi and Yang [108] generalized the concept to general subspaces of a Hilbert space, including a code subspace of a holographic theory [109, 110]. They then discussed its relationship to the causal structure of an emergent bulk theory.

In this paper, we investigate butterfly velocities in holographic theories of general spacetimes, described in Refs. [32, 111]. In particular, we calculate butterfly velocities for bulk local operators in the holographic theory of cosmological flat Friedmann-Robertson-Walker (FRW) spacetimes and analyze their properties. We find that they admit a certain universal scaling, independent of the fluid component and the dimension of the bulk spacetime. This emerges in the limit that the boundary region representing a bulk operator becomes small,

where we expect that the butterfly velocity reflects properties of the underlying theory.

We also provide an extension of the prescription of Ref. [108] for computing the butterfly velocity to include more general operators in the bulk. This generalization allows us to calculate the butterfly velocities of bulk local operators in some entanglement shadow regions.

Together with the monotonicity property of the change of the volume of the holographic space [44, 45, 46] and the behavior of the entanglement entropies of subregions of a holographic space [32, 30], our results provide important data for finding explicit holographic theories of general spacetimes. In particular, our results seem to indicate a certain relation between spatial and temporal scaling in the holographic theory of flat FRW spacetimes.

The organization of the paper is as follows. In Section 3.2, we define the butterfly velocity in holographic theories and discuss (extended) prescriptions of calculating it using the bulk effective theory. In Section 3.3, we compute butterfly velocities in the holographic theory of flat FRW universes and analyze their properties. In Section 3.4, we discuss possible implications of our results.

Throughout the paper, we take units where the bulk Planck length is unity. We assume that the bulk spacetime satisfies the null and causal energy conditions. These impose the conditions $\rho \geq -p$ and $|\rho| \geq |p|$, respectively, on the energy density ρ and pressure p of an ideal fluid component, so that the equation of state parameter, $w = p/\rho$, satisfies $|w| \leq 1$.

3.2 Definition of the Butterfly Velocity in Holographic Theories of General Spacetimes

We are interested in the spread of information in holographic theories of general spacetimes. The butterfly velocity is a quantity that characterizes the spread of correlations of operators acting within a certain subspace of a Hilbert space. In particular, we can restrict our attention to a code subspace of states in which observables correspond to operators acting within the bulk effective theory.

We work within the framework described in Ref. [32]. The theory is defined on the holographic spacetime, which for a fixed semiclassical bulk spacetime corresponds to a holographic screen [42], a special codimension-1 surface in the bulk. The holographic screen is uniquely foliated by surfaces called leaves; this corresponds to a fixed time slicing of the holographic theory. We study how the support of an operator dual to a bulk local operator spreads in time. In Section 5.3, we follow Ref. [108] and define the butterfly velocity in this context. We then describe how to calculate it using the bulk effective theory. We also discuss conceptual issues associated with this procedure. In Section 3.2, we extend the definition to include bulk operators in entanglement shadows.

Butterfly velocities on holographic screens

We are interested in how the support of a holographic representation of a bulk local operator, O, changes in time in the holographic theory.

This analysis is complicated by the fact that each bulk local operator can be represented
in multiple ways in the holographic space (which we may loosely refer to as the boundary,
borrowing from AdS/CFT language) [112, 113, 114]. For example, suppose the operator is
represented over the whole boundary, as in the global representation in AdS/CFT. There
is then no concept of the operator spreading in time. Following Ref. [108], we avoid this
issue by representing a bulk operator at a point p such that p is on the Hubeny-Rangamani-
Takayanagi (HRT) surface [48] of a subregion of the boundary. Specifically, we consider a
subregion A on a leaf σ_0 (not of an arbitrary spatial section of the holographic screen) and
represent a bulk local operator O located on the HRT surface, γ_A, of A. Based on intuition
arising from analyzing tensor network models [110, 115], we expect that such a representation
is unique. We denote the operator in the boundary theory represented in this way on A as
O_A.

We want to know the spatial region B on the leaf $\sigma_{\Delta t}$, which is in the future of σ_0 by
time Δt, such that every operator B supported on B satisfies

$$\langle\Psi_i|[O_A, B]|\Psi_j\rangle = 0. \tag{3.1}$$

Here, $|\Psi_i\rangle$ and $|\Psi_j\rangle$ are arbitrary states in the code subspace. Recall that there is a natural
way of relating regions on different leaves of a holographic screen [46]. The spatial coordinates
on $\sigma_{\Delta t}$ can be defined from those on σ_0 by following the integral curves of a vector field
orthogonal to every leaf on the holographic screen. We can then define the region A' on $\sigma_{\Delta t}$
corresponding to A on σ_0 by following such curves. This allows us to define the distance,
Δd, of the operator spread for each point q on the boundary, $\partial A'$, of A' as the distance from
q to the region B in the direction orthogonal to $\partial A'$.

For an arbitrary operator in A, there is no reason that the distance Δd is independent
of the location on $\partial A'$. The butterfly velocity can then be defined using the largest of Δd
along $\partial A'$ [108]:

$$v_B \equiv \max_{\theta_i} \frac{\Delta d}{\Delta t}, \tag{3.2}$$

where $\{\theta_i\}$ are the coordinates of q on $\partial A'$.

We now discuss how to calculate v_B using the bulk effective theory. For this, we must
understand how time evolved operators in the bulk are represented in the boundary theory.
More specifically, given a particular representation, O_A, of O in the holographic Hilbert
space, what representation of the time evolved bulk operator (within the light cone of p)
does the time evolution of O_A corresponds to? Without an explicit boundary theory it is
not possible to answer this question, but we can still make some headway using intuition.
First, we may expect that the region B on $\sigma_{\Delta t}$ (defined above) fully excludes A'. This is the
statement that the support of the operator does not shrink in any direction. Second, we want
the "minimal necessary extension" of the leaf subregion A. For instance, it seems unphysical
that a bulk operator represented on subregion A should immediately time evolve into the
full boundary representation of the future bulk operator. We thus seek the correspondingly
"maximal" region B whose entanglement wedge does not contain the interior of light cone

of p. Excluding the light cone ensures that no information can be sent in the bulk which
would compromise the commutativity between O_A and B within the code subspace.

From these considerations, we come up with two possible procedures for calculating the
butterfly velocity of a bulk operator at a point p:

1. Maximize the volume of subregion B' subject to the constraint that $A' \cap B' = \emptyset$ and
   that the entanglement wedge of B' does not contain the interior of the light cone of p.
   The resulting subregion then gives B.

2. Find the subregion B with the distance from ∂B to $\partial A'$ being both minimal and inde-
   pendent of the location on ∂B, again subject to the constraint that the entanglement
   wedge of B does not contain the light cone of p.

One can certainly consider other possibilities as well, but these are the two most intuitively
obvious candidates. However, we find that the first possibility leads to discontinuous behavior
of B as p moves across the tip of the HRT surface of a spherical cap region. We therefore
focus on the second possibility, which aligns with Ref. [108].[1]

Essentially, this possibility postulates that the support of the operator O_A spreads uni-
formly:

$$\frac{\partial \Delta d}{\partial \theta_i} = 0. \tag{3.3}$$

We assume that this is indeed the case. The prescription of calculating the butterfly velocity
can then be given explicitly as follows. We first consider a region $B'(\Delta \lambda)$ on $\sigma_{\Delta t}$ which is (i)
$\Delta \lambda$ away from A', i.e. the distance from any point on $\partial A'$ to $B'(\Delta \lambda)$ is $\Delta \lambda$ in the direction
orthogonal to $\partial A'$ and (ii) the entanglement wedge of $B'(\Delta \lambda)$ does not contain the interior
of the light cone of p. The butterfly velocity of O_A is then obtained by finding $B'(\Delta \lambda)$ with
the smallest $\Delta \lambda$

$$v_B = \min_{\Delta \lambda} \frac{\Delta \lambda}{\Delta t}. \tag{3.4}$$

Note that the resulting v_B depends on how the bulk operator O is represented initially, i.e.
A and the location of O on γ_A.

If the assumption of Eq. (3.3) is not valid in general, then our results for the "off-center"
operators, $f \neq 0$, in Section 3.3 (as well as any related results in Ref. [108]) would have to
be reinterpreted as representing something other than v_B defined in Eq. (3.2). However, our
results for the operators at the tip of the HRT surface, $f = 0$, are still correct in this case,
since Eq. (3.3) is guaranteed by the symmetry of the setup.

---

[1]It is possible that the validity of these procedures may be analyzed by explicitly calculating the boundary
dual of bulk local operators located on an HRT surface by using recently proposed methods of entanglement
wedge reconstruction [116, 117].

Bulk operators in entanglement shadows

In the prescription given in the previous subsection, the bulk operator O was on the HRT surface of a subregion A on a leaf. Motivated by the idea that a bulk local operator can be represented in the holographic theory not only at an intersection of HRT surfaces but also at an intersection of the edge of the entanglement wedges (associated with subregions of leaves) [111, 118], we expect that we can similarly calculate the butterfly velocity for an operator O_A corresponding to a bulk operator at a point p on the boundary of the entanglement wedge of A, $EW(A)$.

There is no obstacle in using either of the prescriptions detailed in the previous subsection, except now we take p to be on the edge of the entanglement wedge. In this case, we must be careful to exclude the entire light cone of p when finding B. We find that the behavior of v_B is qualitatively different depending on whether p is on the future or past boundary of $EW(A)$.

Suppose p is on the past boundary of $EW(A)$. In this case, $EW(B)$ is not limited by excluding the part of p's light cone infinitesimally close to p (as is the case when p is on γ_A), but by the part of the light cone that is just to the future of γ_A. Aside from this, there is no other new aspect compared with the case in which p is on γ_A. In particular, A' is forced to spread relative to A in both prescriptions.

There is, however, a subtlety when p is on the future boundary of $EW(A)$. This arises because $EW(\bar{A}')$ automatically excludes the light cone of points located on the future boundary of $EW(A)$. Here, $\bar{A}'$ is the complement of A' on $\sigma_{\Delta t}$. A direct application of the first prescription from the previous subsection would then result in a butterfly velocity of 0 for bulk operators at all points on the future boundary of $EW(A)$. This is due to the constraint that $A' \cap B = \emptyset$, forcing $v_B \geq 0$. This constant $v_B = 0$ behavior may encourage us to abandon the constraint, but doing so leads to severely discontinuous behavior of B. Namely, the resulting region B on $\sigma_{\Delta t}$ is independent of the original region A on σ_0, because B will always find the same global maximum.

The second prescription has more interesting behavior so long as we allow for the distance from ∂B to $\partial A'$ to be negative. Doing so, we see that B is now constrained by excluding the past light cone of p, and for the resulting B, $A' \cap B \neq \emptyset$, so that $v_B \leq 0$. This is interesting because as we move forward in the boundary time, we are actually tracking the past time evolution of a bulk local operator. The shrinking support of O_A could indicate that this is a finely tuned boundary operator.

This generalization to the boundary of entanglement wedges allows us to calculate the butterfly velocity of operator O_A representing a bulk local operator in an entanglement shadow, i.e. a spacetime region in which HRT surfaces do not probe.

3.3 Butterfly Velocities for the Holographic Theory of FRW Universes

In this section, we compute butterfly velocities for the holographic theory of (3+1)-dimensional flat Friedmann-Robertson-Walker (FRW) universes:

$$ds^2 = a^2(\eta)\left[-d\eta^2 + dr^2 + r^2(d\psi^2 + \sin^2\psi \, d\phi^2)\right], \tag{3.5}$$

where $a(\eta)$ is the scale factor with η being the conformal time. We mainly focus on the case in which a universe is dominated by a single ideal fluid component with the equation of state parameter $w = p/\rho$ with $|w| \leq 1$.

In Section 3.3, we derive an analytic expression for the butterfly velocity of a bulk local operator near the holographic screen. In Section 3.3, we numerically calculate the butterfly velocity for a bulk operator located at the tip of an HRT surface with an arbitrary depth. In Section 3.3, we extend the result of Section 3.3 to arbitrary spacetime dimensions.

Local operators near the holographic screen

Consider a spherical cap region

$$\Gamma : 0 \leq \psi \leq \gamma, \tag{3.6}$$

on the leaf at a time η_*, which is located at

$$r = \left.\frac{a(\eta)}{\dot{a}(\eta)}\right|_{\eta=\eta_*} \equiv r_*. \tag{3.7}$$

Following Ref. [32], we go to cylindrical coordinates:

$$\xi = r\sin\psi, \qquad z = r\cos\psi - r_*\cos\gamma, \tag{3.8}$$

in which the boundary of Γ, $\partial\Gamma$, is located at

$$\xi = r_*\sin\gamma \equiv \xi_*, \qquad z = 0. \tag{3.9}$$

In the case that $\gamma \ll 1$, i.e. $\xi_* \ll r_*$, the HRT surface anchored to $\partial\Gamma$ can be expressed in a power series form. Denoting the surface by η and z as functions of ξ, we find

$$\eta(\xi) = \eta_* + \eta^{(2)}(\xi) + \eta^{(4)}(\xi) + \cdots, \tag{3.10}$$
$$z(\xi) = 0, \tag{3.11}$$

where

$$\eta^{(2)}(\xi) = \frac{\dot{a}}{2a}(\xi_*^2 - \xi^2), \tag{3.12}$$

$$\eta^{(4)}(\xi) = -\frac{\dot{a}}{16a^3}(\xi_*^2 - \xi^2)\left\{4\dot{a}^2\xi_*^2 - a\ddot{a}(3\xi_*^2 - \xi^2)\right\}, \tag{3.13}$$
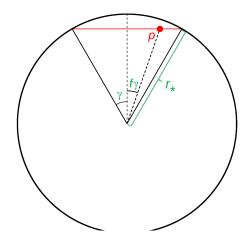
Figure 3.1: A local operator at p, represented by the dot, is on the HRT surface anchored to the boundary of a spherical cap region, $0 \leq \psi \leq \gamma$, on the leaf at time η_*, located at $r = r_*$. Note that the figure suppresses the time direction; for example, the operator is not at the same time as the leaf.

with

$$a \equiv a(\eta_*), \qquad \dot{a} \equiv \frac{da(\eta)}{d\eta}\bigg|_{\eta=\eta_*}, \qquad \ddot{a} \equiv \frac{d^2 a(\eta)}{d\eta^2}\bigg|_{\eta=\eta_*}. \tag{3.14}$$

We consider a bulk local operator on this surface.

We parameterize the location, p, of the operator by a single number f ($0 \leq f < 1$) representing how much fractionally the operator is "off the center," i.e. the operator is located on the surface

$$\psi = f\gamma, \tag{3.15}$$

with η and r determined by the condition that it is also on the HRT surface of Eq. (3.10); see Fig. 3.1. (The value of ϕ is arbitrary because of the symmetry of the problem; below we take $\phi = 0$ without loss of generality.) In cylindrical coordinates, this implies that the location of the operator, $(\eta, \xi, z) = (\eta_B, \xi_B, z_B)$, is given by

$$\eta_B = \eta_* + \frac{\dot{a}}{2a}(\xi_*^2 - \xi_B^2) - \frac{\dot{a}}{16a^3}(\xi_*^2 - \xi_B^2)\big\{4\dot{a}^2\xi_*^2 - a\ddot{a}(3\xi_*^2 - \xi_B^2)\big\}, \tag{3.16}$$

$$\xi_B = \frac{\tan(f\gamma)}{\tan\gamma}\xi_*, \tag{3.17}$$

$$z_B = 0, \tag{3.18}$$

where we have ignored the terms higher order than $\eta^{(4)}(\xi)$ in Eq. (3.10), which are not relevant for our leading order calculation. The future light cone associated with p is then given by

$$\eta = \eta_B + \sqrt{(x - \xi_B)^2 + y^2 + z^2}, \tag{3.19}$$

where we have introduced the coordinates $x = \xi \cos \phi$ and $y = \xi \sin \phi$.

In order to derive the butterfly velocity for the operator at p, we need to find the smallest spherical cap region on the leaf at $\eta = \eta_* + \delta\eta$

$$\Gamma' : 0 \leq \psi \leq \gamma + \delta\gamma, \tag{3.20}$$

so that the entanglement wedge associated with the complement of Γ' on the leaf does not contain the interior of the future light cone of p, Eq. (3.19). This occurs for the value of $\delta\gamma$ at which the HRT surface anchored to $\partial\Gamma'$

$$\begin{aligned}
\eta(\xi) =& \eta_* + \frac{\dot{a}}{2a}(\xi_*^2 - \xi^2) - \frac{\dot{a}}{16a^3}(\xi_*^2 - \xi^2)\left\{4\dot{a}^2\xi_*^2 - a\ddot{a}(3\xi_*^2 - \xi^2)\right\} \\
&+ \delta\eta - \frac{\dot{a}^2}{2a^2}\left(1 - \frac{a\ddot{a}}{\dot{a}^2}\right)(\xi_*^2 - \xi^2)\delta\eta \\
&+ \frac{\dot{a}}{a}\xi_*\delta\xi_* - \frac{\dot{a}}{4a^3}\left\{2\dot{a}^2(2\xi_*^2 - \xi^2) - a\ddot{a}(3\xi_*^2 - 2\xi^2)\right\}\xi_*\delta\xi_*, \tag{3.21}
\end{aligned}$$

$$z(\xi) = \left(1 - \frac{a\ddot{a}}{\dot{a}^2}\right)\cos\gamma\,\delta\eta - \frac{a}{\dot{a}}\sin\gamma\,\delta\gamma, \tag{3.22}$$

is tangent to the light cone. Here,

$$\delta\xi_* = \left(1 - \frac{a\ddot{a}}{\dot{a}^2}\right)\sin\gamma\,\delta\eta + \frac{a}{\dot{a}}\cos\gamma\,\delta\gamma, \tag{3.23}$$

and we have suppressed (some of) the terms that do not contribute to the leading order result.

The conditions for the tangency are given by[2]

$$\eta(x) = \eta_B + \sqrt{(x - \xi_B)^2 + y^2 + z(x)^2}, \tag{3.24}$$

$$\frac{d\eta(x)}{dx} = \frac{x - \xi_B}{\sqrt{(x - \xi_B)^2 + y^2 + z(x)^2}}, \tag{3.25}$$

$$y = 0, \tag{3.26}$$

where the functions $\eta(x)$ and $z(x)$ are given by Eqs. (3.21) and (3.22). These yield the relation between $\delta\eta$ and $\delta\gamma$

$$\delta\eta = \frac{\dot{a}^2}{4a^2}(3\xi_*^2 - 2\xi_B^2)\xi_*\delta\gamma, \tag{3.27}$$

as well as the location in which the HRT surface touches the light cone

$$x = \xi_B - \frac{\dot{a}}{a}\xi_*\xi_B\delta\gamma. \tag{3.28}$$

---

[2]We would like to thank Yiming Chen, Xiao-Liang Qi, and Zhao Yang for correcting the wrong tangency condition in a previous version. The results now agree with the monotonicity statement in Ref. [108], which we believed did not apply to our setup.
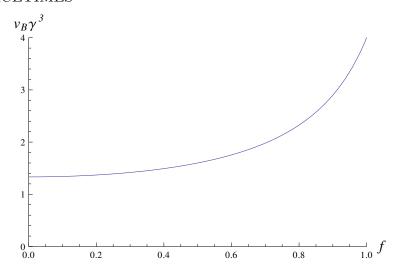
Figure 3.2: Butterfly velocity v_B multiplied by γ^3 as a function of f. Here, γ is the angular size of the leaf region, and f is the fractional displacement of the bulk local operator from the tip of the HRT surface; see Eq. (3.15).

Using Eq. (3.17), Eq. (3.27) becomes

$$\frac{\delta\gamma}{\delta\eta} = \frac{4\dot{a}}{a}\frac{1}{3-2f^2}\frac{1}{\gamma^3},\tag{3.29}$$

where we have used $\xi_* = \gamma a/\dot{a}$; see Eqs. (3.7) and (3.9). Representing the butterfly velocity v_B in terms of the coordinate distance along the holographic space, $\delta\lambda = r_*\delta\gamma$, and the conformal time, we finally obtain

$$v_B \equiv \frac{\delta\lambda}{\delta\eta} = \frac{4}{3-2f^2}\frac{1}{\gamma^3}.\tag{3.30}$$

There are several features one can see in Eq. (3.30). First, the butterfly velocity is non-negative, $v_B \geq 0$, as expected. Second, for $\gamma \ll 1$, which we are focusing on here, the butterfly velocity is much faster than the speed of light. In fact, it diverges as $\gamma \to 0$ with the specific power of γ^{-3}. When the operator is at the tip of the HRT surface, i.e. $f = 0$, the butterfly velocity takes the particularly simple form

$$v_B|_{f=0} = \frac{4}{3}\frac{1}{\gamma^3}.\tag{3.31}$$

In Fig. 3.2, we plot $v_B\gamma^3$ as a function of f. We find that the butterfly velocity increases as the operator moves closer to the holographic screen:

$$\frac{dv_B}{df} = \frac{16f}{(3-2f^2)^2}\frac{1}{\gamma^3} > 0.\tag{3.32}$$

This is consistent with the monotonicity result in Ref. [108].

It is interesting that the scale factor has completely dropped out from the final expression of Eq. (3.30). This implies that regardless of the content of the universe, the short distance behavior of the butterfly velocity is universal in the holographic theory of flat FRW spacetimes. As we will see in the next subsection, the butterfly velocity's dependence on the scale factor appears as we move away from the $\gamma \ll 1$ limit. This suggests that the details of the FRW bulk physics are related with long distance effects in the holographic theory.

Local operators at arbitrary depths

Beyond the $\gamma \ll 1$ limit, we must resort to a numerical method in order to solve for the butterfly velocity. For this purpose, we focus on the case in which the universe is dominated by a single ideal fluid component with the equation of state parameter w. In this case, the scale factor behaves as

$$a(\eta) \propto \left\{ \begin{array}{l} \eta^{\frac{2}{1+3w}} \\ e^{c\eta} \; (c > 0) \end{array} \right. \qquad \text{for} \quad \eta \left\{ \begin{array}{l} \neq -\frac{1}{3} \\ = -\frac{1}{3} \end{array} \right. . \tag{3.33}$$

When the universe is dominated by a single fluid component, the butterfly velocity v_B, expressed in terms of angle γ, does not depend on time η. This can be seen by using appropriate coordinate transformations, in a way analogous to the argument in Section III A 1 of Ref. [32] showing that a screen entanglement entropy normalized by the leaf area does not depend on time.

In Fig. 3.3, we show the results of our numerical calculations of the butterfly velocity, v_B, as a function of γ for a bulk operator located on the tip of the HRT surface, $f = 0$, for $w = 1, 1/3, 0, -1/3$, and $-2/3$. We find that beyond $\gamma \ll 1$, the butterfly velocity deviates from the limiting expression of Eq. (3.31), which is depicted by the dashed curve. In fact, the functional form of $v_B|_{f=0}(\gamma)$ is not universal and depends on w.

We find that for sufficiently large values of w the butterfly velocity $v_B|_{f=0}$ is always faster than the speed of light (depicted by the horizontal dashed line), while for smaller values of w it can be slower than the speed of light for γ close to $\pi/2$ (i.e. when the subregion on the leaf becomes large, approaching a hemisphere). The boundary between the two behaviors lies at $w = -1/3$, when the expansion of the universe changes between deceleration and acceleration.

Arbitrary spacetime dimensions

There is no obstacle in performing the same calculations as in the previous subsections in arbitrary spacetime dimensions. Here we present the analytic results corresponding to those in Section 3.3 for $(d+1)$-dimensional flat FRW universes.

The butterfly velocity, corresponding to Eq. (3.30), is given by

$$v_B = \frac{2}{\frac{d+3}{d+1} - f^2} \frac{1}{\gamma^3}. \tag{3.34}$$
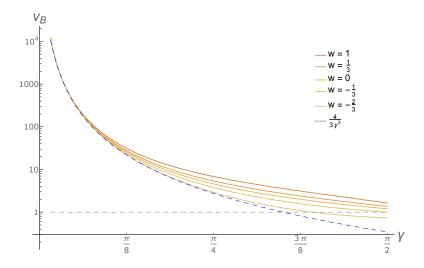
Figure 3.3: Butterfly velocity v_B of a bulk local operator at the tip of the HRT surface, $f = 0$, as a function of the angular size γ of the leaf region for $w = 1$, $1/3$, 0, $-1/3$, and $-2/3$ (solid curves, from top to bottom). The dashed curve represents $v_B = 4/3\gamma^3$, the analytic result obtained for $\gamma \ll 1$ in Eq. (3.31). The horizontal dashed line represents the speed of light.

Again, this is non-negative and does not depend on the scale factor. We also find that the exponent of γ is universal

$$v_B \sim \frac{1}{\gamma^3}, \tag{3.35}$$

regardless of the spacetime dimension. The f dependence of v_B is given by

$$\frac{dv_B}{df} = \frac{4f}{\left(\frac{d+3}{d+1} - f^2\right)^2}\frac{1}{\gamma^3} > 0, \tag{3.36}$$

which is consistent with the monotonicity result of Ref. [108].

3.4   Discussion

Our investigation has used a definition of butterfly velocity that differs from that in the literature regarding lattice systems and spin chains. The main difference is that in our case, the excitations of concern (in the boundary theory) are not local operators. They have support on a large subregion of the space. This is in contrast to the lattice definition which considers commutators of local operators separated in space and time. But the conceptual overlap is clear; we are concerned with when and where operators commute. The investigation of this paper allows us to find the effective "light cone" in the holographic theory.

Sending $\gamma \to 0$ would correspond to a local operator in the holographic theory, and the result that the butterfly velocity diverges in this limit may seem to indicate that the holographic theory is highly nonlocal. However, this is not necessarily the case, as the divergent velocity is integrable. By setting $f = 0$ in Eq. (3.34) and converting λ to γ (see, e.g., Eqs. (3.29) and (3.30)), we obtain

$$\frac{d\gamma}{d\eta} = \frac{q_d}{\eta} \frac{2(d+1)}{(d+3)\gamma^3},\tag{3.37}$$

where $q_d = 2/(d - 2 + dw)$. From this expression, we find

$$\gamma(t_H) = \left[\frac{8(d+1)}{d+3} t_H \right]^{\frac{1}{4}},\tag{3.38}$$

where $t_H = q_d \ln(\eta/\eta_i)$, the number of Hubble times elapsed since the excitation. This shows that the light cone spreads like $t^{1/4}$, regardless of dimension.

Sub-linear growth like this is not an uncommon phenomenon in physics. A localized heat source subject to the heat equation will diffuse as $t^{1/2}$. Even spin chain systems where the Lieb-Robinson bound applies (and suggests a linear dispersion) can admit power law behavior for the effective growth of operators [119]. The specific relationship of $\Delta x \sim \Delta t^{1/4}$ suggests that we should be looking for a theory with dynamical exponent $z = 4$, and the fact that this holds regardless of spacetime dimension may indicate that a Lifshitz field theory with $z = 4$ is the appropriate dual theory for flat FRW spacetimes. Note that results from Ref. [108] show that $v_B \to 1$ as $\gamma \to 0$ for asymptotically AdS spacetimes. Similarly analyzing this result would suggest that a $z = 1$ theory is the appropriate dual for AdS, as is indeed the case. These ideas will be investigated in future work.

Chapter 4

Spacetime from Unentanglement

This chapter is a replication of Nomura, Rath, and Salzetta, "Spacetime from Unentanglement", in: *Phys. Rev.* D97.10 (2018), p. 106010, and is reproduced here in its original form.

4.1   Introduction

It is believed that dynamical spacetime described by general relativity is an emergent phenomenon in the fundamental theory of quantum gravity. Despite this pervasive idea, the materialization of spacetime itself is not fully understood. Holography posits that a fundamental description of quantum gravity resides in a non-gravitational spacetime whose dimension is less than that of the corresponding bulk spacetime [37, 13, 22]. In this paper, we study the emergence of gravitational spacetime in the context of holography, using the renowned anti-de Sitter (AdS)/conformal field theory (CFT) correspondence [14] and a putative holographic theory of Friedmann-Robertson-Walker (FRW) spacetimes [32].

   In this paper, we expound on the intimate relationship between the emergence of spacetime and the lack of maximal entanglement in the boundary state. Through this, we see that the existence of spacetime is necessarily non-generic and that nature seizes the opportunity to construct local spacetime when states deviate from maximal entanglement. A reason why this viewpoint is not heavily emphasized (see, however, e.g. Refs. [111, 120]) in the standard context of AdS/CFT is that one almost always considers states with energy much lower than the cutoff (often sent to infinity). The restriction to these "low energy" states implicitly narrows our perspective to those automatically having non-maximal entropy. However, in a holographic theory with a finite cutoff scale (or a fundamentally nonlocal theory), the regime of maximal entropy is much more readily accessible. This happens to be the case in FRW holography, and perhaps holography in general. Through this lens, we analyze the emergence of spacetime both in the familiar setting of Schwarzschild-AdS spacetime with an infrared cutoff and in flat FRW universes. We explicitly see that the directly reconstructable region of spacetime [111, 118] emerges only as we deviate from maximally entangled states. This

implies that a holographic theory of exact de Sitter space cannot be obtained as a natural limit of theories dual to FRW spacetimes by sending the fluid equation of state parameter, w, to -1. In addition to analyzing these two examples, we prove a theorem demonstrating the lack of directly reconstructable spacetime in the case that a boundary state is maximally entangled.

After surveying the relationship between spacetime and (the lack of) entanglement, we then analyze the deviation from maximal entropy itself. The size of the subregions for which deviations occur reveals valuable information about the underlying holographic theory, and observing the corresponding emergence of spacetime in the bulk provides a glimpse into the mechanism by which nature creates bulk local degrees of freedom. In the case of Schwarzschild-AdS, reconstructable spacetime (the region between the horizon and the cutoff) appears as the temperature in the local boundary theory (the CFT) is lowered, and the resulting entanglement entropy structure (calculated holographically) is consistent with a local theory at high temperature. However, this entanglement structure is not observed in the case of FRW spacetimes as we adjust w away from -1; additionally, the reconstructable region grows from the deepest points in the bulk outward. This suggests that the manner in which entanglement is scaffolded is unlike that of AdS/CFT. In fact, this aberrant behavior leads us to believe that the holographic theory dual to FRW spacetimes has nonlocal interactions.

The relationship between spacetime and quantum entanglement between holographic degrees of freedom is no secret [16, 48, 24, 49, 28, 29, 30], but what *is* spacetime? Undoubtedly, entanglement is a necessity for the existence of spacetime. But, it is indeed possible to have too much of a good thing. The analysis here exposes the inability to construct spacetime from maximally entangled boundary states. Since typical states in a Hilbert space are maximally entangled [75], this implies that states with bulk dual are not typical. We see that spacetime is an emergent property of non-generic states in the Hilbert space with both non-vanishing and non-maximal entanglement for subregions. The existence of entanglement allows for the construction of a code subspace of states [109] in which local, semi-classical bulk degrees of freedom can be encoded redundantly. Simultaneously, the lack of maximal entanglement allows for a code subspace with subsystem recovery—hence partitioning the bulk into a collection of local Hilbert spaces. With this perspective, we see that holographic theories are exceedingly enterprising—once deviating from maximal entanglement, nature immediately seizes the opportunity to construct spacetime. In this sense, spacetime is the byproduct of nature's efficient use of intermediate entanglement to construct codes with subsystem recovery.

For a given spacetime with a holographic boundary, one can calculate the von Neumann entropies for all possible subregions of the boundary via the Hubeny-Rangamani-Ryu-Takayanagi (HRRT) prescription [16, 48, 30]. The corresponding entanglement structure heavily constrains the possible boundary states, but by no means uniquely specifies it. In fact, given an entanglement structure and a tensor product Hilbert space, one can always find a basis for the Hilbert space in which all basis states have the desired entanglement structure. If one considers each of these basis states to be dual to the spacetime reproduc-

ing the entanglement, then by superpositions one could entirely change the entanglement structure, and hence the spacetime. This property naturally raises the question of how the boundary Hilbert space can accommodate states dual to different semiclassical geometries. Fortunately, for generic dynamical systems, the Hilbert space can be binned into energy bands, and canonical typicality provides us with the result that generic states *within these bands* have the same entanglement structure, regardless of the energy band's size. This allows the holographic Hilbert space to contain states dual to many different spacetimes, each of which can have bulk excitations encoded state independently. Importantly, this is contingent on the result that typical states have no spacetime.

Outline

Section 4.2 walks through the statement that maximally entangled (and hence typical) states have no reconstructable spacetime. This is broken down into parts. First, we must define what we mean by reconstructable; this is detailed in Section 4.2, and is very important toward understanding the framework of the rest of the paper. We then use this construction in Section 4.2 to investigate the reconstructable region of AdS with a black hole. We see the expected behavior that the reconstructable region of spacetime vanishes as the temperature of the black hole reaches the cutoff scale, making the state typical. In Section 4.2, we show that de Sitter states are maximally entangled by finding their HRRT surfaces. In Section 4.2, we combine numerical results for flat FRW universes and use the additional property that de Sitter's HRRT surfaces lie on a null cone to show that the reconstructable region vanishes in the de Sitter limit of FRW spacetimes. Motivated by these results, in Section 4.2 we prove a theorem showing that if a state is maximally entangled, then its HRRT surfaces either wrap the holographic space or live on the null cone. This is then used to present the general argument that maximally entangled states have no spacetime.

Section 4.3 compares the emergence of spacetime in the two theories we are considering. Sections 4.3 and 4.3 present results comparing the entanglement structure of AdS black holes and FRW spacetimes, respectively. Section 4.3 interprets these results and argues that the appropriate holographic dual of FRW spacetimes is most likely nonlocal.

In Section 4.4, we put together all of the previous results and explain how one Hilbert space can contain states dual to many different semiclassical spacetimes. Here we discuss the lack of a need for state dependence when describing the directly reconstructable region.

In Appendix 4.6, we analyze two-sided black holes within our construction and discuss how a version of complementarity works in this setup. Appendices 4.6 and 4.6 collect explicit calculations for Schwarzschild-AdS and the de Sitter limit of FRW spacetimes, respectively.

4.2 Maximally Entropic States Have No Spacetime

In this section, we see that maximally entangled states in holographic theories do not have directly reconstructable spacetime. First we lay out the conditions for reconstructability

in general theories of holographic spacetimes. Then we examine the familiar example of a large static black hole in AdS and determine its reconstructable region. We then discuss the de Sitter limit of flat FRW spacetimes. Finally, we prove a theorem establishing that maximally entropic holographic states have no reconstructable spacetime.

Holographic reconstructability

In order to argue that typical states have no reconstructable region, we must first present the conditions for a region of spacetime to be reconstructed from the boundary theory. We adopt the formalism presented first in Ref. [118] but appropriately generalized in Ref. [111] to theories living on holographic screens [42] (which naturally includes the boundary of AdS as in the AdS/CFT correspondence).

The question to answer is: "given a boundary state and its time evolution with a known gravitational bulk dual, what regions of the bulk can be reconstructed?" This may sound tautological, but it is not. Settings in which this question is nontrivial include spacetimes with black holes and other singularities. From entanglement wedge reconstruction [27, 114], we know that the information of a pure black hole is contained in the boundary theory but whether or not the interior is reconstructable is unknown. In holographic theories of general spacetimes, we are interested in describing spacetimes with big bang singularities and a natural question is whether or not the theory reconstructs spacetime arbitrarily close to the initial singularity.

To answer this question, Ref. [118] proposed that reconstructable points in a spacetime are precisely those that can be localized at the intersection of entanglement wedges. This is similar to the proposal in Ref. [121] which advocates that reconstructable points are those located at the intersection of HRRT surfaces anchored to arbitrary achronal subregions of the AdS conformal boundary. However, this construction lacks the ability to localize points in entanglement shadows, which can form in rather tame spacetimes (e.g. a neutron star in AdS), while using the intersection of entanglement wedges allows us to probe these regions.

In order to generalize this to theories living on holographic screens, an essential change is that one can only consider HRRT surfaces anchored to the leaves of a given holographic screen (usually associated to a fixed reference frame) [111]. This is because holographic screens have a unique foliation into leaves that corresponds to a particular time foliation of the holographic theory. Thus the von Neumann entropy of subregions in the holographic theory only makes sense for subregions of a single leaf. Note that despite the lack of a unique time foliation of the conformal boundary, this subtlety is also present in AdS/CFT. Namely, one should consider only a single time foliation of the boundary and the HRRT surfaces anchored to the associated equal time slices even in asymptotically AdS spacetimes [111].[1] This issue becomes manifest when the boundary contains multiple disconnected components, as we discuss in Appendix 4.6.

---

[1]This is related to the work in Ref. [122], which studied the breakdown of the HRRT formula in certain limits of boundary subregions. These breakdowns correspond to disallowed foliations of the boundary theory.

Thus we define the reconstructable region of a spacetime as the union of all points that can be localized at the boundary of entanglement wedges of all subregions of leaves of the holographic screen. Henceforth, we will refer to the regions of spacetime constructed in this way as the directly reconstructable regions (or simply the reconstructable regions when the context is clear), and our analysis will primarily focus on these regions. For a more detailed study of directly reconstructable regions in general spacetimes, see Ref. [111]. In particular, this definition only allows for the reconstruction of points outside the horizon for a quasi-static one-sided black hole, since such a horizon acts as an extremal surface barrier [123].[2] This also prevents the direct reconstruction of points near singularities such as big bang singularities and the black hole singularity of a two-sided black hole.

Now that we have detailed the conditions for regions of spacetime to be directly reconstructable, we must determine a measure of "how much" spacetime is reconstructable. This will allow us to see the loss of spacetime in the limit of states becoming typical. In the context of quantum error correction [109], we are attempting to quantify the factorization of the code subspace, e.g. how many dangling bulk legs exist in a tensor network representation of the code [110, 115]. We expect the spacetime volume of the reconstructable region to be indicative to this property, and we will use it in our subsequent analyses. The bulk spacetime directly reconstructable from a single leaf depends on features of the bulk, for example, the existence of shadows and time dependence. In the case of $(d + 1)$-dimensional flat FRW spacetimes, we find that a codimension-0 region can be reconstructed from a single leaf. On the other hand, in any static spacetime, all HRRT surfaces anchored to one leaf live in the same time slice in the bulk, and hence their intersections reconstruct a codimension-1 surface of the bulk. This is the case in an AdS black hole.

The discrepancy of the dimensions of the directly reconstructable regions for different spacetimes of interest may seem to cause issues when trying to compare the loss of spacetime in these systems. Namely, it seems difficult to compare the loss of reconstructable spacetime in Schwarzschild-AdS as we increase the black hole mass to the loss of spacetime in the $w \to -1$ limit of flat FRW spacetimes. However, in all cases, the spacetime region directly reconstructable from a small time interval in the boundary theory is codimension-0. We can then examine the relative loss of spacetime in both cases (black hole horizon approaching the boundary in AdS space and $w \to -1$ in FRW spacetimes) by taking the ratio of the volume of the reconstructable region to the reconstructable volume of some reference state (e.g. pure AdS and flat FRW with some fixed $w \neq -1$). In static spacetimes, this will reduce to a ratio of the spatial volumes reconstructed on a codimension-1 slice, allowing us to consider only the volume of regions reconstructed from single leaves.

---

[2]This does not exclude the possibility that the holographic theory allows for some effective description of regions other than the directly reconstructable one, e.g. the black hole interior (perhaps along the lines of Ref. [59]). This may make the interior spacetime manifest, perhaps at the cost of losing the local description elsewhere, and may be necessary to describe the fate of a physical object falling into a black hole. We focus on spacetime regions that can be described by the boundary theory without resorting to such descriptions.

Large AdS black holes

Here we will see how spacetime disappears as we increase the mass of the black hole in static Schwarzschild-AdS spacetime, making the corresponding holographic state maximally entangled. We consider a holographic pure state living on the (single) conformal boundary of AdS. We introduce an infrared cutoff $r \leq R$ in AdS space and consider a $d+1$ dimensional large black hole with horizon radius $r = r_+$.

As discussed in Section 4.2, the size of the spacetime region directly reconstructable from the boundary theory is characterized by $V(r_+, R)$, the spatial volume between the black hole horizon and the cutoff. We normalize it by the volume of the region $r \leq R$ in empty AdS space, $V(R)$, to get the ratio

$$f\left(\frac{r_+}{R}\right) \equiv \frac{V(r_+, R)}{V(R)} = (d-1)\frac{r_+^{d-1}}{R^{d-1}} \int_1^{\frac{R}{r_+}} \frac{x^{d-2}}{\sqrt{1 - \frac{1}{x^d}}}\, dx, \tag{4.1}$$

which depends only on r_+/R (and d). As expected, it behaves as

$$f\left(\frac{r_+}{R}\right) \begin{cases} \simeq 1 & (r_+ \ll R) \\ \to 0 & (r_+ \to R), \end{cases} \tag{4.2}$$

in the two opposite limits. The details of this calculation can be found in Appendix 4.6. Here, we plot $f(r_+/R)$ in Fig. 4.1 for various values of d.

In the limit $r_+ \to R$, the HRRT surface, γ_A, anchored to the boundary of subregion A of a boundary space (a constant t slice of the $r = R$ hypersurface) becomes the region A itself or the complement, $\bar{A}$, of A on the boundary space, whichever has the smaller volume.[3] This implies that the entanglement entropy of A, given by the area of the HRRT surface as $S_A = \|\gamma_A\|/4l_{\mathrm{P}}^{d-1}$, becomes exactly proportional to the smaller of the volumes of A and $\bar{A}$ in the boundary theory:

$$S_A = \frac{1}{4l_{\mathrm{P}}^{d-1}} \min\{\|A\|, \|\bar{A}\|\}. \tag{4.3}$$

Here, $\|x\|$ represents the volume of the object x (often called the area for a codimension-2 surface in spacetime), and l_{P} is the $(d+1)$-dimensional Planck length in the bulk. Via usual thermodynamic arguments, we interpret this to mean that the state in the boundary theory is generic, so that it obeys the Page law [75].[4] This in turn implies that the temperature of the system, which is identified as the Hawking temperature T_{H}, is at the cutoff scale.[5] T_{H} is

---

[3]We do not impose a homology constraint, since we consider a pure state in the holographic theory. Additionally, we only consider subregions larger than the cutoff size.

[4]Page's analysis tells us that for a generic state (a Haar random state) in a Hilbert space, the entanglement entropy of a reduced state is nearly maximal. In fact, at the level of the approximation we employ in this paper, $\|A\|/l_{\mathrm{P}}^{d-1} \to \infty$, such a state has the maximal entanglement entropy for any subregion, Eq. (4.3).

[5]When we refer to a high temperature state, we do not mean that the whole holographic state is a mixed thermal state. What we really mean is a high energy state, since we focus on pure states.
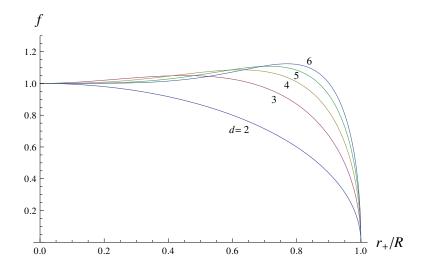
Figure 4.1: The volume $V(r_+, R)$ of the Schwarzschild-AdS spacetime that can be reconstructed from the boundary theory, normalized by the corresponding volume $V(R)$ in empty AdS space: $f = V(r_+, R)/V(R)$. Here, R is the infrared cutoff of $(d+1)$-dimensional AdS space, and r_+ is the horizon radius of the black hole.

related to r_+ by

$$\frac{r_+}{R} = \frac{4\pi l^2}{dR} T_{\mathrm{H}}, \tag{4.4}$$

where l is the AdS radius. Hence, the cutoff scale of the boundary theory is given by [124]

$$\Lambda = \frac{dR}{4\pi l^2}. \tag{4.5}$$

This allows us to interpret the horizontal axis of Fig. 4.1 as T_{H}/Λ from the viewpoint of the boundary theory.

We finally make a few comments. First, it is important to note that by the infrared cutoff, we do not mean that the spacetime literally ends there as in the scenario of Ref. [125]. Such termination of spacetime would introduce dynamical gravity in the holographic theory, making the maximum entropy of a subregion scale as the area, rather than the volume, in the holographic theory. Rather, our infrared cutoff here means that we focus only on the degrees of freedom in the bulk deeper than $r = R$, corresponding to setting the sliding renormalization scale to be $\approx R/l^2$ in the boundary theory. In particular, the boundary theory is still non-gravitational.

Second, to state that spacetime disappears in the limit where the holographic state becomes typical, it is crucial to define spacetime as the directly reconstructable region. This becomes clear by considering a large subregion A on the boundary theory such that A and its HRRT surface γ_A enclose the black hole at the center. If we take the simple viewpoint of

entanglement wedge reconstruction, this would say that spacetime does not disappear even if the black hole becomes large and its horizon approaches the cutoff surface, since the black hole interior is within the entanglement wedge of A so that it still exists in the sense of entanglement wedge reconstruction. We, however, claim that such a region does not exist as a localizable spacetime region, as explained in Section 4.2.

Third, the curves in Fig. 4.1 are not monotonically decreasing as r_+ increases for $d > 2$, despite the fact that

$$\frac{d}{dr_+}\big\{S_{A,\text{max}} - S_{A,\text{BH}}(r_+)\big\} < 0. \tag{4.6}$$

Here, $S_{A,\text{max}}$ and $S_{A,\text{BH}}(r_+)$ are the maximal entropy and the entropy corresponding to the black hole geometry of subregion A, given by

$$S_{A,\text{max}} = \frac{\|A\|}{4l_{\text{P}}^{d-1}}, \qquad S_{A,\text{BH}}(r_+) = \frac{\|A\|}{4l_{\text{P}}^{d-1}}\frac{r_+^{d-1}}{R^{d-1}}. \tag{4.7}$$

This increase in spacetime volume may be demonstrating that the additional entanglement in the boundary state allows for more bulk nodes in the code subspace. Alternatively, this may be a feature of using volume as our measure. Regardless, the decrease observed near the cutoff temperature is the main focus of our attention, and we expect any other reasonable measure to correspondingly vanish.

Finally, the statement that spacetime disappears as the holographic state approaches typicality persists for two-sided black holes. In this setup, there is a new issue that does not exist in the case of single-sided black holes: the choice of a reference frame associated with a relative time shift between the two boundaries. The discussion of two-sided black holes is given in Appendix 4.6.

de Sitter states are maximally entropic

We have seen that a large black hole in AdS with $r_+ \to R$ corresponds to CFT states at the cutoff temperature, and that the holographic states in this limit have the entanglement entropy structure of Eq. (4.3). Below, we refer to states exhibiting Eq. (4.3) as the *maximally entropic states*. Is there an analogous situation in the holographic theory of FRW spacetimes, described in Ref. [32]? Here we argue that the de Sitter limit ($w \to -1$) in flat FRW universes provides one.[6]

We first see that the holographic state becomes maximally entropic in the case that a universe approaches de Sitter space at late times [30]. This situation arises when the universe contains multiple fluid components including one with $w = -1$, so that it is dominated by the $w = -1$ component at late times. This analysis does not apply directly to the case of a single component with $w = -1 + \epsilon$ ($\epsilon \to 0^+$), which will be discussed later.

---

[6]For a simple proof applicable to $2 + 1$ dimensions, see Appendix 4.6.
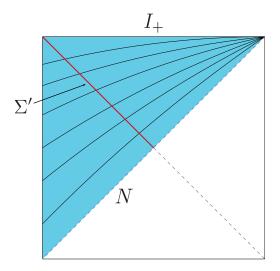
Figure 4.2: The Penrose diagram of de Sitter space. The spacetime region covered by the flat-slicing coordinates is shaded, and constant time slices in this coordinate system are drawn. The codimension-1 null hypersurface Σ' is the cosmological horizon for an observer at $r = 0$, to which the holographic screen of the FRW universe asymptotes in the future.

In the universe under consideration, the FRW metric approaches the de Sitter metric in flat slicing at late times

$$ds^2 = -dt^2 + e^{\frac{2t}{\alpha}}\left(dr^2 + r^2 d\Omega_{d-1}^2\right), \tag{4.8}$$

where α is the Hubble radius, and we have taken the spacetime dimension of the bulk to be $d + 1$. The Penrose diagram of this spacetime is depicted in Fig. 4.2, where constant time slices are drawn and the region covered by the coordinates is shaded; future timelike infinity I_+ corresponds to $t = \infty$, while the null hypersurface N corresponds to $t = -\infty$. At late times, the past holographic screen of the FRW universe asymptotes to the codimension-1 null hypersurface Σ' depicted in the figure. This hypersurface is located at

$$r = \alpha\, e^{-\frac{t}{\alpha}}, \tag{4.9}$$

which corresponds to the cosmological horizon for an observer moving along the $r = 0$ geodesic.

We can now transform the coordinates to static slicing

$$ds^2 = -\left(1 - \frac{\rho^2}{\alpha^2}\right)d\tau^2 + \frac{1}{1 - \frac{\rho^2}{\alpha^2}}d\rho^2 + \rho^2 d\Omega_{d-1}^2. \tag{4.10}$$

In Fig. 4.3, we depict constant τ (red) and constant ρ (blue) slices, with the shaded region being covered by the coordinates. This metric makes it manifest that the spacetime has a Killing symmetry corresponding to τ translation. Using this symmetry, we can map a leaf
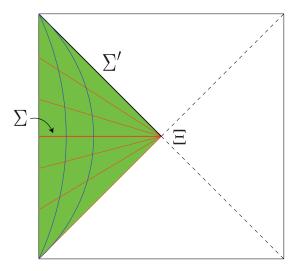
Figure 4.3: Constant time slices and the spacetime region covered by the coordinates in static slicing of de Sitter space. Here, Σ is the $\tau = 0$ hypersurface, and Ξ is the bifurcation surface, given by $\rho = \alpha$ with finite τ.

of the original FRW universe to the $\tau = 0$ hypersurface, Σ. Since the leaf of the universe under consideration approaches arbitrarily close to Eq. (4.9) at late times, the image of the map, Ξ', asymptotes to the bifurcation surface Ξ at

$$\rho = \alpha, \tag{4.11}$$

for a leaf at later times.

Consider an arbitrary subregion A on Ξ' and the minimal area surface γ_A on Σ anchored to the boundary of A, ∂A. Since the geometry of Σ is S^d with Ξ being an equator, the minimal area surface γ_A becomes the region A itself (or its complement on Ξ', whichever is smaller) in the limit $\Xi' \to \Xi$. Strictly speaking, this statement does not apply for a small subset of subregions, since Ξ' is not exactly Ξ unless the leaf under consideration is at strictly infinite time. (For subregions in this subset, the minimal area surfaces probe $\rho \ll \alpha$. For spherical caps, these subregions are approximately hemispheres.) However, the fractional size of the subset goes to zero as we focus on later leaves. Continuity then tells us that our conclusion persists for all subregions.

The surface γ_A found above is in fact an extremal surface, since the bifurcation surface Ξ is an extremal surface, so any subregion of it is also extremal. It is easy to show that this surface is indeed the HRRT surface, the minimal area extremal surface. Suppose there is another extremal surface γ'_A anchored to ∂A. We could then send a null congruence from γ'_A down to Σ, yielding another codimension-2 surface γ''_A given by the intersection of the null congruence and Σ. Because γ'_A is extremal, the focusing of the null rays implies $\|\gamma'_A\| > \|\gamma''_A\|$,

and by construction $\|\gamma_A\| < \|\gamma_A''\|$. This implies that γ_A is the HRRT surface, and hence

$$S_A = \frac{1}{4l_{\mathrm{P}}^{d-1}}\min\{\|A\|, \|\bar{A}\|\}. \tag{4.12}$$

Namely, the holographic state representing an FRW universe that asymptotically approaches de Sitter space becomes a maximally entropic state in the late time limit.

The global spacetime structure in the case of a single fluid component with $w \neq -1$ is qualitatively different from the case discussed above. For example, the area of a leaf grows indefinitely. However, for any finite time interval, the behavior of the system approaches that of de Sitter space in the limit $w \to -1$. In fact, the numerical analysis of Ref. [32] tells us that the holographic entanglement entropy of a spherical cap region becomes maximal in the $w \to -1$ limit. We show in Appendix 4.6 that this occurs for an arbitrary subregion on a leaf.

Spacetime disappears as $w \to -1$ in the holographic FRW theory

We have seen in our AdS/CFT example that as the holographic state approaches typicality, and hence becomes maximally entropic, the directly reconstructable region disappears. On the other hand, we have shown that the entanglement entropies for flat FRW universes approaches the maximal form as $w \to -1$. Does this limit have a corresponding disappearance of reconstructable spacetime? Here we will show that the answer to this question is yes.

From the analysis of Section 4.2, we see that a leaf at late times in universes approaching de Sitter space can be mapped to a surface on the $\tau = 0$ hypersurface Σ, which asymptotes to the bifurcation surface Ξ in the late time limit. From the Killing symmetry, the HRRT surfaces anchored to this mapped leaf must all be restricted to living on Σ. Mapping the HRRT surfaces back to the original location, we see that they asymptote to living on the null hypersurface Σ'. Thus, we find that the HRRT surface for any subregion of a leaf σ_* asymptote to the future boundary of the causal region D_{σ_*}, which we denote by $\partial D_{\sigma_*}^{(+)}$, as a universe approaches de Sitter space. A similar argument holds for universes where $w \to -1$. In Appendix 4.6, we present some examples where we can see this behavior using analytic expressions for HRRT surfaces.

What does this imply for the reconstructable region in de Sitter space? Using the prescription outlined in Section 4.2, we find that spacetime points on the future causal boundary of a leaf, $\partial D_{\sigma_*}^{(+)}$, can be reconstructed. This is a codimension-1 region in spacetime. One might then think that we can reconstruct a codimension-0 region by considering multiple leaves, as was the case in a Schwarzschild-AdS black hole. However, the holographic screen of de Sitter space is itself a null hypersurface, with future leaves lying precisely on the future causal boundary of past leaves. This means that even by using multiple leaves we cannot reconstruct any nonzero measure spacetime region in the de Sitter (and $w \to -1$) limit.

We will now compute the reconstructable region in $(2+1)$-dimensional flat FRW spacetimes. As discussed in Section 4.2, this region is comprised of points that can be localized as the intersection of edges of entanglement wedges. We will be considering the reconstructable

region associated to a single leaf, and hence this prescription reduces to finding points located at the intersection of HRRT surfaces anchored to the leaf. This alone gives us a codimension-0 reconstructable region. In $(2+1)$-dimensional FRW spacetimes, HRRT surfaces are simply geodesics in the bulk spacetime, and this problem becomes tractable.

For a $(2+1)$-dimensional flat FRW universe filled with a single fluid component w, the leaf of the holographic screen at conformal time η_* is located at coordinate radius

$$r_* = \frac{a}{\dot{a}}\bigg|_{\eta=\eta_*} = w\eta_*. \tag{4.13}$$

Let us parameterize the points on the leaf by $\phi \in [0, 2\pi)$. Consider an interval of the leaf at time η_* centered at ϕ_0 with half opening angle ψ. The HRRT surface of this subregion is simply the geodesic connecting the endpoints of the interval: $(\eta, \phi) = (\eta_*, \phi_0 - \psi)$ and $(\eta_*, \phi_0 + \psi)$. It is clear from the symmetry of the setup that if we consider a second geodesic anchored to an interval with the same opening angle but with a center $\phi_0' \in [\phi_0 - 2\psi, \phi_0 + 2\psi]$, then the two geodesics will intersect at a point, specifically where $\phi = (\phi_0 + \phi_0')/2$. Using these pairs of geodesics, it is clear that we can reconstruct all points on all geodesics anchored to the leaf. The union of these points gives us a codimension-0 region.

Can we get a larger region? In $(2+1)$-dimensional flat FRW spacetimes, the answer is no. In higher dimensions, knowing the HRRT surfaces for all spherical cap regions may not be sufficient to figure out reconstructable regions; for example, one may consider using disjoint regions in hopes that the new HRRT surfaces would explore regions inaccessible to the previous HRRT surfaces (although we do not know if this really leads to a larger reconstructable region). However, in $2+1$ dimensions, both connected and disconnected phases of extremal surfaces are constructed from the geodesics already considered, so we gain nothing from considering disconnected subregions. We thus find that the set of all points on HRRT surfaces anchored to arbitrary subregions on a leaf is exactly the reconstructable region from the state on the leaf.

In Fig. 4.4, we show a plot of the reconstructable spacetime volume as a function of w. It shows a qualitatively similar behavior to that of Fig. 4.1, where the reconstructable volume increases and then sharply declines to zero as the holographic state becomes maximally entropic.

We can also perform a similar analysis in higher dimensions. Due to the numerical difficulty in finding extremal surfaces, here we restrict ourselves to the region reconstructable by spherical cap regions (which may indeed be the fully reconstructable region) and to only a few representative values of w. The results are plotted in Fig. 4.5 for $(3+1)$-dimensional FRW universes. These demonstrate the behavior that the extremal surfaces, and hence the reconstructable region, becomes more and more null as $w \to -1$.

The discussion in this subsection says that the reconstructable spacetime region disappears in the holographic theory of FRW spacetimes as the holographic state becomes maximally entropic in the de Sitter limit. While a microstate becoming maximally entropic does not directly mean that states representing the corresponding spacetime become typical
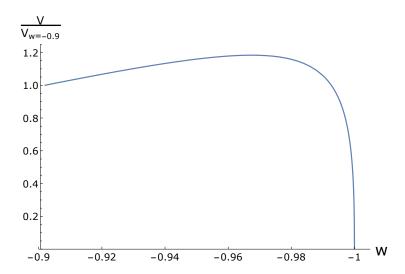
Figure 4.4: The spacetime volume of the reconstructable region in $(2+1)$-dimensional flat FRW universes for $w \in (-0.9, -1)$, normalized by the reconstructable volume for $w = -0.9$.

(a) $w = 1$, $\eta_* = 1$

(b) $w = 0$, $\eta_* = 1$

(c) $w = -4/5$, $\eta_* = -1$
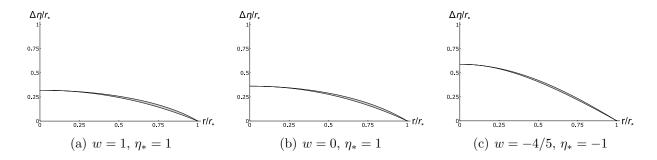
Figure 4.5: Reconstructable spacetime regions for various values of w in $(3+1)$-dimensional flat FRW universes. The horizontal axis is the distance from the center, normalized by that to the leaf. The vertical axis is the difference in conformal time from the leaf, normalized such that null ray from the leaf would reach 1. The full reconstructable region for each leaf would be the gray region between the two lines rotated about the vertical axis.

in the holographic Hilbert space (since the number of independent microstates could still be small), we expect that the former indeed implies the latter as usual thermodynamic intuition suggests; see Section 4.4 for further discussion. In any event, since typical states in a holographic theory are maximally entropic, we expect that the reconstructable spacetime region disappears as the holographic state becomes typical.

An important implication of the analysis here is that a holographic theory of de Sitter space cannot be obtained by taking a limit in the holographic theory of FRW spacetimes. A holographic theory of exact de Sitter space, if any, would have to be formulated in a different

manner.[7]

Maximally entropic states have no spacetime

In this subsection, we provide a proof for the statement that the directly reconstructable region of a maximally entropic leaf is either the leaf itself or a subset of its null cone. We use this result to argue that maximally entropic states have no spacetime. This heavily utilizes the maximin techniques developed in Ref. [76].

Theorem 2. *Consider a compact codimension-2 spacelike surface, σ, with area $\mathcal{A}$, living in a spacetime that satisfies $R_{ab}v^a v^b \geq 0$ for all null vectors v^a. Suppose HRRT surfaces can consistently be anchored to σ.[8] Let $m(\Gamma)$ denote the HRRT surface anchored to the boundary, $\partial\Gamma$, of a subregion Γ of σ.*

If $\|m(\Gamma)\| = min\{\|\Gamma\|, \|\bar{\Gamma}\|\}, \forall \Gamma \subset \sigma$, then either σ is a bifurcation surface or all of the HRRT surfaces of σ lie on a non-expanding null hypersurface connected to σ.

Proof. If Γ_1 and Γ_2 are subregions of σ, we will abbreviate $\Gamma_1 \cup \Gamma_2$ as $\Gamma_1\Gamma_2$. Let $m(\Gamma)_\Sigma$ denote the representative of $m(\Gamma)$ on a complete achronal surface Σ, defined by the intersection of Σ with a null congruence shot out from $m(\Gamma)$. From the extremality of $m(\Gamma)$, $R_{ab}v^a v^b \geq 0$, and the Raychaudhuri equation, $\|m(\Gamma)_\Sigma\| \leq \|m(\Gamma)\|$.

Consider three connected subregions A, B, C of σ such that $\partial A \cap \partial B \neq \emptyset$, $\partial B \cap \partial C \neq \emptyset$ where both such intersections are codimension-3, and $\|A \cup B \cup C\| \leq \|\sigma\|/2$; see Fig. 4.6 for a diagram. By Theorem 17.h of Ref. [76], take $m(ABC)$ and $m(B)$ to be on the same achronal surface, Σ. Now, consider the representatives $m(AB)_\Sigma$ and $m(BC)_\Sigma$. From the properties of representatives and maximin surfaces, we have

$$S(AB) + S(BC) \geq \frac{\|m(AB)_\Sigma\|}{4l_{\mathrm{P}}^{d-1}} + \frac{\|m(BC)_\Sigma\|}{4l_{\mathrm{P}}^{d-1}} \geq S(ABC) + S(B). \qquad (4.14)$$

The assumption of maximal entropies then tells us that strong subadditivity is saturated, and hence

$$\begin{aligned}
\|m(AB)_\Sigma\| &= \|m(AB)\|, \\
\|m(BC)_\Sigma\| &= \|m(BC)\|.
\end{aligned} \qquad (4.15)$$

Additionally, $m(AB)_\Sigma \cap m(BC)_\Sigma \neq \emptyset$.

---

[7]Another instance in which spacetime disappears is when the holographic description changes from that based on a past holographic screen (foliated by marginally anti-trapped surfaces) to a future holographic screen (marginally trapped surfaces). Such a change of description may occur in a spacetime with a late-time collapsing phase, e.g. in a closed FRW universe with the holographic screen constructed naturally in an observer-centric manner. (For an interpretation of such spacetime, see Ref. [32].) Since the leaf at the time of the transition is extremal, the analysis here indicates that the spacetime region reconstructable from a single leaf disappears at that time. This makes the necessity of the change of the description more natural.

[8]This requires the expansion of the two null hypersurfaces bounding $D(\sigma)$ to have $\theta \leq 0$, where $D(\sigma)$ is the interior domain of dependence of some achronal set whose boundary is σ. These HRRT surfaces are guaranteed to exist and satisfy basic entanglement inequalities; see Refs. [30, 126].
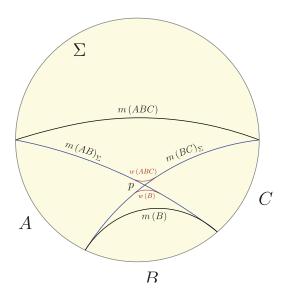
Figure 4.6: Diagrams representing the achronal surface Σ in which two HRRT surfaces, $m(ABC)$ and $m(B)$, live. $m(AB)_\Sigma$ and $m(BC)_\Sigma$ are the representatives of $m(AB)$ and $m(BC)$, respectively. They are shown to be intersecting at p. On a spacelike Σ, one could deform around this intersection to create two new surfaces with smaller areas.

We have two cases depending on the nature of Σ.

Case 1: $m(ABC)$, $m(B)$, $m(AB)_\Sigma$, and $m(BC)_\Sigma$ live on Σ which is a non-null hypersurface.

Suppose $m(AB)_\Sigma \cap m(BC)_\Sigma$ is a codimension-3 surface, meaning they intersect through some surface, p, depicted in Fig. 4.6. One could then smooth out the "corners" around p to create new surfaces homologous to ABC and B. This is depicted through the maroon lines in Fig. 4.6. By the triangle inequality, these new, smoothed out surfaces, $w(ABC)$ and $w(B)$, would have less total area than $m(ABC) \cup m(B)$ because $p \in \Sigma$, which is spacelike. However, this contradicts the minimality of $m(ABC)$ and $m(B)$:

$$(\|A\| + \|B\| + \|C\|) + \|B\| = \|m(ABC)\| + \|m(B)\| \leq \|w(ABC)\| + \|w(B)\|$$
$$< \|m(AB)_\Sigma\| + \|m(BC)_\Sigma\| = (\|A\| + \|B\|) + (\|B\| + \|C\|). \qquad (4.16)$$

Therefore, $m(AB)_\Sigma$ and $m(BC)_\Sigma$ cannot intersect through some codimension-3 surface, yet they must still intersect. This requires $m(AB)_\Sigma$ and $m(BC)_\Sigma$ to coincide somewhere, a neighborhood of x, and by Theorem 4.e of Ref. [76] these two surfaces must coincide at every point connected to x. This means that $m(AB) = m(A) \cup m(B)$ and $m(BC) = m(B) \cup m(C)$. The only way this can consistently occur for all possible A, B, and C is for $m(\Gamma) \subset \sigma$. This means that σ itself is extremal, and hence is a bifurcation surface.
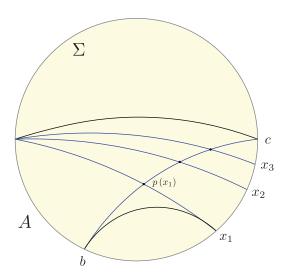
Figure 4.7: This depicts how one can scan across the representative $m(BC)_\Sigma$ by bipartitioning BC on the achronal surface Σ. At each of these intersections, $p(x_i)$, $\theta_u = \theta_v = 0$ if the state on the leaf is maximally entropic and Σ is null and non-expanding.

Case 2: $m(ABC)$, $m(B)$, $m(AB)_\Sigma$, and $m(BC)_\Sigma$ live on hypersurface Σ which is at least partially null.

Suppose $m(AB)_\Sigma \cap m(BC)_\Sigma$ is a codimension-3 surface, p. If at p, Σ is null and non-expanding, then smoothing out the intersection will not result in new surfaces with smaller area. This is the condition that $\theta_u = 0$ on the null hypersurface, Σ_u, coincident with Σ at p, where u is the null vector generating Σ_u at p. Hence, the representatives can intersect at p and simultaneously saturate strong subadditivity. Additionally, because $\|m(BC)_\Sigma\| = \|m(BC)\|$, we know that $\theta_v = 0$ along the hypersurface generating the representatives of $m(BC)$, where v is the null vector generating this hypersurface. Therefore at p, $\theta_u = \theta_v = 0$.

We can now scan across $m(BC)_\Sigma$ by considering its intersection with $m(AB')_\Sigma$ where (B', C') is a bipartition of $B \cup C$ where $\partial B' \cap \partial A \neq \emptyset$, and then considering all such bipartitions. This is illustrated in Fig. 4.7 by splitting up $B \cup C$ at a few points labeled by x_i; for example, $B' = [b, x_3]$ and $C' = [x_3, c]$ is one such allowable bipartition. By continuity, all of $m(BC)_\Sigma$ will be scanned.[9]

By the argument in the previous paragraph, all intersection points along $m(BC)_\Sigma$ must then have $\theta_u = \theta_v = 0$. Assuming nondegeneracy, $m(BC)_\Sigma$ must therefore

---

[9]We believe this is sufficient to scan over the whole surface assuming the spacetime is smooth. Additionally, Eq. (4.15) requires there to be no energy density between an HRRT surface and its representative, this will preclude jumps in the representatives due to entanglement shadows and the like.

be the HRRT surface $m(BC)$. Additionally, every point of $m(BC)$ lives on some null, non-expanding hypersurface and at $\partial m(BC)$ this surface connects to σ. Hence, at $\partial m(BC)$, σ must be marginal. This argument can be repeated for any set of appropriate subregions. This tells us that all HRRT surfaces have the previously stated properties.

Now, by Theorem 17.h of Ref. [76], we can construct an achronal surface, Σ, that is foliated by HRRT surfaces. Each point of Σ must now be null and non-expanding. Additionally, the boundary of Σ, σ, must be marginal. Let k denote the vector in this local marginal direction. This uniquely specifies Σ as the null non-expanding hypersurface generated by k. This is true for all Σ foliated by HRRT surfaces, and each HRRT surface can belong to some foliation of a Σ.[10] Hence all extremal surfaces anchored to σ must belong to a non-expanding null hypersurface.

Back to the beginning, if the intersection of $m(AB)_\Sigma$ and $m(BC)_\Sigma$ is codimension-2, then the argument from Case 1 applies and σ must be extremal.

This concludes the proof of Theorem 2. $\hfill\square$

Corollary 1. *Consider a codimension-2 surface, σ, with area $\mathcal{A}$, living in a spacetime satisfying $R_{ab}v^a v^b \geq 0$. Let $m(\Gamma)$ denote the HRRT surface anchored to $\partial \Gamma$.*
If σ is not marginal, then it cannot satisfy $\|m(\Gamma)\| = min\{\|\Gamma\|, \|\bar{\Gamma}\|\}, \forall \Gamma \subset \sigma$.

Proof. The contrapositive of this statement is proven by Theorem 2. $\hfill\square$

Consider the case that σ is a leaf of a past holographic screen. If the leaf is extremal and the screen is not null, then the directly reconstructable spacetime is just the leaf itself. Additionally, this tells us the holographic screen must halt at this point. This indicates the end of a holographic description based on the past holographic screen. At this point, one can stitch the beginning of a new future holographic screen that starts at a bifurcation surface, patching together two holographic descriptions. This occurs in collapsing universes; see footnote 7.

In the other case, if all of the HRRT surfaces of σ have area corresponding to the maximal entropy, then all of the extremal surfaces must lie on the future null cone of the leaf, where this null cone is non-expanding and compact. This cone itself is the limit of a past holographic screen because $\theta_k = 0$. Barring the existence of a continuum of compact, non-expanding, null hypersurfaces, the holographic screen then follows along this null surface from the leaf. Hence the directly reconstructable region will only be the screen itself, exactly as we observed in the case of de Sitter space. Again, we see that maximal entanglement corresponds to the end of a holographic description, but in this case the screen does not end; this corresponds to a stable final state.

---

[10]Under the assumption of the theorem, the HRRT surface of disconnected subregions will always be disconnected. This is because the disconnected surface is extremal.

In Section 4.2, we took the boundary to be at some large, fixed radius in AdS space. One may be concerned that this cutoff surface is not marginal, and hence Theorem 2 does not apply. However, in the limit that the black hole radius approaches the boundary, then the statement holds because the horizon of the black hole satisfies the needed properties. Note that until this final limit, Corollary 1 tells us that the entanglement of the boundary cannot be maximal.

Finally we are prepared to make a statement about typicality. Typical boundary states are maximally entangled, and hence the argument shows us that for holographic theories living on screens (an instance of which is AdS/CFT), typical states have no directly reconstructable spacetime.

4.3 Spacetime Emerges through Deviations from Maximal Entropy

We have seen that when the holographic state becomes maximally entropic, spacetime defined as the directly reconstructable region disappears. Conversely, bulk spacetime emerges when we change parameters, e.g. the mass of the black hole or the equation of state parameter w, deviating the state from maximal entropy. In this section, we study how this deviation may occur and find qualitative differences between the cases of Schwarzschild-AdS and flat FRW spacetimes. This has important implications for the structures of holographic theories representing these spacetimes.

CFT with subcutoff temperatures

Consider the setup discussed in Section 4.2: a large black hole in asymptotically AdS space. The holographic theory is then a local quantum (conformal) field theory. When the temperature of the system is at the cutoff scale, the holographic state has maximal entropies, Eq. (4.3). As we lower the temperature, the state deviates from a maximally entropic one, and correspondingly bulk spacetime emerges—the horizon of the black hole recedes from the cutoff surface, and the reconstructable spacetime region appears; see Fig. 4.1.

Suppose the temperature of the system T is lower than the cutoff scale, $T < \Lambda$. We are interested in the behavior of von Neumann entropies of subregions of characteristic length L in the boundary theory. These entropies are calculated holographically by finding the areas of the HRRT surfaces anchored to subregions of the cutoff surface $r = R$. We analyze this problem analytically for spherical cap regions in Appendix 4.6. For sufficiently high temperature, $T \gg (\Lambda^{d-2}/l)^{1/(d-1)}$, we find that the entanglement entropy for a subregion A behaves as

$$S_A \approx \begin{cases} cA_{d-2}L^{d-2}\Lambda^{d-2} & \text{for } L \ll L_*, \\ cA_{d-2}\frac{r_+^{d-1}L^{d-1}}{l^{2d-2}} \approx c\left(\frac{T}{\Lambda}\right)^{d-1}A_{d-2}L^{d-1}\Lambda^{d-1} & \text{for } L \gg L_*. \end{cases} \tag{4.17}$$

Here,

$$L_* \approx \frac{l^2 R^{d-2}}{r_+^{d-1}} \approx \frac{\Lambda^{d-2}}{T^{d-1}}, \tag{4.18}$$

$c \approx (l/l_{\mathrm{P}})^{d-1}$ is the central charge of the CFT, and A_{d-2} is the area of the $(d-2)$-dimensional unit sphere. We find that the scaling of the entanglement entropy changes (smoothly) from an area law to a volume law as L increases. For $T \ll (\Lambda^{d-2}/l)^{1/(d-1)}$, i.e. $L_* \gg l$, the entanglement entropy obeys an area law for all subregions. We note that the length in the boundary theory is still measured in terms of the d-dimensional metric at infinity with the conformal factor stripped off. The cutoff length is thus $1/\Lambda \approx O(l^2/R)$, and the size of the boundary space is $\approx O(l)$.

While we have analyzed spherical cap subregions, the behavior of the entanglement entropy found above is more general. When the temperature is lowered from the cutoff scale, the entanglement entropy S_A deviates from the maximal value. Defining

$$Q_A = \frac{S_A}{S_{A,\mathrm{max}}} = \frac{S_A}{\|A\|/4l_{\mathrm{P}}^{d-1}}, \tag{4.19}$$

we find that

$$Q_A \approx \begin{cases} \frac{1}{L\Lambda} & \text{for } L \ll \frac{\Lambda^{d-2}}{T^{d-1}}, \\ \left(\frac{T}{\Lambda}\right)^{d-1} & \text{for } L \gg \frac{\Lambda^{d-2}}{T^{d-1}}. \end{cases} \tag{4.20}$$

Here, we have assumed that subregion A is characterized by a single length scale L, and that the temperature is sufficiently high, $T \gg (\Lambda^{d-2}/l)^{1/(d-1)}$. (If $T \ll (\Lambda^{d-2}/l)^{1/(d-1)}$, $Q_A \approx 1/L\Lambda$ for all subregions.) This behavior is depicted schematically in Fig. 4.8.

We find that as the temperature is lowered from the cutoff scale, two things occur for entanglement entropies:

- For sufficiently large subregions, the entanglement entropies still obey a volume law, but the coefficient becomes smaller.

- The more the temperature is lowered, the further subregions have entanglement entropies obeying an area law. This occurs from shorter scales, i.e. subregions with smaller sizes.

These make the entanglement entropies deviate from the maximal value and lead to the emergence of reconstructable spacetime: the region between the black hole horizon and the cutoff surface, $r_+ < r \leq R$.

FRW universes with $w > -1$

As spacetime emerges by reducing the mass of the black hole in the Schwarzschild-AdS case, a codimension-0 spacetime region that is reconstructable from a single leaf appears when w is increased from -1. As in the AdS case, this appearance is associated with a deviation
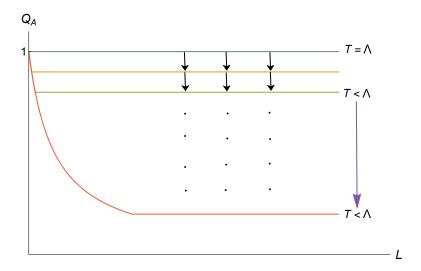
Figure 4.8: A schematic depiction of the entanglement entropy in the Schwarzschild-AdS spacetime, normalized by the maximal value of entropy in the subregion, $Q_A = S_A/S_{A,\max}$, and depicted as a function of the size L of subregion A; see Eq. (4.20). The scales of the axes are arbitrary. As the mass of the black hole is lowered (the temperature T of the holographic theory is reduced from the cutoff Λ), Q_A deviates from 1 in a specific manner.

of entanglement entropies from saturation. However, the manner in which this deviation occurs is qualitatively different in the two cases.

To illustrate the salient points, let us consider flat FRW spacetimes with a single fluid component w and a spherical cap region A on a leaf parameterized by the half opening angle ψ. Below, we focus on entanglement entropies $S_w(\psi)$ of the regions with $\psi \le \pi/2$. Those with $\psi > \pi/2$ are given by the relation $S_w(\psi) = S_w(\pi - \psi)$.

As before, we define

$$Q_w(\psi) = \frac{S_w(\psi)}{S_{\max}(\psi)} = \frac{S_w(\psi)}{\|A\|/4l_{\mathrm{P}}^{d-1}}. \tag{4.21}$$

This quantity was calculated in Ref. [32] in $3+1$ dimensions, which we reproduce in Fig. 4.9. The basic features are similar in other dimensions. In particular, $Q_w(\psi)$ satisfies the properties given in Eqs. (4.57, 4.58) in Appendix 4.6.

We find that the way $Q_w(\psi)$ deviates from 1 as w is increased from -1 is qualitatively different from the way the similar quantity Q_A deviates from 1 in the Schwarzschild-AdS case as the temperature is reduced from the cutoff scale. In particular, we find that in the FRW case

- The deviation from $Q_w(\psi) = 1$ occurs *from larger subregions*. Namely, as w is raised from -1, $Q_w(\psi)$ is reduced from 1 first in the vicinity of $\psi = \pi/2$.
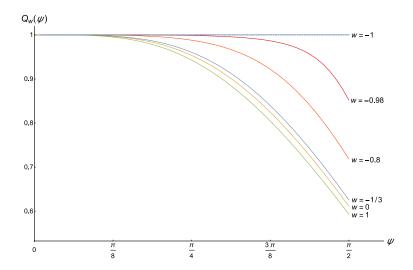
Figure 4.9: The entanglement entropy in the holographic theory of flat FRW spacetimes normalized by the maximal value of entropy in the subregion, $Q_w(\psi) = S_w(\psi)/S_{\max}(\psi)$, as a function of the size of the subregion, a half opening angle ψ. As the equation of state parameter w is increased from -1, $Q_w(\psi)$ deviates from 1 in a way different from the Schwarzschild-AdS case.

- There is no regime in which the entanglement entropy obeys an area law, $Q_w(\psi) \sim 1/\psi$, or a volume law with a reduced coefficient, $Q_w(\psi) = \text{const.} < 1$.

As we will see next, these have profound implications for the nature of the holographic theory of FRW spacetimes.

Locality vs nonlocality

In the following discussion, we assume that the dynamics in the holographic theory are chaotic and non-integrable as expected in a theory of quantum gravity; see, e.g. Ref. [127]. Such systems are expected to satisfy the eigenstate thermalization hypothesis (ETH) [128, 129], so generic high energy eigenstates reproduce the behavior of a thermal Gibbs density matrix. In addition, we note that the dimension of the holographic Hilbert space is large ($\mathcal{A}/4l_P^{d-1} \gg 1$) and finite size effects causing deviations from the thermodynamic limit can be ignored.

We have already seen that one way to obtain a maximally entropic state is to look at high energy states in a local theory. In the context of AdS/CFT, this corresponds to examining black holes with temperature near the cutoff scale. To deviate from maximal entropy, one can then simply lower the energy of the states being considered. For subregions beyond the correlation length, the reduced density matrix is well approximated by a Gibbs density matrix, and hence the entropy obeys a volume law but with a prefactor dependent on the temperature T. For length scales below the correlation length, the von Neumann entropy

is dominated by the area law contribution. Together, these combine to give entanglement entropy curves that have the qualitative behavior shown in Fig. 4.8. Note that in a local theory, lowering the temperature shows deviation from thermal behavior originating at small length scales. Namely, the slope of Q_A begins deviating from 0 at small scales. This entropy deviation at small scales is expected to be a general phenomenon of equilibrium states governed by a local Hamiltonian.

However, the entanglement entropy curves calculated for holographically FRW universes show drastically different behavior; see Fig. 4.9.[11] Namely, the deviations from maximal entropy originate at large length scales, and the entanglement entropy for small subregions is maximal regardless of the fluid parameter w. Additionally, these entropy curves are invariant under time translation. This behavior cannot be achieved by a local theory. One may think that a Lifshitz type theory with large z may be able to accommodate such behavior due to large momentum coupling, but the leading order contribution to the entanglement entropy in d dimensions is believed to be proportional to $(L/\epsilon)^{d-1-1/z}$ for weakly coupled theories [130], where L is the characteristic length of the entangling region and ϵ is the cutoff length. Thus entanglement entropy is proportional to the volume only in the limit that $z \to \infty$, which would be a nonlocal field theory. Indeed, entanglement entropy being maximal for small subregions is observed in a number of nonlocal theories [131, 132, 133, 134, 135, 136] and is likely a generic phenomenon in such theories.

This leads us to believe that an appropriate holographic description of FRW universes would be nonlocal.[12] This provides us with a few possibilities of theories that have the desired qualitative features, all of which have a freedom to tune a parameter which corresponds to changing w (and hence the entropy):

(I) a nonlocal theory with a characteristic length scale below the system size, changing the nonlocal length scale of the theory or energy of the state;

(II) a nonlocal theory coupling sites together at all length scales (like a long-range inter-acting spin chain or a variant of the Sachdev-Ye-Kitaev model [137, 138, 139] with all-to-all random coupling between a fixed number, q, of sites, SYK_q), changing the energy of the state;

(III) a nonlocal theory with a fundamental parameter controlling the coupling at all scales in which variations can change the entropy; for example, changing the number of sites

---

[11] It should be emphasized that we are calculating the entanglement entropy of the boundary state on the holographic screen, not the entropy associated with any bulk quantum fields. We refer to the degrees of freedom on the screen that govern the background gravitation dynamics as the gravitational degrees of freedom. Any low energy bulk excitations (which may include gravitons) are higher order corrections to the entanglement entropy and we do not discuss them.

[12] It is a logical possibility that a local theory could exhibit volume law entropy behavior due to open dynamics. Since the size of the leaf is constantly growing, there are degrees of freedom constantly being added to the system, which could already have long range entanglement. This seems to be an ad hoc solution, and we will not elaborate on this possibility further.

coupled to each other in each term of the Hamiltonian (analogous to changing q in SYK_q).

The ground states of theories in case (I) are explored in Refs. [131, 132, 133] in string theory frameworks. This case can also be realized as a spin chain with interactions that couple all sites within a distance smaller than the characteristic nonlocal length scale. Above the nonlocal length scale an area law term starts to pick up and will eventually dominate. However, because of this eventual turn-on of an area law, the qualitative features of the entropy normalized by volume are different than those exhibited by FRW entropy curves. Namely, the concavity of the Q_A plot beyond the nonlocal length scale is opposite to that observed in the FRW case. This is because beyond the nonlocal length scale the entropy approaches an area law, hence the second derivative of Q_A will be positive, unlike that observed in the FRW case. Raising the temperature will only add an overall constant asymptotic value to Q_A. Hence, the concavity of Q_A forbids the holographic theory of FRW spacetimes from being a theory with a characteristic nonlocal length scale smaller than the system size.

This reasoning leaves us with nonlocal theories with characteristic interaction lengths comparable to the system size—what does this mean? It simply means that a site can be coupled to any other site. For simplicity we will consider SYK-like theories but rather than being zero dimensional we split up the degrees of freedom to live on a lattice but keep the random couplings between them. At first thought, one may think that because of the random, all-to-all coupling the entanglement entropy for all subregions would always be maximal. However this is not the case. The entanglement entropy for small regions is indeed maximal, but then deviates at large length scales [135, 136]. One can intuitively understand this by thinking about the SYK_2 model and Bell pairs. The SYK couplings are random, and some sites will have significantly higher coupling than average. In the ground state, these pairs have a high probability of being entangled, so if the subregion of interest contains only half of one of these special pairs, this will raise the entanglement with the outside. However, once the subregion becomes larger there is a higher probability that a complete Bell pair is contained, and this will drop the entanglement entropy.

From this intuition, one can see that the ground state of SYK-like theories have near maximal entanglement for small regions, which then deviates at large length scales. At higher energies, the probability of minimizing the term in the Hamiltonian coupling these special sites (and creating the effective Bell pair) will be lowered, and hence the entanglement entropy of all subregions will monotonically increase [136, 140]. This behavior is reminiscent of that observed in FRW entanglement entropy if we relate the fluid parameter, w, to the energy of the nonlocal state: the case (II) listed above. The limit of $T \to \infty$ would then correspond to $w \to -1$.

The third possibility (III) is similar to the one just discussed, but with the difference that w is dual not to temperature but to a fundamental parameter dictating the "connectivity" of the boundary theory. In the language of SYK_q, this would correspond to changing q, where q is the number of coupled fermions in each interaction term of the Hamiltonian. As q increases, the ground state entanglement monotonically increases and as $q \to \infty$ becomes

maximal. This would be the limit corresponding to $w \to -1$. However, any possibility like this, which employs a change of a fundamental parameter of the Hamiltonian, will require us to manufacture the whole Hilbert space of the boundary theory by considering the collection of only the low energy states for each value of q. We would like one related class of spacetimes to be dual to one boundary theory, which is not the case in this option. We thus focus on option (II) as the best candidate, but we cannot logically exclude option (III).

It is interesting to observe the relationship between where the deviation from volume law entropy occurs and where the corresponding spacetime emerges. In the Schwarzschild-AdS case, Q_A drops from 1 immediately at small subregions, and the spacetime that emerges is precisely that which is reconstructed from small subregions. Hence the directly reconstructable region appears at the boundary and grows inwards as the temperature of the state is lowered. The converse is true in the case of FRW spacetimes. As we move away from $w = -1$, the entanglement entropy drops from maximal at large subregions and the corresponding spacetime that emerges is constructed by intersecting large surfaces. This is because the HRRT surfaces of small subregions of leaves with w near -1 all lie on the same codimension-1 surface, the future causal boundary of the leaf, analogous to the small surfaces in Fig. 4.13 in Appendix 4.6. The HRRT surfaces for large subregions deviate from this and hence allow for reconstructing a codimension-0 region starting with points deepest in the bulk.

The language of quantum error correction [109] and tensor networks [24, 110, 115] allows for a nice interpretation of this phenomenon. The loss of entanglement in pure gravitational degrees of freedom affords nature the opportunity to redundantly encode local bulk degrees of freedom in the boundary. In AdS, short range entanglement is lost first, and hence there is "room" for the information of local bulk degrees of freedom to be stored. In the case of FRW, long range entanglement is lost first, and subsequently points in the bulk that require large subregions to reconstruct emerge first.

4.4   Holographic Hilbert Spaces

The analysis of the previous sections brings us to a suitable position to discuss the structure of holographic Hilbert spaces. In this section, we propose how a single theory can host states with different spacetime duals while keeping geometric operators linear in the space of microstates for a fixed semiclassical geometry. We use intuition gathered from quantum thermodynamic arguments to guide us. Similar ideas have been discussed in Ref. [53]. Here we present a slightly generalized argument to emphasize its independence of dynamics, and explain its application to our framework.

Let us assume that the entanglement entropy of subregions of a boundary state dual to a semiclassical geometry is calculated via the HRRT prescription. Given a bulk spacetime, one can then find the corresponding entanglement entropies for all subregions of the boundary. Note that here we consider the "classical limit." Namely, all the subregions we consider

contain $O(\mathcal{N})$ degrees of freedom, where

$$\mathcal{N} = \frac{\mathcal{A}}{4l_{\mathrm{P}}^{d-1}}, \tag{4.22}$$

with $\mathcal{A}$ being the volume of the holographic space. The collection of all boundary subregions and their corresponding entanglement entropies will be referred to as the entanglement structure of the state, which we denote by $S(|\psi\rangle)$.

From here, it is natural to ask whether or not all states with the same entanglement structure are dual to the same bulk spacetime. This might indeed be the case, but it leads to some undesirable features. These primarily stem from the fact that given a particular entanglement structure, one can find a basis for the Hilbert space in which all basis states have the specified entanglement structure. For a Hilbert space with a local product structure, one can do this by applying local unitaries to a state—these will retain the entanglement structure and yet generate orthogonal states. This would imply that by generically superposing $e^{O(\mathcal{N})}$ of these states, one could drastically alter the entanglement structure and create a state dual to a completely different spacetime. Hence, geometric quantities could not be represented by linear operators, even in an approximate sense. If this were the case, a strong form of state dependence would be necessary to make sense of dynamics in the gravitational degrees of freedom [111].

However, it is not required that every state in the holographic Hilbert space with the same entanglement structure is dual to the same spacetime. How can this consistently happen? Given an entanglement structure, $S(|\phi\rangle)$, we expect the existence of a subspace in which generic states (within this subspace) have this same entanglement structure up to $O(\mathcal{N}^p)$ corrections with $p < 1$. The existence of a subspace with a unique entanglement structure is not surprising if the dimension of the subspace is $e^{O(\mathcal{N}^p)}$ with $(p < 1)$, since we generally expect

$$S\left(\sum_{i=1}^{e^M} c_i |\psi_i\rangle\right) = S(|\psi\rangle) + O(M), \tag{4.23}$$

where $S(|\psi_i\rangle) = S(|\psi\rangle)$ for all i.

However, we argue further that there exist such subspaces with dimension $e^{O(\mathcal{N})}$, spanned by some basis states $|\psi_i\rangle$ $(i = 1, \cdots, e^{Q\mathcal{N}})$, with

$$S\left(\sum_{i=1}^{e^{Q\mathcal{N}}} c_i |\psi_i\rangle\right) = S(|\psi\rangle) + O(\mathcal{N}^p; \, p < 1), \tag{4.24}$$

where $Q \leq 1$ does not scale with $\mathcal{N}$. The existence of these subspaces with entanglement structures invariant under superpositions is expected from canonical typicality (also referred to as the general canonical principle) [141, 142]. This provides us with the powerful result that generic states in subspaces have the same reduced density matrix for small subsystems (up to small corrections). The proof of this statement is purely kinematical and hence applies

generally. In fact, from canonical typicality the correction term in Eq. (4.24) is exponentially small, $O(e^{-Q\mathcal{N}/2})$.

Canonical typicality is a highly nontrivial statement because the size of the subspaces in question is large enough that one would naively think that superpositions would ruin the entanglement structure at $O(\mathcal{N})$.[13] Therefore, even if one considers an exponentially large superposition of microstates (so long as they are generic states from the same subspace), geometric operators can be effectively linear within this subspace. We propose that states dual to semiclassical geometries are precisely generic states within their respective subspaces.

An example of one of these subspaces would be an energy band of an SYK theory. These harbor an exponentially large number of states, and yet from canonical typicality any superposition of generic states within this band will have the same entanglement entropy. Another example would be states that have energy scaling with the central charge, c, in AdS/CFT. These are dual to large black holes and there are also an exponentially large number of states within the energy band. Despite this, generic states within this energy band will have the same entanglement entropy structure. Essentially, canonical typicality proves the existence of exponentially large subspaces that have entanglement structures preserved under superpositions of just as many states.

We need this strengthened statement because the entanglement entropy calculations for FRW suggest the size of subspaces dual to identical spacetimes are exponentially large. This is because the quantity Q in Eq. (4.24) is related with von Neumann entropies characterizing the whole state, e.g. Q_A in Section 4.3 with A being the half boundary space and $Q_w(\pi/2)$ in Section 4.3. This intuition stems from the statement that the thermal entropy density and entanglement entropy density for states in the thermodynamic limit are approximately equal. For generic states within some energy interval subspace, this holds by canonical typicality. The statement also results from assuming the system satisfies the ETH (like in AdS/CFT). SYK models, however, do not strictly satisfy the ETH; nevertheless, it remains true that Q_A at half system size gives a good approximation for the thermal entropy density, and the discrepancy vanishes as the energy of the states is increased. For these reasons, we expect $Q_w(\pi/2)$ to well approximate the thermal entropy density of states dual to an FRW spacetime with fluid parameter w.

We can now address the properties of typical states within an entire Hilbert space. Consider a holographic Hilbert space of a given theory, e.g. a CFT with a finite cutoff or the holographic theory of FRW spacetimes. If there are multiple superselection sectors in a given theory, then we focus on one of them. In such a Hilbert space, the effective subspace with $Q = 1$ corresponds to typical states. Applying Page's analysis, we can then conclude that the only entanglement structure consistent with Eq. (4.24) where $Q = 1$ must be that of maximal entropy. For example, the number of microstates for a large black hole approaches the dimension of the boundary Hilbert space as $T \to \Lambda$, and these states are maximally entangled. Similarly, using the argument in the previous paragraph, the number of indepen-

---

[13]Note that if one fine-tunes coefficients and selects states in this subspace carefully, one could construct a state with lower entanglement via superposition.

dent microstates in the de Sitter limit approaches the dimension of the boundary Hilbert space, and these states are maximally entangled. As shown in Section 4.2, the directly reconstructable spacetime region vanishes in these cases—an effective subspace with $Q = 1$ does not have reconstructable spacetime. It is in this sense that typical states in the *whole* Hilbert space have no reconstructable spacetime.

On the other hand, if $Q < 1$, the corresponding entanglement structure $S(|\psi\rangle)$ can be non-maximal, and generic states in this subspace may be dual to some bulk spacetime. As discussed in Section 4.3, we expect that dynamics of the boundary theory can naturally select these subspaces, for example by simply lowering the energy of the system in the case of the boundary CFT.

The structure discussed here allows for a single holographic Hilbert space to harbor effective subspaces dual to different geometries, allows for a "generically linear" spacetime operator, and hence eliminates the need for any strong form of state dependence.[14] Because this "spacetime operator" is identical for states of a given entanglement, it will obviously act linearly on generic superpositions of states within one of these dynamically selected, entanglement-invariant subspaces. We suspect that it is only in this thermodynamic sense that classical spacetime emerges from the fundamental theory of quantum gravity.

4.5   Conclusion

Discussion

Our understanding of the relationship between spacetime and entanglement seems to be converging. The necessity of entanglement between boundary degrees of freedom for the existence of spacetime has been known for some time, but this fact may have mistakenly established the intuition that the fabric of spacetime itself is purely this entanglement. However, this cannot be the case. A one-to-one mapping between the entanglement structure of a boundary state and the directly reconstructable bulk spacetime cannot be upheld in a state independent manner. In addition, we see that as boundary entanglement approaches maximality the reconstructable region of the bulk vanishes.

In hindsight, this should not be too surprising. Let us recall Van Raamsdonk's discussion [49] relating spacetime to entanglement by examining the link between mutual information and correlations in a system. The mutual information between two boundary

---

[14]By strong state dependence, we mean a theory that would require state dependence to describe bulk excitations in the directly reconstructable region of a boundary state which is a generic superposition of states dual to a given spacetime. For a more detailed analysis of this statement, we refer the reader to Ref. [111]. The main result is that requiring linearity for the multiple boundary representations of a bulk operator is impossible if the number of geometry microstates is $e^{\mathcal{N}}$. This prohibits the existence of a directly reconstructable region for typical states. Note that the directly reconstructable region does not probe behind black hole horizons, and hence we are not addressing the possibility that state dependence is necessary to recover the black hole interior.

subsystems A and B is defined as

$$I(A, B) = S(A) + S(B) - S(A \cup B). \qquad (4.25)$$

This quantity bounds the correlations in a system between operators $\mathcal{O}_A$ and $\mathcal{O}_B$, supported solely on A and B via the relation

$$I(A, B) \geq \frac{(\langle \mathcal{O}_A \mathcal{O}_B \rangle - \langle \mathcal{O}_A \rangle \langle \mathcal{O}_B \rangle)^2}{2|\mathcal{O}_A|^2|\mathcal{O}_B|^2}. \qquad (4.26)$$

Hence, when the mutual information between two subregions A and B vanishes, the correlation between local operators supported within the subregions must also vanish. Assuming that subregion duality holds, this implies that correlation functions of bulk fields vanish. Generally, correlators between two bulk fields go as

$$\langle \mathcal{O}_1(x_1) \mathcal{O}_2(x_2) \rangle \sim a f(L), \qquad (4.27)$$

where L is the distance of the shortest geodesic connecting x_1 and x_2, a is some theory dependent constant, and $f(z)$ is a decreasing function of z. One can then make the argument that decreasing entanglement between regions will drop the mutual information between the regions, and hence make L effectively infinite. This implies that the spacetime regions dual to subregions A and B are disconnected when the entanglement (and hence mutual information) vanishes. For intuition's sake, one can imagine two subregions of the AdS boundary which are in a connected entanglement phase—increasing the distance between these two subregions will drop the mutual information. This is an argument demonstrating the need for entanglement in a holographic theory dual to spacetime, so long as the holographic theory has subregion duality.

However, there is a different (quite the opposite) way to make the mutual information between small (less than half of the system) subregions vanish, and consequently kill the bulk correlations. This is by considering maximally entropic boundary states—in these, the mutual information will vanish for any pair of subregions. This is the case both in cutoff temperature AdS black holes and in the de Sitter limit of the holographic theory of FRW universes. In these, the boundary states are maximally entropic and hence the bulk correlators must vanish; however, there exist finite length geodesics in the bulk (even if restricted only to the directly reconstructable region) which connect all points on the boundary. This means that the prefactor, a, of Eq. (4.27) must vanish, making the bulk theory ultralocal. In these cases, the maximal entropy implies that there cannot be an extra emergent bulk dimension. This is because the ground state of any quantum field theory quantized on spacelike hypersurfaces must be entangled at arbitrarily short scales, which is violated by the assumption that $a = 0$. However, this is not necessarily unexpected—in both de Sitter space and cutoff temperature black holes, the directly reconstructable regions are codimension-1 null surfaces of the bulk (the de Sitter horizon and black hole horizon respectively). A natural description of the fields on this surfaces would be through null

quantization, which is known to be ultralocal [143]. Accordingly, we see a breakdown in the holographic description.

From the above arguments one can convince themselves that it is not entanglement itself which allows for the construction of spacetime, but rather something related to intermediate entanglement.

How can this be better understood? The framework of tensor networks provides some intuition behind this. Here, a maximally entropic boundary state is most naturally represented by a single bulk node with one bulk leg and multiple boundary legs.[15] Hence the "spacetime" is just one non-localizable bulk region, a "clump" as defined in Ref. [118]. This bulk point can be reconstructed once a subregion of the boundary contains more than half of the boundary legs. Here it is clear that a maximally entropic boundary state has no dual "spacetime," and yet it is possible to encode a bulk code subspace with full recovery once more than half of the boundary is obtained. Note that these typical states will all satisfy (in fact saturate) the holographic entropy cone inequalities [144] simply because a random tensor network accurately describes the state, but this does not mean that there is a reconstructable region of the spacetime.

Additionally, if maximally entropic states did have reconstructable spacetime, then state dependence would be necessary in order to describe bulk excitations in these states, under the assumption that subregion duality holds. This is because the number of microstates with maximal entropy is approximately the dimension of the full boundary Hilbert space, and by the argument in Section V.C. of Ref. [111], it is impossible to find a boundary representation of a bulk operator that has support only on a subregion of the boundary *and* acts approximately linearly on all microstates of a given spacetime. Intuitively, this is because the operator will be over-constrained by insisting it both have support on a subregion of the boundary and act linearly on D microstates, when the dimension of the full boundary space is D. This means that if we require state independence, then the only possible boundary operators representing bulk excitations for a maximally entropic state must have support on the full boundary space.[16] Therefore, the minimum possible subregion in which bulk excitations can be encoded state independently is the whole boundary space; hence there is no directly reconstructable spacetime. This directly highlights the tension between reconstructing spacetime for maximally entropic states (in any manner), and requiring both subregion duality and state independence.

But what happens if we lower the entanglement of the boundary state while keeping the dimension of the boundary Hilbert space constant? Again, we turn to tensor networks for intuition. In these situations, a natural way to encode sub-maximal entanglement (while fixing the bulk leg dimension) is by including more bulk nodes. Therefore, by reducing the

---

[15]Any attempt to create a bulk by artificially including more nodes with extremely large bulk bond dimension can be reduced to the case of one bulk node.

[16]This is not contradicting the statement in the previous paragraph that the sole bulk node's state in a random tensor can be recovered with just more than half of the boundary. In that case, only the recovery of the bulk code subspace for one microstate was considered. State independence would require us to have an operator that acts linearly on *all* microstates of a given spacetime.

boundary entanglement, it is possible to create a bulk code subspace in which subsystem recovery is possible. It seems that quantum gravity naturally utilizes this sub-maximal entanglement in order to encode information via subregion duality. This suggests that perhaps entanglement is not the fundamental constituent of spacetime per se, but rather the avenue by which subregion duality manifests.

Future directions

This paper has attempted to clarify the nature of spacetime in holographic theories and it naturally raises interesting questions to be investigated in future work.

Reconstructability and generalized holographic renormalization

The analysis of this paper utilized the condition for reconstructable spacetime presented in Ref. [118], but appropriately generalized for use in the context of holographic screens [111]. This paper illuminated some highly desirable properties of the directly reconstructable region defined in this manner—namely that one can describe this region state independently. It would be extremely beneficial to attempt to find an explicit way to construct bulk operators using this method, perhaps uniting it with the methods of entanglement wedge reconstruction [116, 117].

It would also be interesting to try and develop new tools for reconstructing the bulk. The relationship between the depth in the bulk and the scale in the boundary theory in AdS/CFT suggests that it may be possible to define the reconstructable region of spacetime as that which is swept through a renormalization procedure. How this manifests in general holography is not clear, but it is suggestive that there exists at least one foliation where one can "pull" the leaf inward while retaining the ability to consistently apply the HRRT prescription. Because the area of these renormalized leaves are monotonically decreasing, it is natural that this "pulling" may correspond to some renormalization procedure. The decrease in area also happens locally, which can be seen by generalizing the spacelike monotonicity theorem of Ref. [32].

One guess as to how to construct the renormalized leaf is to first pick the coarse graining scale of the boundary, and then define the new leaf as the collection of all of the deepest points of the extremal surfaces anchored to subregions with the size of the coarse graining scale. In AdS/CFT this will pull the boundary in along the z direction as expected, while in FRW spacetimes this will pull the leaf along the null direction if the coarse graining scale is small. Using this method, one can renormalize to a given scale in a number of different ways. For example, one could perform many small renormalization steps or one large one. The renormalized leaves in the two cases will generically differ, and this may correspond to the difference between one-shot renormalization and a renormalization group method. The collection of all renormalized leaves may then determine the reconstructable

region.[17] Theorem 2 tells us that once the renormalized state becomes maximally entropic, the renormalization procedure must halt. Furthermore, because extremal surfaces for non-maximally entropic states probe the bulk, this renormalization procedure will continue until the leaf becomes maximally entangled. Thus, this renormalization group flow will halt only once a bifurcation surface or a null non-expanding surface is reached. In this language, maximally entropic states correspond to fixed points. This is speculation, but may shed some light on the nature of renormalization in general holographic theories.

Cosmic equilibration

In Section 4.2, we proved that maximally entropic states have no directly reconstructable spacetime. Additionally, we argued that if one desires a state on a holographic screen to be maximally entropic and evolve in time, then the holographic screen is a null non-expanding surface and the directly reconstructable region is no more than the screen itself. This suggests that in a holographic theory of cosmological spacetimes, if a state becomes maximally entropic and the screen does not halt, then the holographic description approaches that of de Sitter space. Consequently, the area of the screen is constant. It would be interesting to investigate the result from the other direction. By first assuming that the screen approaches a constant area, one may be able to argue that the leaves would then approach maximal entropy, and hence the holographic description approaches that of de Sitter space. This could provide another way to consider equilibrating to de Sitter type solutions; see Ref. [145].

Complementarity

In Appendix 4.6, we highlighted the dependence of the reconstructable region on the frame of reference. In the case of the two-sided AdS black hole, we considered different reference frames corresponding to different time slicings in the same boundary theory—as one shifts the difference in the two boundary times, one recovers more and more of the black hole interior. This is an example of complementarity. It would be interesting to pursue this idea further and investigate the directly reconstructable region of a two-sided black hole.

One intriguing aspect of the two-sided black hole is that the directly reconstructable region does not extend beyond the extremal surface barrier; this is a *macroscopic* distance away from the future singularity, regardless of the boundary frame. Does this mean that the boundary CFT cannot describe semiclassical physics behind this barrier, even where curvature is small? Perhaps this means that there is a different description for the interior, living on a different holographic space.

---

[17]Using this construction, it is not possible to extend reconstruction beyond horizons, but it is possible to reach behind entanglement shadows.

Fundamentality of subregion duality

In many of the discussions throughout this paper, we either required subregion duality or saw that it naturally arose from other considerations. This seems to suggest that subregion duality is a fundamental characteristic of general holography. Investigating the manner in which subregion duality arises in AdS/CFT may shed light on holography in general spacetimes.

Holographic theory of flat FRW spacetimes

One of the most obvious open problems is that of finding an effective holographic theory applicable beyond asymptotically AdS spacetimes. In this paper and throughout previous work, we have focused on the case of flat FRW universes and assumed that a theory exists on the holographic screen in which the generalized HRRT prescription holds. Investigations into this has led to a deeper understanding of the nature of entanglement in constructing spacetime, along with (the lack of) state dependence in holographic theories.

It seems that a consistent theory is possible, and the most promising candidate for a theory describing the gravitational degrees of freedom is a theory with long-range interactions in which the energy of the states are dual to the fluid parameter of the FRW universe. We know that it cannot be entirely nonlocal because this would prohibit the existence of entanglement phase transitions. A theory with long range interactions would accurately reproduce the entanglement entropy structure we observe for FRW universes and would allow for a universal theory describing the single class of spacetimes. Beyond this, we have some additional data about the properties of the boundary theory.

We know that a code subspace of states manifests, and these states are dual to bulk excitations. Assuming subregion duality holds, one can ask the question of whether or not nonlocality/very long-range interactions in the gravitational degrees of freedom prohibits the local propagation of bulk excitations in the boundary theory. We expect that the operators dual to bulk excitations are weakly coupled to the gravitational degrees of freedom, and that a local description of these bulk operators exists in the boundary. In fact, this is what happens when one renormalizes the AdS boundary down to a single AdS volume [146]. This renormalization induces an infinite set of interactions which makes the resulting theory on the renormalized boundary nonlocal. Despite this, the renormalized theory still describes bulk physics through subregion duality. Hence, the nonlocality of the boundary theory does not seem to be a fundamental obstacle in describing low energy excitations using local dynamics in the boundary theory.[18] The dynamics of boundary operators dual to bulk excitations in flat FRW spacetimes was studied in Ref. [33] and it was determined that regardless of dimension and fluid parameter, the spread of these operators was characteristic of a theory with $z = 4$ Lifshitz scaling. This provides extra constraints for finding a candidate theory.

---

[18]It would be interesting to study this effective boundary theory, induced in AdS/CFT by renormalizing all the way down to the AdS scale. The holographic theory capturing sub-AdS locality could be very closely related to the theory on holographic screens.

Holographic theory for general spacetimes

It might appear that defining quantum gravity using holography, as envisioned here, is background dependent. Namely, the holographic theory is given for each class of background spacetimes, e.g. asymptotically AdS spacetimes and flat FRW spacetimes. This situation is analogous to defining string theory on the worldsheet, which is defined separately on each target space background. From the perspective of the worldsheet, different backgrounds correspond to different theories living on the two dimensional spacetime. Nevertheless, we believe there exists some unified framework encompassing all these possibilities. Similarly, in the case of holographic theories, it is plausible that the resultant theories for different background spacetimes correspond to different sectors described within a single framework.

4.6 Appendix

Reconstructability of Two-sided Black Holes and Complementarity

In the main part of the text, we have focused on spacetimes having a simply connected boundary. It is interesting to consider when this is not the case and examine which (if any) results persist. For definiteness, we here analyze the case of a two-sided eternal black hole in asymptotically AdS space. In this case, the holographic screen is the union of the two asymptotic boundaries at spacelike infinity. The boundary theory comprises two CFTs, CFT_L and CFT_R, which are decoupled from each other. Hence, the Hamiltonian for the system is given by

$$H_{\text{total}} = H_L + H_R. \tag{4.28}$$

The times t_L and t_R associated respectively with H_L and H_R run in opposite directions along the two asymptotic boundaries.

Since the theories are decoupled, it might appear that one could evolve each of the theories independently—effectively foliating the holographic screen by two independent parameters, (t_L, t_R). Per the construction outlined in Section 4.2, the directly reconstructable region would then be the union of all points localized by intersecting entanglement wedges of HRRT surfaces individually anchored to "one" leaf, each of which is labeled by (t_L, t_R). Here, "one" leaf corresponds to picking a connected, equal time slice of the left boundary and independently a connected, equal time slice of the right boundary. If this were the case, the reconstructable region would be most of the spacetime, including a macroscopic portion of the interior (aside from a region near the singularity with $r < r_+/2^{1/d}$, where r_+ is the horizon radius) [147].

However, a theory described by Hamiltonian dynamics should have a single time parameter. To make the holographic theory compatible with this, we postulate that there is a single parameter t that foliates the multiple disconnected components of the holographic screen. From this assumption, there are multiple suitable foliations, and among them we

must pick one—this corresponds to choosing a reference frame, a gauge for the holographic redundancy [43]. In the case of a two-sided black hole, this gives us a one parameter family of foliations corresponding to the freedom in choosing the relative time shift between t_L and t_R in the CFTs, even after choosing a natural foliation at each boundary.

In general, each of these individual foliations reconstruct a different region of the bulk spacetime. For example, adopting the usual thermofield double state construction [148] corresponds to choosing a reference frame

$$t_L = t_R = t, \tag{4.29}$$

in which the $t = 0$ slice in the bulk is the one passing through the bifurcation surface. Since time translation is a Killing symmetry in this spacetime, and the bifurcation surface is invariant under this translation, the HRRT surfaces for any time t never enter the interior of the black hole. Connected HRRT surfaces always pass through the bifurcation surface in such a situation (unless the subregion has support on only one of the boundaries, in which case the HRRT surface stays in one side of the black hole). The reconstructable region in this reference frame, therefore, does *not* include the interior of the black hole.

However, one could alternatively consider a reference frame in which there is a relative shift in the two times

$$t_L = t + \Delta, \quad t_R = t. \tag{4.30}$$

In this case, the connected HRRT surfaces would not necessarily pass through the bifurcation surface and could probe regions of the interior, and hence parts of the interior will be reconstructable. We can interpret this foliation dependence of the reconstructable region as a version of complementarity [39]. In this light, the canonical thermofield double time foliation corresponds to an entirely exterior description of the black hole, while increasing Δ allows for more of the region behind the horizon to be reconstructed. An important point is that we should not consider leaves with different Δ's in a single description—they correspond to different descriptions in different reference frames. We also note that regardless of the foliation, we cannot reconstruct near the singularity because of the extremal surface barrier located at $r = r_+/2^{1/d}$. This suggests that in order to probe physics of the singularity we must use a different method.

With this interpretation of bulk reconstruction, we would like to examine whether or not spacetime "disappears" as we approach maximal entropy. A priori, it seems that a macroscopic spacetime region would remain as we increase the black hole radius because some portion of the interior is reconstructable. However, this apparent contradiction is resolved by considering a finite coordinate time interval and examining the reconstructable volume as one increases the temperature.

Consider any foliation where the relative time shift between t_L and t_R has been fixed. In order to carry out the analysis analogous to Section 4.2, we fix an interval of coordinate time Δt and fix the cutoff surface at $r = R$. Increasing the temperature of the black hole moves the horizon closer and closer to the cutoff surface, which can be represented in the Penrose diagram as in Fig. 4.10. The allowed range of times is depicted by the constant time surfaces
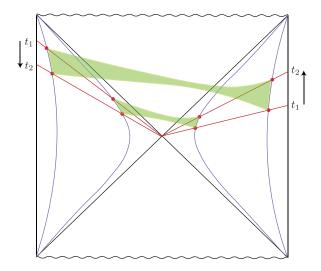
Figure 4.10: The spacetime regions reconstructable using connected HRRT surfaces anchored to subregions with support on both asymptotic boundaries within the range $t \in [t_1, t_2]$ are depicted (green shaded regions) for two different values of black hole horizon radius r_+ in a two-sided eternal AdS black hole. The holographic screen (blue) in both cases is the cutoff surface $r = R$. Here, we superimpose the respective Penrose diagrams in the two cases to compare the amount of reconstructable spacetime volume available by allowing connected HRRT surfaces.

t_1 and t_2. As we take the limit $r_+ \to R$, which corresponds to taking the temperature of the black hole $T_{\mathrm{H}} \to \Lambda$ where Λ is the cutoff in the boundary theory, the finite range of time collapses down to the bifurcation surface on both sides. Thus, the relative reconstructable spacetime volume shrinks to zero.

We find that our claim persists despite the addition of a disconnected boundary region that allows for the reconstruction of spacetime behind a black hole horizon.

Calculations for the Schwarzschild-AdS Spacetime

In this appendix, we provide explicit calculations of the spatial volume and HRRT surfaces of the Schwarzschild-AdS spacetime.

Reconstructable volume

The Schwarzschild-AdS spacetime in $d + 1$ dimensions is described by the metric

$$ds^2 = -\left(\frac{r^2}{l^2} + 1 - \frac{2\mu}{r^{d-2}}\right)dt^2 + \frac{dr^2}{\frac{r^2}{l^2} + 1 - \frac{2\mu}{r^{d-2}}} + r^2 d\Omega_{d-1}^2, \qquad (4.31)$$

where l is the AdS radius, and μ is related with the black hole horizon radius r_+ as

$$2\mu = \frac{r_+^d}{l^2}\left(1 + \frac{l^2}{r_+^2}\right). \tag{4.32}$$

The Hawking temperature of the black hole is given by

$$T_{\mathrm{H}} = \frac{dr_+^2 + (d-2)l^2}{4\pi r_+ l^2}. \tag{4.33}$$

Consider a large AdS black hole $r_+ \gg l$. In this limit,

$$2\mu = \frac{r_+^d}{l^2}, \qquad T_{\mathrm{H}} = \frac{dr_+}{4\pi l^2}, \tag{4.34}$$

and the metric is well approximated by

$$ds^2 = -\left(\frac{r^2}{l^2} - \frac{r_+^d}{l^2 r^{d-2}}\right)dt^2 + \frac{dr^2}{\frac{r^2}{l^2} - \frac{r_+^d}{l^2 r^{d-2}}} + r^2 d\Omega_{d-1}^2. \tag{4.35}$$

Let us now introduce an infrared cutoff $r \leq R$ and consider the spatial volume between the black hole horizon and the cutoff

$$
\begin{aligned}
V(r_+, R) &= A_{d-1} \int_{r_+}^{R} \frac{r^{d-1}}{\sqrt{\frac{r^2}{l^2} - \frac{r_+^d}{l^2 r^{d-2}}}}\, dr \\
&= \frac{2\pi^{d/2}}{\Gamma(d/2)} \, l \, r_+^{d-1} \int_1^{\frac{R}{r_+}} \frac{x^{d-2}}{\sqrt{1 - \frac{1}{x^d}}}\, dx,
\end{aligned} \tag{4.36}
$$

where $A_{d-1} = 2\pi^{d/2}/\Gamma(d/2)$ is the area of the $(d-1)$-dimensional unit sphere. Here, we have focused on the spatial volume because the system is static.

We normalize this volume by the volume of the region $r \leq R$ in empty AdS space

$$
\begin{aligned}
V(R) &= A_{d-1} \int_0^{R} \frac{r^{d-1}}{\sqrt{\frac{r^2}{l^2} + 1}}\, dr \\
&= \frac{2\pi^{d/2}}{(d-1)\Gamma(d/2)} \, l \, R^{d-1},
\end{aligned} \tag{4.37}
$$

where we have used $R \gg l$ in the second line. This gives us the quantity quoted in Eq. (4.1):

$$f\left(\frac{r_+}{R}\right) \equiv \frac{V(r_+, R)}{V(R)} = (d-1)\frac{r_+^{d-1}}{R^{d-1}} \int_1^{\frac{R}{r_+}} \frac{x^{d-2}}{\sqrt{1 - \frac{1}{x^d}}}\, dx. \tag{4.38}$$

HRRT surfaces

Consider a large black hole in asymptotically AdS space. The holographic theory is then a CFT. Suppose the temperature of the system T is lower than the cutoff scale, $T < \Lambda$. Here we study the behavior of the von Neumann entropy of a spherical cap region A on $r = R$ in this setup.

The region is specified by a half opening angle ψ

$$0 \leq \theta \leq \psi, \tag{4.39}$$

where θ is a polar angle parameterizing S^{d-1} with constant t and r. The HRRT surface γ_A is then given by function $r(\theta)$, which is determined by minimizing the area functional:

$$\|\gamma_A\| =$$

$$\underset{r(\theta)}{min} \left[A_{d-2} \int_0^\psi r^{d-2} \sin^{d-2}\theta \sqrt{r^2 + \frac{(\frac{dr}{d\theta})^2}{\frac{r^2}{l^2}+1-\frac{2\mu}{r^{d-2}}}} \, d\theta \right], \text{(4.40)} \text{with the boundary condition}$$

$$r(\psi) = R, \tag{4.41}$$

where A_{d-2} is the area of the $(d-2)$-dimensional unit sphere, and μ is given by Eq. (4.31). Here and below, we assume $\psi \leq \pi/2$. For $\psi > \pi/2$, the entropy of A is determined by $S(\psi) = S(\pi - \psi)$.

The surface γ_A is well approximated to consist of two components: (i) a "cylindrical" piece with $\theta = \psi$, which is perpendicular to the cutoff surface $r = R$ and extends down to $r = r_0 \ (< R)$ and (ii) the "bottom lid" with $r = r_0$ and $0 \leq \theta \leq \psi$; see Fig. 4.11. The area of the surface is then given by

$$\|\gamma_A\| = \min_{r_0} \left[A_{d-2} \sin^{d-2}\psi \int_{r_0}^R \frac{r^{d-2}}{\sqrt{\frac{r^2}{l^2} - \frac{r_+^d}{l^2 r^{d-2}}}} \, dr + A_{d-2} \, r_0^{d-1} \int_0^\psi \sin^{d-2}\theta \, d\theta \right], \tag{4.42}$$

where r_+ is the horizon radius, and we have used the approximation that $r_+ \gg l$ and hence Eq. (4.34). The value of r_0 is determined by the minimization condition

$$\sqrt{r_0^2 - \frac{r_+^d}{r_0^{d-2}}} = \frac{\sin^{d-2}\psi}{(d-1) \int_0^\psi \sin^{d-2}\theta \, d\theta} l. \tag{4.43}$$

As discussed in Section 4.2, the cutoff at $r = R$ in our context simply means that the renormalization scale in the boundary theory is lowered; in particular, it does not mean that the theory is modified by actually terminating space there. The length in the boundary theory, therefore, is still measured in terms of the d-dimensional metric at infinity, $r = \infty$, with the conformal factor stripped off. The radius of the region A is then given by

$$L = l \, \psi, \tag{4.44}$$
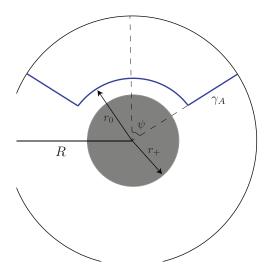
Figure 4.11: The HRRT surface γ_A in the Schwarzschild-AdS spacetime can be well approximated by consisting of two components: a "cylindrical" piece with $\theta = \psi$ and a "bottom lid" piece with $r = r_0$.

and not $R\psi$. Since the cutoff length is $1/\Lambda \approx l^2/R$, we should only consider the region $\psi \gtrsim l/R$.

The solution of Eq. (4.43) behaves as

$$\text{(i)} \quad r_0 = \frac{l}{\psi} \ (\gg r_+) \qquad\qquad \text{for } \frac{l}{R} < \psi \ll \frac{l}{r_+}, \tag{4.45}$$

$$\text{(ii)} \quad r_0 - r_+ = \frac{l^2}{d\psi^2 r_+} \ (\ll \frac{r_+}{d}) \quad \text{for } \frac{l}{r_+} \ll \psi \ll 1, \tag{4.46}$$

$$\text{(iii)} \quad r_0 - r_+ = O(1)\frac{l^2}{r_+} \qquad\qquad \text{for } \psi \approx O(1). \tag{4.47}$$

In the case of (i), $\|\gamma_A\|$ is dominated by the first term in Eq. (4.42), so that

$$\|\gamma_A\| = \frac{A_{d-2}}{d-2} l R^{d-2} \psi^{d-2}. \tag{4.48}$$

Here and below, we assume $d > 2$. We thus obtain an area law for the entropy

$$S_A = \frac{\|\gamma_A\|}{4l_{\mathrm{P}}^{d-1}} \approx c A_{d-2} L^{d-2} \Lambda^{d-2}, \tag{4.49}$$

where $c \approx (l/l_{\mathrm{P}})^{d-1}$ is the central charge of the boundary CFT.

In the case of (ii), $\|\gamma_A\|$ is given by

$$\|\gamma_A\| = \frac{A_{d-2}}{d-2} l R^{d-2} \psi^{d-2} + \frac{A_{d-2}}{d-1} r_+^{d-1} \psi^{d-1}. \tag{4.50}$$

We find that the first (second) term is larger for

$$\psi < (>) \frac{d-1}{d-2} \frac{l R^{d-2}}{r_+^{d-1}}, \tag{4.51}$$

so that the entanglement entropy behaves as

$$S_A \approx \begin{cases} c A_{d-2} L^{d-2} \Lambda^{d-2} & \text{for } L \ll L_*, \\ c A_{d-2} \frac{r_+^{d-1} L^{d-1}}{l^{2d-2}} \approx c \left(\frac{T}{\Lambda}\right)^{d-1} A_{d-2} L^{d-1} \Lambda^{d-1} & \text{for } L \gg L_*, \end{cases} \tag{4.52}$$

where

$$L_* \approx \frac{l^2 R^{d-2}}{r_+^{d-1}} \approx \frac{\Lambda^{d-2}}{T^{d-1}}. \tag{4.53}$$

For $\psi \approx O(1)$, i.e. case (iii), we find

$$S_A \approx c \left(\frac{T}{\Lambda}\right)^{d-1} A_{d-2} L^{d-1} \Lambda^{d-1}. \tag{4.54}$$

Combining the results in all three cases gives the expression in Eqs. (4.17, 4.18).

Calculations for the de Sitter Limit of FRW Universes

This appendix collects explicit calculations for entropies and HRRT surfaces in the de Sitter limit of FRW spacetimes.

Entropies in the case of (2 + 1)-dimensional bulk

Here we see that for $(2+1)$-dimensional FRW spacetimes, the results of Ref. [32] immediately tell us that the entanglement entropy of an arbitrary (not necessarily connected) subregion A is maximal in the de Sitter limit:

$$S_{A,w\to-1} = \frac{1}{4l_P} \min\{\|A\|, \|\bar{A}\|\}. \tag{4.55}$$

Consider an FRW universe in $d+1$ dimensions dominated by a single ideal fluid component with the equation of state parameter $w = p/\rho$ ($|w| \le 1$). From the analysis of Ref. [32], we know that the holographic entanglement entropy of a spherical cap region A on a leaf—parameterized by the half opening angle ψ as viewed from the center of the bulk—scales with the smaller of the volumes of A and $\bar{A}$. The proportionality constant

$$Q_w(\psi) \equiv \frac{S(\psi)}{\frac{1}{4l_P^{d-1}} \min\{\|A\|, \|\bar{A}\|\}}, \tag{4.56}$$

satisfies the properties

$$Q_w(\psi \to 0) \to 1, \qquad Q_{w\to-1}(\psi) \to 1, \tag{4.57}$$
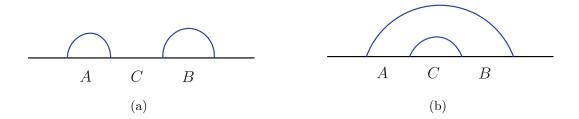
Figure 4.12: Two possible extremal surfaces anchored to the boundary of a subregion AB on a leaf, given by the union of two disjoint intervals A and B. The areas of the surfaces depicted in (a) and (b) are denoted by $E_{\text{disconnected}}(AB)$ and $E_{\text{connected}}(AB)$, respectively.

$$\frac{\partial Q_w(\psi)}{\partial \psi}\bigg|_{\psi=0} = 0, \qquad \frac{\partial Q_w(\psi)}{\partial \psi}\bigg|_{\psi<\frac{\pi}{2}} \leq 0, \qquad \frac{\partial Q_w(\psi)}{\partial w} < 0. \tag{4.58}$$

(The original analysis was performed for $(3 + 1)$-dimensional FRW universes, but these properties persist in arbitrary spacetime dimensions.)

The second relation in Eq. (4.57) implies that in the de Sitter limit, $w \to -1$, the holographic entanglement entropy of a spherical cap region is maximal. Now, consider $(2 + 1)$-dimensional FRW universes, in which a leaf has only one spatial dimension. We consider a subregion on the leaf consisting of the union of two small intervals A and B. Note that a similar setup is often discussed in AdS/CFT, where two possible extremal surfaces homologous to the subregion compete, so that a phase transition from the disconnected to connected HRRT surfaces occurs as the regions A and B are taken to be closer; see Fig. 4.12. We want to understand what happens in the case of FRW spacetimes.

We denote the areas of two possible extremal surfaces by

$$\begin{aligned} E_{\text{disconnected}}(AB) &= E(A) + E(B) \\ &= Q_w(A) \, \|A\| + Q_w(B) \, \|B\|, \end{aligned} \tag{4.59}$$

and

$$\begin{aligned} E_{\text{connected}}(AB) &= E(ABC) + E(C) \\ &= Q_w(ABC) \, \|ABC\| + Q_w(C) \, \|C\|, \end{aligned} \tag{4.60}$$

where A, B, and C are defined in Fig. 4.12. A phase transition can occur when

$$E_{\text{disconnected}}(AB) = E_{\text{connected}}(AB). \tag{4.61}$$

The condition of Eq. (4.61) can be satisfied for any w away from the de Sitter limit because of the second relation in Eq. (4.58). Since a larger region has a greater volume

but also has a smaller coefficient, it is possible for the two extremal surfaces to compete. However, in the de Sitter limit the requirement for a phase transition becomes

$$\|ABC\| + \|C\| = \|A\| + \|B\|, \tag{4.62}$$

which is clearly impossible because the left hand side is always greater. Since a general subregion of the leaf is a union of disconnected intervals, the above argument implies that the entanglement entropy is merely the sum of each interval's volume for sufficiently small regions. Extending the argument to large regions in which their complements matter, we can conclude that arbitrary subregions have maximal entanglement entropies in a $(2 + 1)$-dimensional de Sitter universe.

Entropies in the $w \to -1$ limit of FRW spacetimes

The global spacetime structure in the case of a single fluid component with $w \neq -1$ is qualitatively different from the case discussed mainly in Section 4.2, i.e. the case in which a universe approaches de Sitter space at late times. Nevertheless, here we show that the holographic entanglement entropy of an arbitrary subregion on a leaf becomes maximal in the $w \to -1$ limit.

Let us consider an FRW universe filled with a single fluid component with the equation of state w. The scale factor is then given by

$$a(t) = c \, t^{\frac{2}{d(1+w)}}, \tag{4.63}$$

where $c > 0$ is a constant. We focus on a leaf σ_* at time t_* and the causal region D_{σ_*} associated with it. Following Ref. [32], we perform t_*-dependent coordinate transformation on the FRW time and radial coordinates t and r:

$$\eta = \frac{2}{d - 2 + dw} \left\{ \left(\frac{t}{t_*} \right)^{\frac{d-2+dw}{d(1+w)}} - 1 \right\}, \tag{4.64}$$

$$\rho = \frac{2}{d(1 + w)} c \, t_*^{-\frac{d-2+dw}{d(1+w)}} r. \tag{4.65}$$

This converts the metric into the form

$$ds^2 = \left(\frac{\mathcal{A}_*}{A_{d-1}} \right)^{\frac{2}{d-1}} \left(\frac{d - 2 + dw}{2} \eta + 1 \right)^{\frac{4}{d-2+dw}} \left(-d\eta^2 + d\rho^2 + \rho^2 d\Omega_{d-1}^2 \right), \tag{4.66}$$

where A_{d-1} is the area of the $(d - 1)$-dimensional unit sphere, defined below Eq. (4.36), and $\mathcal{A}_*$ is the volume of the leaf σ_*

$$\mathcal{A}_* = \left(\frac{d(1 + w)}{2} \right)^{d-1} A_{d-1} \, t_*^{d-1}. \tag{4.67}$$

In these coordinates, D_{σ_*} is mapped into the region $\eta \in [-1, 1]$ and $\rho \in [0, 1 - |\eta|]$.[19]

We can now take $w = -1 + \epsilon$ in Eq. (4.66) and expand it around $\epsilon = 0$. This gives

$$ds^2 = \left(\frac{\mathcal{A}_*}{A_{d-1}} \right)^{\frac{2}{d-1}} \left(\frac{1}{(1-\eta)^2} - d\frac{\eta + (1-\eta)\ln(1-\eta)}{(1-\eta)^3}\epsilon + \cdots \right) \left(-d\eta^2 + d\rho^2 + \rho^2 d\Omega_{d-1}^2 \right). \quad (4.68)$$

The leading order term describes the causal region inside a leaf of volume $\mathcal{A}_*$ in de Sitter space with conformal coordinates. The time translational Killing symmetry in these coordinates is

$$\eta \to a\eta + 1 - a, \quad (4.69)$$

$$\rho \to a\rho. \quad (4.70)$$

The expansion in Eq. (4.68) is not valid when $\eta \lesssim 1 - \epsilon$. However, this occurs only for a small subset of all the subregions on σ_*, which becomes measure zero when $\epsilon \to 0$. Continuity then tells us that the entanglement entropy S_A of any subregion A on σ_* takes the same value as that calculated in de Sitter space in the $\epsilon \to 0$ limit. However, we have already concluded from the argument in Section 4.2 that the entanglement entropies take the maximal form in de Sitter space, hence

$$S_A \xrightarrow[w \to -1]{} \frac{1}{4l_{\mathrm{P}}^{d-1}} \min\{\|A\|, \|\bar{A}\|\}. \quad (4.71)$$

Note that the area of the leaf, $\mathcal{A}_*$, keeps growing indefinitely, so that D_{σ_*} at each time t_* is mapped to a different auxiliary de Sitter space. The ratio $Q_w(A) = S_A/(\min\{\|A\|, \|\bar{A}\|\}/4l_{\mathrm{P}}^{d-1})$, however, depends only on w and not t_*.

HRRT surfaces

Here we present two examples in which one can analytically see the convergence of the HRRT surfaces onto the future boundary of the causal region of a leaf in the de Sitter limit.

The de Sitter limit of FRW universes in $2+1$ dimensions

As the first example, consider the de Sitter limit of FRW universes in $2 + 1$ dimensions

$$ds^2 = a^2(\eta) \left(-d\eta^2 + dx^2 + dy^2 \right). \quad (4.72)$$

Here, $\eta \in (-\infty, 0)$ is the conformal time, and the scale factor is given by

$$a(\eta) = \frac{c}{\eta}, \quad (4.73)$$

---

[19]For $w \geq -1 + 4/d$, the region D_{σ_*} hits the big bang singularity, so we need to restrict our attention to a portion of D_{σ_*}, e.g. $D_{\sigma_*}^+ = \{p \in D_{\sigma_*} \mid t(p) \geq t_*\}$. This issue is not relevant to our discussion here.

where c is a positive constant. In this case, we can obtain an analytic solution for HRRT surfaces, which are geodesics in $2+1$ dimensions.

In order to find a spacelike geodesic anchored to two points on the leaf, we can use the symmetry of the problem to rotate our axes so that the points lie at constant $y = y_0$. To find a geodesic, we need to extremize the distance functional

$$\mathcal{D} = \int d\eta \, \frac{c}{\eta} \sqrt{\dot{x}^2 - 1}, \tag{4.74}$$

where $\dot{x} = dx/d\eta$, and we have used the fact that the geodesic lies on the $y = y_0$ hypersurface. This functional has no explicit dependence on x, which means the existence of a quantity that is conserved along the geodesic

$$\frac{\partial \mathcal{D}}{\partial \dot{x}} = \frac{c \dot{x}}{\eta \sqrt{\dot{x}^2 - 1}} \equiv p_x. \tag{4.75}$$

Using this, we obtain a first-order ordinary differential equation

$$\frac{d\eta}{dx} = \sqrt{1 - \frac{c^2}{p_x^2 \eta^2}}, \tag{4.76}$$

which can be easily solved to give the analytic expression for the geodesic

$$\begin{cases} \eta(x) & = -\sqrt{x^2 + \frac{c^2}{p_x^2}}, \\ y(x) & = y_0. \end{cases} \tag{4.77}$$

The holographic screen of FRW universes in the de Sitter limit lies on

$$\eta = -\sqrt{x^2 + y^2} \equiv -r. \tag{4.78}$$

Consider a leaf at $\eta = \eta_* = -r_*$ and a subregion on it specified by a half opening angle ψ $(0 \leq \psi \leq \pi)$. The end points of the HRRT surface are then at

$$(x, y) = (\mp \eta_* \sin \psi, -\eta_* \cos \psi). \tag{4.79}$$

This can be used to determine p_x and y_0 in Eq. (4.77), giving the final expression for the geodesic

$$\begin{cases} \eta(x) & = -\sqrt{x^2 + y_0^2}, \\ y(x) & = y_0, \end{cases} \tag{4.80}$$

where $y_0 = -\eta_* \cos \psi$. By varying the angle ψ, the HRRT surfaces sweep a codimension-1 surface in the bulk, which is indeed the future boundary of the causal region of the leaf:

$$\eta = -r, \qquad 0 \leq r \leq r_* \, (= -\eta_*). \tag{4.81}$$

These surfaces are depicted in x-y-η space in Fig. 4.13. We can clearly see that all the HRRT surfaces are spacelike, except for that corresponding to $\psi = \pi/2$ which is null.
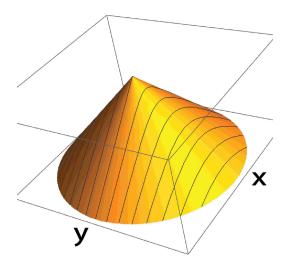
Figure 4.13: HRRT surfaces anchored to subregions on a leaf in $(2+1)$-dimensional de Sitter space. They all lie on the future boundary of the causal region associated with the leaf.

Small spherical caps in FRW universes in $d+1$ dimensions

Another example in which simple analytic expressions are obtained is the limit of small spherical cap regions, $\psi \ll 1$, on a leaf. Consider a flat FRW universe in $d+1$ dimensions

$$ds^2 = a(\eta)^2\big(-d\eta^2 + dr^2 + r^2 d\Omega_{d-1}^2\big), \tag{4.82}$$

filled with a single fluid component with the equation of state w. We consider the leaf σ_* at $\eta = \eta_*$, which is located at

$$r = \frac{a}{\dot{a}}. \tag{4.83}$$

The future boundary F_* of the causal region D_{σ_*} is then given by

$$F_* : \eta(r) = \eta_* + \frac{a}{\dot{a}} - r. \tag{4.84}$$

Here and below, the scale factor and its derivatives without an argument represent those at $\eta = \eta_*$:

$$a \equiv a(\eta_*), \qquad \dot{a} \equiv \left.\frac{da(\eta)}{d\eta}\right|_{\eta=\eta_*}, \qquad \ddot{a} \equiv \left.\frac{d^2a(\eta)}{d\eta^2}\right|_{\eta=\eta_*}. \tag{4.85}$$

We consider a spherical cap region A on the leaf σ_*, specified by a half opening angle ψ

$$0 \leq \theta \leq \psi, \tag{4.86}$$

where θ is a polar angle parameterizing S^{d-1} with constant η and r. Following Ref. [32], we go to cylindrical coordinates:

$$\xi = r\sin\theta, \qquad z = r\cos\theta - \frac{a}{\dot{a}}\cos\psi. \tag{4.87}$$
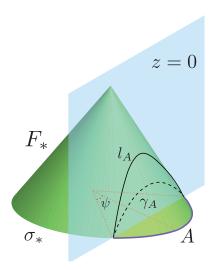
Figure 4.14: The HRRT surface γ_A for subregion A of a leaf σ_* specified by a half opening angle ψ is on the $z = 0$ hypersurface. It approaches the surface l_A, the intersection of the null cone F_* and the $z = 0$ hypersurface, in the de Sitter limit.

In these coordinates, the null cone F_* in Eq. (4.84) is given by

$$F_* : \eta(\xi) = \eta_* + \frac{a}{\dot{a}} - \sqrt{\xi^2 + \left(z + \frac{a}{\dot{a}}\cos\psi\right)^2}, \tag{4.88}$$

and the boundary of A, ∂A, is located at

$$\eta = \eta_*, \qquad \xi = \frac{a}{\dot{a}}\sin\psi \equiv \xi_*, \qquad z = 0. \tag{4.89}$$

The HRRT surface γ_A anchored to ∂A is on the $z = 0$ hypersurface [32]. We would like to compare this HRRT surface with the intersection of F_* and $z = 0$:

$$l_A : \eta(\xi) = \eta_* + \frac{a}{\dot{a}} - \sqrt{\xi^2 + \frac{a}{\dot{a}}\cos\psi}, \tag{4.90}$$

see Fig. 4.14. Using Eq. (4.89) and expanding in powers of $\psi \sim \xi/(a/\dot{a})$, this can be written as

$$l_A : \eta(\xi) = \eta_* + \frac{\dot{a}}{2a}(\xi_*^2 - \xi^2) + \frac{\dot{a}^3}{8a^3}(\xi_*^2 - \xi^2)^2 + \cdots. \tag{4.91}$$

For $\psi \ll 1$, the HRRT surface can be expressed in a power series form

$$\gamma_A : \eta(\xi) = \eta_* + \eta^{(2)}(\xi) + \eta^{(4)}(\xi) + \cdots, \tag{4.92}$$

where

$$\eta^{(2)}(\xi) = \frac{\dot{a}}{2a}(\xi_*^2 - \xi^2), \tag{4.93}$$

$$\eta^{(4)}(\xi) = -\frac{\dot{a}}{8a^3(d+1)}(\xi_*^2 - \xi^2)$$
$$\times \left[\dot{a}^2\{(d+5)\xi_*^2 - (d-3)\xi^2\} - a\ddot{a}\{(d+3)\xi_*^2 - (d-1)\xi^2\}\right]. \tag{4.94}$$

In the universe dominated by a single fluid component, the scale factor behaves as

$$a(\eta) \propto \eta^{\frac{2}{d-2+dw}}. \tag{4.95}$$

Plugging this into Eq. (4.94), we obtain

$$\eta^{(4)}(\xi) = \frac{\dot{a}^3}{16(d+1)a^3}(\xi_*^2 - \xi^2)\left[\{2 - (1+3w)d - (1+w)d^2\}\xi_*^2 - \{2 + (3+w)d - (1+w)d^2\}\xi^2\right]. \tag{4.96}$$

We find that for $w = -1$, the surface given by Eqs. (4.92, 4.93, 4.96) agree with l_A in Eq. (4.91). Namely, the HRRT surface γ_A is on the null cone F_*.

One can see how γ_A approaches F_* as $w \to -1$ by subtracting Eq. (4.92) from Eq. (4.91):

$$\eta^{l_A}(\xi) - \eta^{\gamma_A}(\xi) = \frac{\dot{a}^3}{16a^3}\frac{d}{d+1}(1+w)(\xi_*^2 - \xi^2)\{(d+3)\xi_*^2 - (d-1)\xi^2\}$$
$$\geq 0. \tag{4.97}$$

The inequality is saturated only for $w = -1$ (except at the end points at $\xi = \xi_*$).

Chapter 5

Pulling the Boundary into the Bulk

This chapter is a replication of Nomura, Rath, and Salzetta, "Pulling the Boundary into the Bulk", in *Phys. Rev.* D98.2 (2018), p. 026010, and is reproduced here in its original form.

5.1 Introduction

The holographic duality between asymptotically Anti-de Sitter (AdS) spacetimes in $d +$ 1 dimensions and conformal field theories (CFTs) in d dimensions is perhaps the closest realization of a complete theory of quantum gravity [14, 82, 15]. One of the most intriguing results stemming from this correspondence is the renowned Ryu-Takayanagi formula relating entanglement entropy in time independent CFTs to the area of minimal surfaces in the bulk spacetime [16]. The covariant extension of this formula to include time dependent cases was obtained by Hubeny-Rangamani-Takayanagi and uses extremal bulk surfaces (henceforth referred to as the HRRT prescription) [48]. Remarkably, by including quantum corrections to this formula, one obtains entanglement wedge reconstruction [27, 114]. These investigations have shed light on the deep connection between entanglement in the boundary and emergent gravitational physics in the bulk.

However, there is reason to believe that these results extend beyond the scope of AdS/CFT. The Bekenstein-Hawking formula [8, 6] and the covariant entropy bound [21] provide us with holographic bounds on entropy in general spacetimes. These suggest that gravitational physics may inherently be holographic [37, 13]. Furthermore, the areas of extremal surfaces anchored to any convex boundaries satisfy all known entropic inequalities [126, 144, 30, 149]. In isometric tensor networks, calculating the entanglement entropy of a subregion of boundary sites reduces to finding the minimum cut across the network [50]. A version of entanglement wedge reconstruction also holds in perfect and random tensor networks [110, 115]. This evidence seems to indicate that the HRRT prescription may in fact generalize to spacetimes outside of AdS.

It is with this perspective that we have pursued investigations of quantum gravity beyond AdS/CFT. We postulate that the HRRT prescription (with quantum corrections [28,

[29] to allow for entanglement wedge reconstruction) applies to general convex boundaries. In particular, we assume the existence of a quantum state that "lives" on the convex boundary and encodes the bulk geometry of the interior. Our previous work [32, 111, 34] has focused primarily on investigating this assumption applied to holographic screens [42], but holographic screens are only special in the sense that they are the largest surfaces in which we can apply the HRRT prescription in general spacetimes. In this paper, we have relaxed this condition and look at general convex surfaces—in particular this allows us to consider asymptotically AdS spacetimes.

We emphasize that the postulate we adopt here is falsifiable. At any point in the analysis, had the geometric properties of general relativity prohibited a consistent boundary interpretation, the program would have failed. Through the present, however, no such roadblock has presented itself. In fact, we can view the self-consistency of this work as further evidence that the relationship between entanglement and geometry prevails in general spacetimes.

The present framework allows us to consider a nested family of convex surfaces each of which contains less bulk information than the previous. Taking a natural continuum version of these convex surfaces yields a surface which we dub the *holographic slice*. As has proved historically useful, studying covariantly defined geometric objects yields insights into holographic theories, and the holographic slice is such an object. In particular, the slice allows us to visualize the coarse-graining of holographic states and provides us with a method to categorize bulk regions as being "more IR" than others.

The construction of the slice is purely perturbative, and thus does not allow us to analyze complex quantum gravitational states formed as superpositions of many geometries. It is inherently tied to one background geometry, but this is no more restrictive than the HRRT prescription itself. For a simply connected boundary, the slice seems to sweep the maximal bulk region that can be perturbatively reconstructed, i.e. it pulls the boundary in through shadows all the way to black hole horizons, and contracts no further. It was the study of extremal surfaces in maximally entangled pure states that initiated this work, where it was realized that maximally entangled states were fixed points of flow in the direction of small HRRT surfaces [34].[1]

Overview

In Section 5.2, we offer the intuitive motivation for the construction of the holographic slice. This reveals the connection to coarse-graining and provides a basic definition for the object. In Section 5.3, we geometrically define the object rigorously and then illustrate some of its most important properties. These properties must necessarily be satisfied for a consistent interpretation as coarse-graining of a boundary state. Section 5.4 goes through multiple explicit examples of the slice in different spacetimes.

---

[1]By maximally entangled, we mean that the von Neumann entropy of any subregion saturates the Page curve [75]. This was referred to as maximally entropic in Ref. [34].

After introducing the holographic slice as a geometric object, we are poised to analyze its boundary interpretation in Section 5.5. Here we delve into its relationship to coarse-graining and emphasize that the slice encodes a sequence of codimension-0 bulk regions, not merely the codimension-2 bulk convex surfaces. We also describe the relationship to tensor networks, particularly continuous tensor networks [150]. Because the holographic slice is constructed from one boundary time slice, it can be used as a novel gauge fixing of the bulk—this is discussed in the final subsection of Section 5.5. Since the slice grants us a way to uniquely pull in the boundary, it is natural to consider its connection to renormalization. This is explored in Section 5.6. We conclude with discussing the slice's place in the wider view of quantum gravity in Section 6.4. The appendices contain proofs of various geometric statements made in the body of the text.

Preliminaries

This paper will work in the framework of holography for general spacetimes proposed in Ref. [32]. We will highlight the applications to AdS/CFT but use language from generalized holography. In particular, the term "boundary" will refer to the holographic screen, which reduces to the conformal boundary of AdS. Additionally, holographic screens have a unique time foliation into codimension-2 surfaces called leaves [44]. This uniqueness is lost in the case of AdS because of the asymptotic symmetries, but to remain consistent within the generalized framework we must choose a particular time foliation of the boundary of AdS [111]. We will then refer to a time slice of this foliation as a leaf.

For a subregion, A, of a leaf, we will denote its HRRT surface as $\gamma(A)$ and its entanglement wedge as EW(A). EW(A) is defined as the domain of dependence of any closed, compact, achronal set with boundary $A \cup \gamma(A)$.[2] Throughout this paper, we will work at the lowest order in bulk Newton's constant. In particular, we will only consider extremal surfaces found by extremizing the area, not the generalized entropy. We expect that by making appropriate modifications, along the lines of Refs. [28, 29, 77], our results can be extended to higher orders.

For an achronal codimension-2 surface ω, we denote the domain of dependence of any achronal set with boundary ω as $D(\omega)$. Wherever $G_{\mathrm{N}} = l_{\mathrm{P}}^{d-1}$ appears, it represents Newton's constant in the bulk spacetime.

---

[2]In standard AdS/CFT, reflective boundary conditions are imposed at the conformal boundary. This extends the domain of dependence of $A \cup \gamma(A)$ to include the boundary domain of dependence of A. However, for holographic screens there are no such impositions on the screen (they can even be spacelike), and thus EW(A) generally does not include any portion of the screen other than A itself. In particular, there is no generalization of causal wedges to holographic screens.

5.2   Motivation

Amongst other things, the concept of subregion duality in holographic theories allows us to address questions regarding where bulk information is stored in the boundary theory [**Bousso:2012sj**, 112, 151, 152, 113, 76, 153, 27, 114]. This line of inquiry has provided us with the intuition that bulk geometric information is encoded redundantly in the boundary theory. In particular, a bulk local operator can be represented in multiple different regions of the boundary, a special case being the whole boundary space. However, despite this seemingly democratic distribution of bulk information throughout boundary degrees of freedom, lack of access to a boundary region necessarily prohibits the reconstruction of a corresponding bulk region. Namely, if one removes a subregion A from a leaf σ, the maximum possible bulk region reconstructed from the remaining region, $\overline{A}$, will be the entanglement wedge of $\overline{A}$, $\mathrm{EW}(\overline{A})$. This implies that indispensable information of the region $\mathrm{EW}(A)$ is stored in A.

Suppose one were to coarse-grain over all boundary subregions of balls of radius δ. From the logic above, the bulk region whose information can remain is given by

$$R(B_\delta) = \bigcap_{p \in \sigma} \mathrm{EW}\big(\overline{B_\delta(p)}\big), \tag{5.1}$$

where $B_\delta(p)$ is a ball of radius δ centered at point p on the boundary leaf σ. Because the intersection of domains of dependence is itself a domain of dependence,[3] $R(B_\delta)$ is a domain of dependence of some achronal set, and thus has a unique boundary, $\sigma(B_\delta)$.

Motivated by ideas of holographic renormalization in AdS/CFT [154, 155, 146, 156, 157], surface state correspondence [126], and previous work on holographic screens [30, 32, 111, 34], we conjecture that there exists a holographic state living on $\sigma(B_\delta)$ which encodes aspects of the bulk geometry to its interior. A check of this proposal is that the HRRT prescription can be consistently applied, in the sense that the areas of these HRRT surfaces obey the known holographic entropy inequalities. Given this consistency check, we conjecture that "coarse-grained subregion duality" holds—namely that entanglement wedge reconstruction holds on this new leaf.

Now suppose one wants to coarse-grain over some scale on this new leaf, $\sigma(B_\delta)$. This will produce a new leaf even deeper in the bulk. Repeating this process will in turn produce a series of new leaves, henceforth called renormalized leaves. Sending the coarse-graining scale at each step to zero in a consistent manner will produce a continuous family of renormalized leaves that sweep out a smooth surface through the bulk, Υ. The manner in which Υ is constructed naturally reveals its relationship to holographic coarse-graining. This prompts us to assert that the continuous coarse-graining of a holographic state pulls the boundary slice in along the slice Υ.

---

[3]We could not find a proof of this statement, so we have included one in Appendix 5.8.

5.3   Holographic Slice

The geometric object Υ is what we will refer to as the holographic slice. In this section, we give a more rigorous definition of holographic slices and highlight some of the salient properties of them.

Definition

Consider a closed codimension-2 achronal surface σ living in a $(d+1)$-dimensional spacetime M. Denote the two future-directed null orthogonal directions as k and l. Suppose the null expansions along these directions satisfy $\theta_k \leq 0$ and $\theta_l > 0$.[4] For concreteness, one could imagine σ to be a leaf of a past holographic screen ($\theta_k = 0$, $\theta_l > 0$) or a time slice of the (regularized) boundary of AdS. Borrowing this language, we will call σ a leaf. From Ref. [30], we know that the boundary of the domain of dependence of σ, $D(\sigma)$, is an extremal surface barrier for HRRT surfaces anchored to σ. In addition, the boundary of an entanglement wedge of a subregion Γ on σ serves as an extremal surface barrier for all extremal surfaces anchored within EW(Γ).

Now, on σ, consider a family of open, codimension-0 (within the leaf) smooth subregions, with an injective mapping from points on the leaf, p, to subregions, $C(p)$, with the constraint that $p \in C(p)$ and that $C(p)$ varies continuously with p. For example, one may take $C(p)$ to be open balls of radius δ centered at p, $B_\delta(p)$. Now, let

$$R(C) = \bigcap_{p \in \sigma} \text{EW}\big(\overline{C(p)}\big), \tag{5.2}$$

where $\overline{C(p)}$ is the complement of $C(p)$ in σ. From Appendix 5.8, we know that $R(C)$ itself is a domain of dependence of some achronal sets, all of which share a unique boundary, σ_C^1, called a renormalized leaf; see Fig. 5.1.

Provided the characteristic scale of EW($C(p)$) is sufficiently smaller than the extrinsic curvature scale of σ, we can identify all points on σ_C^1 with those on σ. At each point on σ, consider the plane generated by k and l. This will intersect σ_C^1 at one point so long as adjacent planes do not intersect at a caustic before hitting σ_C^1, which is guaranteed if we take $C(p)$ to be sufficiently small. We now have a natural identification of the points on σ with points on σ_C^1. In particular, we can identify the length scale δ on σ to the appropriate scale on σ_C^1. Moreover, since $\sigma_C^1 \subseteq \text{EW}(\overline{C(p)})$ $\forall p$ and $\text{EW}(\overline{C(p)})$ serves as an extremal surface barrier for all surfaces anchored within $\text{EW}(\overline{C(p)})$, all extremal surfaces anchored to σ_C^1 are contained within $R(C) = D(\sigma_C^1)$. If we interpret the area of these extremal surfaces as entanglement entropies for the associated subregions, convexity of $R(C)$ and the null energy condition ensure that all known holographic entanglement inequalities are satisfied. This allows us to interpret these extremal surfaces as HRRT surfaces.

---

[4]Appropriate modifications can be made to extend to surfaces where $\theta_k \geq 0$ and $\theta_l < 0$.
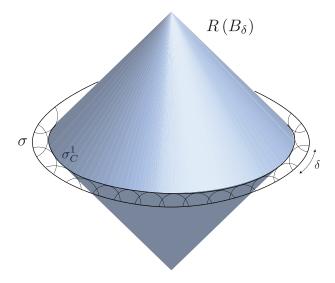
Figure 5.1: $R(B_\delta)$ is the entanglement wedge associated with the new leaf σ_C^1, where we have taken $C(p) = B_\delta(p)$. It is formed by intersecting the entanglement wedges associated with the complements of spherical subregions of size δ on the original leaf σ.

Utilizing coarse-grained subregion duality, we can repeat the construction above but with new subregions, $C^1(p)$, on the renormalized leaf, σ_C^1. This yields a new leaf σ_C^2. We can associate points on σ_C^2 with those on σ_C^1, and hence on σ, as was done above. All we require of the new subregions is that the size scale of $C^i(p)$ match with that of $C(p)$ under the natural identification described previously. This procedure can be repeated until stringy effects become important, i.e. when the size of the renormalized leaf is $O(l_{\rm s})$.

In the limit of sending the size of $C(p)$ to 0 for all p, the collection of all renormalized leaves in M, $\Upsilon = \{\sigma_C^i\}$ sweeps out a continuous surface. This is a holographic slice. Note that we can take the $G_{\rm N} \to 0$ limit in discussing classical spacetime, so we may take $C(p) \to 0$ thus making Υ continuous in this limit. We can then label the renormalized leaves of Υ by some continuous parameter λ, corresponding to the depth of the renormalized leaf, i.e. $\sigma(\lambda)$ is some σ_C^i and $\sigma(0) = \sigma$. Below we take λ to decrease as i increases, so that $\lambda \leq 0$.

Properties

Uniqueness

Υ is dependent on an extraordinary number of degrees of freedom, namely the shape $C(p)$ at each point on σ. Despite this freedom, we find that Υ is unique provided some mild assumptions hold.

In particular, imposing homogeneity and isotropy on $C(p)$ (and each subsequent $C^i(p)$) yields a unique holographic slice. For example, one can restrict themselves to the case where

$C^i(p)$ are composed of the same shape and with random orientations. These all reduce to the slice formed by considering balls of constant radius for $C(p)$ and mapping these balls to the subsequent renormalized leaves. We will focus on this preferred slice for the remainder of the paper.

A full discussion of uniqueness is provided in Appendix 5.8. However, one of the primary results is that the vector s, which is tangent to Υ and radially evolves the leaf inward is given by

$$s = \frac{1}{2}(\theta_k l + \theta_l k). \tag{5.3}$$

This tells us that for a (non-renormalized) leaf of a holographic screen, $s \propto k$ and $\theta_s = 0$. In these situations, the holographic slice initially extends in the null direction and the leaf area remains constant.

In fact, the s vector coincides with the Lorentzian generalization of the mean curvature vector of the leaf [158, 159]. This preferred holographic slice is then realized as the mean curvature flow of the initial leaf.

Monotonicity of Renormalized Leaf Area

One of the most important features of the holographic slice is that the area of the renormalized leaves decreases monotonically as λ decreases. This is crucial to the interpretation as coarse-graining. This property can be shown in a manner similar to Ref. [46], but only after showing that $\theta_k \leq 0$ and $\theta_l \geq 0$ for each renormalized leaf. This is proved in Appendix 5.8.

Armed with this knowledge, consider a point p on σ and the s vector (defined in the previous section) orthogonal to the leaf σ at p. The integral curves of s passing through p provide a mapping of p to a unique point on each $\sigma(\lambda)$. Now consider an infinitesimal area element δA around p. The rate at which this area changes as one flows along s is measured by the expansion

$$\theta_s = \theta_k \theta_l \leq 0, \tag{5.4}$$

as found in Appendix 5.8.

Since the area for all infinitesimal area elements decreases on flowing along s, the total leaf area also decreases. In fact, this property holds locally. For any subregion of a renormalized leaf, as one flows inward along the holographic slice the area of the subregion decreases monotonically.

Monotonicity of Entanglement Entropy

Along with the fact that the renormalized leaf area shrinks, the entanglement entropy of subregions also decreases monotonically. This must necessarily happen for a consistent interpretation that the coarse-graining procedure continuously removes short range entanglement.

This is precisely the spacelike monotonicity theorem of Ref. [32], so we will only sketch the idea.[5]

Consider a leaf $\sigma = \sigma(\lambda_0)$ and a renormalized leaf obtained after some small amount of radial evolution, $\sigma' = \sigma(\lambda_0 + \delta\lambda)$, where $\delta\lambda < 0$. A subregion A of σ is mapped to subregion A' of σ' by following the integral curves of s.

Suppose the HRRT surface $\gamma(A')$ anchored to A' is the minimal surface on a spacelike slice Σ'. Now extend Σ' by including the portion of the holographic slice between σ and σ', such that Σ' is now an achronal slice with boundary σ. Now consider the minimal surface $\Xi(A)$ anchored to A on this extended Σ'. $\Xi(A)$ has a portion in the exterior of σ' which can be projected down to σ' using the normal vector s. This projection, denoted by $\Xi(A) \to \pi(\Xi(A))$, decreases the area of $\Xi(A)$ due to the spacelike signature of Σ'. This projection results in a surface anchored to A', which must have an area greater than that of $\gamma(A')$. On the other hand, due to the maximin procedure [76], $\Xi(A)$ must also have an area less than the area of the HRRT surface $\gamma(A)$ anchored to A. In summary,

$$\|\gamma(A')\| \leq \|\pi(\Xi(A))\| \leq \|\Xi(A)\| \leq \|\gamma(A)\|, \tag{5.5}$$

where $\|x\|$ represents the volume of the object x (often called the area for a codimension-2 surface in spacetime). The inequalities arise from minimization, projection, and maximization, respectively.

Subregion Flow Contained within Entanglement Wedge

Suppose one were given access to a finite subregion A on the leaf σ and chose to apply the holographic slice construction only to this subregion. The result would be a sequence of renormalized leaves given by $\sigma(\lambda) = A(\lambda) \cup \overline{A}$, with $A(\lambda)$ denoting the sequence of subregions that result from radially evolving A as illustrated in Fig. 5.2.

An interpretation of this procedure as coarse-graining requires that it should not add any further information than what was already available. Thus, it should not allow one to reconstruct points in the bulk beyond what was already accessible from A, i.e. $\text{EW}(A)$. This is ensured by the fact that the boundary of $\text{EW}(A)$ acts as an extremal surface barrier for HRRT surfaces anchored to points inside $\text{EW}(A)$, and thus, at no step does $A(\lambda)$ cross outside $\text{EW}(A)$. In fact, if there were a non-minimal extremal surface anchored to A which is contained within $\text{EW}(A)$, the holographic slice would not be able to go beyond this. This would be the case if one were to consider A to be a large subregion of the boundary dual to an AdS black hole.

Probes Directly Reconstructable Region

Using the definition of Ref. [111], we define the directly reconstructable region of spacetime as the set of bulk points which can be localized by the intersections of some set of boundary

---

[5]This interpretation may in fact be the most natural explanation of why the spacelike monotonicity theorem holds.
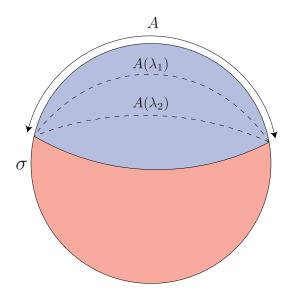
Figure 5.2: The radial evolution procedure when restricted to a subregion A results in a new leaf $\sigma(\lambda) = A(\lambda) \cup \overline{A}$, where A is mapped to a subregion $A(\lambda)$ contained within EW(A) (blue). The figure illustrates this for two values of λ with $\lambda_2 < \lambda_1 < 0$ (dashed lines).

anchored HRRT surfaces and the boundary of their entanglement wedges. Boundary operators corresponding to the maximally localizable bulk operators are dual to local operators in the directly reconstructable region [118].

As argued in Ref. [111], the interior of an equilibrated black hole cannot be reconstructed using the intersection of entanglement wedges. Since the horizon acts as a barrier for all extremal surfaces anchored to points outside the black hole, $\sigma(\lambda)$ stays outside the horizon at each step. Thus, the holographic slice cannot enter the black hole interior. This implies that bulk regions that are not directly reconstructable using the entire holographic screen are inaccessible to any holographic slice.

In fact, as long as $\sigma(\lambda)$ does not become extremal, the holographic slice procedure can continue moving the leaf spatially inward. This is a consequence of Theorem 1 in Ref. [34]. As we will see later, the radial evolution will only halt once the boundary state on the renormalized leaf no longer has distillable local correlations. This can happen in two ways. The first is that the surface closes off to zero area (corresponding to the vanishing of the coarse-grained Hilbert space). The second is if the surface asymptotes to a bifurcation surface or Killing horizon (corresponding to a maximally entangled state).

Holographic slices probe entanglement shadows, the spacetime regions which cannot be probed by HRRT surfaces anchored to a non-renormalized leaf σ. The extremal surfaces anchored to σ that probe the shadow regions are non-minimal. This prevents the reconstruction of points in these regions by using intersection of HRRT surfaces anchored to σ. However, the set of HRRT surfaces used for constructing subsequent renormalized leaves

need not be minimal on σ; they need only be minimal on the renormalized leaf at hand. Since non-minimal surfaces anchored to σ become minimal when anchored to an appropriately renormalized leaf $\sigma(\lambda)$, the holographic slice can flow through entanglement shadows. We will see an example of this in the next section.

Not only will the holographic slice itself flow through entanglement shadows, HRRT surfaces anchored to a renormalized leaf will probe regions behind shadows of the original leaf. Again, this is because the minimal extremal surfaces anchored to renormalized leaves need not be portions of minimal extremal surface anchored to the original leaf. In fact, one immediately starts recovering portions of shadow regions once the boundary is pulled in. This is what occurs in dense stars and conical AdS. In these cases, more and more of the shadow is recovered as the boundary is pulled in, and the entire shadow is only recovered once the slice contracts to a point.[6]

Because the holographic slices pass through shadows, it seems that the collection of all holographic slices anchored to boundary leaves will sweep out the directly reconstructable region. However, this breaks down if one considers a disconnected boundary. Consider the case of a two-sided AdS black hole. The directly reconstructable region can include regions behind the horizon if one picks a foliation of the left and right boundaries with an offset in time (see Appendix A of Ref. [34]). The intersection of HRRT surfaces anchored to large subregions with support on both boundaries allow for the reconstruction of points behind the horizon. On the other hand, the holographic slice is built from infinitesimal HRRT surfaces anchored to individual boundaries and hence cannot recover regions built from these long range correlations. In the two-sided black hole (no matter what the offset in boundary times), the holographic slice will always connect through the bifurcation surface and never probe behind the horizon; Section 5.4 explains this in detail.

5.4   Examples

In this section, we illustrate salient properties of the holographic slice using a few example spacetimes.

Conical AdS

We first consider conical AdS$_3$ to illustrate that the holographic slice probes regions inside entanglement shadows. In order to obtain conical AdS$_3$, we start with the AdS$_3$ metric

$$ds^2 = -\left(1 + \frac{r^2}{L^2}\right)dt^2 + \left(1 + \frac{r^2}{L^2}\right)^{-1}dr^2 + r^2d\theta^2, \tag{5.6}$$

---

[6]This will be explored in future work. This is similar to how entanglement of purification probes portions of shadow regions [160]. However, to recover the entire shadow region using entanglement of purification, one must impose additional conditions on the purification [161, 162].
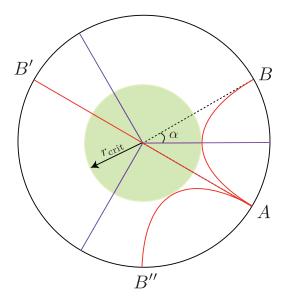
Figure 5.3: The case of conical AdS$_3$ with $n = 3$. The points B, B', and B'' are identified. There are 3 geodesics from A to B, of which generically only one is minimal. Here, we have illustrated the subregion AB with $\alpha = \pi/6$, where two of the geodesics are degenerate. This is the case in which the HRRT surface probes deepest into the bulk, leaving a shadow region in the center. Nevertheless, the holographic slice spans the entire spatial slice depicted.

where L is the AdS length scale. We then perform a $\mathbb{Z}_n$ quotient, so that the angular coordinate θ has periodicity $2\pi/n$. Locally, this spacetime is identical to AdS$_3$, and solves the Einstein equations for a negative cosmological constant away from $r = 0$. However, there is a conical defect at $r = 0$ introduced by the $\mathbb{Z}_n$ quotient.

HRRT surfaces in this spacetime simply correspond to minimal length geodesics anchored to subregions at the conformal boundary. As illustrated in Fig. 5.3, there are n geodesics in the parent AdS$_3$ spacetime which are candidate extremal surfaces for a given subregion. However, generically only one of them is minimal and corresponds to the HRRT surface. The geodesics in AdS$_3$ are described by the equation

$$\tan^2\theta = \frac{r^2 \tan^2\alpha - L^2}{r^2 + L^2}, \tag{5.7}$$

where α is the half-opening angle of the subregion being considered. Since the angular coordinate θ has a periodicity of $2\pi/n$, the minimal length geodesic that probes deepest into the bulk is obtained when $\alpha = \pi/2n$. From Eq. (5.7), this gives a critical radius of [163]

$$r_{\mathrm{crit}}(n) = L \cot\left(\frac{\pi}{2n}\right), \tag{5.8}$$

which takes a nonzero finite value for $n \neq 1$. Thus, the region $r < r_{\mathrm{crit}}(n)$ is an entanglement shadow, which cannot be probed by HRRT surfaces anchored to the conformal boundary.

The holographic slice is constructed by finding infinitesimal HRRT surfaces starting from the (regularized) conformal boundary. Since the spacetime is locally AdS_3, the HRRT surfaces for small regions are identical to those in AdS_3. Because of the static and spherically symmetric nature of AdS_3, the renormalized leaves correspond to surfaces of constant r and t. Now, since $r_{\text{crit}}(n)$ is not an extremal surface barrier, as can be seen from the existence of non-minimal extremal surfaces penetrating it, the holographic slice suffers no obstruction in crossing over to the entanglement shadow. This implies that the holographic slice is simply given by a constant time slice that covers all of the spatial region $r \in [0, \infty)$.

In general, holographic slices do not have any difficulty in going into entanglement shadow regions, since these shadows are not associated with extremal surface barriers which any extremal surfaces anchored to the outside cannot penetrate [123]. In fact, holographic slices also sweep entanglement shadows other than those in the centers of conical AdS, e.g. regions around a dense star [164].

Black Holes

Consider a two-sided eternal AdS_{d+1} Schwarzschild black hole. The metric is given by

$$ds^2 = -f(r)\, dt^2 + \frac{1}{f(r)} dr^2 + r^2 d\Omega_{d-1}^2, \tag{5.9}$$

where

$$f(r) = 1 + \frac{r^2}{L^2} - \left(\frac{r_+}{r}\right)^{d-2}\left(1 + \frac{r_+^2}{L^2}\right), \tag{5.10}$$

with r_+ being the horizon radius. As can be seen in Fig. 5.4, the two exterior regions have a timelike Killing vector. Thus, the HRRT surfaces anchored to subregions with support only on one boundary respect the Killing symmetry and lie on the constant t slice connecting the respective boundary to the bifurcation surface. Subregions anchored on both boundaries could potentially lie on a different spatial slice if the HRRT surface is connected. However, since we are considering the holographic slice being built up using HRRT surfaces anchored to infinitesimal subregions, those anchored on both sides always stay disconnected.

Thus, the holographic slice, as seen in Fig. 5.4, is the union of static slices in both exterior regions and terminates at the bifurcation surface. As shown in Ref. [34], the bifurcation surface itself is extremal and lies on a Killing horizon, and hence the process of renormalizing leaves must asymptote to this surface.

The phenomenon of a holographic screen being terminated at a nontrivial surface requires the existence of a bifurcation surface, which is absent in most physical situations. For example, consider an AdS-Vaidya metric where a black hole is formed from the collapse of a thin null shell of energy [165]. The metric in ingoing Eddington-Finkelstein coordinates is given by

$$ds^2 = -f(r, v)\, dv^2 + 2dv\, dr + r^2 d\Omega_{d-1}^2, \tag{5.11}$$
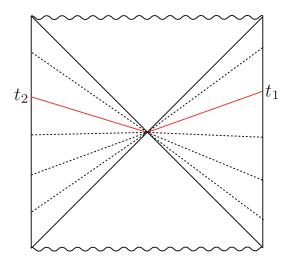
Figure 5.4: The exterior of a two-sided eternal AdS black hole can be foliated by static slices (black dotted lines). The holographic slice (red) connects the boundary time slices at $t = t_1$ on the right boundary and $t = t_2$ on the left boundary to the bifurcation surface along these static slices.

where

$$f(r, v) = 1 + \frac{r^2}{L^2} - \theta(v) \left(\frac{r_+}{r} \right)^{d-2} \left(1 + \frac{r_+^2}{L^2} \right), \tag{5.12}$$

with

$$\theta(v) = \begin{cases} 0 & \text{for } v < 0 \\ 1 & \text{for } v > 0. \end{cases} \tag{5.13}$$

The null shell lies at $v = 0$, and this spacetime is obtained simply by stitching together an AdS-Schwarzschild metric to the future of the shell and a pure AdS metric to the past. The composite global spacetime is time-dependent, but each of the building blocks admits a timelike Killing vector locally as shown in Fig. 5.5. As discussed earlier, since the HRRT surfaces relevant to the holographic slice are those of infinitesimal subregions, they only sense the local spacetime, which is static. This allows us to construct the holographic slice independently in each region. The static slices can then be stitched together to obtain the holographic slice as shown in Fig. 5.5.

An important feature here is that at late times, i.e. sufficiently after the black hole has stabilized, the holographic slice constructed from a leaf stays near the horizon for long time. Eventually, this flow terminates at $r = 0$. This behavior of holographic slices is, in fact, general in one-sided black holes; see Fig 5.6 for a schematic depiction.

Note that the picture of Fig 5.6 is obtained in the $G_N \to 0$ limit. When $G_N \neq 0$, renormalized leaves will hit the stretched horizon [39], where the semiclassical description of spacetime breaks down, before being subjected to the long flow near the horizon.
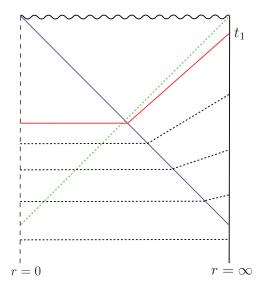
Figure 5.5: Penrose diagram of an AdS Vaidya spacetime formed from the collapse of a null shell (blue), resulting in the formation of an event horizon (green). Individual portions of the spacetime, the future and past of the null shell, are static. Thus, the holographic slice (red) can be constructed by stitching together a static slice in each portion.

FRW Spacetimes

We now discuss a nontrivial example in a time-dependent spacetime, away from the standard asymptotically AdS context. Consider a $(d+1)$-dimensional flat Friedmann-Robertson-Walker (FRW) spacetime containing a single fluid component with equation of state parameter w

$$ds^2 = a(\eta)^2 \left(-d\eta^2 + dr^2 + r^2 d\Omega_{d-1}^2 \right). \tag{5.14}$$

Here,

$$a(\eta) = c \, |\eta|^q, \tag{5.15}$$

where $c > 0$ is a constant, and

$$q = \frac{2}{d - 2 + dw}. \tag{5.16}$$

The discontinuity of q at $w = (2-d)/d$ is an artifact of choosing conformal time, and physics is smooth across this value of w.

The spherically symmetric holographic screen is located at

$$r(\eta) = \frac{a(\eta)}{\frac{da}{d\eta}(\eta)} = \frac{\eta}{q}. \tag{5.17}$$

By spherical symmetry, the holographic slice must be a codimension-1 surface of the form $\eta = g(r)$, where each renormalized leaf is an $\mathbb{S}^{d-1}$. Consider a renormalized leaf at $\eta = \eta_*$
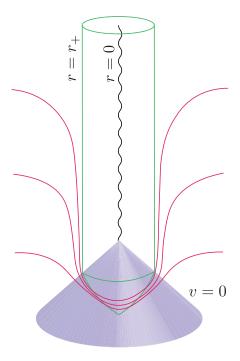
Figure 5.6: A schematic depiction of holographic slices for a spacetime with a collapse-formed black hole in ingoing Eddington-Finkelstein coordinates.

and $r = r_*$. Generalizing the results from Refs. [34, 33], HRRT surfaces anchored to a small spherical cap of half-opening angle γ of the renormalized leaf are given by

$$\eta(\xi) = \eta_* + \frac{\dot{a}}{2a}\left(\xi_*^2 - \xi^2\right) + \dots, \tag{5.18}$$

where $\xi = r\sin\theta$ and $\xi_* = r_*\sin\gamma$ with θ being the polar angle, and $a \equiv a(\eta_*)$ and $\dot{a} \equiv da/d\eta(\eta_*)$. We refer the reader to Appendix C.3 of Ref. [34] for more details.

The next renormalized leaf is generated by joining together the deepest point of each such HRRT surface. Suppose $\Delta\eta$ and Δr represent the change in conformal time and radius from one renormalized leaf to the next. Then we have

$$\Delta\eta = \frac{\dot{a}}{2a}\xi_*^2 + \dots, \tag{5.19}$$

$$\Delta r = -(r_* - r_* \cos\gamma), \tag{5.20}$$

so that

$$\frac{\Delta\eta}{\Delta r} = -\frac{\frac{\dot{a}}{2a}r_*^2\sin^2\gamma}{r_*(1 - \cos\gamma)} = -\frac{\dot{a}}{a}r_*. \tag{5.21}$$
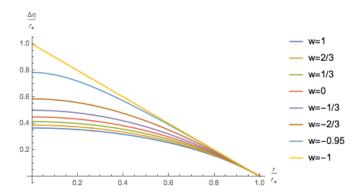
Figure 5.7: Holographic slices of $(3+1)$-dimensional flat FRW universes containing a single fluid component with equation of state parameter w.

Taking the limit $\gamma \to 0$, we obtain a differential equation for the radial evolution of the holographic slice

$$\frac{d\eta}{dr} = -\frac{qr}{\eta}. \tag{5.22}$$

Integrating this equation gives us

$$\eta^2 + qr^2 = \eta_*^2 + qr_*^2 = \frac{1+q}{q}\eta_0^2, \tag{5.23}$$

where η_0 is the conformal time of the original non-renormalized leaf.

Let us highlight a few interesting features of this holographic slice. First, it spans the entire interior region of the holographic screen. Next, substituting $r = \eta/q$ into Eq. (5.22) tells us that the holographic slice starts out in the null direction from the leaf; see Eq. (5.17). This is because the k direction locally has zero expansion there, as discussed in Section 5.3. As we move inward along the radial flow, however, the slope becomes flatter, and eventually the surface reaches the highest point given by

$$\eta(r=0) = \eta_0\sqrt{\frac{1+q}{q}}. \tag{5.24}$$

In Fig. 5.7 we have depicted holographic slices, given by Eq. (5.23), for several values of w with $d = 3$.

Asymptotically AdS and Flat Spacetimes

Here we discuss certain subtleties associated with holographic screens that lie on an asymptotic boundary. First, consider a $(d+1)$-dimensional asymptotically AdS spacetime, which

can be expanded in a Fefferman-Graham series [166] near the boundary

$$ds^2 = \frac{L^2}{z^2}\big\{ g_{ab}(x^a, z)dx^a dx^b + dz^2 \big\}, \tag{5.25}$$

where L is the AdS length scale, and

$$g_{ab}(x^a, z) = g_{ab}^{(0)}(x^a) + z^2 g_{ab}^{(2)}(x^a) + \dots. \tag{5.26}$$

Here, $g_{ab}^{(0)}$ represents the conformal boundary metric, and the subleading corrections represent deviations as one moves away from the boundary at $z = 0$.

In an asymptotically AdS spacetime, the holographic screen H formally lies at spacelike infinity. In order to construct a holographic slice in such a situation, one needs to first consider a regularized screen H' at $z = \epsilon$ and then take the limit $\epsilon \to 0$ after constructing the slice. Suppose that a leaf is given by a constant t slice of H', with h_{ij} representing the induced metric on the leaf. The null normals are then given by

$$k_\mu = dz - dt + O(\epsilon^2), \tag{5.27}$$
$$l_\mu = -dz - dt + O(\epsilon^2), \tag{5.28}$$

where the $O(\epsilon^2)$ corrections arise due to deviations away from the boundary. The null expansions are

$$\begin{aligned} \theta_k &= h^{ij}\Gamma_{ij}^z - h^{ij}\Gamma_{ij}^t \\ &= -\frac{\epsilon(d-1)}{L} + O(\epsilon^2), \end{aligned} \tag{5.29}$$

$$\begin{aligned} \theta_l &= -h^{ij}\Gamma_{ij}^z - h^{ij}\Gamma_{ij}^t \\ &= \frac{\epsilon(d-1)}{L} + O(\epsilon^2). \end{aligned} \tag{5.30}$$

Thus, we see that the expansion θ_k vanishes only in the limit $\epsilon \to 0$.

This implies that a leaf σ' of a regularized screen H' ($\epsilon \neq 0$) is, in fact, a renormalized leaf ($\theta_k \neq 0$), and thus the results in Section 5.3—that the holographic slice initially extends in the null direction and the leaf area remains constant—do not apply. In fact, the holographic slice extending from σ' initially evolves inward along the z direction up to corrections of $O(\epsilon)$, as can be seen from the fact that $\theta_k = -\theta_l$ up to $O(\epsilon)$. In the limit $\epsilon \to 0$, both θ_k and θ_l vanish simultaneously. This leads to a holographic screen at spacelike infinity in a formal sense.[7]

A similar situation arises in asymptotically flat spacetimes. A general asymptotically flat spacetime can be expanded in the Bondi-Sachs form [167, 168] as

$$\begin{aligned} ds^2 = &-\frac{V}{r}e^{2\beta}du^2 - 2e^{2\beta}dudr \\ &+ r^2 h_{AB}\big(dx^A - U^A du\big)\big(dx^B - U^B du\big), \end{aligned} \tag{5.31}$$

---

[7] Strictly speaking, this does not satisfy the definition of the holographic screen in Section 5.3, which requires θ_l to be strictly positive.

where each of the functions admits a large r expansion with the following behavior:

$$V = r + O(1), \qquad \beta = O\left(\frac{1}{r^2}\right), \tag{5.32}$$

$$U^A = O\left(\frac{1}{r^2}\right), \qquad h_{AB} = O(1). \tag{5.33}$$

In order to construct a holographic slice, the holographic screen H must be regularized to become a timelike surface H' at $r = R$, where we can eventually take the limit $R \to \infty$. The null normals of a leaf on a constant time slice are

$$k_\mu = du, \tag{5.34}$$

$$l_\mu = -\frac{V}{r}du - 2dr, \tag{5.35}$$

giving the null expansions near the boundary

$$\theta_k = -\frac{2}{R} + O\left(\frac{1}{R^2}\right), \tag{5.36}$$

$$\theta_l = \frac{2}{R} + O\left(\frac{1}{R^2}\right). \tag{5.37}$$

Thus, similar to the case of asymptotically AdS spacetimes, a leaf of a regularized holographic screen is a renormalized one, and both $\theta_k, \theta_l \to 0$ simultaneously as $R \to \infty$.

As a simple example, we illustrate the case of a Minkowski spacetime in Fig. 5.8. As the limit $R \to \infty$ is taken, the holographic slices become complete Cauchy hypersurfaces which are constant time slices anchored to spatial infinity. In the limit $t \to +\infty$ $(-\infty)$, future (past) null and timelike infinities are obtained as a holographic slice. In this situation, time evolution of the boundary theory from $t \to -\infty$ to $+\infty$ corresponds to an S-matrix description of the bulk.

5.5 Interpretation and Applications

We have introduced the geometric definition of the holographic slice and demonstrated some of its properties. But what does the slice correspond to in the boundary theory? What questions can it help us address? The construction of the slice naturally lends itself to an interpretation of eliminating information at small scales, and hence can be well understood in the context of coarse-graining. Through this, we can think of the slice as an isometric tensor network. This provides us with a new way to think about holographic tensor networks and the bulk regions of spacetime that they encode.

Throughout this section we will be talking about various Hilbert spaces in which holographic states belong. To do so, we will be taking G_N to be finite but small. This is an appropriate approximation for classical spacetimes provided we only concern ourselves with length scales sufficiently larger than the Planck length.
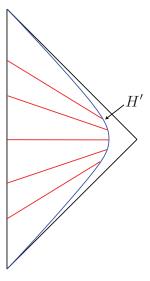
Figure 5.8: Penrose diagram of a Minkowski spacetime. The holographic slices (red) are anchored to the regularized holographic screen H' (blue). As the limit $R \to \infty$ is taken, the holographic slices become complete Cauchy slices.

Coarse-Graining

We take the view that a boundary state, $|\psi(0)\rangle$, lives on the original leaf, $\Upsilon(0)$, i.e. it lives in an effective Hilbert space, $\mathcal{H}$, having a local product space structure with dimension $\log|\mathcal{H}| = \|\Upsilon(0)\|/4G_\mathrm{N}$. The HRRT prescription says that the emergent bulk geometry is intricately related to the entanglement of the boundary state. In particular, despite the fact that bulk information is delocalized in the boundary theory, a bulk region cannot be reconstructed if some boundary subregions are ignored. The size of the smallest subregion for this to occur gives us some idea of what scale of boundary physics this bulk region is encoded in. Using this intuition, we can then attempt to address what coarse-graining the boundary state corresponds to in the bulk.

At each step in the construction of the holographic slice, we eliminate the region of spacetime associated with a small length scale, δ, of the boundary. In particular, this is the region of spacetime whose information is necessarily lost if we cannot resolve below length scale δ. In this sense, we are coarse-graining over the scale δ and obtaining a new bulk region whose information has not been lost. Recursively doing this and sending δ to zero produces a continuum of bulk domains of dependence with unique boundaries sweeping out the holographic slice, $\Upsilon(\lambda)$. This is depicted in Fig. 5.9.

A consistency check for this interpretation is that the size of the effective Hilbert space should necessarily decrease as we coarse-grain over larger and larger scales. This is precisely the monotonicity property listed in Section 5.3: as one flows along the holographic slice, the area of the renormalized leaves decreases. This tells us that the size of the effective Hilbert
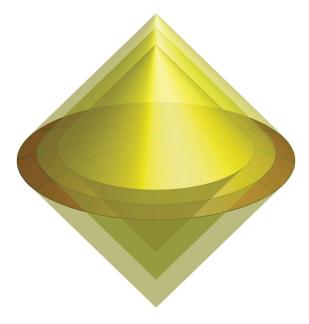
Figure 5.9: This depicts the holographic slice (maroon), and the successive domains of dependence encoded on each renormalized leaf.

space describing the bulk domain of dependence also decreases.

As the coarse-graining procedure progressively removes information at small scales, a corresponding removal of bulk information closest to the renormalized leaf occurs. Given this global removal of short range information, one should expect the entanglement between any region and its complement to correspondingly decrease. This is precisely the monotonicity of entanglement entropy property observed in Section 5.3. This is consistent with the interpretation that at each step we are removing short range entanglement.

Using the holographic slice, we can address the question of how much entanglement between a subregion and its complement is sourced by physics at different scales. By following the integral curves of s for the subregion, we can stop at whatever scale we desire and use the HRRT prescription on the renormalized leaf. This gives us the entanglement entropy sourced by physics at length scales larger than that associated with the renormalized leaf.

Radial Evolution of States

We will now be more explicit in describing the framework for coarse-graining holographic states. Given a bulk region $D(\Upsilon(0))$, there exists a quantum state $|\psi(0)\rangle$ living in some fundamental holographic Hilbert space, $\mathcal{H}_{\mathrm{UV}}$, in which the bulk information of $D(\Upsilon(0))$ is encoded via the HRRT prescription. This implies that $\mathcal{H}_{\mathrm{UV}}$ has a locally factorizable structure. On the other hand, the area of $\Upsilon(0)$ provides an upper bound for the dimension of effective Hilbert space that $|\psi(0)\rangle$ lives in, which we call $\mathcal{H}_{\Upsilon(0)}$. That is, $|\psi(0)\rangle \in \mathcal{H}_{\Upsilon(0)} \subset$

$\mathcal{H}_{\mathrm{UV}}$. The dimension, $|\mathcal{H}_{\Upsilon(0)}|$, of the effective Hilbert space is defined as

$$\ln |\mathcal{H}_{\Upsilon(0)}| = \sum_i S_i = \frac{\|\Upsilon(0)\|}{4G_{\mathrm{N}}}. \tag{5.38}$$

Here, S_i represents the entanglement entropy of $|\psi(0)\rangle$ in an infinitesimally small subregion, A_i, of the holographic space Ω on which $\mathcal{H}_{\mathrm{UV}}$ is defined. We sum over all of these small subregions such that $\Omega = \cup_i A_i$ and $A_i \cap A_j = \emptyset$ $(i \neq j)$. This reduces to calculating the area of $\Upsilon(0)$ because of the HRRT prescription. Namely, the size of the effective Hilbert space that $|\psi(0)\rangle$ lives in is determined by the entanglement between the fundamental degrees of freedom of $\mathcal{H}_{\mathrm{UV}}$, and $\|\Upsilon(0)\|/4G_{\mathrm{N}}$ is the thermodynamic entropy associated with this entanglement structure.

As one continuously coarse-grains $|\psi(0)\rangle$, information encoded in small scales is lost. Correspondingly, information of the bulk geometry that is stored in small scales is lost, and the dimension of the effective Hilbert space that the coarse-grained state lives in decreases. At a given scale of coarse-graining corresponding to λ, the new state, $|\psi(\lambda)\rangle$, lives in the same Hilbert space as the original leaf, $\mathcal{H}_{\mathrm{UV}}$, but now in an effective subspace, $\mathcal{H}_{\Upsilon(\lambda)}$, with dimension given by $\ln |\mathcal{H}_{\Upsilon(\lambda)}| = \|\Upsilon(\lambda)\|/4G_{\mathrm{N}}$. Additionally, $|\psi(\lambda)\rangle$ only contains information of $D(\Upsilon(\lambda))$, as we have explicitly lost the information necessary to reconstruct any part of $D(\Upsilon(0)) \setminus D(\Upsilon(\lambda))$.

Because all of the coarse-grained states live in the same Hilbert space, $\mathcal{H}_{\mathrm{UV}}$, we can consider the coarse-graining procedure as a unitary operation that takes us from state to state, along the lines of the work of Ref. [169]. That is,

$$|\psi(\lambda)\rangle = U(\lambda, 0)|\psi(0)\rangle. \tag{5.39}$$

We can write $U(\lambda_1, \lambda_2)$ as

$$U(\lambda_1, \lambda_2) = P \exp\left[-i \int_{\lambda_2}^{\lambda_1} K(\lambda) d\lambda\right], \tag{5.40}$$

where P represents path-ordering. $K(\lambda)$ is a Hermitian operator removing physical correlations between nearby subregions at the length scale, l_λ, associated to λ on Ω. Some appropriate measures of physical correlations would be the mutual information $(I(A, B))$, entanglement negativity $(N(A, B))$, or the entanglement of purification $(E(A, B))$ between neighboring small subregions of the leaf under consideration, $\Upsilon(\lambda)$. Note that as the boundary state becomes maximally entangled, all three of these measures will vanish. This also happens if the boundary state in consideration has no entanglement, i.e. is a product state.

Of the three measures, entanglement of purification already has a bulk description that naturally characterizes some measure of moving into the bulk. In particular, Refs. [**Takayanagi:2017knl, Nguyen:2017yqw**] proposed that the entanglement of purification of two boundary subregions, A and B, is calculated by the minimum cross section, ζ, of a bipartition of the extremal surface anchored to $A \cup B$; see Fig. 5.10. Considering the case where ∂A and ∂B
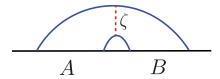
Figure 5.10: Let A and B two boundary subregions. The blue lines represent the HRRT surface of $A \cup B$ and ζ the minimal cross section. The entanglement of purification of A and B is given by $\|\zeta\|/4G_N$. In the limit that A and B share a boundary point, ζ probes the depth of the extremal surface.

coincide at some point, and whose connected phase is the appropriate extremal surface, the entanglement of purification gives some measure of the depth of the extremal surface. In bulk dimensions higher than $2 + 1$, $\|\zeta\|$ will not be in units of length, but it is still related to the depth of the extremal surface. Thus it seems natural that $K(\lambda)$ is some (quasi-)local function, F, of physical correlations, including but not necessarily limited to quantum entanglement, at the scale l_λ. For example, it may be related to the entanglement of purification:

$$K(\lambda) \sim \int d^{d-1}\mathbf{x}\, F\big(E_\lambda(\mathbf{x})\big), \tag{5.41}$$

where $\mathbf{x}$ are the coordinates of Ω. Here, $E_\lambda(\mathbf{x})$ is the "density" of the entanglement of purification between the degrees of freedom in two neighboring regions on $\sigma(\lambda)$ around $\mathbf{x}$.

Alternately, the case of subregion coarse-graining as in Fig. 5.2 motivates the usage of results from Ref. [116], which can be used to map the state from σ to $\sigma(\lambda)$. In AdS/CFT, modular evolution allows one to explicitly reconstruct bulk operators on the HRRT surface. With our assumption that the HRRT formula holds (with quantum corrections), a similar construction should be possible given complete knowledge of the boundary theory. $K(\lambda)$ may then be better understood as a convolution over modular evolutions with infinitesimal boundary subregions:

$$K(\lambda) \sim \int d^{d-1}\mathbf{x}\, F\big(\kappa_\lambda(\mathbf{x})\big), \tag{5.42}$$

where $\kappa_\lambda(\mathbf{x})$ is the modular Hamiltonian density on $\sigma(\lambda)$ at $\mathbf{x}$. It would be interesting to make the connection of $K(\lambda)$ to modular evolution clearer in the future.

The process of removing short range correlations continues until all correlations at the scale l_λ have been removed, and hence no more bulk spacetime can be reconstructed. This can happen when the slice contracts to a point and no local product structure exists in the effective Hilbert space $\mathcal{H}_{\Upsilon(\lambda)}$. Note that in $\mathcal{H}_{\mathrm{UV}}$ this state corresponds to a product state, so that $S_i = 0$ for every subregion in $\mathcal{H}_{\mathrm{UV}}$. The other way in which all relevant correlations vanish is when the coarse-grained state becomes maximally entangled in $\mathcal{H}_{\Upsilon(\lambda)}$. In $\mathcal{H}_{\mathrm{UV}}$, this corresponds to a state which satisfies $S_A = \sum_{i \subset A} S_i$ for all subregions, A, of Ω.

When the coarse-grained state becomes maximally entangled in $\mathcal{H}_{\Upsilon(\lambda)}$, $U(\lambda + d\lambda, \lambda)$ becomes the identity for Eq. (5.41) as $K(\lambda)$ becomes 0. Hence, the state remains invariant

under the coarse-graining operation. There are two ways for this to happen geometrically. One is if the slice approaches a bifurcation surface; then the extremal surfaces coincide with the renormalized leaf, hence preventing any further movement into the bulk. This is the case for eternal two-sided black holes. The second is if the slice approaches a null, non-expanding horizon and the state is identical along the horizon. This is the case in de Sitter space. This result is complementary to Theorem 1 of Ref. [34], which proves that if a boundary state is maximally entangled, it must either live on a bifurcation surface or a null, non-expanding horizon.

This may initially seem like a contradiction—that both the state becomes maximally entangled and that there are no more correlations to harvest. However, it is precisely because we are examining correlations at *small* scales that this occurs. A small boundary region is maximally entangled with the entire rest of the boundary, and hence the short range entanglement must vanish. One can quantify this by examining the entanglement negativity of bipartitions of small subregions on $\sigma(\lambda)$. As states become maximally entangled, the entanglement negativity vanishes for two small subregions. This places an upper bound on the real, distillable entanglement between these subregions. Hence, the true quantum entanglement at small scales vanishes as a state becomes maximally entangled. Correspondingly, the coarse-graining procedure halts. This is indeed what happens to the holographic slice.

The same can also be seen by considering the modular evolution, Eq. (5.42), of a maximally entangled subregion. In this case, the modular evolution is proportional to the identity operator, and hence the modular flow of the state is stationary. This corresponds to no movement into the bulk as expected by the properties of the holographic slice for maximally entangled states.

Tensor Network Picture

In this language the relationship to tensor networks is very clear. The holographic slice arises as the continuous limit of a tensor network that takes a boundary state and disentangles below a certain scale, reducing the effective Hilbert space size. This is a slight generalization of continuous Multiscale Entanglement Renormalization Ansatz (cMERA) [150], which is restricted to hyperbolic geometries.

In general, we can consider a tensor network as a non-continuum modeling of the holographic slice, which isometrically embeds boundary states into spaces of lower effective dimension by removing short range correlations; see Fig. 5.11. In the ground state of AdS/CFT, this corresponds to an instance of Multiscale Entanglement Renormalization Ansatz (MERA) [25]. Each layer of the tensor network then lives on the corresponding renormalized leaf of the discrete version of Υ. From this we see that the tensor network lives on this discrete version of the holographic slice. Because isometric tensor networks obey a form of HRRT, one may mistakenly conclude that the cut through the network computes the area of the corresponding surface in the bulk along the holographic slice. This is generally not the case; the maximin method tells us that this area provides only a lower bound on the entanglement. The entanglement calculated in this way instead corresponds to the area of
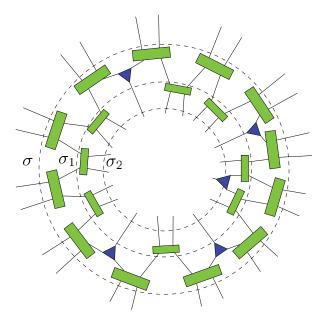
Figure 5.11: A tensor network for a non-hyperbolic geometry. The green rectangles correspond to disentanglers while the blue triangles are coarse-graining isometries. Each internal leg of the tensor network has the same bond dimension. We are imagining that σ corresponds to a leaf of a holographic screen and each successive layer (σ_1 and σ_2) is a finite size coarse-graining step of the holographic slice. Through this interpretation, the tensor network lives on the holographic slice. However, the entanglement entropy calculated via the min-cut method in the network does not correspond to the distance of the cut along the holographic slice in the bulk. It corresponds to the HRRT surface in the appropriate domain of dependence. The locations of σ_1 and σ_2 in the bulk are found by convolving the HRRT surfaces for the small regions being disentangled and coarse-grained. The holographic slice is a continuous version of this tensor network.

the HRRT surface anchored to the appropriate subregion of a renormalized leaf. In other words, the tensor network should not be viewed as a discretization of the holographic slice, but rather as a set of boundary states dual to successively smaller domains of dependence.

In fact, this interpretation can be applied to any isometric tensor network, and we argue that this is the proper way to view tensor networks representing bulk spacetimes. That is, given a state represented by an isometric tensor network, one can find a set of states by pushing the boundary state through the tensors one layer at a time such that no two layers have the same boundary legs.[8] These successive states are then dual to bulk domains of dependence that are successively contained in each other, and whose boundaries lie on (a

---

[8]This picture can perhaps be used to show that the dynamical holographic entropy cone is contained within the holographic entropy cone [144]. By explicitly constructing the holographic slice tensor network that encodes a state of a time dependent geometry, we will have found a model that encodes the entropies in a way that ensures containment within the holographic entropy cone.

discrete version of) the holographic slice.

Time Evolution and Gauge Fixing

The preferred holographic slice of Section 5.3 provides us with a novel way to foliate space-times. By applying the holographic slice procedure to each boundary time slice, one foliates the bulk spacetime with holographic slices.

In order for this to provide a good gauge fixing, the holographic slices generated from different boundary time slices must not intersect. In spherically symmetric cases, these intersections do not occur. From the spherical symmetry of the spacetime, the renormalized leaves must also be spherical. Thus, if two holographic slices did intersect, they must intersect at a renormalized leaf. However, the evolution of the slice is unique from this leaf, and hence these two slices do not intersect. Furthermore, the reverse flow is also unique and hence the slices must exactly coincide. This prevents ambiguities in the gauge fixing of the bulk spacetime.

Outside of spherically symmetric cases, if $\text{sgn}(K)$, the sign of the extrinsic curvature of the slice, is constant over the slice then no slices will intersect. By joining a slice with the past (future) portion of the holographic screen in the $K \geq 0$ (≤ 0) case, one can create a barrier for extremal surfaces anchored in the interior of the barrier. This implies that any slice constructed from a leaf cannot penetrate slices generated from leaves towards its future (past) if $K \geq 0$ (≤ 0).

As explained in Sections 5.3 and 5.4, the foliation generated by the holographic slices will not probe behind late-time horizons. Thus this foliation provides a gauge fixing of the region of spacetime exterior to black hole horizons. In this region, the foliation provides a covariant map from boundary time slices to bulk time slices.

5.6 Relationship to Renormalization

In this section, we discuss how our coarse-graining procedure is related to conventional renormalization, both in the context of standard quantum field theories and AdS/CFT.

Analogy to Renormalization in Quantum Field Theories

We first draw an analogy between pulling in the boundary along the holographic slice and standard renormalization in quantum field theories. In particular, we liken the limitations of fixed order perturbation theory with the existence of reconstructable shadows. We begin by reviewing renormalization in quantum field theories phrased in a way to make the relationship clear.

Suppose one computes the amplitude of a process involving two widely separated mass scales m and E in fixed order perturbation theory. In terms of a renormalized coupling

constant g, it is given generally in the form

$$\mathcal{M} = \sum_{n=0}^{\infty} c_n \left(\frac{g}{16\pi^2} \ln \frac{E}{m} \right)^n, \tag{5.43}$$

where c_n's are of the same order. This implies that even if $g/16\pi^2$ is small, this perturbation theory breaks down when $\ln(E/m) \sim 16\pi^2/g$.

There is, however, a way to resum these logarithms—the renormalization group. Introducing the concept of running coupling constant, $g(\mu)$, defined at a sliding scale μ, the amplitude of Eq. (5.43) can be written as

$$\mathcal{M} = \sum_{n=0}^{\infty} c_n \left(\frac{g(\mu)}{16\pi^2} \ln \frac{E}{\mu} \right)^n. \tag{5.44}$$

The process can now be calculated perturbatively as long as both $g(m)/16\pi^2$ and $g(E)/16\pi^2$ are small, where $g(m)$ and $g(E)$ are related by a continuous renormalization group evolution. In general, the range of validity of this renormalization group improved perturbation theory is larger than that of fixed order perturbation theory.

This phenomenon is analogous to the existence of shadows in the holographic reconstruction. If one tries to reconstruct the bulk in a "single shot" using HRRT surfaces anchored to the original leaf, then there can be regions in spacetime (shadows) that cannot be reconstructed. This, however, is not a fundamental limitation of the perturbative reconstruction of the bulk. As we have seen, we can reconstruct a portion of entanglement shadows by performing a reconstruction in multiple steps: first renormalizing the leaf and then using HRRT surfaces anchored to the renormalized leaf. By doing this renormalization with more steps, one can progressively probe deeper into shadow regions. Going to the continuum limit (the holographic slice), we find that we can describe physics in shadows without difficulty.

Even with the renormalization group improvement, the perturbative description of physics stops working when $g(\mu)$ hits a Landau pole or approaches a strongly coupled fixed point. This is analogous to the fact that the evolution of the holographic slice halts, $U(\lambda_1, \lambda_2) \propto 1$ in Eq. (5.40), once the renormalized leaf contracts to a point or approaches a horizon. Incidentally, this picture is consonant with the idea that describing the interior of a black hole would require "nonperturbative" physics.[9]

We stress that from the boundary point of view, renormalization of a leaf corresponds to coarse-graining of a state at a fixed time. A natural question is if there is an effective theory relating coarse-grained states at different times. We do not see a reason to doubt the existence of such a theory, at least for degrees of freedom sufficiently deep in the bulk. Since the coarse-graining depends on the state, however, the resulting description may well be applicable only within a given geometry, i.e. a selected semiclassical branch of the fundamental state in quantum gravity.

---

[9]In particular, an interior description may require changing the basis of multiple black hole microstates [62, 170], each of which can be viewed as having different background geometries corresponding to slightly different black hole masses [84, 86].

Comparison to Holographic Renormalization in AdS/CFT

How is the holographic slice related to holographic renormalization in asymptotically AdS spacetimes? There has been extensive literature devoted to the latter subject. Here we will highlight the essential difference between our renormalization procedure and the perspective of Susskind and Witten [124].

If one kept N^2 (the number of field degrees of freedom) fixed per cutoff cell and applied the Susskind-Witten method of regularization deeper in the bulk, a local description of physics on the boundary would break down once $R \approx l_{\text{AdS}}$. Here, R and l_{AdS} are the radius of the cutoff surface and the AdS length scale, respectively. This is because the number of degrees of freedom within an l_{AdS}-sized bulk region is of order $(l_{\text{AdS}}/l_{\text{P}})^{d-1}$, which is just N^2. Here, l_{P} is the Planck length in the bulk.

However, holography extends to sub-AdS scales, and the extremal surfaces anchored to a cutoff at l_{AdS} satisfy the appropriate properties to be interpreted as entanglement entropies [126, 30]. As emphasized throughout the text, the connection between entanglement and geometric quantities seems to extend beyond AdS/CFT [115, 55]. Because of this, we expect that there should be some way to renormalize the boundary state in such a way to preserve the HRRT prescription at all scales. This is, however, prohibited if we fix N^2 because already at an l_{AdS}-sized region we lose the ability to talk about the entanglement of boundary subregions (as there is only one boundary cell).

Therefore, if one wants to preserve the ability to use the HRRT prescription, N^2 must change as the boundary is pulled in. Simply requiring that $N^2 \geq 1$ per cell will allow renormalization down to l_{P}. This is easily seen by noticing that the number of cells for a boundary moved in to radius R ($\leq l_{\text{AdS}}$) is given by the total number of bulk degrees of freedom, $(R/l_{\text{P}})^{d-1}$, divided by N^2. This implies that when $R = l_{\text{P}}$ the number of cells is of order unity, and the holographic description must break down. In fact, the bulk description is expected to break down before this happens. Suppose that the gauge coupling, g, of the boundary theory stays constant. Then the requirement of a large 't Hooft coupling, $N^2 \geq 1/g^4 = (l_{\text{s}}/l_{\text{P}})^{d-1}$, implies that the bulk spacetime picture is invalidated when $R \lesssim l_{\text{s}}$. Here, l_{s} is the string length. Assuming the existence of a renormalization scheme preserving the HRRT prescription implies that there exists a way to redistribute the original N^2 degrees of freedom spatially on a coarse-grained holographic space.

The construction of the holographic slice requires extremal surfaces to be anchored to renormalized leaves, so the renormalization procedure utilized must necessarily preserve the ability to use the HRRT prescription. The holographic slice, therefore, must employ the special renormalization scheme described above.

5.7 Discussion

The holographic slice is defined using HRRT surfaces, and hence is inherently background dependent. This prohibits the use of the holographic slice as some way to analyze the coarse-

grained behavior of complex quantum gravitational states with no clear bulk interpretation. In particular, if a state is given by a superposition of many different semiclassical geometries,

$$|\Psi\rangle = c_1|\psi_1\rangle + c_2|\psi_2\rangle + \cdots , \tag{5.45}$$

then the holographic slice prescription can be applied to each branch of the wavefunction, $|\psi_i\rangle$, independently. However, there is no well-defined slice for $|\Psi\rangle$. This is the same limitation one would face when considering the entanglement wedge of similar states. Despite this, for superpositions of states within the code subspace, the analyses of Refs. [111, 53] tell us the holographic slice construction is well defined.

Regardless, the holographic slice sheds light on the nature of bulk emergence. The construction of the slice harvests short range entanglement between small subregions, not in the form of entanglement entropy. It is precisely this that allows the slice to flow into the bulk and through entanglement shadows. This work emphasizes the idea that entanglement entropy as measured by von Neumann entropy is not sufficient to characterize the existence of a semiclassical bulk viewed from the boundary. Other measures of entanglement (negativity, entanglement of purification, etc.) may be more useful to analyze bulk emergence. This was explored extensively in Ref. [34].

The slice additionally provides a very natural interpretation for non-minimal extremal surfaces as the entanglement entropy for subregions of coarse-grained states. Because the coarse-graining procedure mixes up the boundary degrees of freedom while removing the short range information, the interpretation of non-minimal extremal surfaces in terms of purely UV boundary terms will necessarily be very complicated [163]. However, once coarse-graining occurs these complicated quantities manifest with a simple interpretation. This is also what is seen in the entanglement of purification calculations.

By assuming that the holographic states all live within the same infinite dimensional Hilbert space, $\mathcal{H}_{\text{UV}}$, we were able to discuss the mapping from a boundary state to a coarse-grained version of itself. This is what gave rise to the $K(\lambda)$ operator in Section 5.5. Alternatively, rather than use $\mathcal{H}_{\text{UV}}$ to discuss coarse-graining, one can use it to talk about time evolution in the boundary theory. One of the major hurdles in formulating theories for holographic screens is the fact that the area of the screens are non-constant. If one were to view this area as determining the size of the true Hilbert space the state lived in, then time evolution would require transitions between Hilbert spaces. However, by viewing the leaf area as a measure of the size of the effective subspace that the state lives in, we are free from this complication. In fact, modeling time evolution is similar to performing the reverse of the coarse-graining operation. This introduces entanglement at shorter and shorter scales, which increases the effective subspace's size. Of course, time evolution must account for other complex dynamics, but simply increasing the screen area is no difficulty. This interpretation suggests that the area of holographic screens is a thermodynamic entropy measure, rather than a measure of the fundamental Hilbert space size.

Concluding, the holographic slice is a novel, covariantly defined geometric object. It encodes the bulk regions dual to successively coarse-grained states and we propose that the

flow along the slice is governed by distillable correlations at the shortest scales. This may be related to the entanglement of purification of small regions or the modular evolution of such regions. Investigation of the explicit boundary flow along the slice seems to be the most promising avenue of future work. It may also be fruitful to study the mean curvature vector flow of codimension-2 convex surfaces in Lorentzian spacetimes, as characterizing solutions to this flow may provide insights into the coarse-graining operation.

5.8   Appendix

Intersection of Domains of Dependence

Lemma 1. *Let Σ be a closed, achronal set and $D(\Sigma)$ be the domain of dependence of Σ. Let p and q be points in $D(\Sigma)$, and λ a causal curve such that $\lambda(0) = p$ and $\lambda(1) = q$ where p lies to the past of q. Then, all points $r = \lambda(t)$ for $t \in [0, 1]$ are contained in $D(\Sigma)$.*

Proof. Suppose such a point r does not belong to $D(\Sigma)$. Then, there must exist an inextendible causal curve λ' that passes through r and does not intersect Σ. Without loss of generality, assume that r lies to the past of Σ. Consider a causal curve composed of λ to the past of r and λ' to the future of r. This would then be an inextendible causal curve passing through p but not intersecting Σ, implying that p does not belong to $D(\Sigma)$, thus contradicting the assumption. □

Lemma 2. *Let R be a closed set such that every causal curve connecting two points in R lies entirely in R. Let Σ be the future boundary of R defined by points $p \in R$ such that $\exists$ a timelike curve λ passing through p that does not intersect R anywhere in the future. Then,*

   1. Σ is an achronal set.

   2. $R \subseteq D(\Sigma)$.

Proof. We first show that Σ is an achronal set. Suppose there exist two points p and q in Σ that were timelike related. Without loss of generality, assume that p lies to the past of q. Consider an open neighborhood of p denoted by $U(p)$. Consider a point r such that $r \in \{I_+(p) \cap U(p)\} \backslash R$. By continuity, $\exists$ a timelike curve λ connecting r to q. λ can then be extended to pass through p in the past. Thus, we have found a causal curve that connects points p and q, both of which belong to R, and passes through $r \notin R$. This contradicts the assumption, and hence, Σ must be an achronal set.

Now, we can show that $R \subseteq D(\Sigma)$. Consider a point p such that $p \in R \backslash \Sigma$. Then, $I_+(p)$ must intersect Σ. To show this, suppose it were not true and consider a future causal curve λ from p which does not intersect Σ. The boundary point of $\lambda \cap R$ then also has a timelike curve through it which does not intersect R anywhere in the future, and thus should be included in the set Σ. Therefore, $I_+(p)$ either intersects Σ everywhere in the interior of Σ or

intersects some portion of the boundary of Σ. In the first case, all inextendible causal curves through p necessarily pass through Σ, and hence $p \in D(\Sigma)$. In the second case, extend Σ in a spacelike manner to an open neighborhood around Σ where a point q outside Σ is timelike related to p. Causal curves from p to q would not intersect Σ since q is spacelike related to all points on Σ. Consider the intersection of this curve with R. It must have a boundary point which does not belong to Σ. This point would then have inextendible timelike curves through it that do not intersect R in the future. This contradicts the assumption that this point was not in Σ. This implies that the second case is impossible. Hence, we have proved that $R \subseteq D(\Sigma)$. $\qquad\square$

Theorem 3. *Consider two codimension-1 spacelike subregions Σ_1 and Σ_2 that are compact. Let their domains of dependence be $D(\Sigma_1) = D_1$ and $D(\Sigma_2) = D_2$. Then $D = D_1 \cap D_2$ is the domain of dependence of the future boundary of D denoted by Σ.*

Proof. Consider any two points p and q that belong to D. Both p and q belong to D_1 and D_2. Using Lemma 1, we can conclude that all points on a causal curve joining p and q belong to both D_1 and D_2. Hence, any such point also belongs to D. Thus, D satisfies the condition required for R above in Lemma 2. Using Lemma 2 then tells us that $D \subseteq D(\Sigma)$.

Since Σ is defined to be the future boundary of D, Σ itself is necessarily contained in D. Now consider any $p \in D(\Sigma)$. Any causal curve λ passing through p intersects Σ by definition. However, since $\Sigma \subseteq D$, all inextendible causal curves through Σ necessarily intersect both Σ_1 and Σ_2. Thus, all inextendible causal curves through p also pass through both Σ_1 and Σ_2. This implies $D(\Sigma) \subseteq D$.

Combining the above two results, we have shown that $D = D(\Sigma)$. Namely, the intersection of two domains of dependence is also a domain of dependence. $\qquad\square$

Uniqueness of the Holographic Slice

Consider a codimension-2, closed, achronal surface σ in an arbitrary $(d+1)$-dimensional spacetime M. Suppose σ is a convex boundary. We assume that both M and σ are sufficiently smooth so that variations in the spacetime metric $g_{\mu\nu}$ and induced metric on σ, denoted by h_{ij}, occur on characteristic length scales L and L_σ, respectively.

Theorem 4. *Consider subregion R of characteristic length $\delta \ll L, L_\sigma$ on σ. To leading order, the extremal surface anchored to ∂R lives on the hypersurface generated by the vector $s = \theta_t t - \theta_z z$ normal to σ. Here, t and z are orthonormal timelike and spacelike vectors perpendicular to σ, and $\theta_t = h^{ij} K_{ij}^t$ and $\theta_z = h^{ij} K_{ij}^z$ where K_{ij}^t and K_{ij}^z are the extrinsic curvature tensors of σ for t and z, respectively. This property is independent of the shape of R.*

Proof. Start from a point $p \in R$ and set up Riemann normal coordinates in the local neighborhood of p.

$$g_{\mu\nu}(x) = \eta_{\mu\nu} - \frac{1}{3} R_{\mu\rho\nu\sigma} x^\rho x^\sigma + O(x^3). \tag{5.46}$$

In these coordinates, we are considering a patch of size δ around the origin p with $R_{\mu\rho\nu\sigma} \sim O(1/L^2)$. Equivalently, we could consider a conformally rescaled metric

$$x^\mu = \epsilon y^\mu, \tag{5.47}$$

$$ds^2 = \epsilon^2 g_{\mu\nu}(\epsilon y)\, dy^\mu dy^\nu, \tag{5.48}$$

$$d\tilde{s}^2 = g_{\mu\nu}(\epsilon y)\, dy^\mu dy^\nu$$
$$= \tilde{g}_{\mu\nu}(y)\, dy^\mu dy^\nu, \tag{5.49}$$

where $\epsilon = \delta/L \ll 1$.

In this alternate way of viewing the problem, we have a patch of size L with the metric varying on a larger length scale L/ϵ. In these coordinates, each derivative of the conformal metric brings out an extra power of ϵ; for example,

$$\frac{\partial^2}{\partial y^\rho \partial y^\sigma} \tilde{g}_{\mu\nu} = \epsilon^2 \frac{\partial^2}{\partial x^\rho \partial x^\sigma} g_{\mu\nu} \sim \frac{\epsilon^2}{L^2}. \tag{5.50}$$

The connection coefficients $\Gamma^\mu_{\rho\sigma}$ vanish at p due to our choice of Riemann normal coordinates. This implies that for points in the neighborhood of p, we can Taylor expand to find

$$\Gamma^\mu_{\rho\sigma} \sim \frac{\epsilon^2}{L}, \tag{5.51}$$

$$R_{\mu\rho\nu\sigma} \sim \frac{\epsilon^2}{L^2}. \tag{5.52}$$

Note that these quantities are obtained using the rescaled metric $\tilde{g}_{\mu\nu}$ in the y^μ coordinates.

Since there is still a remaining $SO(d,1)$ symmetry that preserves the Riemann normal coordinate form of the metric, we can use these local Lorentz boosts and rotations to set t and z as the coordinates in the normal direction to σ at p while y^i parameterize the tangential directions. This is a convenient choice to solve the extremal surface equation in a perturbation series order by order. The extremal surface equation is given by [48]

$$\tilde{g}^{\rho\sigma}\left(\partial_\rho \partial_\sigma Y^\mu + \Gamma^\mu_{\lambda\eta} \partial_\rho Y^\lambda \partial_\sigma Y^\eta - \Gamma^\lambda_{\rho\sigma} \partial_\lambda Y^\mu\right) = 0. \tag{5.53}$$

This is a set of $d+1$ equations for the embedding of the extremal surface Y^μ, which are functions of $d-1$ independent coordinates. The equations in the tangential directions are trivially satisfied by taking the $d-1$ parameters to be y^i. This leaves only two equations in the normal directions to be solved.

From the discussion above, when restricted to the local patch of size L, we have

$$\tilde{g}^{\mu\nu} = \eta^{\mu\nu} + O(\epsilon^2), \tag{5.54}$$

$$\Gamma^\mu_{\rho\sigma} = O\left(\frac{\epsilon^2}{L}\right). \tag{5.55}$$

Assuming the extremal surface is smooth, derivatives of Y^μ typically bring down a power of L_σ. Thus,

$$\partial Y \sim O(1), \tag{5.56}$$

$$\partial^2 Y \sim O\left(\frac{1}{L_\sigma}\right). \tag{5.57}$$

Using this, at the leading order in ϵ and $\epsilon_\sigma = \delta/L_\sigma$, the extremal surface equations simply become

$$\delta^{ij}\partial_i\partial_j Y^\mu = 0, \tag{5.58}$$

where μ takes the t and z directions. We write these as

$$\nabla^2 t_{\mathrm{E}} = \nabla^2 z_{\mathrm{E}} = 0, \tag{5.59}$$

where t_{E} and z_{E} are functions of y^i.

Let K_{ij}^t, K_{ij}^z denote the extrinsic curvature tensors for the t and z normals, respectively. Following the above scaling arguments, K_{ij}^t, $K_{ij}^z \sim \epsilon/L_\sigma$. Here, we have assumed that $L_\sigma \lesssim L$, although this is not essential for the final result. Because t and z are normal to the leaf, the equations for the leaf, described by $t_{\mathrm{L}}(y^i)$ and $z_{\mathrm{L}}(y^i)$, can be Taylor expanded in the neighborhood R as

$$t_{\mathrm{L}}(y^i) = -\frac{1}{2}K_{ij}^t y^i y^j + O\left(\frac{\epsilon^2 y^3}{L_\sigma^2}\right), \tag{5.60}$$

$$z_{\mathrm{L}}(y^i) = \frac{1}{2}K_{ij}^z y^i y^j + O\left(\frac{\epsilon^2 y^3}{L_\sigma^2}\right), \tag{5.61}$$

where the negative sign in the first line is due to the timelike signature of the t normal. The boundary conditions for the extremal surface equation are

$$t_{\mathrm{E}}(\partial R) = t_{\mathrm{L}}(\partial R), \tag{5.62}$$

$$z_{\mathrm{E}}(\partial R) = z_{\mathrm{L}}(\partial R). \tag{5.63}$$

Now, consider $\delta t = t_{\mathrm{E}} - t_{\mathrm{L}}$ and $\delta z = z_{\mathrm{E}} - z_{\mathrm{L}}$. The extremal surface equations are then given by

$$\nabla^2 \delta t = -\nabla^2 t_{\mathrm{L}} = \theta_t \left\{1 + O(\epsilon_\sigma)\right\}, \tag{5.64}$$

$$\nabla^2 \delta z = -\nabla^2 z_{\mathrm{L}} = -\theta_z \left\{1 + O(\epsilon_\sigma)\right\}, \tag{5.65}$$

where $\theta_t = h^{ij}K_{ij}^t$ and $\theta_z = h^{ij}K_{ij}^z$. Note that $h_{ij} = \eta_{ij}$ at this order. The boundary conditions are given by

$$\delta t\,(\partial R) = \delta z\,(\partial R) = 0. \tag{5.66}$$

It is now clear that at leading order $\delta t / \theta_t$ and $-\delta z / \theta_z$ satisfy the same equation with the same boundary conditions. Thus,

$$\frac{\delta t}{\delta z} = -\frac{\theta_t}{\theta_z} + O(\epsilon_\sigma), \tag{5.67}$$

for all points on the extremal surface. Rewritten, the extremal surface lives on the hypersurface generated by $s = \theta_t t - \theta_z z$, orthogonal to σ.

This result is independent of the explicit shape of subregion R. $\qquad\square$

Theorem 4 essentially brings us to the uniqueness of the holographic slice. The new surface, σ', is generated by a convolution of the "deepest" points on each $\gamma(R)$. Considering balanced shapes such that the "deepest" point corresponds to $y^i = 0$, $\delta t / \delta z$ has the interpretation of the slope of the evolution vector s from p which takes it to the new leaf σ'. Slight imbalances in the shape would only affect the slope at subleading order in $\epsilon, \epsilon_\sigma$ and thus, the slope of s is determined in a shape independent manner in the limit $\epsilon, \epsilon_\sigma \to 0$. In order to move to σ', we must also specify the distance, $\delta\lambda(p)$, by which we move along s at each step. If the size of $C(p)$ is homogeneous across σ, then $\delta\lambda(p)$ is independent of p to leading order. Thus, the new leaf σ' obtained at each stage is unique up to small error terms. Following a similar procedure at each stage, e.g. by choosing random uncorrelated shapes of size δ' (found by mapping length δ to σ' by s) for subregions $C'(p)$ at each point p, ensures that the error terms do not add up coherently. This implies that the holographic slice is obtained by following the integral curves of the evolution vector s starting from each point $p \in \sigma$, and hence is unique.

Corollary 2. *Construct a holographic slice such that $C^i(p)$ is homogeneous and uncorrelated with $C^j(p)$, $j \neq i$. Let the sizes of $C^i(p)$ be determined by mapping the characteristic length, δ, of $C(p)$ on σ to σ^i by s. The continuum version (sending $\delta \to 0$) of all such slices are identical.*

As an aside, there are certain interesting features that this analysis highlights. Consider a generic leaf of a holographic screen σ and the future directed orthogonal null vectors k and l normalized as $k \cdot l = -2$. The t and z vectors are then given by

$$t = \frac{1}{2}(k + l), \qquad z = \frac{1}{2}(k - l). \tag{5.68}$$

From the linearity of extrinsic curvature, this leads to

$$\theta_t = \frac{1}{2}(\theta_k + \theta_l), \qquad \theta_z = \frac{1}{2}(\theta_k - \theta_l). \tag{5.69}$$

The evolution vector s and its associated expansion θ_s are given by

$$s = \theta_t t - \theta_z z = \frac{1}{2}(\theta_k l + \theta_l k), \tag{5.70}$$

and

$$\theta_s = \theta_t^2 - \theta_z^2 = \theta_k \theta_l \leq 0, \tag{5.71}$$

respectively.

At the holographic screen, $\theta_k = 0$. This leads to

$$s \propto k, \qquad \theta_s = 0. \tag{5.72}$$

Namely, the initial evolution of the holographic slice from a non-renormalized leaf occurs in the k direction with a non-expanding or contracting leaf area.

Convexity of Renormalized Leaves

Definition. *On a spacelike slice Σ, a compact set S is defined to be convex if all the codimension-1 minimal surfaces $\gamma(A)$ anchored to a codimension-2 region $A \subset S$ are such that $\forall A$, $\gamma(A) \subset S$.*

Lemma 3. *S is convex if and only if $K_\Sigma(\partial S) \leq 0$, where $K_\Sigma(\partial S)$ is the trace of the extrinsic curvature of ∂S embedded in Σ for the normal pointing inward.*

Proof. This follows from the fact that if $K_\Sigma(\partial S) \leq 0$, ∂S acts as a minimal surface barrier and hence, all the minimal surfaces must be contained within S. For the converse, suppose $K_\Sigma(\partial S) > 0$ somewhere on ∂S, then by considering small enough subregions anchored to this portion of ∂S, one can explicitly construct minimal surfaces that are outside S.   □

Definition. *In a spacetime M, a codimension-2 compact surface σ is called a convex boundary if on every codimension-1 spacelike slice Σ such that $\sigma \subset \Sigma$, the closure of the interior of σ is a convex set.*

Theorem 5. *σ is a convex boundary if and only if the null expansions in the inward direction, i.e. θ_k and θ_{-l}, are both non-positive.*

Proof. An inward normal n on a spacelike slice Σ is given by a linear superposition of k and l, i.e. $n = \alpha k - \beta l$ with some $\alpha, \beta \geq 0$. If $\theta_k \leq 0$ and $\theta_l \geq 0$, then $K_\Sigma(\sigma) = \theta_n = \alpha \theta_k - \beta \theta_l \leq 0$ for all choices of $\alpha, \beta \geq 0$. Thus, from Lemma 3, σ would be convex on all Σ containing σ. For the converse, suppose $\theta_k > 0$. One can then choose Σ such that $K_\Sigma(\sigma) > 0$ by taking $\beta \ll \alpha$. Thus, from Lemma 3, σ would not be convex on Σ, and hence σ would not be a convex boundary. The same argument applies if $\theta_l < 0$.   □

Fact. *A leaf of a holographic screen is a convex boundary. The boundary of any entanglement wedge is also a convex boundary.*

Theorem 6. *The intersection of the interior domains of dependence of two convex boundaries σ_1 and σ_2, represented by D_1 and D_2 is the interior domain of dependence of a convex boundary σ'.*

Proof. As shown in Appendix 5.8, $D' = D_1 \cap D_2$ is the interior domain of dependence of some σ'. We only need to show that σ' is convex. In order to show this, we can consider two slices Σ_1 and Σ_2 passing through σ_1 and σ_2 such that they are identical in the interior of σ' and are disjoint in the exterior of σ'. Let us denote the slice through the interior of σ' to be Σ'. Now consider any codimension-2 region $A \subset \Sigma'$. Then, from the convexity of σ_1, the minimal surface $\gamma(A)$ is contained in the interior of σ_1 on Σ_1. Similarly, $\gamma(A)$ is contained in the interior of σ_2 on Σ_2. This is only possible if $\gamma(A)$ is contained in the interior of σ' on Σ'. This is true for arbitrary Σ' and hence, by definition, σ' is a convex boundary. The maximin process can now be applied to σ'. $\qquad\square$

Corollary 3. *In a black hole spacetime or the case of a spacelike screen in an FRW spacetime, the coarse-graining procedure moves away from the singularity in the direction where the expansions θ_k and θ_l have opposite signs. At each step of coarse-graining, θ_k and θ_l in general have opposite signs.*

Chapter 6

Holographic Entanglement Entropy in TT Deformed CFTs

This chapter is a replication of Murdia et al. "Comments on holographic entanglement entropy in $T\overline{T}$ deformed conformal field theories", in *Phys. Rev.* D100.2 (2019), p. 026011, and is reproduced here in its original form.

6.1 Introduction

Gauge-gravity duality, specifically AdS/CFT, is our best known example of a holographic description of quantum gravity [14]. The so-called GKPW dictionary [82, 15] relating bulk physics to boundary dynamics takes the form

$$Z_{\text{CFT}}[\gamma_{ij}] = e^{-I_{\text{bulk}}[g_{\mu\nu}]},\tag{6.1}$$

where γ_{ij} is the background metric of the space in which the boundary CFT lives, and $g_{\mu\nu}$ is the bulk metric. A particularly consequential holographic correspondence given by this duality is the Ryu-Takayanagi (RT) formula

$$S(A) = \min_{\partial\Gamma=\partial A}\left[\frac{\|\Gamma\|}{4G}\right],\tag{6.2}$$

which relates the entanglement entropy of a subregion A of the boundary space to the area of the bulk extremal surface Γ anchored to the entangling surface ∂A [16, 47, 48]. Throughout, we will work to leading order in the bulk Newton's constant, G, and suppress all bulk fields aside from $g_{\mu\nu}$. Higher order effects are well understood in the context of AdS/CFT [28, 29].

Other holographic dualities with similar features have been proposed. In particular, the $T\overline{T}$ deformation of 2-dimensional CFTs and its appropriate generalizations to higher dimensions have been argued to have holographic duals [36, 171, 172]. Of crucial importance to our discussion is that the proposed dictionary relating the boundary and bulk observables

in these theories takes the same form as Eq. (6.1), except that now Dirichlet boundary
conditions are imposed on a cutoff surface in the bulk.

The simple idea we would like to highlight is that Eq. (6.2) was derived in the context of
AdS/CFT from Eq. (6.1) under rather tame assumptions [23]. The same argument, therefore,
can be used to show that the RT formula holds for all dualities adopting dictionaries of the
form of Eq. (6.1). This straightforward result is known in the community; however, careful
consideration of it resolves subtleties involving counterterms when calculating entanglement
entropy in TT deformed theories.

We start by reviewing some aspects of entanglement entropy from a field theory perspec-
tive in Section 6.2. We then proceed to a calculation in the particular case of TT deformed
theories in Section 6.2. We discuss the general holographic argument for the RT formula in
Section 6.3, which is followed by a sample calculation in cutoff AdS in Section 6.3. Along the
way, we address some subtleties related to holographic renormalization. We conclude with
a discussion about the consequences for holography in general spacetimes in Section 6.4.

Note that several calculations of entanglement entropy in TT deformed theories have
appeared recently [173, 174, 175, 176, 177, 178, 179]. Our goal is to emphasize the generality
of the arguments leading to an agreement between boundary entanglement entropy and the
RT formula and clarify some of the calculations performed in these works.

Conventions

The background metric of the space in which the boundary field theory lives is denoted by
γ_{ij}, while h_{ij} refers to the bulk induced metric on the cutoff surface at $r = r_c$. These are
related by $h_{ij} = r_c^2 \gamma_{ij}$.

6.2   Field Theory Calculation

Preliminaries

Consider a D-dimensional CFT with action $I[\phi] = \int d^D x \sqrt{\gamma}\, \mathcal{L}[\phi]$. One can prepare a density
matrix ρ on a spatial slice Σ using an appropriate Euclidean path integral. In order to
compute the entanglement entropy $S(A)$ of a subregion A of Σ, one can use the replica trick
as follows:

$$
\begin{aligned}
S(A) &= \lim_{n \to 1} \frac{\log\left(Z^{(b)}[M_n]\right) - n \log\left(Z^{(b)}[M_1]\right)}{1 - n} \\
&= \left(1 - n\frac{d}{dn}\right) \log\left(Z^{(b)}[M_n]\right)\bigg|_{n \to 1},
\end{aligned}
\tag{6.3}
$$

where

$$
Z^{(b)}[M] = \int D\phi \, \exp\left(-\int_M d^D x \sqrt{\gamma}\, \mathcal{L}[\phi]\right)
\tag{6.4}
$$

is the "bare" partition function computed by the path integral on a given manifold M. M_1
is the manifold used to compute $\text{Tr}\,\rho$, while M_n is an n-sheeted version of M_1 which is a
branched cover with a conical excess of angle $\Delta\phi = 2\pi(n-1)$ localized at the $(D-2)$-
dimensional submanifold ∂A.

The bare partition function $Z^{(b)}[M]$ typically diverges and takes the form

$$\log\left(Z^{(b)}[M]\right) = c_1(\Lambda a)^D + c_2(\Lambda a)^{D-2} + \dots, \tag{6.5}$$

where Λ is a UV cutoff and a is the length scale associated with the manifold M [180]. What
are the contributions of these divergences to entanglement entropy? These divergence can
be expressed as local integrals of background quantities [181, 182, 183]. (In even dimensions,
there is a logarithmic divergence which cannot be expressed in this manner.) This implies
that their contributions cancel in Eq. (6.4) everywhere away from ∂A, since M_n and n copies
of M_1 are identical manifolds except at ∂A. However, M_n has extra divergent contributions
coming from curvature invariants localized at ∂A. This leads to

$$S(A) = \sum_{k=1}^{\lfloor D/2 \rfloor} a_k \Lambda^{D-2k} \int_{\partial A} d^{D-2}x \sqrt{H}\left[\mathcal{R}, \mathcal{K}^2\right]^{k-1}, \tag{6.6}$$

where $\left[\mathcal{R}, \mathcal{K}^2\right]^{k-1}$ represents all possible scalar intrinsic and extrinsic curvature invariants of
∂A of mass dimension $2k-2$, with their coefficients collectively written as a_k, and H_{ab} is
the intrinsic metric of ∂A. Here, we have suppressed possible finite terms to focus on the
leading divergences. This is the famous "area law" associated with entanglement entropy,
which comes from the short distance correlations between A and $\bar{A}$.

Since the above behavior is sensitive to the cutoff, one often considers a renormalized
version of entropy. In particular, the divergences in Eq. (6.5) can be subtracted (except for
logarithmic ones) by introducing a counterterm action I_{ct} which involves local integrals of
curvature invariants:

$$I_{\text{ct}} = \sum_{k=1}^{\lfloor D/2 \rfloor+1} b_k \Lambda^{D-2k+2} \int_M d^D x \sqrt{\gamma}\,\mathcal{R}^{k-1}. \tag{6.7}$$

Here, $\mathcal{R}^{k-1}$ represents all possible scalar curvature invariants of M that one can write down
at mass dimension $2k-2$, and their coefficients b_k can be tuned exactly to cancel the
divergences. The renormalized entropy is then given by

$$S_{\text{ren}}(A) = \lim_{n\to 1} \frac{\log\left(Z_{\text{ren}}[M_n]\right) - n\log\left(Z_{\text{ren}}[M_1]\right)}{1-n}, \tag{6.8}$$

where Z_{ren} is the renormalized partition function which is computed using the action with
the counterterms in Eq. (6.7). This renormalized entropy is universal, i.e. UV regulator
independent in the continuum limit, and has been discussed previously in the literature
[183]. A closely related version of renormalized entropy was discussed in Ref. [182]. These
two are not identical, but they both extract the appropriate universal behavior in the CFT
limit by subtracting the power divergences.

Entanglement Entropy in TT Deformed Theories

We now specialize to the case of a D-dimensional CFT deformed by a particular composite
operator X_D of the stress tensor [172]. The presence of this deforming irrelevant operator
breaks conformal invariance and gives rise to a QFT that is conjectured to be holographically
dual to AdS with a finite cutoff radius, where Dirichlet boundary conditions are imposed.

We will focus on computing the partition function of this TT deformed theory on the
manifold S^D of radius R:

$$\gamma_{ij} = R^2 d\Omega_D^2. \tag{6.9}$$

The theory is defined by the flow equation dictated by X_D, and using this we obtain

$$\langle T_i^i \rangle = -D\lambda \langle X_D \rangle, \tag{6.10}$$

where λ is the deformation parameter. T_{ij} is the renormalized stress tensor, whose trace
vanishes up to conformal anomalies in the CFT limit $\lambda \to 0$. The bare stress tensor $T_{ij}^{(b)}$ is
related to the renormalized one[1] as

$$\langle T_{ij}^{(b)} \rangle = \langle T_{ij} \rangle - C_{ij}, \tag{6.11}$$

where C_{ij} represent various terms involving the background metric γ_{ij} that arise from vari-
ation of the counterterm action, which in the CFT limit is given by Eq. (6.7). For finite λ,
the cutoff of the theory is provided by the deformation itself, so that Λ is replaced by—or
identified with—$\lambda^{-1/D}$ in Eqs. (6.5 – 6.7). Since S^D is a maximally symmetric space, the one point function of the stress tensor
takes the form

$$\langle T_{ij} \rangle = \omega_D(R) \, \gamma_{ij}, \tag{6.12}$$

$$\langle T_{ij}^{(b)} \rangle = \omega_D^{(b)}(R) \, \gamma_{ij}. \tag{6.13}$$

Using the flow equation, one can solve for $\omega_D(R)$ and $\omega_D^{(b)}(R)$ as has been done in Ref. [178],
yielding

$$\omega_D(R) = -\frac{D-1}{2D\lambda}\sqrt{1 + \frac{L_D^2}{R^2}} + \frac{D-1}{2D\lambda}$$
$$+ \sum_{k=1}^{\lfloor (D-1)/2 \rfloor} \frac{f_{k,D}}{\lambda} \left(\frac{L_D}{R}\right)^{2k}, \tag{6.14}$$

$$\omega_D^{(b)}(R) = -\frac{D-1}{2D\lambda}\sqrt{1 + \frac{L_D^2}{R^2}}, \tag{6.15}$$

---

[1]The bare stress tensor is related to the Brown-York stress tensor [184], while the renormalized stress
tensor is related to the Balasubramanian-Kraus stress tensor [185] by a factor of r_c^{d-2}.

where $L_D^2 = 2D(D-2)\alpha_D\lambda^{2/D}$ with α_D being quantities related to the central charges of the field theory, and $f_{k,D}$ are dimension dependent constants. (Note that $\alpha_D \propto 1/(D-2)$, so that $L_2 \neq 0$.) We stress that while $\omega_D(R)$ has been represented schematically, the expression for $\omega_D^{(b)}(R)$ is exact. The explicit expressions for $\omega_D(R)$ can be found in Ref. [178].

Now using these results, we can compute the bare partition function as

$$\frac{d}{dR}\log Z_{S^D}^{(b)} = -\frac{1}{R}\int_{S^D} d^D x\sqrt{\gamma}\,\langle T_i^{i(b)}\rangle, \tag{6.16}$$

obtaining

$$\log Z_{S^D}^{(b)} = -D\Omega_D\int_0^R dR\,\omega_D^{(b)}(R)\,R^{D-1}$$
$$= \frac{\Omega_D L_D R^{D-1}}{2\lambda}\,{}_2F_1\left[-\frac{1}{2}, \frac{D-1}{2}; \frac{D+1}{2}; -\frac{R^2}{L_D^2}\right], \tag{6.17}$$

where Ω_D is the volume of a unit S^D. The entanglement entropy of a subregion A which is a hemisphere of the spatial S^{D-1} can then be computed by a simple trick described in Ref. [174]:

$$S(A) = \left(1 - n\frac{d}{dn}\right)\log\left(Z^{(b)}[S_n^D]\right)\Big|_{n\to 1}$$
$$= \left(1 - \frac{R}{D}\frac{d}{dR}\right)\log Z_{S^D}^{(b)}. \tag{6.18}$$

This gives us the answer

$$S(A) = \frac{\pi\Omega_{D-2}L_D R^{D-1}}{D(D-1)\lambda}\,{}_2F_1\left[\frac{1}{2}, \frac{D-1}{2}; \frac{D+1}{2}; -\frac{R^2}{L_D^2}\right]. \tag{6.19}$$

We can also compute the renormalized entanglement entropy in multiple different ways, e.g. using Eq. (6.8), which results in a universal answer in the CFT limit [183]. Alternately, one can use the version employed in Ref. [182]. For finite λ these two versions give different answers, which explains the discrepancy in Ref. [179] between the field theory calculation and the renormalized entropy.

We, however, emphasize that the TT deformation provides a particular physical regulator for the entropy, so one need not focus their attention on the renormalized entropy. This regularization has a simple interpretation in field theory, which also has a geometric bulk interpretation. Specifically, on the field theory side one only includes the energy levels below the shock singularity, above which the energies take complex values. The existence of this regularization naturally leads us to consider the bare entanglement entropy in Eq. (6.19), which captures all the information about correlations between A and $\bar{A}$.

6.3 Bulk Calculation

Holographic Duality

Using the holographic dictionary in Eq. (6.1), the entanglement entropy $S(A)$ of a boundary subregion A can be calculated as

$$S(A) = \lim_{n \to 1} \frac{I_{\text{bulk}}[B_n] - n I_{\text{bulk}}[B_1]}{n - 1}, \tag{6.20}$$

where B_n and B_1 are the saddle point bulk solutions dual to the boundary conditions dictated by the field theory path integral on M_n and M_1, respectively [23]. Notably, the action I_{bulk} dual to the bare partition function is the usual Einstein-Hilbert action supplemented by the Gibbons-Hawking-York boundary term. Assuming that the solution B_n preserves the $\mathbb{Z}_n$ symmetry of the boundary, Ref. [23] showed that the contribution to the above expression is localized to the extremal surface Γ, resulting in the RT formula

$$S(A) = \min_{\partial \Gamma = \partial A} \left[\frac{\|\Gamma\|}{4G} \right]. \tag{6.21}$$

Our simple observation is that this proof carries through unmodified as long as one is computing the bare partition function. The TT theory must then obey the RT formula by construction.

Counterterms added to the boundary action are well understood to correspond to boundary terms added to the bulk action [185, 186]. Per the discussion in Section 6.2, these terms give rise to extra contributions to $S(A)$ localized to the entangling surface ∂A. The saddle point solutions are not modified by the inclusion of these terms, which are pure functionals of the induced metric h_{ij}. This implies that the renormalized entropy can be calculated holographically as

$$S_{\text{ren}}(A) = \min_{\partial \Gamma = \partial A} \left[\frac{\|\Gamma\|}{4G} \right] + \tilde{S}(\partial A), \tag{6.22}$$

where the form of $\tilde{S}(\partial A)$ is discussed in Ref. [183].

RT Formula in Cutoff AdS

As a simple check, we now compare the result of the RT formula to the entanglement entropy obtained in Section 6.2. On the bulk side, we need to compute the minimal surface Γ anchored to the entangling surface ∂A on the cutoff surface at $r = r_c$, on which the induced metric is given by

$$h_{ij} = r_c^2 R^2 d\Omega_D^2 \equiv r_0^2 d\Omega_D^2. \tag{6.23}$$

This calculation was performed in Ref. [179] and the answer obtained is

$$S(A) = \frac{r_0^{D-1}\Omega_{D-2}}{4G(D-1)} \, _2F_1\left[\frac{1}{2}, \frac{D-1}{2}; \frac{D+1}{2}; -\frac{r_0^2}{l^2}\right],$$ (6.24)

where l is the AdS radius. By using the holographic identifications

$$\lambda = \frac{4\pi Gl}{Dr_c^D},$$ (6.25)

$$l^2 = 2D(D-2)\alpha_D\lambda^{2/D}r_c^2 = L_D^2 r_c^2,$$ (6.26)

we find that this is identical to Eq. (6.19).

6.4 Discussion

Holographic Dictionary

As emphasized throughout, if there exists a holographic duality between Einstein gravity
in the bulk and a quantum field theory on the boundary such that the two are related
by Eq. (6.1), then the RT formula will hold. This is true independent of the details of
the bulk spacetime and the boundary field theory. Indeed, we have shown that the TT
deformed CFT provides an explicit example of the validity of the Lewkowycz-Maldacena
(LM) proof beyond AdS/CFT at the conformal boundary.[2] In fact, all the results based
only on this dictionary element will hold in any such duality, at least in a perturbative
expansion in G. Two salient examples include the prescription for calculating refined Rényi
entropies presented in Ref. [188] and generalizations of the RT formula in higher curvature
gravity [189]. Though the robustness of the LM proof is far from unknown, we hope that
highlighting this feature helps solidify the relationship between entanglement entropy and
geometry in general spacetimes.

Holographic Renormalization and Counterterms

In CFT calculations, one often considers only renormalized quantities because these are
universally well-defined and survive the continuum limit. However, entanglement entropy
is not one of these quantities. Nevertheless, since the TT operator implements a particular
physical cutoff which has a simple geometric dual, it is sensible to consider bare quantities. In
particular, TT deformations with different background geometries would implement different
regularizations, leading to different entanglement entropies. On the bulk side, this manifests
as different choices of the cutoff surface. This provides a better understanding of the UV-IR
correspondence.

---

[2]An important assumption is the $\mathbb{Z}_n$ symmetry in the bulk. It is plausible that the argument holds after
relaxing this assumption; See, e.g., Ref. [187].

The handling of counterterms is the only additional subtlety encountered when calculating entanglement entropy in TT deformed CFTs. For finite deformations, all quantities are automatically regulated and hence the previous distinction between finite and divergent terms becomes muddled. We aimed to clarify the conceptual aspects of these terms and how they are related with the holographic result.

The fundamental idea is that the dictionary relation

$$Z_{\text{CFT}}[\gamma_{ij}] = e^{-I_{\text{bulk}}[g_{\mu\nu}]} \tag{6.27}$$

is precisely between the *bare* CFT on the boundary and Einstein-Hilbert gravity (plus the necessary Gibbons-Hawking-York term) in the bulk, both of which have divergent partition functions. This is the arena in which the RT formula was shown to hold. If one now chooses to introduce specific counterterms to renormalize the CFT stress tensor, then this will correspondingly alter the gravity side of the dictionary (specifically by adding terms localized to the boundary of the bulk). In particular, the addition of counterterms will alter the RT prescription to include terms beyond the standard area piece. This addition manifests as integrals of local geometric invariants at the entangling surface. In the CFT limit these are used to cancel power divergences, but with finite deformations one need not add a counterterm. Indeed, calculations including counterterms [174, 179] would necessarily miss the area law piece for $D > 2$, which is finite for finite deformations.

Holography in General Spacetimes

The explicit verification of the RT formula beyond AdS/CFT at the conformal boundary of AdS provides a strong footing for the surface-state correspondence [126] and related constructions to understand holography in general spacetimes via entanglement entropy [30, 32, 111, 34, 31]. In previous work, the RT formula was used as an assumption to investigate properties of a hypothetical boundary theory and self consistency checks provided confidence in that assumption. Now, the evidence that a duality in the form of Eq. (6.1) exists beyond basic AdS/CFT, and the RT formula along with it, suggests that a duality may indeed exist for general spacetimes and bolsters our confidence in previous work.

The results of TT deformations provide a particularly promising avenue to investigate flat space holography, since they hold down to scales below the AdS radius l. This contrasts with the conventional UV-IR correspondence, which would result in a single matrix-like theory describing an AdS volume [124]. It suggests that there is a way to redistribute degrees of freedom on the boundary theory in a way that maintains local factorization, and the TT deformation implements this. This is explicitly seen in the calculation of entanglement entropy in the fact that it does not face an obstruction when a volume law scaling is reached at $r_0 \approx l$. Volume law scaling of entanglement entropy suggests that the boundary theory for asymptotically flat space is non-local, as is expected from the TT deformation. Corresponding behavior is seen in cosmological spacetimes [34], and investigating properties of highly deformed CFTs may shed light on these theories. Since the TT operator naturally imple-

ments some sort of coarse graining, it would be interesting to relate this to the geometric coarse graining procedure developed in Ref. [31].

Bibliography

[1] Steven Weinberg. *The Quantum theory of fields. Vol. 1: Foundations.* Cambridge University Press, 2005. ISBN: 9780521670531, 9780511252044.

[2] Michael E. Peskin and Daniel V. Schroeder. *An Introduction to quantum field theory.* Reading, USA: Addison-Wesley, 1995. ISBN: 9780201503975, 0201503972. URL: http://www.slac.stanford.edu/~mpeskin/QFT.html.

[3] John F. Donoghue. "Introduction to the effective field theory description of gravity". In: *Advanced School on Effective Theories Almunecar, Spain, June 25-July 1, 1995.* 1995. arXiv: gr-qc/9512024 [gr-qc].

[4] Michael B. Green, J. H. Schwarz, and Edward Witten. *SUPERSTRING THEORY. VOL. 1: INTRODUCTION.* Cambridge Monographs on Mathematical Physics. 1988. ISBN: 9780521357524. URL: http://www.cambridge.org/us/academic/subjects/physics/theoretical-physics-and-mathematical-physics/superstring-theory-volume-1.

[5] J. Polchinski. *String theory. Vol. 1: An introduction to the bosonic string.* Cambridge Monographs on Mathematical Physics. Cambridge University Press, 2007. ISBN: 9780511252273, 9780521672276, 9780521633031. DOI: 10.1017/CBO9780511816079.

[6] S. W. Hawking. "Particle Creation by Black Holes". In: *Commun. Math. Phys.* 43 (1975). [,167(1975)], pp. 199–220. DOI: 10.1007/BF02345020,10.1007/BF01608497.

[7] S. W. Hawking. "Black hole explosions". In: *Nature* 248 (1974), pp. 30–31. DOI: 10.1038/248030a0.

[8] Jacob D. Bekenstein. "Black holes and entropy". In: *Phys. Rev.* D7 (1973), pp. 2333–2346. DOI: 10.1103/PhysRevD.7.2333.

[9] J. D. Bekenstein. "Black holes and the second law". In: *Lett. Nuovo Cim.* 4 (1972), pp. 737–740. DOI: 10.1007/BF02757029.

[10] James M. Bardeen, B. Carter, and S. W. Hawking. "The Four laws of black hole mechanics". In: *Commun. Math. Phys.* 31 (1973), pp. 161–170. DOI: 10.1007/BF01645742.

[11] G. W. Gibbons and S. W. Hawking. "Cosmological Event Horizons, Thermodynamics, and Particle Creation". In: *Phys. Rev.* D15 (1977), pp. 2738–2751. DOI: `10.1103/PhysRevD.15.2738`.

[12] Ted Jacobson. "Thermodynamics of space-time: The Einstein equation of state". In: *Phys. Rev. Lett.* 75 (1995), pp. 1260–1263. DOI: `10.1103/PhysRevLett.75.1260`. arXiv: `gr-qc/9504004 [gr-qc]`.

[13] Leonard Susskind. "The World as a hologram". In: *J. Math. Phys.* 36 (1995), pp. 6377–6396. DOI: `10.1063/1.531249`. arXiv: `hep-th/9409089 [hep-th]`.

[14] Juan Martin Maldacena. "The Large N limit of superconformal field theories and supergravity". In: *Int. J. Theor. Phys.* 38 (1999). [Adv. Theor. Math. Phys.2,231(1998)], pp. 1113–1133. DOI: `10.1023/A:1026654312961,10.4310/ATMP.1998.v2.n2.a1`. arXiv: `hep-th/9711200 [hep-th]`.

[15] Edward Witten. "Anti-de Sitter space and holography". In: *Adv. Theor. Math. Phys.* 2 (1998), pp. 253–291. DOI: `10.4310/ATMP.1998.v2.n2.a2`. arXiv: `hep-th/9802150 [hep-th]`.

[16] Shinsei Ryu and Tadashi Takayanagi. "Holographic derivation of entanglement entropy from AdS/CFT". In: *Phys. Rev. Lett.* 96 (2006), p. 181602. DOI: `10.1103/PhysRevLett.96.181602`. arXiv: `hep-th/0603001 [hep-th]`.

[17] Wendy L. Freedman et al. "Final Results from theHubble Space TelescopeKey Project to Measure the Hubble Constant". In: *The Astrophysical Journal* 553.1 (May 2001), pp. 47–72. DOI: `10.1086/320638`. URL: `https://doi.org/10.1086%2F320638`.

[18] N. Jarosik et al. "Seven-year Wilkinson Microwave Anisotropy Probe (WMAP) Observations: Sky Maps, Systematic Errors, and Basic Results". In: *The Astrophysical Journal Supplement Series* 192.2 (Jan. 2011), p. 14. DOI: `10.1088/0067-0049/192/2/14`. URL: `https://doi.org/10.1088%2F0067-0049%2F192%2F2%2F14`.

[19] P. A. R. Ade et al. "Planck 2013 results. I. Overview of products and scientific results". In: *Astron. Astrophys.* 571 (2014), A1. DOI: `10.1051/0004-6361/201321529`. arXiv: `1303.5062 [astro-ph.CO]`.

[20] Adam G. Riess et al. "Large Magellanic Cloud Cepheid Standards Provide a 1% Foundation for the Determination of the Hubble Constant and Stronger Evidence for Physics beyond ΛCDM". In: *Astrophys. J.* 876.1 (2019), p. 85. DOI: `10.3847/1538-4357/ab1422`. arXiv: `1903.07603 [astro-ph.CO]`.

[21] Raphael Bousso. "A Covariant entropy conjecture". In: *JHEP* 07 (1999), p. 004. DOI: `10.1088/1126-6708/1999/07/004`. arXiv: `hep-th/9905177 [hep-th]`.

[22] Raphael Bousso. "The Holographic principle". In: *Rev. Mod. Phys.* 74 (2002), pp. 825–874. DOI: `10.1103/RevModPhys.74.825`. arXiv: `hep-th/0203101 [hep-th]`.

[23] Aitor Lewkowycz and Juan Maldacena. "Generalized gravitational entropy". In: *JHEP* 08 (2013), p. 090. DOI: `10.1007/JHEP08(2013)090`. arXiv: `1304.4926 [hep-th]`.

[24] Brian Swingle. "Entanglement Renormalization and Holography". In: *Phys. Rev. D86* (2012), p. 065007. DOI: `10.1103/PhysRevD.86.065007`. arXiv: `0905.1317 [cond-mat.str-el]`.

[25] G. Vidal. "Entanglement Renormalization". In: *Phys. Rev. Lett.* 99 (22 Nov. 2007), p. 220405. DOI: `10.1103/PhysRevLett.99.220405`. URL: `https://link.aps.org/doi/10.1103/PhysRevLett.99.220405`.

[26] G. Vidal. "Class of Quantum Many-Body States That Can Be Efficiently Simulated". In: *Phys. Rev. Lett.* 101 (2008), p. 110501. DOI: `10.1103/PhysRevLett.101.110501`. arXiv: `quant-ph/0610099 [quant-ph]`.

[27] Daniel L. Jafferis et al. "Relative entropy equals bulk relative entropy". In: *JHEP* 06 (2016), p. 004. DOI: `10.1007/JHEP06(2016)004`. arXiv: `1512.06431 [hep-th]`.

[28] Thomas Faulkner, Aitor Lewkowycz, and Juan Maldacena. "Quantum corrections to holographic entanglement entropy". In: *JHEP* 11 (2013), p. 074. DOI: `10.1007/JHEP11(2013)074`. arXiv: `1307.2892 [hep-th]`.

[29] Netta Engelhardt and Aron C. Wall. "Quantum Extremal Surfaces: Holographic Entanglement Entropy beyond the Classical Regime". In: *JHEP* 01 (2015), p. 073. DOI: `10.1007/JHEP01(2015)073`. arXiv: `1408.3203 [hep-th]`.

[30] Fabio Sanches and Sean J. Weinberg. "Holographic entanglement entropy conjecture for general spacetimes". In: *Phys. Rev. D94.8* (2016), p. 084034. DOI: `10.1103/PhysRevD.94.084034`. arXiv: `1603.05250 [hep-th]`.

[31] Yasunori Nomura, Pratik Rath, and Nico Salzetta. "Pulling the Boundary into the Bulk". In: *Phys. Rev. D98.2* (2018), p. 026010. DOI: `10.1103/PhysRevD.98.026010`. arXiv: `1805.00523 [hep-th]`.

[32] Yasunori Nomura et al. "Toward a Holographic Theory for General Spacetimes". In: *Phys. Rev. D95.8* (2017), p. 086002. DOI: `10.1103/PhysRevD.95.086002`. arXiv: `1611.02702 [hep-th]`.

[33] Yasunori Nomura and Nico Salzetta. "Butterfly Velocities for Holographic Theories of General Spacetimes". In: *JHEP* 10 (2017), p. 187. DOI: `10.1007/JHEP10(2017)187`. arXiv: `1708.04237 [hep-th]`.

[34] Yasunori Nomura, Pratik Rath, and Nico Salzetta. "Spacetime from Unentanglement". In: *Phys. Rev. D97.10* (2018), p. 106010. DOI: `10.1103/PhysRevD.97.106010`. arXiv: `1711.05263 [hep-th]`.

[35] Chitraang Murdia et al. "Comments on holographic entanglement entropy in $T\overline{T}$ deformed conformal field theories". In: *Phys. Rev. D100.2* (2019), p. 026011. DOI: `10.1103/PhysRevD.100.026011`. arXiv: `1904.04408 [hep-th]`.

[36] Lauren McGough, Mark Mezei, and Herman Verlinde. "Moving the CFT into the bulk with $T\overline{T}$". In: *JHEP* 04 (2018), p. 010. DOI: `10.1007/JHEP04(2018)010`. arXiv: `1611.03470 [hep-th]`.

[37] Gerard 't Hooft. "Dimensional reduction in quantum gravity". In: *Conf. Proc.* C930308 (1993), pp. 284–296. arXiv: `gr-qc/9310026 [gr-qc]`.

[38] W. Fischler and Leonard Susskind. "Holography and cosmology". In: (1998). arXiv: `hep-th/9806039 [hep-th]`.

[39] Leonard Susskind, Larus Thorlacius, and John Uglum. "The Stretched horizon and black hole complementarity". In: *Phys. Rev.* D48 (1993), pp. 3743–3761. DOI: `10.1103/PhysRevD.48.3743`. arXiv: `hep-th/9306069 [hep-th]`.

[40] Yasunori Nomura. "Physical Theories, Eternal Inflation, and Quantum Universe". In: *JHEP* 11 (2011), p. 063. DOI: `10.1007/JHEP11(2011)063`. arXiv: `1104.2324 [hep-th]`.

[41] Raphael Bousso and Leonard Susskind. "The Multiverse Interpretation of Quantum Mechanics". In: *Phys. Rev.* D85 (2012), p. 045007. DOI: `10.1103/PhysRevD.85.045007`. arXiv: `1105.3796 [hep-th]`.

[42] Raphael Bousso. "Holography in general space-times". In: *JHEP* 06 (1999), p. 028. DOI: `10.1088/1126-6708/1999/06/028`. arXiv: `hep-th/9906022 [hep-th]`.

[43] Yasunori Nomura. "Quantum Mechanics, Spacetime Locality, and Gravity". In: *Found. Phys.* 43 (2013), pp. 978–1007. DOI: `10.1007/s10701-013-9729-1`. arXiv: `1110.4630 [hep-th]`.

[44] Raphael Bousso and Netta Engelhardt. "New Area Law in General Relativity". In: *Phys. Rev. Lett.* 115.8 (2015), p. 081301. DOI: `10.1103/PhysRevLett.115.081301`. arXiv: `1504.07627 [hep-th]`.

[45] Raphael Bousso and Netta Engelhardt. "Proof of a New Area Law in General Relativity". In: *Phys. Rev.* D92.4 (2015), p. 044031. DOI: `10.1103/PhysRevD.92.044031`. arXiv: `1504.07660 [gr-qc]`.

[46] Fabio Sanches and Sean J. Weinberg. "Refinement of the Bousso-Engelhardt Area Law". In: *Phys. Rev.* D94.2 (2016), p. 021502. DOI: `10.1103/PhysRevD.94.021502`. arXiv: `1604.04919 [hep-th]`.

[47] Shinsei Ryu and Tadashi Takayanagi. "Aspects of Holographic Entanglement Entropy". In: *JHEP* 08 (2006), p. 045. DOI: `10.1088/1126-6708/2006/08/045`. arXiv: `hep-th/0605073 [hep-th]`.

[48] Veronika E. Hubeny, Mukund Rangamani, and Tadashi Takayanagi. "A Covariant holographic entanglement entropy proposal". In: *JHEP* 07 (2007), p. 062. DOI: `10.1088/1126-6708/2007/07/062`. arXiv: `0705.0016 [hep-th]`.

[49] Mark Van Raamsdonk. "Comments on quantum gravity and entanglement". In: (2009). arXiv: `0907.2939 [hep-th]`.

[50] Brian Swingle. "Constructing holographic spacetimes using entanglement renormalization". In: (2012). arXiv: `1209.3304 [hep-th]`.

[51] Juan Maldacena and Leonard Susskind. "Cool horizons for entangled black holes". In: *Fortsch. Phys.* 61 (2013), pp. 781–811. DOI: `10.1002/prop.201300020`. arXiv: `1306.0533 [hep-th]`.

[52] Michael Freedman and Matthew Headrick. "Bit threads and holographic entanglement". In: *Commun. Math. Phys.* 352.1 (2017), pp. 407–438. DOI: `10.1007/s00220-016-2796-3`. arXiv: `1604.00354 [hep-th]`.

[53] Ahmed Almheiri, Xi Dong, and Brian Swingle. "Linearity of Holographic Entanglement Entropy". In: *JHEP* 02 (2017), p. 074. DOI: `10.1007/JHEP02(2017)074`. arXiv: `1606.04537 [hep-th]`.

[54] Yasunori Nomura et al. "Spacetime Equals Entanglement". In: *Phys. Lett.* B763 (2016), pp. 370–374. DOI: `10.1016/j.physletb.2016.10.045`. arXiv: `1607.02508 [hep-th]`.

[55] Daniel Harlow. "The Ryu-Takayanagi Formula from Quantum Error Correction". In: *Commun. Math. Phys.* 354.3 (2017), pp. 865–912. DOI: `10.1007/s00220-017-2904-z`. arXiv: `1607.03901 [hep-th]`.

[56] Ahmed Almheiri et al. "Black Holes: Complementarity or Firewalls?" In: *JHEP* 02 (2013), p. 062. DOI: `10.1007/JHEP02(2013)062`. arXiv: `1207.3123 [hep-th]`.

[57] Ahmed Almheiri et al. "An Apologia for Firewalls". In: *JHEP* 09 (2013), p. 018. DOI: `10.1007/JHEP09(2013)018`. arXiv: `1304.6483 [hep-th]`.

[58] Donald Marolf and Joseph Polchinski. "Gauge/Gravity Duality and the Black Hole Interior". In: *Phys. Rev. Lett.* 111 (2013), p. 171301. DOI: `10.1103/PhysRevLett.111.171301`. arXiv: `1307.4706 [hep-th]`.

[59] Kyriakos Papadodimas and Suvrat Raju. "Remarks on the necessity and implications of state-dependence in the black hole interior". In: *Phys. Rev.* D93.8 (2016), p. 084049. DOI: `10.1103/PhysRevD.93.084049`. arXiv: `1503.08825 [hep-th]`.

[60] Kyriakos Papadodimas and Suvrat Raju. "An Infalling Observer in AdS/CFT". In: *JHEP* 10 (2013), p. 212. DOI: `10.1007/JHEP10(2013)212`. arXiv: `1211.6767 [hep-th]`.

[61] Erik Verlinde and Herman Verlinde. "Black Hole Entanglement and Quantum Error Correction". In: *JHEP* 10 (2013), p. 107. DOI: `10.1007/JHEP10(2013)107`. arXiv: `1211.6913 [hep-th]`.

[62] Yasunori Nomura and Jaime Varela. "A Note on (No) Firewalls: The Entropy Argument". In: *JHEP* 07 (2013), p. 124. DOI: `10.1007/JHEP07(2013)124`. arXiv: `1211.7033 [hep-th]`.

[63] Bryce S. DeWitt. "Quantum Theory of Gravity. 1. The Canonical Theory". In: *Phys. Rev.* 160 (1967). [3,93(1987)], pp. 1113–1148. DOI: `10.1103/PhysRev.160.1113`.

[64] J. A. Wheeler. "SUPERSPACE AND THE NATURE OF QUANTUM GEOMETRO-DYNAMICS". In: *Adv. Ser. Astrophys. Cosmol.* 3 (1987). [,C67(1968)], pp. 27–92.

[65] Raphael Bousso and Joseph Polchinski. "Quantization of four form fluxes and dynamical neutralization of the cosmological constant". In: *JHEP* 06 (2000), p. 006. DOI: 10.1088/1126-6708/2000/06/006. arXiv: hep-th/0004134 [hep-th].

[66] Shamit Kachru et al. "De Sitter vacua in string theory". In: *Phys. Rev.* D68 (2003), p. 046005. DOI: 10.1103/PhysRevD.68.046005. arXiv: hep-th/0301240 [hep-th].

[67] Leonard Susskind. "The Anthropic landscape of string theory". In: (2003), pp. 247–266. arXiv: hep-th/0302219 [hep-th].

[68] Michael R. Douglas. "The Statistics of string / M theory vacua". In: *JHEP* 05 (2003), p. 046. DOI: 10.1088/1126-6708/2003/05/046. arXiv: hep-th/0303194 [hep-th].

[69] Yasunori Nomura. "The Static Quantum Multiverse". In: *Phys. Rev.* D86 (2012), p. 083505. DOI: 10.1103/PhysRevD.86.083505. arXiv: 1205.5550 [hep-th].

[70] Yasunori Nomura, Jaime Varela, and Sean J. Weinberg. "Low Energy Description of Quantum Gravity and Complementarity". In: *Phys. Lett.* B733 (2014), pp. 126–133. DOI: 10.1016/j.physletb.2014.04.027. arXiv: 1304.0448 [hep-th].

[71] S. A. Hayward. "General laws of black hole dynamics". In: *Phys. Rev.* D49 (1994), pp. 6467–6474. DOI: 10.1103/PhysRevD.49.6467.

[72] Sean A. Hayward. "Unified first law of black hole dynamics and relativistic thermodynamics". In: *Class. Quant. Grav.* 15 (1998), pp. 3147–3162. DOI: 10.1088/0264-9381/15/10/017. arXiv: gr-qc/9710089 [gr-qc].

[73] Abhay Ashtekar and Badri Krishnan. "Dynamical horizons: Energy, angular momentum, fluxes and balance laws". In: *Phys. Rev. Lett.* 89 (2002), p. 261101. DOI: 10.1103/PhysRevLett.89.261101. arXiv: gr-qc/0207080 [gr-qc].

[74] Abhay Ashtekar and Badri Krishnan. "Dynamical horizons and their properties". In: *Phys. Rev.* D68 (2003), p. 104030. DOI: 10.1103/PhysRevD.68.104030. arXiv: gr-qc/0308033 [gr-qc].

[75] Don N. Page. "Average entropy of a subsystem". In: *Phys. Rev. Lett.* 71 (1993), pp. 1291–1294. DOI: 10.1103/PhysRevLett.71.1291. arXiv: gr-qc/9305007 [gr-qc].

[76] Aron C. Wall. "Maximin Surfaces, and the Strong Subadditivity of the Covariant Holographic Entanglement Entropy". In: *Class. Quant. Grav.* 31.22 (2014), p. 225007. DOI: 10.1088/0264-9381/31/22/225007. arXiv: 1211.3494 [hep-th].

[77] Raphael Bousso and Netta Engelhardt. "Generalized Second Law for Cosmology". In: *Phys. Rev.* D93.2 (2016), p. 024025. DOI: 10.1103/PhysRevD.93.024025. arXiv: 1510.02099 [hep-th].

[78] Wei Li and Tadashi Takayanagi. "Holography and Entanglement in Flat Spacetime". In: *Phys. Rev. Lett.* 106 (2011), p. 141301. DOI: 10.1103/PhysRevLett.106.141301. arXiv: 1010.3700 [hep-th].

[79] Gia Dvali. "Black Holes and Large N Species Solution to the Hierarchy Problem". In: *Fortsch. Phys.* 58 (2010), pp. 528–536. DOI: `10.1002/prop.201000009`. arXiv: `0706.2050 [hep-th]`.

[80] Luca Bombelli et al. "A Quantum Source of Entropy for Black Holes". In: *Phys. Rev.* D34 (1986), pp. 373–383. DOI: `10.1103/PhysRevD.34.373`.

[81] Mark Srednicki. "Entropy and area". In: *Phys. Rev. Lett.* 71 (1993), pp. 666–669. DOI: `10.1103/PhysRevLett.71.666`. arXiv: `hep-th/9303048 [hep-th]`.

[82] S. S. Gubser, Igor R. Klebanov, and Alexander M. Polyakov. "Gauge theory correlators from noncritical string theory". In: *Phys. Lett.* B428 (1998), pp. 105–114. DOI: `10.1016/S0370-2693(98)00377-3`. arXiv: `hep-th/9802109 [hep-th]`.

[83] Yasunori Nomura and Sean J. Weinberg. "Entropy of a vacuum: What does the covariant entropy count?" In: *Phys. Rev.* D90.10 (2014), p. 104003. DOI: `10.1103/PhysRevD.90.104003`. arXiv: `1310.7564 [hep-th]`.

[84] Yasunori Nomura, Fabio Sanches, and Sean J. Weinberg. "Black Hole Interior in Quantum Gravity". In: *Phys. Rev. Lett.* 114 (2015), p. 201301. DOI: `10.1103/PhysRevLett.114.201301`. arXiv: `1412.7539 [hep-th]`.

[85] Yasunori Nomura, Fabio Sanches, and Sean J. Weinberg. "Relativeness in Quantum Gravity: Limitations and Frame Dependence of Semiclassical Descriptions". In: *JHEP* 04 (2015), p. 158. DOI: `10.1007/JHEP04(2015)158`. arXiv: `1412.7538 [hep-th]`.

[86] Yasunori Nomura and Nico Salzetta. "Why Firewalls Need Not Exist". In: *Phys. Lett.* B761 (2016), pp. 62–69. DOI: `10.1016/j.physletb.2016.08.003`. arXiv: `1602.07673 [hep-th]`.

[87] Robert M. Wald. *General Relativity*. Chicago, USA: Chicago Univ. Pr., 1984. DOI: `10.7208/chicago/9780226870373.001.0001`.

[88] Raphael Bousso, Ben Freivogel, and Stefan Leichenauer. "Saturating the holographic entropy bound". In: *Phys. Rev.* D82 (2010), p. 084024. DOI: `10.1103/PhysRevD.82.084024`. arXiv: `1003.3012 [hep-th]`.

[89] Alan H. Guth. "The Inflationary Universe: A Possible Solution to the Horizon and Flatness Problems". In: *Phys. Rev.* D23 (1981). [Adv. Ser. Astrophys. Cosmol. 3, 139 (1987)], pp. 347–356. DOI: `10.1103/PhysRevD.23.347`.

[90] Andrei D. Linde. "A New Inflationary Universe Scenario: A Possible Solution of the Horizon, Flatness, Homogeneity, Isotropy and Primordial Monopole Problems". In: *Phys. Lett.* 108B (1982). [Adv. Ser. Astrophys. Cosmol.3,149(1987)], pp. 389–393. DOI: `10.1016/0370-2693(82)91219-9`.

[91] Andreas Albrecht and Paul J. Steinhardt. "Cosmology for Grand Unified Theories with Radiatively Induced Symmetry Breaking". In: *Phys. Rev. Lett.* 48 (1982). [Adv. Ser. Astrophys. Cosmol.3,158(1987)], pp. 1220–1223. DOI: `10.1103/PhysRevLett.48.1220`.

[92] Sidney R. Coleman and Frank De Luccia. "Gravitational Effects on and of Vacuum Decay". In: *Phys. Rev.* D21 (1980), p. 3305. DOI: `10.1103/PhysRevD.21.3305`.

[93] Alan H. Guth, David I. Kaiser, and Yasunori Nomura. "Inflationary paradigm after Planck 2013". In: *Phys. Lett.* B733 (2014), pp. 112–119. DOI: `10.1016/j.physletb.2014.03.020`. arXiv: `1312.7619 [astro-ph.CO]`.

[94] Yasunori Nomura. "A Note on Boltzmann Brains". In: *Phys. Lett.* B749 (2015), pp. 514–518. DOI: `10.1016/j.physletb.2015.08.029`. arXiv: `1502.05401 [hep-th]`.

[95] Don N. Page and William K. Wootters. "EVOLUTION WITHOUT EVOLUTION: DYNAMICS DESCRIBED BY STATIONARY OBSERVABLES". In: *Phys. Rev.* D27 (1983), p. 2885. DOI: `10.1103/PhysRevD.27.2885`.

[96] Anthony Aguirre, Sean M. Carroll, and Matthew C. Johnson. "Out of equilibrium: understanding cosmological evolution to lower-entropy states". In: *JCAP* 1202 (2012), p. 024. DOI: `10.1088/1475-7516/2012/02/024`. arXiv: `1108.0417 [hep-th]`.

[97] Alan H. Guth and Erick J. Weinberg. "Could the Universe Have Recovered from a Slow First Order Phase Transition?" In: *Nucl. Phys.* B212 (1983), pp. 321–364. DOI: `10.1016/0550-3213(83)90307-3`.

[98] Alexander Vilenkin. "The Birth of Inflationary Universes". In: *Phys. Rev.* D27 (1983), p. 2848. DOI: `10.1103/PhysRevD.27.2848`.

[99] Andrei D. Linde. "Eternally Existing Selfreproducing Chaotic Inflationary Universe". In: *Phys. Lett.* B175 (1986), pp. 395–400. DOI: `10.1016/0370-2693(86)90611-8`.

[100] Andrei D. Linde. "ETERNAL CHAOTIC INFLATION". In: *Mod. Phys. Lett.* A1 (1986), p. 81. DOI: `10.1142/S0217732386000129`.

[101] Sean M. Carroll and Jennifer Chen. "Spontaneous inflation and the origin of the arrow of time". In: (2004). arXiv: `hep-th/0410270 [hep-th]`.

[102] Lisa Dyson, Matthew Kleban, and Leonard Susskind. "Disturbing implications of a cosmological constant". In: *JHEP* 10 (2002), p. 011. DOI: `10.1088/1126-6708/2002/10/011`. arXiv: `hep-th/0208013 [hep-th]`.

[103] Andreas Albrecht. "Cosmic inflation and the arrow of time". In: (2002), pp. 363–401. arXiv: `astro-ph/0210527 [astro-ph]`.

[104] Don N. Page. "Is our universe likely to decay within 20 billion years?" In: *Phys. Rev.* D78 (2008), p. 063535. DOI: `10.1103/PhysRevD.78.063535`. arXiv: `hep-th/0610079 [hep-th]`.

[105] Stephen H. Shenker and Douglas Stanford. "Black holes and the butterfly effect". In: *JHEP* 03 (2014), p. 067. DOI: `10.1007/JHEP03(2014)067`. arXiv: `1306.0622 [hep-th]`.

[106] Daniel A. Roberts, Douglas Stanford, and Leonard Susskind. "Localized shocks". In: *JHEP* 03 (2015), p. 051. DOI: `10.1007/JHEP03(2015)051`. arXiv: `1409.8180 [hep-th]`.

[107]   Daniel A. Roberts and Brian Swingle. "Lieb-Robinson Bound and the Butterfly Effect in Quantum Field Theories". In: *Phys. Rev. Lett.* 117.9 (2016), p. 091602. DOI: `10.1103/PhysRevLett.117.091602`. arXiv: `1603.09298 [hep-th]`.

[108]   Xiao-Liang Qi and Zhao Yang. "Butterfly velocity and bulk causal structure". In: (2017). arXiv: `1705.01728 [hep-th]`.

[109]   Ahmed Almheiri, Xi Dong, and Daniel Harlow. "Bulk Locality and Quantum Error Correction in AdS/CFT". In: *JHEP* 04 (2015), p. 163. DOI: `10.1007/JHEP04(2015)163`. arXiv: `1411.7041 [hep-th]`.

[110]   Fernando Pastawski et al. "Holographic quantum error-correcting codes: Toy models for the bulk/boundary correspondence". In: *JHEP* 06 (2015), p. 149. DOI: `10.1007/JHEP06(2015)149`. arXiv: `1503.06237 [hep-th]`.

[111]   Yasunori Nomura, Pratik Rath, and Nico Salzetta. "Classical Spacetimes as Amplified Information in Holographic Quantum Theories". In: *Phys. Rev.* D97.10 (2018), p. 106025. DOI: `10.1103/PhysRevD.97.106025`. arXiv: `1705.06283 [hep-th]`.

[112]   Alex Hamilton et al. "Holographic representation of local bulk operators". In: *Phys. Rev.* D74 (2006), p. 066009. DOI: `10.1103/PhysRevD.74.066009`. arXiv: `hep-th/0606141 [hep-th]`.

[113]   Bartlomiej Czech et al. "The Gravity Dual of a Density Matrix". In: *Class. Quant. Grav.* 29 (2012), p. 155009. DOI: `10.1088/0264-9381/29/15/155009`. arXiv: `1204.1330 [hep-th]`.

[114]   Xi Dong, Daniel Harlow, and Aron C. Wall. "Reconstruction of Bulk Operators within the Entanglement Wedge in Gauge-Gravity Duality". In: *Phys. Rev. Lett.* 117.2 (2016), p. 021601. DOI: `10.1103/PhysRevLett.117.021601`. arXiv: `1601.05416 [hep-th]`.

[115]   Patrick Hayden et al. "Holographic duality from random tensor networks". In: *JHEP* 11 (2016), p. 009. DOI: `10.1007/JHEP11(2016)009`. arXiv: `1601.01694 [hep-th]`.

[116]   Thomas Faulkner and Aitor Lewkowycz. "Bulk locality from modular flow". In: *JHEP* 07 (2017), p. 151. DOI: `10.1007/JHEP07(2017)151`. arXiv: `1704.05464 [hep-th]`.

[117]   Jordan Cotler et al. "Entanglement Wedge Reconstruction via Universal Recovery Channels". In: *Phys. Rev.* X9.3 (2019), p. 031011. DOI: `10.1103/PhysRevX.9.031011`. arXiv: `1704.05839 [hep-th]`.

[118]   Fabio Sanches and Sean J. Weinberg. "Boundary dual of bulk local operators". In: *Phys. Rev.* D96.2 (2017), p. 026004. DOI: `10.1103/PhysRevD.96.026004`. arXiv: `1703.07780 [hep-th]`.

[119]   David J. Luitz and Yevgeny Bar Lev. "Information propagation in isolated quantum systems". In: *Phys. Rev.* B96.2 (2017), p. 020406. DOI: `10.1103/PhysRevB.96.020406`. arXiv: `1702.03929 [cond-mat.dis-nn]`.

[120]   Ning Bao and Aidan Chatwin-Davies. "Puzzles and pitfalls involving Haar-typicality in holography". In: *SciPost Phys.* 4.6 (2018), p. 033. DOI: 10.21468/SciPostPhys.4.6.033. arXiv: 1708.08561 [hep-th].

[121]   Daniel Kabat and Gilad Lifschytz. "Local bulk physics from intersecting modular Hamiltonians". In: *JHEP* 06 (2017), p. 120. DOI: 10.1007/JHEP06(2017)120. arXiv: 1703.06523 [hep-th].

[122]   Yuya Kusuki, Tadashi Takayanagi, and Koji Umemoto. "Holographic Entanglement Entropy on Generic Time Slices". In: *JHEP* 06 (2017), p. 021. DOI: 10.1007/JHEP06(2017)021. arXiv: 1703.00915 [hep-th].

[123]   Netta Engelhardt and Aron C. Wall. "Extremal Surface Barriers". In: *JHEP* 03 (2014), p. 068. DOI: 10.1007/JHEP03(2014)068. arXiv: 1312.3699 [hep-th].

[124]   Leonard Susskind and Edward Witten. "The Holographic bound in anti-de Sitter space". In: (1998). arXiv: hep-th/9805114 [hep-th].

[125]   Lisa Randall and Raman Sundrum. "An Alternative to compactification". In: *Phys. Rev. Lett.* 83 (1999), pp. 4690–4693. DOI: 10.1103/PhysRevLett.83.4690. arXiv: hep-th/9906064 [hep-th].

[126]   Masamichi Miyaji and Tadashi Takayanagi. "Surface/State Correspondence as a Generalized Holography". In: *PTEP* 2015.7 (2015), 073B03. DOI: 10.1093/ptep/ptv089. arXiv: 1503.03542 [hep-th].

[127]   Juan Maldacena, Stephen H. Shenker, and Douglas Stanford. "A bound on chaos". In: *JHEP* 08 (2016), p. 106. DOI: 10.1007/JHEP08(2016)106. arXiv: 1503.01409 [hep-th].

[128]   Mark Srednicki. "Chaos and quantum thermalization". In: *Phys. Rev. E* 50 (2 Aug. 1994), pp. 888–901. DOI: 10.1103/PhysRevE.50.888. URL: https://link.aps.org/doi/10.1103/PhysRevE.50.888.

[129]   Rahul Nandkishore and David A. Huse. "Many body localization and thermalization in quantum statistical mechanics". In: *Ann. Rev. Condensed Matter Phys.* 6 (2015), pp. 15–38. DOI: 10.1146/annurev-conmatphys-031214-014726. arXiv: 1404.0686 [cond-mat.stat-mech].

[130]   M. Reza Mohammadi Mozaffar and Ali Mollabashi. "Entanglement in Lifshitz-type Quantum Field Theories". In: *JHEP* 07 (2017), p. 120. DOI: 10.1007/JHEP07(2017)120. arXiv: 1705.00483 [hep-th].

[131]   Jose L. F. Barbon and Carlos A. Fuertes. "Holographic entanglement entropy probes (non)locality". In: *JHEP* 04 (2008), p. 096. DOI: 10.1088/1126-6708/2008/04/096. arXiv: 0803.1928 [hep-th].

[132]   Willy Fischler, Arnab Kundu, and Sandipan Kundu. "Holographic Entanglement in a Noncommutative Gauge Theory". In: *JHEP* 01 (2014), p. 137. DOI: 10.1007/JHEP01(2014)137. arXiv: 1307.2932 [hep-th].

[133] Joanna L. Karczmarek and Charles Rabideau. "Holographic entanglement entropy in nonlocal theories". In: *JHEP* 10 (2013), p. 078. DOI: `10.1007/JHEP10(2013)078`. arXiv: `1307.3517 [hep-th]`.

[134] Noburo Shiba and Tadashi Takayanagi. "Volume Law for the Entanglement Entropy in Non-local QFTs". In: *JHEP* 02 (2014), p. 033. DOI: `10.1007/JHEP02(2014)033`. arXiv: `1311.1643 [hep-th]`.

[135] Wenbo Fu and Subir Sachdev. "Numerical study of fermion and boson models with infinite-range random interactions". In: *Phys. Rev.* B94.3 (2016), p. 035135. DOI: `10.1103/PhysRevB.94.035135`. arXiv: `1603.05246 [cond-mat.str-el]`.

[136] Chunxiao Liu, Xiao Chen, and Leon Balents. "Quantum Entanglement of the Sachdev-Ye-Kitaev Models". In: *Phys. Rev.* B97.24 (2018), p. 245126. DOI: `10.1103/PhysRev B.97.245126`. arXiv: `1709.06259 [cond-mat.str-el]`.

[137] Subir Sachdev and Jinwu Ye. "Gapless spin fluid ground state in a random, quantum Heisenberg magnet". In: *Phys. Rev. Lett.* 70 (1993), p. 3339. DOI: `10.1103/PhysRev Lett.70.3339`. arXiv: `cond-mat/9212030 [cond-mat]`.

[138] Alexei Kitaev. *A simple model of quantum holography*. Talks given at *The Kavli Institute for Theoretical Physics*, University of California, Santa Barbara. Apr. 2015. URL: `%7Bhttp://online.kitp.ucsb.edu/online/entangled15/kitaev/%7D`.

[139] Juan Maldacena and Douglas Stanford. "Remarks on the Sachdev-Ye-Kitaev model". In: *Phys. Rev.* D94.10 (2016), p. 106002. DOI: `10.1103/PhysRevD.94.106002`. arXiv: `1604.07818 [hep-th]`.

[140] Yichen Huang and Yingfei Gu. "Eigenstate entanglement in the Sachdev-Ye-Kitaev model". In: *Phys. Rev.* D100.4 (2019), p. 041901. DOI: `10.1103/PhysRevD.100.041901`. arXiv: `1709.09160 [hep-th]`.

[141] Sheldon Goldstein et al. "Canonical Typicality". In: *Phys. Rev. Lett.* 96.5 (2006), p. 050403. DOI: `10.1103/PhysRevLett.96.050403`. arXiv: `cond-mat/0511091 [cond-mat.stat-mech]`.

[142] Sandu Popescu, Anthony J. Short, and Andreas Winter. "Entanglement and the foundations of statistical mechanics". In: *Nature Physics* 2.11 (Nov. 2006), pp. 754–758. DOI: `10.1038/nphys444`. arXiv: `quant-ph/0511225 [quant-ph]`.

[143] Aron C. Wall. "A proof of the generalized second law for rapidly changing fields and arbitrary horizon slices". In: *Phys. Rev.* D85 (2012). [erratum: Phys. Rev.D87, no.6, 069904 (2013)], p. 104049. DOI: `10.1103/PhysRevD.87.069904,10.1103/PhysRevD.85.104049`. arXiv: `1105.3445 [gr-qc]`.

[144] Ning Bao et al. "The Holographic Entropy Cone". In: *JHEP* 09 (2015), p. 130. DOI: `10.1007/JHEP09(2015)130`. arXiv: `1505.07839 [hep-th]`.

[145] Sean M. Carroll and Aidan Chatwin-Davies. "Cosmic Equilibration: A Holographic No-Hair Theorem from the Generalized Second Law". In: *Phys. Rev.* D97.4 (2018), p. 046012. DOI: 10.1103/PhysRevD.97.046012. arXiv: 1703.09241 [hep-th].

[146] Vijay Balasubramanian and Per Kraus. "Space-time and the holographic renormalization group". In: *Phys. Rev. Lett.* 83 (1999), pp. 3605–3608. DOI: 10.1103/PhysRevLett.83.3605. arXiv: hep-th/9903190 [hep-th].

[147] Leonard Susskind. "Entanglement is not enough". In: *Fortsch. Phys.* 64 (2016), pp. 49–71. DOI: 10.1002/prop.201500095. arXiv: 1411.0690 [hep-th].

[148] Juan Martin Maldacena. "Eternal black holes in anti-de Sitter". In: *JHEP* 04 (2003), p. 021. DOI: 10.1088/1126-6708/2003/04/021. arXiv: hep-th/0106112 [hep-th].

[149] Massimiliano Rota and Sean J. Weinberg. "New constraints for holographic entropy from maximin: A no-go theorem". In: *Phys. Rev.* D97.8 (2018), p. 086013. DOI: 10.1103/PhysRevD.97.086013. arXiv: 1712.10004 [hep-th].

[150] Jutho Haegeman et al. "Entanglement Renormalization for Quantum Fields in Real Space". In: *Phys. Rev. Lett.* 110.10 (2013), p. 100402. DOI: 10.1103/PhysRevLett.110.100402. arXiv: 1102.5524 [hep-th].

[151] Alex Hamilton et al. "Local bulk operators in AdS/CFT: A Holographic description of the black hole interior". In: *Phys. Rev.* D75 (2007). [Erratum: Phys. Rev. D75, 129902 (2007)], p. 106001. DOI: 10.1103/PhysRevD.75.106001,10.1103/PhysRevD.75.129902. arXiv: hep-th/0612053 [hep-th].

[152] Idse Heemskerk et al. "Bulk and Transhorizon Measurements in AdS/CFT". In: *JHEP* 10 (2012), p. 165. DOI: 10.1007/JHEP10(2012)165. arXiv: 1201.3664 [hep-th].

[153] Matthew Headrick et al. "Causality & holographic entanglement entropy". In: *JHEP* 12 (2014), p. 162. DOI: 10.1007/JHEP12(2014)162. arXiv: 1408.6300 [hep-th].

[154] Emil T. Akhmedov. "A Remark on the AdS / CFT correspondence and the renormalization group flow". In: *Phys. Lett.* B442 (1998), pp. 152–158. DOI: 10.1016/S0370-2693(98)01270-2. arXiv: hep-th/9806217 [hep-th].

[155] Enrique Alvarez and Cesar Gomez. "Geometric holography, the renormalization group and the c theorem". In: *Nucl. Phys.* B541 (1999), pp. 441–460. DOI: 10.1016/S0550-3213(98)00752-4. arXiv: hep-th/9807226 [hep-th].

[156] Kostas Skenderis and Paul K. Townsend. "Gravitational stability and renormalization group flow". In: *Phys. Lett.* B468 (1999), pp. 46–51. DOI: 10.1016/S0370-2693(99)01212-5. arXiv: hep-th/9909070 [hep-th].

[157] Jan de Boer, Erik P. Verlinde, and Herman L. Verlinde. "On the holographic renormalization group". In: *JHEP* 08 (2000), p. 003. DOI: 10.1088/1126-6708/2000/08/003. arXiv: hep-th/9912012 [hep-th].

[158] Lars Andersson and Jan Metzger. "The Area of horizons and the trapped region". In: *Commun. Math. Phys.* 290 (2009), pp. 941–972. DOI: `10.1007/s00220-008-0723-y`. arXiv: `0708.4252 [gr-qc]`.

[159] Marc Mars. "Stability of Marginally Outer Trapped Surfaces and Geometric Inequalities". In: *Fundam. Theor. Phys.* 177 (2014), pp. 191–208. DOI: `10.1007/978-3-319-06349-2_8`.

[160] Ricardo Espindola, Alberto Guijosa, and Juan F. Pedraza. "Entanglement Wedge Reconstruction and Entanglement of Purification". In: *Eur. Phys. J.* C78.8 (2018), p. 646. DOI: `10.1140/epjc/s10052-018-6140-2`. arXiv: `1804.05855 [hep-th]`.

[161] Ning Bao and Illan F. Halpern. "Holographic Inequalities and Entanglement of Purification". In: *JHEP* 03 (2018), p. 006. DOI: `10.1007/JHEP03(2018)006`. arXiv: `1710.07643 [hep-th]`.

[162] Ning Bao. Private communications.

[163] Vijay Balasubramanian et al. "Entwinement and the emergence of spacetime". In: *JHEP* 01 (2015), p. 048. DOI: `10.1007/JHEP01(2015)048`. arXiv: `1406.5859 [hep-th]`.

[164] Ben Freivogel et al. "Casting Shadows on Holographic Reconstruction". In: *Phys. Rev.* D91.8 (2015), p. 086013. DOI: `10.1103/PhysRevD.91.086013`. arXiv: `1412.5175 [hep-th]`.

[165] Veronika E. Hubeny and Henry Maxfield. "Holographic probes of collapsing black holes". In: *JHEP* 03 (2014), p. 097. DOI: `10.1007/JHEP03(2014)097`. arXiv: `1312.6887 [hep-th]`.

[166] C. Fefferman and C. R. Graham. "Conformal invariants". In: *Elie Cartan et les Mathematiques d'Aujourd'hui, "Asterisque, hors serie"* (1985), pp. 95–116.

[167] H. Bondi, M. G. J. van der Burg, and A. W. K. Metzner. "Gravitational waves in general relativity. 7. Waves from axisymmetric isolated systems". In: *Proc. Roy. Soc. Lond.* A269 (1962), pp. 21–52. DOI: `10.1098/rspa.1962.0161`.

[168] R. K. Sachs. "Gravitational waves in general relativity. 8. Waves in asymptotically flat space-times". In: *Proc. Roy. Soc. Lond.* A270 (1962), pp. 103–126. DOI: `10.1098/rspa.1962.0206`.

[169] Masahiro Nozaki, Shinsei Ryu, and Tadashi Takayanagi. "Holographic Geometry of Entanglement Renormalization in Quantum Field Theories". In: *JHEP* 10 (2012), p. 193. DOI: `10.1007/JHEP10(2012)193`. arXiv: `1208.3469 [hep-th]`.

[170] Ning Bao et al. "Branches of the Black Hole Wave Function Need Not Contain Firewalls". In: *Phys. Rev.* D97.12 (2018), p. 126014. DOI: `10.1103/PhysRevD.97.126014`. arXiv: `1712.04955 [hep-th]`.

[171] Marika Taylor. "TT deformations in general dimensions". In: (2018). arXiv: `1805.10287 [hep-th]`.

[172] Thomas Hartman et al. "Holography at finite cutoff with a T^2 deformation". In: *JHEP* 03 (2019), p. 004. DOI: 10.1007/JHEP03(2019)004. arXiv: 1807.11401 [hep-th].

[173] Soumangsu Chakraborty et al. "Entanglement beyond AdS". In: *Nucl. Phys.* B935 (2018), pp. 290–309. DOI: 10.1016/j.nuclphysb.2018.08.011. arXiv: 1805.06286 [hep-th].

[174] William Donnelly and Vasudev Shyam. "Entanglement entropy and $T\overline{T}$ deformation". In: *Phys. Rev. Lett.* 121.13 (2018), p. 131602. DOI: 10.1103/PhysRevLett.121.131602. arXiv: 1806.07444 [hep-th].

[175] Bin Chen, Lin Chen, and Peng-Xiang Hao. "Entanglement entropy in $T\overline{T}$-deformed CFT". In: *Phys. Rev.* D98.8 (2018), p. 086025. DOI: 10.1103/PhysRevD.98.086025. arXiv: 1807.08293 [hep-th].

[176] Victor Gorbenko, Eva Silverstein, and Gonzalo Torroba. "dS/dS and $T\overline{T}$". In: *JHEP* 03 (2019), p. 085. DOI: 10.1007/JHEP03(2019)085. arXiv: 1811.07965 [hep-th].

[177] Chanyong Park. "Holographic Entanglement Entropy in Cutoff AdS". In: *Int. J. Mod. Phys.* A33.36 (2019), p. 1850226. DOI: 10.1142/S0217751X18502263. arXiv: 1812.00545 [hep-th].

[178] Pawel Caputa, Shouvik Datta, and Vasudev Shyam. "Sphere partition functions & cut-off AdS". In: *JHEP* 05 (2019), p. 112. DOI: 10.1007/JHEP05(2019)112. arXiv: 1902.10893 [hep-th].

[179] Aritra Banerjee, Arpan Bhattacharyya, and Soumangsu Chakraborty. "Entanglement Entropy for TT deformed CFT in general dimensions". In: (2019). arXiv: 1904.00716 [hep-th].

[180] Zohar Komargodski. "Renormalization group flows and anomalies". In: *Les Houches Lect. Notes* 97 (2015), pp. 255–271. DOI: 10.1093/acprof:oso/9780198727965.003.0011.

[181] Ling-Yan Hung, Robert C. Myers, and Michael Smolkin. "Some Calculable Contributions to Holographic Entanglement Entropy". In: *JHEP* 08 (2011), p. 039. DOI: 10.1007/JHEP08(2011)039. arXiv: 1105.6055 [hep-th].

[182] Hong Liu and Mark Mezei. "A Refinement of entanglement entropy and the number of degrees of freedom". In: *JHEP* 04 (2013), p. 162. DOI: 10.1007/JHEP04(2013)162. arXiv: 1202.2070 [hep-th].

[183] Marika Taylor and William Woodhead. "Renormalized entanglement entropy". In: *JHEP* 08 (2016), p. 165. DOI: 10.1007/JHEP08(2016)165. arXiv: 1604.06808 [hep-th].

[184] J. David Brown and James W. York Jr. "Quasilocal energy and conserved charges derived from the gravitational action". In: *Phys. Rev.* D47 (1993), pp. 1407–1419. DOI: 10.1103/PhysRevD.47.1407. arXiv: gr-qc/9209012 [gr-qc].

[185] Vijay Balasubramanian and Per Kraus. "A Stress tensor for Anti-de Sitter gravity". In: *Commun. Math. Phys.* 208 (1999), pp. 413–428. DOI: `10.1007/s002200050764`. arXiv: `hep-th/9902121 [hep-th]`.

[186] Kostas Skenderis. "Lecture notes on holographic renormalization". In: *Class. Quant. Grav.* 19 (2002), pp. 5849–5876. DOI: `10.1088/0264-9381/19/22/306`. arXiv: `hep-th/0209067 [hep-th]`.

[187] Joan Camps and William R. Kelly. "Generalized gravitational entropy without replica symmetry". In: *JHEP* 03 (2015), p. 061. DOI: `10.1007/JHEP03(2015)061`. arXiv: `1412.4093 [hep-th]`.

[188] Xi Dong. "The Gravity Dual of Renyi Entropy". In: *Nature Commun.* 7 (2016), p. 12472. DOI: `10.1038/ncomms12472`. arXiv: `1601.06788 [hep-th]`.

[189] Xi Dong. "Holographic Entanglement Entropy for General Higher Derivative Gravity". In: *JHEP* 01 (2014), p. 044. DOI: `10.1007/JHEP01(2014)044`. arXiv: `1310.5713 [hep-th]`.